INVESTIGATION OF THE PHASE TRANSITIONS OF PREGELATINIZED WAXY MAIZE
STARCH AT LOW MOISTURE CONTENTS

BY

RACHEL WICKLUND

DISSERTATION

Submitted in partial fulfillment of the requirements
for the degree of Doctor of Philosophy in Food Science and Human Nutrition
in the Graduate College of the
University of Illinois at Urbana-Champaign, 2016

Urbana, Illinois

Doctoral Committee:

    Research Assistant Professor Dawn Bohn, Chair
    Professor Shelly J. Schmidt, Director of Research
    Professor Nicki Engeseth
    Assistant Professor Youngsoo Lee

ABSTRACT

A sub-Tg endotherm has been identified in many cereal-based, low moisture food systems, including several commercial varieties of crackers. Given the similarity of this endotherm to the retrogradation endotherm of amylopectin under higher moisture conditions, the presence of this endotherm may indicate structural changes in amylopectin occurring at low moisture contents that could lead to textural changes in the corresponding food system. Pregelatinized waxy maize starch was studied by MDSC as a function of moisture content and storage temperature. A sub-Tg endotherm was observed between 45-65°C in the non-reversing signal for pregelatinized waxy maize starch stored between 0 and 72% RH and over a storage temperature range from 5 to 35°C. The enthalpy of this transition was independent of storage temperature, but exhibited an exponential relationship with increasing moisture content. FTIR-ATR and ^{13}C CP/MAS NMR identified the fundamental structural cause of the endotherm as the reorganization of amylopectin into double helices following gelatinization, but without the aggregation of the double helices into crystalline arrays that can occur during the full retrogradation process. The reorganization into double helices, and hence the development of the sub-Tg endotherm, was observed to increase with time according to Avrami kinetics, which is often used to describe crystallization processes. The Avrami exponent, n, was estimated at 0.24 and was found to be independent of starch moisture content. The Avrami rate constant, K, was exponentially correlated with starch moisture content similar to the enthalpy of the sub-Tg endotherm. In a model wheat-flour based cracker system the development of the sub-Tg endotherm, due to reformation of amylopectin double helical structure, was also found to follow Avrami kinetics and was correlated with a decrease in the hardness and an increase in the toughness of the crackers. This work confirms that staling and associated textural changes in low moisture starch-based food systems, such as crackers, is a result of reformation of amylopectin double helices without crystallization or aggregation of those helices that develops in high moisture starch-based food systems, such as bread.

TABLE OF CONTENTS

CHAPTER 1
INTRODUCTION

1.1 Rationale and significance

Starch is an integral ingredient in many food products, primarily for its viscosifying and texturizing properties. Thus, recognizing the physical states and transitions undertaken by starch is fundamental in understanding the behavior of more complex food systems.

Undoubtedly, the most important phase transitions for starch in a food system, in terms of the impact on food texture and quality, are starch gelatinization and retrogradation. Atwell and others (1988) proposed definitions for starch transitions including describing gelatinization as "the collapse of molecular orders within the starch granule" whereas pasting was referred to as "the phenomena following gelatinization in the dissolution of starch." Similarly, the definition of retrogradation was proposed as "a process that occurs when the molecules comprising gelatinized starch begin to associate in an ordered structure." Gelatinization and retrogradation are, in many ways, considered to be opposite events in that gelatinization involves a loss of birefringence, loss of double helical structure, loss of crystallinity and an endothermic melting or dissociation event, whereas retrogradation results in an increase in double helical structure and crystallinity.

In terms of direct impact on the food industry, starch retrogradation has long been associated with the staling of bread, the rate of which is often described by the Avrami equation (Fearn and Russell 1982). As starch gels are considered meta-stable, non-equilibrium states, they will undergo structural transformations, including chain aggregation and crystallization, during storage (Biliaderis and Zawistowski 1990). Additionally, the crystallization of amylose is generally accepted to occur rapidly and is often essentially completed by the time the baked item has cooled to room temperature, whereas the staling process occurs over a time period of days and is genreally associated with the recrystallization of amylopectin (Biliaderis and others 1996).

Similar to the starch amylopectin retrogradation endotherm at higher moisture contents, the presence of a sub-Tg endotherm in starch-based food systems at low moisture contents has also been identified. This sub-Tg endotherm occurs over a similar temperature span and possesses many of the same characterisitics of retrogradation, except that the system is below its glass transition temperature at ambient conditions, unlike in retrogradation. While the origin of

1

this sub-Tg endotherm remains controversial, the most prevalent theories involve (1) "melting" of water-carbohydrate interactions and (2) physical aging, also referred to as enthalpy relaxation. However, similarities of the sub-Tg endotherm to the amylopectin retrogradation endotherm and associated process also require consideration.

As many food products, especially those at lower moisture contents, have shelf-lifes on the order of months to a year or more, it is vitally important to understand textural and quality changes that may be occurring during long-term storage. Thus, the aim of this work is to understand phase transitions occuring in starch at low moisture contents that may lead to associated textural changes in starch-based low moisture food systems.

1.2 Objectives

The major objectives of this research were to:

1) Characterize the development of the sub-Tg endotherm in pregelatinized waxy maize starch as a function of moisture content and storage temperature.

2) Identify structural changes in the pregelatinized waxy maize starch that may lead to the development of the sub-Tg endotherm.

3) Determine the kinetics for the development of the sub-Tg endotherm, which may, in turn, relate to shelf-life of certain starch-based low moisture food systems.

4) Correlate the development of the sub-Tg endotherm with textural changes in a low moisture, starch-based cracker model system.

1.3 References

Atwell WA, Hood LF, Lineback DR, Varriano-Marston E, Zobel HF. 1988. The terminology and methodology associated with basic starch phenomena. Cereal Foods World 33:306-11.

Biliaderis CG, Prokopowich DJ, Jacobson MR, BeMiller JN. 1996. Effect of n-alkyl glucosides on waxy maize and wheat starch retrogradation. Carbohydr. Res. 280(1):157-69.

Biliaderis CG, Zawistowski J. 1990. Viscoelastic behavior of aging starch gels - effects of concentration, temperature, and starch hydrolysates on network properties Cereal Chem. 67(3):240-6.

Fearn T, Russell PL. 1982. A kinetic study of bread staling by differential scanning calorimetry - the effect of loaf specific volume J. Sci. Food Agric. 33(6):537-48.

CHAPTER 2
REVIEW OF LITERATURE

2.1 A review of the proposed mechanisms for the formation of a sub-Tg endotherm in glassy polymers and its relationship to starch and its thermal transitions

2.1.1 Abstract

The occurrence of an endothermic event, typically observed below the conventional glass transition, is a common feature of many polymer systems, including starch and other polysaccharides. The most prevalent theories for the origin of this sub-Tg endotherm are the "melting" of water-carbohydrate interactions and physical aging, also referred to as enthalpy relaxation. The water-carbohydrate theory centers on the principle that water-carbohydrate interactions are more easily formed or disrupted than carbohydrate-carbohydrate interactions, particularly below the glass transition where the carbohydrate is essentially immobile. Physical aging is thought to be the result of the spontaneous relaxation of a polymer that occurs in the glassy state as a result of its non-equilibrium state. Both hypotheses assume that the polymer is aged below Tg, although there have been reports of this peak occurring in systems both above and below the system Tg. The aim of this review is to describe the proposed origins of this sub-Tg endothermic event and how it may relate to starch and its thermal transitions, in particular the similarity between physical aging and the retrogradation of starch.

2.1.2 Introduction

In aqueous starch systems, 4 types of thermal events are generally encountered: (1) a sub-Tg endotherm, (2) a glass transition, (3) various crystal melting processes and (4) a high-temperature endotherm which marks the transition into a thermoplastic melt (Thiewes and Steeneken 1997). The occurrence of an endothermic event, typically observed below the conventional glass transition, is a common feature of many semicrystalline polymers, including starch, which develops semi-crystalline shells termed "growth rings" through the organization of amylopectin molecules (Perez and Bertoft 2010). This sub-Tg thermal event has been reported for synthetic semicrystalline polymers (Beckmann and others 1997; Struik 1987), starch (Chung and others 2002; Kalichevsky and others 1992a; Kim and others 2001; Shogren 1992; Yuan and

Thompson 1994), maltodextrin (Descamps and others 2009), confectionary wafers (Livings and others 1997), and cornflakes (Gonzalez and others 2010; Li 2010). While the origin of this sub-Tg thermal event remains controversial, the most prevalent theories involve (1) "melting" of water-carbohydrate interactions and (2) physical aging.

Physical aging, also referred to as enthalpy relaxation, occurs for a glassy material as a result of the non-equilibrium state spontaneously relaxing to a more energetically favorable state. Physical aging is a general, thermoreversible phenonmenon, occurring for any glassy material as a result of its non-equilibrium state attempting to regain equilibrium (Perera 2003).

Alternatively, the endothermic peak has also been attributed to the melting of water-carbohydrate interactions, in particular, the disruption of the hydrogen-bond network involving water and polysaccharides (Appelqvist and others 1993; Yuan and Thompson 1994). This hypothesis relies on the assumption that large molecular weight carbohydrates, such as starch, are effectively immobile below the glass transition, preventing carbohydrate-carbohydrate interactions, whereas water-carbohydrate interactions between residues can still be formed or disrupted (Appelqvist and others 1993).

The presence of this sub-Tg endothermic event has practical implications for carbohydrate and starchy food systems in that it is also typically accompanied by physical changes directly impacting the texture and quality of the food system. In particular, foods that are classified as being in the "glassy" state may be affected, although the prevailing assumption has been that the physical characteristics of such food systems are kinetically stable. However, recently, Li (2010) observed the presence of an endothermic event with a peak temperature near 60°C during DSC analysis of cornflakes that was independent of moisture content over a relative humidity range from 11.3 to 68.9%. The features of this thermal event were similar to what has been described with the exception that the event was observed both below and above the glass transition of the cornflakes. The aim of this review is to describe the proposed origins of this sub-Tg endothermic event of semicrystalline polymers with the intention of gaining insight into the endothermic event ocurring in starchy foods such as cornflakes, below and above the glass transition, and how this relates to the thermal transitions of starch.

2.1.3 Melting of water-carbohydrate interactions

It has been reported that the endothermic peak is a result of the dirsuption of the hydrogen-bonding network between water and polysaccharides (Appelqvist and others 1993; Gidley and others 1993; Yuan and Thompson 1994). It is generally thought that kinetic immobilization below the glass transition determines the material properties of low moisture polysaccharides due to the fact that water-carbohydrate interactions are considred to be equivalent to water-water interactions (Slade and Levine 1991). As such, below the glass transition, water is considered to interact via entropic and free volume effects and should have no net enthalpic interaction with carbohydrates. However, Appelqvist and others (1993) reported the presence of an endothermic "melting" event for a variety of polysaccharides occurring significantly below the glass transition that was more akin to a first order phase transition, which is difficult to reconcile with a completely "glassy" system. A more plausible model might be that glass formation reflects effective prevention of backbone (glycosidic) reorientation, whereas water-carbohydrate interactions between residues can still be formed or disrupted.

Gidley and others (1993) suggested that in high concentrations of carbohydrates, an increase in microviscosity occurs, which leads to lifetimes of associations between water and carbohydrates being sufficiently long enough to be detectable by physical measurements such as DSC. Appelqvist and others (1993) showed that an endothermic event in the temperature range of 50-70°C was observed for materials that show melting rather than glass to rubber transitions upon heating, such as agar and κ-carrageenan, while dextran and pullulan, which do show glass transition behavior, exhibited a similar endohtermic peak in the same temeprature region. The difference in behavior between the polysaccharides was attributed to differences in the geometry and orientation of the glycosidic bond, leading to a variety of "immobilizaiton" mechanims, of which, glass formation is only one.

In a study of a variety of polysaccharides, including pullulan, waxy maize starch, dextran, xanthan gum, agar, alginate, pectin and guar gum, among others, an endothermic event followed by material softening was observed between 45 and 80°C, having the following common features (Appelqvist and others 1993):

1) DSC peak temperature showed no systemic dependence on polymer type or water content

2) The enthalpy of the transition was influenced by water content, although each polymer family may have its own dose-response curve. The event was not detectable above the glass transition (for those systems that typcially show glass transition behavior)

3) Peak was not immediately seen upon rescan in the DSC, but recovery of the endothermic behavior did occur within hours/days, and was quicker for aging temperatures near the glass transition (for those systems which show such behavior). For example, the peak was not evident on immediate rescan of pullulan, but 60-70% was recovered after room temperature storage for 7 days. Additionally, lower moisture content samples, which were 65-75°C below Tg, had slower recovery than higher moisture samples that were 30-40°C below Tg, under the same storage conditions.

4) Detectable softening of the material as measured by DMTA was also evident in the same temperature range, and the softening effect was independent of DMTA frequency, which is more characteristic of a structural melting or first order phase transition rather than a relaxation process.

To study the role of starch hydroxyl groups in the formation of this sub-Tg endotherm, Yuan and Thompson (1994) compared amylopectin and amylopectin triacetate, which has had all of the free hydroxyl groups substituted with acetyl groups, and found that the sub-Tg peak disappeared after complete acetylation of waxy starch. This result suggests that water-starch hydroxyl groups play a role in the formation of the peak, although it should also be noted that complete acetylation also renders the starch insoluble.

Yuan and Thompson (1994) also studied ß-limit dextrin for the presence of the sub-Tg peak due to its reduced tendency to form double helices. If the peak is due to double helical formation, as has been suggested for physical aging, then no or little peak should be observed for aged dextrin. However, the authors found that the enthalpy change for dextrin was greater than for waxy starch at a similar moisture content.

Furthermore, Yuan and Thompson (1994) found that conditioning starch at low moisture (~2% at constant temperature) after previously conditioning at 43, 65 and 75% relative humidity resulted in the disappearance of the sub-Tg endotherm. The authors argued that if the sub-Tg peak that was present when the starch was conditioned at the higher relative humidities was due to enthalpy relaxation, then loss of moisture at constant temperature would be extremely difficult to result in the recovery of entropy, as would be necessary to result in the loss of an endotherm

due to relaxation. Rather, this observation supports the hypothesis that water-starch interactions are the underlying cause of the sub-Tg peak rather than enthalpy relaxation.

According to Yuan and Thompson (1994), the water-starch hyroxyl group interactions can be disrupted by:

1) heating the sample above the dissociaiton temperature (in this case, around 50°C)

2) removing water from the sample by reducing the vapor pressure above the sample (such as by placing the sample above P_2O_5)

3) Drastically increasing the mobility of the carbohydrate backbone by increasing the moisture content so that the carbohydrate is in the rubbery state

Using thermodynamic clustering theory, Kilburn and others (2005) expanded on the role of water in amorphous carbohydrate polymers by analyzing the size of intermolecular voids between polymer chains. In low-moisture carbohydrate systems, water uptake leads to a strong increase in the size of the holes between the polymer chains in both the glassy and rubbery state. The authors proposed that water dynamically disrupts the hydrogen-bonding between carbohydrate chains, leading to an expansion of the matrix at the nanolevel and increasing the degrees of freedom of the carbohydrate chains. In contrast, low molecular weight sugars did not modify the interactions between carbohydrate chains, but owing to their small size, reduced the average number of polymer entanglements and thus enabled polymer reorganizations in the glassy state. This improved molecular packing of carbohydrates containing low molecular weight sugars in the glassy state increased the matrix density, which could explain the reduced mobility of these systems despite a lower glass transition temperature.

In general, the key mechanistic features for the formation of the sub-Tg endothermic peak due to the melting of water-carbohydrate interactions can be summarized as (Appelqvist et al., 1993):

1) Disruption of energetic associations between water molecules and hydrophilic groups on the carbohydrate

2) Development of the endotherm requires a long range connectivity between associating units, which may require days to develop

3) Increasing, but restricted, mobility results in faster development of the endotherm and greater cooperativity of structural disordering

2.1.4 Physical aging

Physical aging, also termed enthalpy relaxation, encompasses a wide variety of physical properties, all characterized by the same general phenomenon of an observed change in the property of the material during storage at constant temperature and zero stress and under no influence from any other external condition. In contrast to chemical or biological aging, which involve irreversible changes in polymer structure primarily through chemical modification, physical aging involves only reversible changes in physical properties such as elastic modulus, fracture stress, enthalpy, dielectric constant, diffusion coefficients and refractive index (Hutchinson 1995).

Physical aging is the spontaneous relaxation of a polymer that occurs in the glassy state as a result of its non-equilibrium state (Perera 2003). Glassy materials are kinetic solids, and as such, are not thermodynamically stable. At temperatures greater than the glass transition temperature, (T>Tg), there is greater polymer mobility so that as temperature is decreased, thermodynamic properties such as enthalpy and entropy can follow equilibrium conditions. However, for temperatures below the glass transition, (T<Tg), long range cooperative motions of the polymer chains are frozen, and thus, the mobility of the polymer is greatly reduced. In such instances, as temperature is decreased, the rate of change of the enthalpy and entropy of the system is slower than the temperature change, creating a non-equilibrium state. During storage, the polymer structure "relaxes" towards equilibrium, or the state that would have been reached if relaxation limits were not reached during cooling, resulting in a spontaneous decrese in enthalpy, specific volume, entropy and other physical properties (Badii and others 2005).

In a DSC scan, the result of enthalpy relaxation from physical aging can be observed by the enthalpy recovery peak as the energy is lost from the relaxation process to a more ordered state. The enthalpy relaxation process has been observed for gelatin (Badii et al., 2005), synthetic polymers (Beckmann and others 1997; Struik 1987), starch (Chung and others 2004a; Chung and others 2002; Chung and Lim 2004; Chung and others 2004b; Chung and others 2005; Jang and Pyun 1997; Kim and others 2001; Lourdin and others 2002; Shogren 1992; Steeneken and Woortman 2009; Thiewes and Steeneken 1997) maltodextrin (Descamps and others 2009), cornflakes (Gonzalez and others 2010; Li 2010), and confectionary wafers (Livings and others 1997). To further support the assumption that the endothermic peak is a result of enthalpy relaxation, Livings and others (1997) scanned confectionary wafers in the DSC at different

heating rates and then extrapolated the data using least squares fit, resulting in an intersection with the x-axis at approximately zero. That is, for a zero scan rate, no endothermic transition is observed, implying that for very slow scan rates, the sample has sufficient time to relax back to its equilbrium position, and hence, no peak is seen.

Physical aging is related to conformational rearrangement of polymers with increased molecular pakcing and densification that occurs in the absence of a phase change (e.g., crystallization), or chemical reaction (e.g. photo chemical degradation). The rate at which conformational rearrangements are occuring in the enthalpy relaxation process is dependent on aging time and moisture content of the material (Badii and others 2005; Kilburn and others 2005; Livings and others 1997). In general, as moisture content increased, enthalpy of the peak increased, while the temperature of the peak was independent of moisture content (Badii and others 2005; Chung and others 2002; Shogren 1992; Thiewes and Steeneken 1997).

Additionally, a linear relationship between the peak temperature and the logarithm of the aging time has been observed for both normal and waxy rice starches (Chung and others 2004a; Chung and Lim 2004), maltose and a starch-sorbitol mixture (Lourdin and others 2002) and for starch, maltodextrin and maltose (Noel and others 2005). In starchy systems, the rate of relaxation decreased as aging time progressed (Chung and Lim 2004). In the beginning, the relaxation was rapid since the starch chains had sufficient mobility, but as aging time increased, the relaxation rate decreased as the starch chains became less mobile on approaching equilibrium. Thus, the rate of the increase in relaxation temperature was dependent on the residual crystallinity of the starch (Chung and others 2004a). Similarly, cross-linking of starch with sodium tripolyphospate (STPP) was found to result in a greater extent of relaxation, presumably, because the large phosphate groups increased the free volume, allowing for more mobility (Chung and others 2004b).

However, it should be noted that Gonzalez and others (2010) did not find a relationship between peak temperature and log aging time in cornflakes, although the study employed a lower and more narrow range of moisture contents. On ther other hand, Gonzalez and others (2010) also concluded that molecular relaxation occurred faster as starch became more fragmented during the shearing process for cornflakes. The authors contended that the shear during flaking provided the activation energy needed for molecular rearrangement towards a more ordered,

equilibrium state such that relaxation of depolymerized starch could occur faster upon subsequent aging.

Physical aging is a general phenomenon that occurs for amorphous materials. To provide a link between the sub-Tg endotherm and physical aging, Kim and others (2001) ball-milled starch in order to destroy its crystallinity and form a completely amorphous structure. This system was found to still contain a sub-Tg endotherm around 50-60°C at 16% moisture, which the authors attributed to enthalpy relaxation. Additionally, the authors noted that the peak could not be due to melting because the ball-milled starch was shown to be completely amorphous using x-ray diffraction.

Another feature of the sub-Tg endoherm, as it relates to physical aging, is the dependence of the sample on thermal history. In general, the peak is not seen upon immediate rescan in the DSC, and furthermore, upon aging, aging temperature was found to have more of an effect on the peak magnitude than the relative humidity storage conditions for 21DE maltodextrin (Descamps and others 2009). That is, temperature plasticization was more efficient to release energy than water plasticization owing to the different kinetics of structural recovery in temperature-jump experiments compared to relative humidity-jump experiments with longer recovery times experienced for relative-humidity jumps. Thus, the sub-Tg peak seemed to correspond more to a partial structural recovery from the onset of molecular mobility that was occurring below Tg.

Thiewes and Steenenken (1997) summarized the properties of the sub-Tg endotherm, as it relates to physical aging, as:

1) Physical aging is only possible below Tg; above Tg, the process is referred to as annealing
2) Endotherm is asymmetrical
3) Endotherm increases in magnitude and shifts to a higher temperature as aging time and relative humidity storage conditions increase
4) For long times and higher temperatures, the endotherm may be super-imposed on the glass transition
5) The peak temperature of the endothermic event is a linear function of temperature and log aging time

2.1.5 Physical aging of semicrystalline polymers

In a study involving DSC analysis of cornflakes, Li (2010) noted the occurrence of the sub-Tg endothermic peak occuring for cornflakes both below and above the conventional glass transition of the system, which would suggest that the peak is not due to physical aging as it is a phenomenon that occurs only in the glassy state. However, as noted by Perera (2003), semicrystalline polymers distinguish themselves from completely amorphous systems by their relatively broad and complicated glass transition, and by the fact that physical aging has been found to occur at temperatures above Tg, in fact, as high as 100°C above Tg.

This observation led to the development of an "extended glass transition" due to restricted mobility domains in semicrystalline polymers (Struik 1987; Struik 1989b; Struik 1989a). This model assumes that the amporphous regions near crystallites are constrained by their proximity to the crystalline region, such that it remains in the glassy state well above the conventional Tg of the polymer. Therefore, the polymer no longer has a single Tg, but a Tg-distribution. For example, Shogren (1992) suggested that the upper Tg for corn starch may be as high as 100°C above the lowest observed Tg.

In general, semicrystalline polymers are considered to consist of 3 phases (Struik 1987):

1) *Mobile amorphous phase*, in which thermal transitions are linked to relaxations occuring in the bulk amorphous phase. This portion of the non-crystalline region in a polymer gains mobility at the glass transition.

2) *Rigid amorphous phase*, in which thermal transitions are linked to relaxations occuring in the amorphous region tied to the crystalline lamellae; this portion remains immobile across the normal glass transition and does not contribute to the traditional Tg peak observed by DSC. This region may still undergo structural rearrangements and reductions in free volume leading to physical aging at conditions above the normal Tg of the polymer.

3) *Crystalline phase*, in which thermal transitons are linked to local mobility in crystallites

Thus, the Tg of the mobile amorphous phase is not the same as the Tg of the rigid amorphous phase. In fact, the Tg of the rigid amorphous phase will be affected not only by molecular structure, but also by kinetic restrainsts such as the availability of water, degree of crystallinity, structure of crystalline lamellae, etc. (Liu and Shi 2006).

2.1.6 Physical aging of starch

Starch is a semicrystalline polymer composed of two polymers, amylose and amlopectin. The structure of a starch granule consists of stacks of semicrystalline regions separated by amorphous growth rings. In each semicrystalline ring, there are alternating crystalline lamellae and amorphous lamellae, in which the crystalline lamellae are comprised of double helices from the outer chains of amylopectin and the amorphous lamellae contain glucose units of amylopectin near the branch points. As a result of differences in fine structure and molecular arrangemnt, the crystalline laemllae and amorphous lamellae have different densities and water contents (Liu and Shi 2006; Perez and Bertoft 2010).

Using dynamic DSC (DDSC), Liu and Shi (2006) found that stepwise changes in heat capacity overlapped with the melting of crystallites in starch, which suggested that the rigid amorphous fraction corresponded to the interlamellar noncrystalline regions close to crystallites which became mobile only in the melting region. The rigid amorphous fraction was constrained by the double helices formed at the branch points in the amorphous lamellae as well as by the crystalline structure packing, leading to an increase in the energy barrier needed for segmental movememnt of these amylopectin molecules. As such, the T_g of the rigid amorphous region should be substantially higher than that of the mobile amorphous growth rings.

Native rice starch was found to exhibit a smaller endothermic enthalpy and broader temperature range than gelatinized rice starch (Chung and others 2002), which may have been due to the greater amount of amorphous material in gelatinized starch, but may also be a result of the crystalline lamellae broadening the endotherm as a result of the constraints placed on the amorphous lamellae. Using DSC, Chung and Lim (2004) observed dual glass transitions (56.7 and 71.4°C at 14.5% moisture) for normal rice starch, but only one glass transition for waxy rice starch, suggesting heterogeniety in the amorphous structure of normal rice starch, for example, a less restricted and more restricted amorphous region. Normal corn starch also exhibited dual glass transitions, and the lower T_g overlapped the enthalpy relaxation peak while the upper T_g did not, allowing for observations of changes in the upper T_g upon aging (Chung and others 2005). The authors observed that the temperautre of the upper T_g increased as aging time increased, with a significant rate of increase intially, followed by a slowing of the rate as the system approached equilibrium and it became more difficult for conformation changes to occur as the rigidity of the matrix increased. By extension, the upper T_g should reach a maximum

12

when the system is at equilibrium. Furthermore, the Cowie and Ferguson model could be used to explain the kinetics of the relaxation/aging process where

$$\Delta H(t_a, T_a) = \Delta H_\infty(T_a)[1 - \exp\{(\frac{-t_a}{t_c})^\beta\}]$$ Equation 2.1

where ΔH_∞ represents the maximum equilibrium enthalpy, t_c is the average relaxation time, and β is the width of the relaxation time distribution. Nonlinear curve-fitting analysis can be used to calculate these parameters in order to provide useful information on the kinetics of relaxation at a given aging time and temperature (t_a and T_a), which may then correspond to the kinetics related to changes in physical properties such as break strength and texture.

During the relaxation process, X-ray diffraction data of aged, wheat-based confectionary wafers indicated the presence of a small, but well-defined peak at 2θ angle of 20° superimposed on the broad amorphous halo, typical of gelatinized starch products, which was not found in freshly prepared wafers. The position and d-spacing of this peak was characteristic of a 6-fold helical structure that corresponded to the 310 reflection of V-type amylose, which is typically observed when amylose complexes with lipids (Livings and others 1997). However, amylose-lipid melting typically occurs at much higher temperatures (95-130°C in excess water and higher for limited water conditions) than the temperature range of the sub-Tg endotherm. Rather, the authors proposed that on aging below Tg, short chain amylopectin domains with helical ordering form but without the aggregation of these to give crystals.

Liu and others (2010b) also recognized the importance of double helical formation in the effects of physical aging in the development of the "gel-ball" structure model. In a previous study, the double helical crystalline structures formed by short, branced chain amylopectin were found to be torn apart during gelatinization (Yu and Christie 2005). Liu and others (2010b) expanded on this finding to suggest that these short, branched chains remain in a regular pattern, retaining a certain "memory," that can lead to the formation of "gel-balls" that are comprised mainly of chains from the same sub-main chain that can then organize into a relatively separate "super-globe." The molecular entanglements between gel-balls and super-globes are much less than those between linear polymer chains due to their size and length. Thus, these gel-balls require less energy to move than long, linear chains, especially in the presence of a plasticizer such as water.

2.1.7 Starch retrogradation

The sub-Tg endotherm occurs around 60°C, which is similar to that of the retrogradation of amylopectin under high moisture conditions. However, retrogradation, which is a recrystallization process, should not occur below Tg, but its similarity to this sub-Tg peak warrants further investigation as amylopectin retrogradation is often attributed as the cause of a variety of physical and textural changes in a wide range of food systems. In particular, the recrystallization of the outer chains of amylopectin has been linked to the staling endotherm of baked foods (Jang and Pyun 1997).

Retrogradation is a multistage process, similar to the crystallization of other semicrystalline polymers. The recrystallization process can be descirbed in 3 phases: (1) nucleation, or the initiation of oriented chain segments, (2) propagation (crystal growth), and (3), maturation during which crystal perfection and growth continue. Overall, the rate of crystallization depends on nucleation and rate of crystal growth. During retrogradation of starch, the peak temperature of the retrogradation endotherm increases as the storage temperature increases, but the peak width and enthalpy decrease, resulting in the formation of a more perfect crystal structure. Nucleation rate and propagation rate can be converted into enthalpy and peak temperature in DSC measurements since higher enthalpy corresponds to greater nucleation rate and higher preak temperatures correlate with faster propagation rates (Jang and Pyun 1997).

Due to their different structures, amylose and amylopectin have different rates of relaxation and/or potential reassociation rates, which leads to differences in the rate of retrogradation (Gonzalez and others 2010). Crystallization of amylose dominates the short-term development of gel-structure, while amylopectin crystallizatin dominates the long-term development. Owing to the fact that retrogradation is a kinetic process, other factors such as starch concentration, water content, and storage time and temperature will also have an impact on the rate of retrogradation (Liu and others 2010a).

For waxy corn starch, the rate of crystallization was found to follow a bell-shaped curve versus temperature with the maximum occurring about 65°C above Tg (De Meuter and others 1999). Similarly, Jang and Pyun (1997) observed the bell-shape curve versus moisture for the staling endotherm, with the peak occurring at 50-60% moisture, which would be within the temperature range based on Tg, reported above. At really low temperatures, the crystallization rate decreases due to viscosity limitations such that the transport of starch chains to the boundary

of the starch crystal is restricted and thereby the crystallization rate is diffusion-controlled. At higher temperatures, the crystallization rate is limited by a reduction in the thermodynamic driving force (primary and secondary nucleation).

The endotherms for the amylopectin contribution of retrograded starch are closely related to the endotherms of starch gelatinization, typically referred to as G and M1, although the peak temperature is lower and the enthalpy is smaller for retrograded starch (Chang and Liu 1991; Liu and others 2010a). The smaller peak observed for retrogradation versus gelatinization implies that retrograded starch is less stable than native starch. During storage of gelatinized starch, the enthalpy progressively increases, in a nonlinear fashion, until a certain limit is reached, which is about 78% of the enthalpy of starch gelatinization for waxy corn starch and only about 45% for normal corn starch (Liu and others 2007; Liu and others 2010a). Similarly, in gelatinized waxy cornstarch that was allowed to retrograde, x-ray diffraction analysis indicated about 5.5% crystallinity in the retrograded starch compared to 24% crystalinity in the native starch (Kalichevsky and others 1992a). Liu and Thompson (1998) suggested that the reformation of double helices to give retrograded amylopectin is favored in molecules in which the orientation of the chains is similar to the initial double helical conformation, and that after gelatinization, the amylose serves to dilute the amylopectin double helices and sterically hinder their formation, leading to a decreased number of restored double helices. In retrograded potato starch gels (30% w/w), the crystalline domains were on the size order of about 5 nm, which is much smaller than that seen in native starch. Furthermore, the super-helical structure formed by the crystalline domains in the native starch was not seen in the retrograded starch, which suggests that long-range reordering is not regained during retrogradation (Keetels and others 1996a).

Additionally, cereal amylopectins have a reduced rate of retrogradation compared to tuber and pulse starches, which has been linked to their shorter average chain lengths (Kalichevsky and others 1990). Amylopectin typically has a bimodal molecular weight distribution with degrees of polymerization (DP) of the chains ranging from about 40 to 60 and about 15-20, with a greater abundance of the shorter chains in cereal starches (Hizukuri 1985). Retrogradation/reassociation of amylopectin in cereal starch gels was found to occur over 16 glucose residues, compared to 18 for pea amylopectin and 19 for tuber starches. Additionally, the peak temperature for the retrogradation endotherm occurred at lower value than it did for pea and potato, which may also depend on the size and perfection of the crystallized amylopectin as well

as the length of the chains involved (Kalichevsky and others 1990). It would be interesting to determine if the same trend holds for the physical aging of starch, since theoretically, shorter chain lengths may have more mobility below the glass transition, which could lead to faster rates of relaxation.

2.1.8 Starch retrogradation and physical aging

In principle, starch retrogradation occurs at temperatures above Tg, while physical aging occurs below Tg, although the similarity between the endotherms developed for each transition are quite similar. Both peaks occur in the same temperature region and have similar dependencies with storage time. Additionally, during physical aging, short chain amylopectin domains with helical ordering form, but without the aggregation of these to give crystals, as may occur during retrogradation (Livings and others 1997). It is possible that during retrogradation, relaxation occurs first followed by association and crystallization of the larger polymer chains, resulting in a larger endotherm. Further work is needed to verify this hypothesis.

2.1.9 Summary and conclusions

The occurrence of an endothermic event, typically observed below the conventional glass transition, is a common feature of many carbohydrates and carbohydrate-based systems, including starch, as well as for synthetic semicrystalline polymers. Literature accounts of the observation of this sub-Tg peak are summarized in Table 2.1.

The most prevalent theories for the origin of this sub-Tg endotherm are the "melting" of water-carbohydrate interactions and physical aging. The water-carbohydrate theory centers on the principle that water-carbohydrate interactions are more easily formed or disrupted than carbohydrate-carbohydrate interactions, particularly below the glass transition where the carbohydrate is essentially immobile. Physical aging is thought to be the result of the spontaneous relaxation of a polymer that occurs in the glassy state as a result of its non-equilibrium state. Both theories have validity as well as inconsistencies with what has actually been observed, and the arguments for and against each theory are summarized in Table 2.2.

Furthermore, starch presents a unique system that also exhibits this sub-Tg endortherm. Starch is a semicrystalline polymer that consists of stacks of crystalline regions separated by amorphous growth rings. Like other semicrystalline polymers, starch has been found to have

more than one glass transition due ot the presence of a mobile amorphous phase and a rigid amorphous phase. The relaxation of amylopectin near the branch points in the rigid amorphous phase is thought to be responsible for the physical aging of starch below the conventional glass transition.

In starch, the thermal transitons involved in physical aging are quite similar to the thermal transitions occurring for retrogradation. It is hypothesized that relaxation may be the first step in retrogradation, followed by crystallization. Below Tg, only relaxation may be occuring, but above Tg, relaxation and crystallization can occur. Further work is needed to verify this hypothesis.

2.2 A review of starch retrogradation and its relationship to the sub-Tg endotherm in starch

2.2.1 Introduction

Starch is an integral ingredient in many food products, primarily for its viscosifying and texturizing properties. Thus, understanding the physical states and transitions undertaken by starch is fundamental in understanding the behavior of more complex food systems.

Starch is a semicrystalline polymer composed of two glucose polymers, amylose and amylopectin. The structure of a starch granule consists of stacks of semicrystalline regions separated by amorphous growth rings. In each semicrystalline ring, there are alternating crystalline lamellae and amorphous lamellae, in which the crystalline lamellae are comprised of double helices from the outer chains of amylopectin and the amorphous lamellae contain glucose units of amylopectin near the branch points (Perez and Bertoft 2010).

In general, semicrystalline polymers are considered to consist of 3 phases (Struik 1987):

4) *Mobile amorphous phase*, in which thermal transitions are linked to relaxations occurring in the bulk amorphous phase. This portion of the non-crystalline region in a polymer gains mobility at the glass transition.

5) *Rigid amorphous phase*, in which thermal transitions are linked to relaxations occurring in the amorphous region tied to the crystalline lamellae; this portion remains immobile across the normal glass transition and does not contribute to the traditional Tg peak observed by DSC. This region may still undergo structural rearrangements and reductions

in free volume leading to physical aging at conditions above the normal Tg of the polymer.

6) *Crystalline phase*, in which thermal transitions are linked to local mobility in crystallites.

Owing to the direct relationship between starch thermal transitions and food texture, manipulation of these processes, in particular the glass transition and crystallization processes, can then be used to alter the texture of starch-based foods. Below the glass transition, glassy materials are hard and brittle, since molecular motion is suspended and energy cannot be absorbed by changes in molecular conformation. Above the glass transition, molecular motion increases and the materials become more elastic and less brittle. For examples, plasticizers, namely water, can be used to encourage transitions from glassy to rubbery such as in the cooking of spaghetti (Morris 1990).

Undoubtedly, the most important phase transitions for starch in a food system, in terms of the impact on food texture and quality, are starch gelatinization and retrogradation. Atwell and others (1988) proposed definitions for starch transitions including describing gelatinization as "the collapse of molecular orders within the starch granule" whereas pasting was referred to as "the phenomena following gelatinization in the dissolution of starch." Similarly, the definition of retrogradation was proposed "a process that occurs when the molecules comprising gelatinized starch begin to associate in an ordered structure." Gelatinization and retrogradation are, in many ways, considered to be opposite events in that gelatinization involves a loss of birefringence, loss of double helical structure, loss of crystallinity and an endothermic melting or dissociation event whereas retrogradation results in an increase in double helical structure and crystallinity.

In terms of direct impact on the food industry, starch retrogradation has long been associated with the staling of bread, the rate of which is often described by the Avrami equation (Fearn and Russell 1982). As starch gels are considered meta-stable, non-equilibrium states, they will undergo structure transformation, including chain aggregation and crystallization, during storage (Biliaderis and Zawistowski 1990). Additionally, the crystallization of amylose is generally accepted to occur rapidly and is often essentially completed by the time the baked item has cooled to room temperature whereas the staling process occurs over a time period of days and is genreally associated with the recrystallization of amylopectin (Biliaderis and others 1996).

As most food products have shelf-lifes on the order of months to year or more, it is vitally important to understand textural and quality changes that may be occurring during long-term

storage. Thus, the aim of this review is to understand phase transitions occuring in starch with a particular emphasis on retrogradation.

2.2.2 Starch gelatinization

As gelatinization and retrogradation are directly linked, to understand the processes and changes occurring during retrogradation, an understanding of gelatinization is also required. When a starch granule is heated in excess water, an order-disorder phase transition, termed gelatinization, occurs, accompanied by near swelling and solubilization of the granule, melting of crystallites, separation of amylose from amylopectin and disentanglement of non-covalent bonds (Keetels and others 1996c). At a minimum, gelatinization entails the nearly concurrent processes of (1) loss of crystallinity as measured by loss of birefringence and its x-ray diffraction pattern, (2) uptake of heat as the conformation of the starch is altered, (3) hydration of the starch, accompanied by swelling of the granule, and (4) decrease in relaxation time of the water molecules (Donovan 1979).

When examining the gelatinization processes by temperature scanning calorimetric measurements (e.g. DSC), up to 4 thermal transitions can be observed depending on the water content and final heating temperature (Goldstein and others 2010; Randzio and others 2002):

1) A single endotherm, genreally referred to as the G endotherm, occurring at ~60-70°C in excess water (usually >50% wet basis). This endotherm, if present, occurs at constant temperature regardless of the amount of water present in the system. The enthalpy change increases with increasing water content.

2) A second endothermic peak, commonly called the M1 endotherm, may partially overlap the G endotherm and is observed at higher temperatures as the starch to water ratio increases. As water content is sufficiently increased, the G and M1 endotherm converge, resulting in a single endothermic peak as previously described.

3) As water content further decreases, the G endotherm disappears, and the M1 endotherm shifts to higher temperatures.

4) Two transitions, occurring at temperatures higher than the G and M1 endotherms have also been observed and are typically linked to the melting of amylose and amylose-lipid complexes.

19

Using a combination of techniques, such as small- and wide-angle X-ray scattering, differential scanning calorimetry and small-angle neutron scattering, several models for the gelatinization process have been proposed over the years. The earliest model is that of Donovan (1979), which describes gelatinization as a regular equilibrium process consisting of the swelling of the amorphous regions of starch resulting in the "stripping" of starch chains from the surface of crystallites. In low water conditions, water is not evenly distributed within the granule giving rise to separate crystallite "stripping" and melting events and the two endotherm peaks typically observed for starch systems under low moisture. As water content is increased, crystallite "stripping" dominates, leaving no crystallites remaining to undergo melting at higher temperatures and only one endothermic peak is observed. Since crystallite "stripping" may result in both the unfolding and hydration of double helices in starch, this model is consistent with the observation of concurrent loss of crystalline order and molecular order, but the model fails to address the process of swelling that would need to occur in the amorphous regions in order to result in gelatinization and "striping" of crystalline regions as well as the non-equilibrium nature of the process.

According to Russell (1987), the most appropriate model for gelatinization involves a glass transition, perhaps due to plasticization of the amorphous fraction, as well as two phase transitions. The G endotherm is thought to be due to the disordering of double helices of short-range order as a consequence of chain mobilization in the amorphous rings due to gross swelling and crystallite disruption in excess water, and the M1 endotherm was assigned to the disordering of the amylopectin crystallites. Under conditions of limiting water, the crystallites are unaffected by the disruption of the amorphous regions, causing them to melt out at higher temperatures.

Biliaderis and others (1996) suggested that the two DSC endotherms are a consequence of partial melting followed by recrystallization and then final melting. When examining the gelatinization process at different heating rates, Biliaderis and others (1996) observed the merging of the G and M1 endotherms, which was attributed to insufficient time for recrystallization. At slower heating rates and in excess water, it was suggested that a glass transition within the bulk amorphous phase was occurring simultaneously with the melting and recrystallization processes. As water content was reduced, the difference between the glass transition and crystallite melting increased, allowing for separation of the peaks in DSC studies. However, the effect of heating rate on the two endotherms can also be explained in terms of

differences in resolution of the DSC instrument, and furthermore, recrystallization has not been observed in x-ray studies of partially gelatinized starch prepared by extracting samples during gelatinisation in limiting water (Jenkins and Donald 1998).

However, more recent work by Liu and others (1991) utilizing X-ray diffraction to study the gelatinization processes, contradicts this theory that granule crystallinity is lost throughout both the G and M1 endotherms. Furthermore, the combination of ^{13}C NMR, which detects order corresponding to double-helix content, x-ray diffraction studies, which detects order related to crystallites, and DSC thermograms has led to the conclusion that crystalline and molecular order are lost concurrently during gelatinization, and the DSC endothermic enthalpies primarily reflect the loss of double helical order rather than the melting of crystalline regions (Cooke and Gidley 1992; Liu and others 1991; Randzio and others 2002).

Using a combination of techniques, small- and wide-angle X-ray scattering, differential scanning calorimetry and small-angle neutron scattering, Jenkins and Donald (1998) concluded that most of the cyrstallinity was lost during the gelatinization endotherm, but this occurred only after a significant amount of water had already entered the amorphous background region. The amorphous background was where all of the initial swelling was concentrated, presumably as a result of a strong driving force pulling water out of the amorphous lamellae and into the amorphous background region, since the rate of transport from water outside of the granule would not be sufficiently fast on its own to result in swelling of the granule. Only once a large amount of swelling had occurred in the amorphous background region was there sufficient stress imposed between the growth rings and the semicrystalline lamellae to start disrupting the crystallites. This final loss of crystallinity and ultimate breakdown of the granule occurred late in the process and rather beyond the end of the endotherm revealed by DSC.

Waigh and others (2000) proposed a liquid crystalline approach to starch gelatinization in which, during gelatinization, upon separation of the double helices from their lamellar crystallites, a true helix-coil transition occurs. Those amylopectin side chains intertwined in double helices can strongly interact with not only their helical duplex partners but also with neighboring chains in other helices, leading to a dissociation of helices side-by-side and an unwinding of the coil. It is theorized that dissociation of the double helices occurs from the ends, and past the point of dissociation, the free ends of the amylopectin helices mix up producing constraints that discourage the re-assembly of the double helices such that they now interact with

parts of the amylopectin molecule other than their original helical duplex partner, forming physical junctions (new double helices) and creating more general amorphous hydrogen bonded associations.

The kinetically limiting-step for this unwinding rotation is possible rotation of the helices, and as such the ease of rotation could thus affect the rate of gelatinization. This theory predicts that long unit chain lengths, such as found in A-type starches, would encourage rapid dissociation due to the increased flexibility. A-type starches generally have a higher proportion of longer amylopectin branch chains than their counterparts, those displaying a B-type pattern. Starch granule swelling, gelatinization and pasting properties have previously been correlated with amylopectin branch chain length and distribution with those starches with a larger proportion of longer amylopectin chains with a degree of polymerization of 18-21, in general, had lower gelatinization temperatures (Jane and others 1999; Kim and Huber 2010; Qi and others 2003; Singh and others 2010; Srichuwong and others 2005). Additionally, several other factors may be involved including the proportion of double helices, the level of crystallinity and the presence of amylose–lipid inclusions (Shi and Seib 1992; Tananuwong and Reid 2004).

According to Waigh and others (2000), this model of helix–helix dissociation followed by a helix–coil transition provides a framework within which to understand the water content dependent DSC traces of starch gelatinization. In excess water, the difference between the DSC endotherms for the helix-helix dissociation and the unwinding transition of the helices is immeasurably small and they are assumed to occur simultaneously, but as the water content is decreased, the difference in energy of the two transitions allows for separation of the DSC endotherms (G and M1). Patel and Seetharaman (2010) observed a kinetic limitation to the complete melting of the M1 endother, which under this theory, would further suggest that unwinding of the double helices is the rate-limiting step.Thus, in order to predict the molecular behavior of the amylopectin during gelatinization, the lamellar order parameter, the orientational order parameter of the amylopectin double helices and the helicity of the amylopectin (helix:coil ratio) need to be characterized.

Using specialized differential scanning calorimetry (DSC) techniques, Randzio and others (2002) further expanded upon the observations of Waigh and others (2000) and observed 5 types of phase transitions occurring in starch-water systems in the course of gelatinization

1) Sharp endothermic transition occurring between 46 and 60°C that was independent of the water content. The transition was associated with the melting of the crystalline part of the starch granule followed by a helix-coil transformation in amylopectin;

2) Water content-dependent, slow exothermic transition connected with the reassociation of the unwound helixes of amylopectin with parts of other amylopectin molecules (other than their original helix duplex partner);

3) Water content-dependent, low-temperature exothermic transition associated with recrystallization of partly dehydrated starch;

4) High-temperature endothermic transformation associated with a nematic-isotropic transition, which is in agreement with the liquid crystalline approach to the gelatinization of starch;

5) Continuous slow exothermic transformation associated with the softening of the amorphous growth rings of the starch granule due to increasing water content in the granule during gelatinization.

In general, it can be concluded that the gelatinization process consists of 3 general structural changes in the starch granule: (1) increased starch polymer mobility in the amorphous regions due to water absorption in the granule, (2) rearrangement of amylopectin in the amorphous regions as a result of the formation of new intermolecular interactions, and (3) further increased mobility of the starch polymers as water content further increases, causing a loss of these intermolecular interactions and a breakdown in granule structure (Ratnayake and Jackson 2007). The energy absorbed during gelatinization is sufficient to not only melt crystallites, but also lead to a structural re-ordering process consisting of helical-helical dissociation and helical-coil transitions.

2.2.3 Amylose retrogradation

Textural changes in food during storage as a result of structural changes in starch are often, however misleading, associated with amylose retrogradation. While amylose retrogradation is often thought to be a negative side effect, in some food products, such as starch jelly candies and other confectionary products, it is often desired and promoted. Amylose gels are opaque, and the opacity arises from a phase separation of the amylose into polymer-rich and polymer-deficient regions upon gelation (Miles and others 1985). The gelation

process is considered to be a 2-stage process with an initial, rapid change in structural properties followed by a slower change due to crystallization of the amylose in the polymer-rich regions of the gel (Ring and others 1987). Amylose crystallizes independently from amylopectin, which can result in amylose leaching and phase separation during thermal treatment. These crystallites are generally acid-resistant and relatively heat stable (melting temperature >100°C) with a degree of polymerization of 35-40 glucose units. On the contrary, amylopectin crystallites are heat and acid labile with a degree of polymerization of approximately 15 (Mestres and others 1988).

Initially, the amylose polymer chains adopt double helical structures followed by helix-helix aggregation, thereby leading to increased turbidity and for sufficiently long polymer chains, cross-linked network formation and gelation (Hoover 1995). It has been theorized that the double helix formation probably occurs at the ends of the molecules, favoring chain elongation. Once helix formation has occurred, lateral association of the double helices may occur through crystallization, creating stiff double helices within crystallite junction zones (Leloup and others 1992; Morris 1990). Most of the textural changes associated with amylose retrogradation and gelation occur in the first stage as a substantial part (>80%) of the crystallization of the amylose was found to occur after the shear modulus had reached a constant value ((Biliaderis and Zawistowski 1990; Miles and others 1985).

The physical form of the amylose polymers (precipitate or gel), kinetics of aggregation and variation of the gel strength have been correlated with amylose chain length. Chain lengths less than 100 glucose residues precipitate in aqueous solution, whereas chain lengths between 250 and 600 residues undergo precipitation and gelation, and chain lengths greater than 1100 residues favor gelation (Hoover 1995; Shi and Seib 1992). Overall, the increase in the shear modulus (G') observed with amylose retrogradation was found to be dependent on the amylose concentration while the kinetics of the increase in gel stiffness and rate of crystallization was independent of amylose concentration (Doublier and Choplin 1989).

Amylose retrogradation can be observed by DSC measurement as an endotherm occurring near 160°C (Mestres and others 1988). Upon gelling and crystallization, amylose adopts a B-type crystalline pattern along with the reappearance of birefringence. The birefringence reassembly appears to be based on longitudinal growth of amylose crystallites, as related to the phase separation process and the creation of a network. This birefringence is

different from that in native starch granules, which results from radial orientation of spherulites leading to a polarization cross (Mestres and others 1988).

2.2.4 Amylopectin retrogradation

2.2.4.1 Structural changes occurring during retrogradation

In many respects, the retrogradation of amylopectin is the reverse event of gelatinization occurring upon cooling of the gelatinized starch, or as described by Biliaderis and others (1996), the underlying molecular changes associated with amylopectin retrogradation are adoption of double helical structures and chain aggregation. Upon cooling a gelatinized starch suspension, the amylopectin molecules may reassociate through crystallization of the branches into parallel double helices linked by amorphous sections containing loosely organized chains (Putaux and others 2000; van Soest and others 1994). Similarly, Farhat and others (2000b) applied the Lauritzen-Hoffman theory of chain-folded crystals of synthetic polymers to describe amylopectin retrogradation. The theory of polymer crystallization developed by Lauritzen and Hoffman (1973) considers the growth of chain-folded polymer crystals by the deposition of polymer chains on an already-existing crystal substrate. It is assumed that the chains are deposited at adjacent positions on the crystal growth face by the polymer chain emerging from the crystal and then folding back on itself. In the case of amylopectin, the double helices comprising the external, short chains form the crystallites while the branching points constitute the "folds."

Using a combination of acid hydrolysis, gel permeation chromatography and X-ray diffraction, Ring and others (1987) showed that the associated regions with an amylopectin gel contained branched fragments comprised of individual chains with an average degree of polymerization (DP) of 15. The smaller chains are believed to be attached as clusters on the longer chains, and as such, inter-chain association can only extend over about 15 residues before it is interrupted by a branch point (Miles and others 1985). The crystalline part of starch is also derived from short amylopectin chains (DP =15) (Hoover 1995). It was further demonstrated that the nanocrystals of amylopectin form from the short side or external branches of the molecule, as evidenced by the inability of the beta-limit dextrin to retrograde (Hoover 1995; Putaux and others 2000; Ring and others 1987).

Additionally, studies of native starches indicate that the average chain length of amylopectin is the main determinant in the polymorphic crystalline form (A-type or B-type). An A-type structure has a nearly close-packed array of double helices whereas the B-type form consists of more open-packing and holds 4 times as many water molecules. Due to the close-packing of the A-type structure and its lower free energy, amylopectin glucan chains would be expected to have a greater entropy barrier to recrystallize in the A-form rather than the B-form. In terms of retrogradation, lower temperatures would be expected to favor more rapid crystallization and therefore favor the polymorphic form requiring the least entropy change (B-type), the kinetic product. At higher temperatures, crystallization would be slower and tend to favor the most stable polymorph (A-type), the thermodynamic product (Gidley 1987). Similarly, Farhat and others (2000b), in studying nonexpanded waxy maize starch extrudates, found that at low moisture content and high storage temperature, the A-type polymorph was obtained, while at high water content and low storage temperature, the B-type polymoph appeared.

Unlike amylose gels, amylopectin gels are thermoreversible (Miles and others 1985; Ring and others 1987). Additionally, when measured by DSC, the midpoint temperature and enthalpy value for the transition marking amylopectin retrogradation is similar to, though always less than, the gelatinization temperature of the starch granule (Miles and others 1985), and the endotherm temperature range is usually broader than that of gelatinization (Goldstein and others 2010). The retrogradation endotherm may be as much as 10-26°C less than the gelatinization endotherm and 60-80% of the gelatinization enthalpy (Goldstein and others 2010), and less than that (as low as 45%) for amylose-containing starches, which may interfere with the reformation of the amylopectin double helices (Liu and others 2010a). These observations suggest that the crystalline forms that appear during storage of amylopectin gels are different and weaker than those of native granules. Studies conducted by Lv and others (2011) proved that structure changes in starch occurring during gelatinization and retrogradation affected the availability, quality and number of sites on the amylopectin molecules that were able to participate in water binding. Furthermore, the maximum retrogradation enthalpy typically occurs at 50-60% starch concentration and falls close to 0 at 10 and 80% starch (Zeleznak and Hoseney 1986).

In freshly gelatinized starch, the amylopectin is completely amorphous, and the water within the granule is nearly uniformly distributed. The degree to which the amylopectin will retrograde or recrystallize depends on the temperature as it relates to the mobility of the

amylopectin chains and their ability to reassociate. At low water content, the amylopectin is mainly assumed to be in the glassy state, and as such mobility is hindered to the point at which recrystallization either does not occur or is very slow. As water content increases, the glass transition temperature decreases due to the more effective plasticization provided by the water and recrystallization of amylopectin may progress. At excessively high moisture contents, recrystallization may decreases as a consequence of dilution (Gudmundsson 1994).

2.2.4.2 Amylopectin retrogradation as a crystallization process

Starch retrogradation is a non-equilibrium thermoreversible recrystallization process which is governed by a consecutive three step mechanism of nucleation, propagation and maturation (Slade and Levine 1988a). After gelatinization, the reordering of the amylopectin molecules results in heterogeneous recrystallization that is responsible for the broad endotherm observed by DSC in which the least stable crystals melt out at lower temperatures and the remaining crystallites, of higher quality, melt at higher temperatures (Elfstrand and others 2004).

Because nucleation and propagation is a liquid state event which requires orientational mobility of the polymer chains in the amylopectin molecule, the crystallization process can only occur in the temperature range between the glass transition temperature and the melting temperature, e.g. in the range of approximately 25 and 60°C for a starch gel containing 50% water (Silverio and others 2000). Thus, the crystallization behavior can be related to Tg, which allows for prediction of starch crystallization behavior and stability of products containing starch.

For example, the temperature difference between the storage temperature and glass transition temperature (T- Tg) for gelatinized starch affects both the extent of crystallization and the melting behavior of the crystallites formed. Crystallization under low T-Tg conditions appears to produce smaller and less perfect crystallites than those produced under high T-Tg conditions, due to lower molecular mobility (Jouppila and Roos 1997). Furthermore, the kinetics of starch retrogradation exhibit a strong temperature dependence because the nucleation rate increases exponentially with decreasing temperature down to the glass transition temperature, while the propagation rate increases exponentially with increasing temperature up to the melting temperature (Silverio and others 2000), and the retrogradation rate should be greatest at a temperature between the optimal temperatures for nucleation and progpagation, somewhere between Tg and Tm (Jacobson and BeMiller 1998).

Thus, the crystallization and retrogradation of amorphous starch is similar to the crystallization behavior of semicrystalline synthetic polymers, such as styrene. Mizuno and others (1998) showed that the effect of cross-linking on crystallization behavior (in terms of elevating the glass transition temperature) was similar for starch and styrene cross-linked with divinylbenzene, despite the differences in the types of cross-linking; the cross-linking in starch is thought to be mainly caused by hydrogen bonding rather than covalent bonds that join the polymer chains in styrene.

In terms of nucleation, the double helices of amylopectin can act as nuclei and increase the rate of nucleation. Elfstrand and others (2004) discovered that acid hydrolysis of starch led to more retrogradation than did mechanical treatment in producing starches of similar mechanical weight, the only difference being that acid hydrolysis left intact granules while mechanical treatment created completely amorphous, broken granules. The authors postulated that the presence of already crystalline material or granular remnants could serve as nucleation points and favor recrystallization in acid hydrolyzed starch compared to mechanically treated starch. However, amylopectin molecular weight and its relation to ability to reform double helices, was important in terms of the number of starch crystallites formed and the overall amount of crystallinity, but it was not important in terms of the stability of the recrystallized polymer. Degree of polymerization, degree of branching and unit chin length distribution controlled the stability of the recrystallites.

Silverio and others (2000) also demonstrated a dependence on the rate of amylopectin recrystallization and the time-temperature cycles imparted on the starch. Alternating between a temperature favoring nucleation and a temperature favoring propagaion decreased the quantity of recrystallized starch, but the crystallites that were obtained were of a higher quality and more temperature stable. Zhou and others (2010) observed a similar effect for normal and waxy corn starches in that fewer crystallites might be formed under the temperature cycles compared to isothermal storage, but the crystallites formed under temperature cycling appeared more homogeneous than those under isothermal storage. This result could possibly be interpreted as an annealing effect, allowing for the growth of more stable crystallites at the expense of less stable crystallites. Such an effect could be related to the bimodal endotherm that often develops for retrogradation of potato, waxy maize and pea starches (Fredriksson and others 1998).

28

Storage time may also have a similar effect in terms of producing more or less stable recrystallites. Durrani and Donald (1995) found that amylopectin gels stored at 4°C for different times showed an endotherm at 40-65°C, but the final temperature of the melting transition was 65°C regardless of storage time while the peak temperature moved to lower temperatures as storage time decreased. The authors hypothesized that increasing storage time allowed for the development of more perfect crystals, and it was the perfection, rather than the number, of crystallites which provided stability to the recrystallized amylopectin gel.

2.2.4.3 Amylopectin retrogradation kinetics

The kinetics describing the retrogradation and recrystallization of amylopectin are often fit to the Avrami equation, in which the rate follows an s-type shape and is slow in the beginning and end but rapid in between. Using DSC to measure the extent of retrogradation of waxy cornstarch with intermediate water content, Liu and others (2010a) found that the M1r endotherm appeared after 2 hours of storage and developed rapidly but only changed slightly after 5 hours of storage. Similarly, the Gr endotherm was detected after 5 hours and increased rapidly up to 1 day of storage, after which it was seen to reach a limiting value (Liu and others 2007).

Retrogradation behavior is often modeled using classical Avrami kinetics for polymer crystallization (Marsh and Blanshard 1988; Zhang and Jackson 1992) even though the Avrami equation assumes thermodynamic equilibrium and the retrogradation process is known to be nonequilibrium. In studying native wheat starch gels, retrogradation appeared to follow a mechanism of "rod-like growth from instantaneous nuclei" based on the Avrami model, though the Avrami exponents were not integers, which suggests that starch retrogradation is a more complex process and the Avrami equation is not a good theoretical model to explain crystalline growth and nucleation during retrogradation (Zhang and Jackson 1992).

Marsh and Blanshard (1988) further expanded upon the rates of crystallization by applying the Lauritzen-Hoffman theory for the growth of polymer crystals. The theory of polymer crystallization developed by Lauritzen and Hoffman (1973) considers the growth of chain-folded polymer crystals by the deposition of polymer chains on an already-existing crystal substrate. It is assumed that the chains are deposited at adjacent positions on the crystal growth face by the polymer chain emerging from the crystal and then folding back on itself. Using this

theory, a glass transition temperature, Tg, for this 50% wheat starch gel was calculated as approximately 200K (-73°C), which was similar to a value calculated using free volume theory.

Bulkin and others (1987) described the kinetics for the retrogradation of waxy maize and potato starch composites as consisting of 4 distinct phases:

1. Stage 1 – closely approximates 1st order kinetics. Crystallinity does not develop, indicating that only short-range, conformational ordering is occurring, possibly the formation of double helices within an amylopectin molecule.
2. Stage 2 – plateau region. This stage was postulated to be the induction time before the onset of crystal growth.
3. Stage 3 – linear change with time (zero order kinetics). The authors observed the development of crystallinity during this stage and described this phase as the primary crystallization step.
4. Stage 4 – linear change with time (zero order kinetics). Crystallinity was seen to further increase due to the development of more long-range order. This stage was described as the crystalline propagation and perfection step.

Thus, whether describing the kinetics of amylopectin retrogradation or structural changes occuring within the granule during, starch retrogradation can most simply be described as a thermoreversible recrystallization process which is governed by a consecutive three step mechanism of nucleation, propagation and maturation (Slade and Levine 1988a).

2.2.4.4 Textural changes and bread staling

Starch retrogradation is most thought of, in terms of its importance to the food industry, for its impact on food texture. Retrograded starch may increase the hardness, elasticity, water-biding and many other important textural properties of the food. The cooling of gelatinized starch pastes is generally seen to increase the storage modulus (G') and decrease the loss modulus (G"), and the degree of this affect has been correlated with the molecular weight of the amylopectin and the chain length distribution (Chung and others 2008).

In particular, the recrystallization of the outer chains of amylopectin has been linked to the staling endotherm of baked foods (Jang and Pyun 1997). In studying the effect of the glycerol monostearate (GMS) as a dough constituent on bread staling, Russell (1983b) observed a reduction in the rate constant for the development of the Gr endotherm though not in the limiting

enthalpy. At the same time, addition of GMS also led to a reduction in the rate constant for bread crumb firming. Fearn and Russell (1982) used DSC and crumb compressibility measurements to correlate changes in the starch fraction of bread with changes in the texture of the bread crumb, as fitted to the Avrami equation.

Bread crumb firming is probably the change most widely associated with bread staling. Changes in starch structure, namely gelatinization and retrogradation of starch, contribute to changes in texture from soft to firm (Hibi 2001). Retrogradation in wheat starch gels was controlled by the amount of water present during aging, regardless of the amount present during gelatinization. It was also found that solubilized amylopectin did retrograde, and as with starch, the extent of retrogradation was controlled by the amount of water present. However, bread baked with several different anti-staling agents and aged at different moisture levels were not significantly different in the amount of recrystallization. Thus, the anti-staling agents did not alter the amount of water available for crystallization, and therefore, the anti-staling properties brought about by these compounds must be through a different mechanism (Zeleznak and Hoseney 1986).

Aguirre and others (2011) used X-ray diffraction and water activity measurments to examine the effect of storage temperature on starch retrogradation and bread staling. The authors found that the storage temperature affected not only the mobility of the molecules but also the phase that they form. Recrystallization was still seen to occur at -18°C (below the glass transition) but only crystal growth occurred at this temperature, whereas at 25 and 4°C, crystal growth and formation of new crystals occurred.

2.2.5 Factors affecting amylopectin retrogradation

2.2.5.1 Effect of starch botanical origin

Starch botanical origin can have a significant impact on the tendency of the starch to retrograde. Through observation of the shear modulus over time, pea starch gels were observed to retrograde at a greater extent than potato, then maize, and then wheat starch, and this effect became more pronounced as the starch concentration increased (Orford and others 1987). Retrogradation in stored (4°C for 56 days) 2% pastes prepared by atmospheric cooking under mild shear conditions of starches from various botanical sources as determined quantitatively by

turbidometric analysis revealed that retrogradation rates followed the order wheat, common corn > rice, tapioca, potato >> waxy maize (Jacobson and others 1997). Paredes-lopez and others (1994) observed a lower tendency to retrograde for amaranth starch than for waxy corn or normal corn starch.

In general, cereal starch amylopectins tend to retrograde to a lesser extent than pea or potato starches, which has been attributed to the shorter average chain lengths found in cereal starches (Fredriksson and others 1998; Kalichevsky and others 1990). Similarly, in the study of different cultivars of sorghum, those cultivars with amylopectin fine structures with a lower proportion of long B-chains were found to be less likely to retrograde and stale (Matalanis and others 2009).

2.2.5.2 Effect of amylopectin chain size

Native wheat starches were treated with acid to develop different molecular profiles, and different retrogradation behaviors were seen due to smaller size amylopectin fragments, narrowed linear chain length distribution, and decreased branching which were attributed to the molecular changes of the starches. The increased initial retrogradation rate was due to increased mobility of smaller size amylopectin fragments, and the narrowed linear chain length distribution with decreased branch points (increased molecular homogeneity). The final similar enthalpy level of retrogradation indicated the retention of native amylopectin side chain patterns in the smaller amylopectin fragments (Zhang and Jackson 1992).

Mua and Jackson (1998) and Chang and Lin (2007) have observed a dependency of retrogradation on molecular weight and degree of branching, while Kohyama and others (2004) has linked wheat starches which contained longer side chains of amylopectin with increased retrogradation. In terms of molecular chain lengths, the extent of retrogradation has been found to be proportional to the mole fraction of unit chains with a degree of polymerization of 14-24 and inversely proportional to the mole fraction of unit chains with DP 6-9 (Shi and Seib 1992). Vandeputte and others (2003) also observed an inhibition of retrogradation for relatively high amounts of amylopectin chains with DP 6-9 and DP >25 whereas relative amounts of DP 12-22 led to an increase in retrograded amylopectin and enthalpy as measured by DSC.

2.2.5.3 Effect of temperature

In general, the rate of retrogradation follows a bell-shaped curve with storage temperature (Farhat and others 2000b) though when tested under limited temperature conditions, it may appear to be increasing with increasing storage temperature (Jouppila and others 1998). Slade and Levine (1988a) showed that the rate of nucleation increased exponentially as temperatre decreased to Tg, but the rate of propagation increased exponentially as temperature increased to just below the melting point (Tm) of the crystallites; thus, the fastest rate of retrogradation should ocurr at the midpoint between Tg and Tm. Additionally, the shift of the curve describing the rate versus temperature is explained in terms of the role of water in plasticizing the polymer and consequently, decreasing Tg and Tm (Farhat and others 2000b).

Yu and others (2010) studied the effects of freezing rates and storage temperature on starch retrogradation and textural properties of cooked rice. Starch retrogradation and hardness increased as the freezing rate decreased, but the adhesiveness or stickiness of the rice increased as freezing rate increased. Additionally, when stored at 4°C, the cooked rice lost all of the advantages of fast freezing within 3 days, but rice stored at -18°C maintained its textural properties over 7 month storage. Therefore, high quality cooked rice can be produced by combining rapid freezing with frozen storage. Jacobson and BeMiller (1998) used these proprerites to develop a simple method to accelerate and quantitate retrogradation that does not require special equipment. The authors found that freezing and then thawing starch pastes at temperatures greater than 30°C produced staling endotherms and x-ray diffraction patterns nearly identical to those that form during isothermal storage at 4°C.

2.2.5.4 Effect of lipids

Monoglycerides and other emulsifiers have long been known for their antistaling action, and thus are frequently used in bread formulations to improve crumb softness and extend the shelf-life of the product (Biliaderis and others 1996). Proposed mechanisms of action include (1) complex formation between lipids and starch components, (2) surface adhesion of the lipids on the amylopectin chains or on the granule surface, hinder recrystallization, or (3) decreased mobility, due to water-water interactions and/or increase in local viscosity (Hoover 1995).

Eliasson and Ljunger (1988) reported increased efficacy for retarding retrogradation using monoglyceride additives with one hydrocarbon chain compared to those with 2 or 3

33

hydrocarbon chains. The authors hypothesized that amylopectin has similar interactions with lipids as amylose does, i.e. ability to form complexes with the outer branch of the amylopectin molecule assisting in the formation of a helical inclusion complex with the acyl chains of a suitable lipid. DSC and X-ray diffraction further supported this hypothesis for the interaction of the surfactants sodium dodecyl sulphate (SDS), cetyltrimethylammonium bromide (CTAB) and monogylcerides (Gudmundsson and Eliasson 1990).

Lipids are more commonly thought to form inclusion complexes with amylose, but they may also form complexes with amylopectin, though this is limited when the amylopectin is present in the native starch granule due to structural restrainment. Gudmundsson and Eliasson (1990) summarized the effect of surfactants and lipids on amylopectin retrogradation as follows:

1) Greatest reduction in retrogradation for the formation of a complex with 100% amylopectin and suitable lipids since no other constituents are present to disturb this effect.

2) Retrogradation may be reduced in mixtures containing 50-90% amylopectin, though this is more likely a result of a reduction in amylose retrogradation. In such mixtures, lipids are more likely to complex with free amylose.

3) In mixtures containing less than 50% amylopectin, the lipids also primarily form complexes with amylose. As a result, the amylose cannot co-crystallize with the amylopectin and the surfactants cannot affect the amylopectin, leading to a smaller reduction in the extent of retrogradation.

2.2.5.5 Effect of salts

For most salts, increasing concentration results in decreased retrogradation, and in general, the effect of various ions follows the lyotropic series. That is, retrogradation rates in wheat starch gels were found to increase by anions in the order $I^- < Br^- < Cl^- < F^-$ and by cations in the order $K^+ < Li^+ < Na^+$ (Hoover 1995). Generally, increased salt concentration reduced the rate constants for development of the storage modulus during gel ageing and gels with salt showed an additional peak at higher temperatures whose limiting size was proportional to salt content, suggesting that salt inhibits the re-ordering of the amylopectin fraction of starch gels during ageing and induces the separation of domains within this fraction (Russell and Oliver 1989). Additionally, Mita (1992) observed a decrease in the rate of storage modulus increase for

potato starch gels as the NaCl concentration increased. Introduction of starch modification such as substitution with acetyl, hydroxypropyl and phosphate groups into the starch molecule interferes with retrogradation due to stearic hindrance between the amylose chains and the outer linear chains of amylopectin. This effect may be further enhanced due to the interaction of these groups with salts such as phosphate (in high concentration in potato starches) with sodium chloride (Hoover 1995).

2.2.5.6 Effect of sugars

The addition of sucrose, glucose or ribose, added to wheat starch gels at a ratio of 1:1:1 (sugar: water: starch) has been found to reduce the firmness of the gels and the level of B-type crystallization. The effectiveness of the sugars in reducing firmness and crystallinity followed the order ribose> sucrose> glucose (Cairns and others 1991; Ianson and others 1990). Additionally, increasing molecular weight of the sugars has preliminarily been associated with a reduction in rate of crystallization (Cairns and others 1991). Additionally, while sugars generally acted in such a way as to decrease firmness and starch crystallinity (Ward and others 1994), fructose was the exception. For waxy-maize starch extrudates, fructose considerably increased the rate of retrogradation and the increase was proportional to the sugar concentration (Farhat and others 2000a).

Several mechanisms have been proposed for the effect of sugars on delaying starch retrogradation. Spies and Hoseney (Spies and Hoseney 1982) proposed that sucrose interacts with starch in the amorphous region to form bridges between the chains. Other theories include (1) the binding of water by sucrose thus limiting water availability to the starch (Cameron and Donald 1993), (2) a decrease in water mobility due to sucrose addition (Lim and others 1992; Spies and Hoseney 1982) and (3) and an antiplasticization effect of sugars (Slade and Levine 1988a). Using NMR, Le Botlan and Desbois (1995) concluded that sucrose interacted completely in the liquid phase with 4.6 molecules of water, and the water-sucrose entity acted as a plasticizing agent during retrogradation. Later, Farhat *et al.* Farhat and others (2000a) found that sugars enhanced the transformation of the A-type polymorph to a so-called pseudo B-type polymorph with a similar X-ray pattern as B-type amylopectin. With just water and amylopectin, the A-type polymorph formed during retrogradation.

2.2.6 Methods used to assess amylopectin retrogradation

A range of physical and chemical techniques, including viscometry and rheological measurements, turbidity measurements, FTIR, NMR , X-ray diffraction, and differential scanning calorimetry, have been used to study the retrogradation of amylopectin. These methods differ in the level to which the starch is probed, from the macroscopic to the molecular level, and as such, each can give a different view as to changes occurring during and after retrogradation. In general, using a combination of 2 to 3 methods allows for cross comparison and provide a more complete understanding of the retrogradation process (Karim and others 2000).

2.2.6.1 Turbidity measurements

During storage, amylopectin gels become turbid and finally opaque, allowing for measurement of turbidity as a means to assess retrogradation. The increase in turbidity is indicative of changes occurring in the refractive index distribution and, hence, of the density distribution in the gel. For 20% amylopectin gels, the turbidity reached a limiting value after 4-5 days, but quantitiative analysis is difficult due to sensitivity at low concentrations and during the early stages of retrogradation (Ring and others 1987).

2.2.6.2 Rheology

Textural changes of starch pastes, as related to retrogradation during storage, can typically be monitored through examination of changes in the dynamic viscoelastic properties. This method is advantageous in that the sample volume is relatively large, so that the measurement averages out sample inhomogeneity. Changes in the viscoelastic properties of starch gels during storage primarily reflect the effect of amylopectin crystallization on the rigidity of the entire gel structure (Roulet and others 1988). During storage, a 20% amylopectin solution changed from a viscoelastic material which flowed under an applied small, constant stress to a gel with a corresponding increase in the storage modulus, G', that reached a limiting value after 30-40 days (Ring and others 1987). Similarly, Mita (1992) found that the storage modulus of potato starch pastes increased rapidly with time for the first few hours, but attained equilibrium after a long period of ageing. Additionally, the rate of storage modulus increase decreased with increasing concentrations up to 10%, and at higher concentrations little or no increase was observed.

Large deformation properties, including the stress at fracture and Young's modulus, for concentrated starch pastes were found change during storage (Keetels and others 1996c). An increase in Young's Modulus was attributed to an increase in the stiffness of the swollen granules as a result of the reordering of amylopectin. The increase in fracture stress may be related to (1) changes in the amylose matrix gel surrounding the swollen granules, which most likely occurs within the first day of storage and (2) an increase in the rigidity of the hooks between adjacent, irregularly shaped swollen granules during deformation due to the increased stiffness of the swollen granules.

2.2.6.3 Dilatometry

Dilatometry is a thermo-analytical method based on volume changes occurring over a specified temperature range. Dilatometry has been used to study phase transitions occurring during gelatinization and retrogradation of starch in which the observed volume changes are indicative of changes in strength, number and symmetry of interactions between molecules. Retrogradation of 20% amylopectin solution was found to result in isothermal volume increases that approached a limiting value during storage and the magnitude of this change was much larger for amylopectin than for amylose (Ring and others 1987).

2.2.6.4 Thermogravimetric analysis

Tian and others (2011) employed thermogravimetric analysis (TGA) to study the retrogradation properties of rice starch. The authors found that the bound water content significantly increased during storage and through comparison with DSC, the increase was related with changes occurring as a result of the retrogradation process. Additionally, the kinetics of this change was also seen to follow the Avrami model.

2.2.6.5 DSC

Whenever a material undergoes a change in physical state (e.g. melting), or transforms from one crystalline form to another, or whenever it reacts chemically, heat is either absorbed (endothermic) or liberated (exothermic). Basically, DSC is a technique whereby the difference in energy input into a substance and a reference material is measured as a function of temperature while both materials are subjected to programmed heating or cooling.

DSC is sensitive to structural effects caused by long-range ordering of chains into microcrystalline domains (Biliaderis and Zawistowski 1990). DSC measures the amount of enthalpy required to disrupt or melt those crystallites, and DSC is arguably the most common method to assess the extent of retrogradation. In terms of the properties and transitions of starch, DSC can be used to measure gelatinization of starch and percent crystallinity or changes in crystallinity during storage (Thomas and Schmidt 2010).

DSC has been successfully used to study the gelatinization of starch (Biliaderis and others 1996; Russell 1987; Tananuwong and Reid 2004), retrogradation kinetics (Liu and others 2007; Liu and others 2010a; Roulet and others 1988; Zhang and Jackson 1992), and a wide variety of factors known to influence the retrogradation process (Eliasson and Ljunger 1988; Fisher and Thompson 1997; Jang and Pyun 1997; Russell 1983b; Shi and Seib 1992).

2.2.6.6 X-ray diffraction

X-ray diffraction is commonly used together with DSC to assess starch retrogradation. Starch granules, being partially crystalline, give distinct X-ray diffraction patterns (Sarko and Wu 1978). Powder diffraction patterns of starch show relatively broad peaks superimposed on an amorphous "halo." The relative intensity of these two features is used to estimate the level of crystalline order; for example, broad diffraction peaks indicate either imperfect or relatively small crystallites (Cooke and Gidley 1992). One drawback to x-ray diffraction is the relatively small amount of crystallized material present in retrograded starch. Only about 15% of the available amylopectin is crystallized in fully retrograded starch and so the effective sample volume is small relative to the total sample volume. Additionally, the total volume sampled by x-rays is also small, which means that sample inhomogeneity can have a large impact on the results obtained from this technique (Roulet and others 1988).

2.2.6.7 FTIR

As with other aqueous solutions of polysaccharides, the Fourier-transform infrared (FTIR) spectra of starch solutions in the 1300-800 cm^{-1} region is sensitive to the structural conformation. Most bands in this region arise from highly coupled C-C and C-O stretching modes, that while difficult to assign, changes in these modes can be measured over time as a means to assess the extent of retrogradation (Goodfellow and Wilson 1990; Wilson and others 1987). During

gelatinization, the most intense band was observed at 1022 cm^{-1} with a noticeable shoulder on the high frequency side, and after retrogradation, this peak had resolved into two distinct bands at 1019 and 1046 cm^{-1} (Wilson and others 1987). Similarly, Smits and others (1998) used diffuse reflectance Fourier transform infrared (DRIFT) to assess retrogradation by changes in the lineshapes and intensities in the characteristic area between 995 and 1020 cm^{-1}.

Since A and B-type starches differ only in the packing of their helices and their IR spectra are indistinguishable in the characteristic 1300-800 cm^{-1} region, changes in this region due to retrogradation must be due to changes in short-range conformation (Goodfellow and Wilson 1990). For amylopectin, these changes involve an initial fast change for a coil to helix transformation for amylopectin side chains followed by a slower aggregation of these helices to produce crystallinity. FTIR was successfully used to separate the multiple stages occurring during retrogradation (formation of helices and induction time for helix aggregation followed by primary aggregation and crystallization) and evaluate the effect of glycerol on the retrogradation kinetics of waxy maize starch (van Soest and others 1994).

2.2.6.8 NMR

NMR spectra of starch granules can be analysed in terms of a combination of amorphous and ordered components. As NMRspectroscopy is a short-distance range probe, it is considered that detected "order" corresponds to double-helix content in contrast to X-ray diffraction, which detects only those double helices that are packed in regular arrays (Cooke and Gidley 1992). Jane and others (1985) first used NMR to detect the formation of helical complexes from a random coil to a helix in aged starch solutions. Because the conformation of the starch polymer changes about the glycosidic linkage, the change in torsion angle around this linkage affects the pattern of electron distribution, which can be detected by NMR as a change in the shielding of the atoms involved in the linkage. At the time, the authors felt that ^{13}C NMR was more useful than proton NMR because of the fast exchange rate of the hydroxyl protons causing sensitivity issues.

However, Wu and Eads (1993) successfully applied ^{1}H cross-relaxation NMR and high resolution NMR to study the ageing of gelatinized waxy maize starch gels. The authors observed starch polymer chains in three different motional states: (1) The most flexible with fairly narrow resonances in high resolution ^{1}H NMR spectra; (2) The most rigid, giving rise to a very broad component in the cross-relaxation spectrum; and, (3) The less rigid with motions intermediate

between those in crystalline and dissolved states, producing the narrower component of the cross-relaxation spectra. Additionally, Lewen and others (2003) observed that the value for T2b, the solid transverse relaxation time, did not change with starch concentration or time indicating that the mobility of the solid component did not change over time despite the conversion of the highly mobile starch fraction to the less mobile solid state during retrogradation.

Pulsed NMR (PNMR) has also been used to analyze the retrogradation of rice starches (Yao and Ding 2002). The authors also attempted to fit the measured signal corresponding to the relative solid content to the Avrami equation since the crystallite growth of amylopectin accounts for the increase of this signal under the experimental conditions used. The Avrami exponent n increased and the crystallization rate constant k decreased when the moisture content increased, which the authors explained by the effects of water on the nucleation mechanism, the concentration of nuclei, and the migration distance among amylopectin external chains.

2.2.7 Summary and conclusions

Starch retrogradation is a complex process that can have a direct and measurable impact on food texture and quality. During starch gelatinization, a loss of double helical order and crystallinity occurs in the granule with a loss of birefringence as witnessed by an endothermic melting event. During retrogradation, the starch attempts to regain that double helical structure and crystallinity, though at most 60-80% of the original structure is rebuilt. Many factors can influence the extent of retrogradation, including starch botanical origin, amylopectin chain size and chain length distribution, presence of salts, sugars and lipids and temperature. Several techniques are available to assess retrogradation such as DSC, X-ray diffraction, rheological measurements, and spectroscopy including FTIR and NMR. By measuring and understanding the retrogradation process and those factors that influence it, improved or novel food products can be designed with improved texture and quality with minimal changes occurring during storage.

2.3 A review of bread staling and its relationship to the recrystallization of amylopectin

2.3.1 Introduction

While recognized and investigated for centuries, bread staling still results in substantial economic losses to both the baking industry and the consumer. The generally accepted definition

of staling is as "a term which indicates decreasing consumer acceptance of bakery products caused by changes in crumb other than those resulting from the action of spoilage organisms" (Bechtel and others 1953). Macroscopically, staling is characterized by a time-dependent firming of the crumb, flavor changes and loss of crispy crust. Microscopically, moisture migration and redistribution, recrystallization of starch components and changes in interactions between the protein and starch fractions may contribute to the global processes known as staling.

Bread formulations contain several ingredients, each of which may undergo changes during both the breadmaking process and the aging of the final product. Changes in crumbliness, water sorption capacity, crumb compressibility, amount of soluble starch, susceptibility to enzymes, X-ray diffraction patterns and thermal properties have all been measured and used as indices of staling, but as the rate at which these parameters changes is different as the product ages, no single parameter can give a complete description of the degree of staling as perceived by the consumer (Fearn and Russell 1982).

Bread can be viewed as a complex, unstable, elastic solid foam consisting of a continuous starch fraction interwoven by a continuous protein matrix among a discontinuous phase of entrapped and partially gelatinized, swollen starch granules (Hug-Iten and others 2003; Aguirre and others 2011). While the multicomponent and multiphase nature of bread should be considered when investigating quality changes in bread as a result of aging, the staling mechanism, when considered solely as a crumb firming process, is generally considered to be primarily a result of the recrystallization or retrogradation of the amylopectin component of the starch present in the bread product.

Bread staling is unquestionably a complex process, even when just considering changes as a result of amylopectin recrystallization. Many factors affect amylopectin recrystallization, and consequently, staling and the rate of staling, including formulation, processing conditions, and storage temperature and conditions. As a recrystallization process, staling would only be expected to occur for products in the rubbery state and not those in the glassy state where molecular immobility may inhibit the interactions necessary to promote a crystallization process. However, the texture of low moisture baked food products such as crackers, biscuits and breakfast cereals have been shown to be dependent on many of the same factors that influence bread staling. The intent of this review is to provide a cursory overview of the factors that promote staling, particularly as it relates to the starch and amylopectin contributions to staling

41

with the aim of understanding how the staling phenomenon might be extended to low moisture systems.

2.3.2 Crust staling

Bread staling can fall into two categories: crust staling and crumb staling. When bread is freshly baked, the crust is dry and crispy due to its lower moisture content than the crumb. As reported by Kulp and Ponte (1981), typical fresh white pan bread contains, on average, 38% moisture, but the crumb moisture content may be as high as 45% while the crust portion may be as low as 12% moisture. As moisture migrates from the interior of the loaf to the crust to equilibrate moisture content, the crust becomes soft and leathery with a loss of crust crispness while both the moisture content and water activity of the crumb decreases (Aguirre and others 2011; Baik and Chinachoti 2000; Piazza and Masi 1995).

This moisture redistribution could affect the localized water activity and the localized amylopectin recrystallization kinetics (Czuchajowska and Pomeranz 1989). Differential scanning calorimetry (DSC) and x-ray diffraction detected an increase in crystallinity due to amylopectin retrogradtion in bread crust stored for 20 days in a closed box, but amylopectin retrogradation was not evidenced after 1 day of storage and was barely detectable by 2 days of storage (Primo-Martin and others 2007). Thus, amylopectin retrogradation, which is the main process responsible for the staling of bread crumb, cannot be responsible for crispness deterioration of the crust as the loss of bread crust crispness proceeds over shorter times than the time frame under which amylopectin retrogradation in the crust was observed.

Rather, textural changes associated with crust staling is generally attributed to a transition from the glassy to rubbery state as a result of the change in moisture content (Bhatt and Nagaraju 2009; Lin and Lineback 1990). The glass transition changes the physical properties of the crust, for example, a transition from the glassy to rubbery state results in an increase in entropy and heat capacity and a decrease in rigidity and viscosity (Roudaut and others 2004). Zeleznak and Hoseney (1986) observed an increase in the glass transition temperature of crystalline starch compared to amorphous starch at the same water content; thus, the extent of starch crystallinity after baking will influence the kinetics of crust staling and with that the loss of crust crispness.

Ironically, crust staling is promoted by packaging of bread in moisture-proof packaging which do not allow for moisture to migrate from the crumb to the crust and then to the

42

atmosphere. Even for specialty breads which may not be packaged in moisture-proof packaging, high atmospheric humidity may also promote staling (Maga and Ponte 1975). However, those measures which may slow crust staling may also promote crumb staling. However, bread crumb firmness has been found to increase for those samples stored with and without crust. Thus, keeping crumb moisture content constant by storing bread without crust does not necessarily prevent firming or staling of the bread, and in most instances, crust staling is tolerated at the expense of maintaining crumb freshness (Baik and Chinachoti 2000).

2.3.3 Role of starch and amylopectin in bread staling

The retrogradation of starch polymers was first proposed as a mechanism for staling based on evidence of the similarity in x-ray diffraction patterns between fresh bread and freshly gelatinized wheat starch as well as between stale bread and retrograded starch (Gray and Bemiller 2003). When starch granules are gelatinized, a portion of the amylose may diffuse into the interstitial environment, concentrate, and quickly undergo retrogradation upon cooling. Thus, even if amylose leaches from the starch granules during the baking process, by the time the bread has completely cooled, any interstitial amylose will have retrograded and become insoluble, and therefore, unlikely to play a role in any future staling events (Kim and Dappolonia 1977c; Kim and Dappolonia 1977a; Kim and Dappolonia 1977b). Starch is a 2-component polymer, composed of amylose and amylopectin, and if changes in starch structure is at least partly responsible for the staling phenomenon, then the amylopectin fraction must be the responsible party.

Wheat flour, the primary component of bread, contains approximately 84 to 88% (db) starch. During baking, the starch gelatinizes, leading to the formation of a continuous starch network. As a consequence of gelatinization, amylopectin crystallites are melted, leading to amylopectin in the amorphous plasticized state in the fresh bread crumb and phase separation of the amylopectin and amylose components (Hug-Iten and others 1999). The amylopectin is located primarily inside the starch granule, though some amylopectin side chains may protrude into the intergranular space, as well as into the amylose-rich granule center. Reorganization of the amylopectin results in reformation of its double helical structures which can repack into crystallites upon aging. This reorganization imparts rigidity to both the swollen granule and the intergranular material by acting as physical crosslinks in the overall gel structure. As a network,

the influence of even very low levels of crystallinity is magnified in their effect on crumb firmness (Hug-Iten and others 2003; Ribotta and others 2004). For example, Ribotta and Le Bail (2007) witnessed changes in the thermo-mechanical profile of aged bread crumb by dynamic mechanical analysis (DMA), and it was showed that a greater amount of retrograded starch affected significantly the contraction capacity of bread crumb.

Regardless of the initial crystalline pattern of the starch (i.e., A-type, B-type, C-type), under most conditions, recrystallization of amylopectin results in a supermolecular structure containing B-type crystalline regions with incorporation of water molecules into the crystal lattice during formation of the B-type polymorph (Mihhalevski and others 2012; Imberty and others 1988). Thus, a redistribution of moisture occurs, and this process has been demonstrated by a progressive decrease in the percentage of "freezable" water as bread was stored over 11 days (Slade and Levine 1991). The water molecules that are part of the crystal lattice are not available for plasticization, so the result is the perceived drier, firmer texture characteristic of stale bread. Furthermore, Mihhalevski and others (2012) demonstrated that the starch in rye sourdough bread crystallized in different polymorphs than in wheat bread, leading to different proportions of water incorporation into the crystal lattice during staling, and consequently, a slower rate of staling for rye bread compared to wheat bread.

In fact, a decrease in water mobility during staling of starch-based foods has been well documented, primarily through NMR techniques, by Wynne-Jones and Blanshard (1986), Kimshin and others (1991), and Chen and others (1997). The decrease in water mobility has been attributed to one or more of the following reasons: (1) some water molecules were initially at more mobile states, and were subsequently locally incorporated into the starch matrix upon staling; or (2) water molecules initially associated with the amorphous regions of amylopectin may be trapped inside the partially crystalline structure of the retrograding starch; or (3) water migration between starch and gluten molecules and hence reassociation of water with these molecules may result in a change in the mobility of water molecules, or (4) loss of moisture from crumb to crust as previously discussed (Chen and others 1997).

2.3.4 Staling kinetics as related to amylopectin recrystallization

Most of the proposed models used to predict the kinetics of bread staling, as it relates to amylopectin recrystallization, are based on the Avrami equation, originally derived to describe

polymer crystallization from melt (Avrami 1939; Avrami 1940; Avrami 1941). The Avrami equation can be represented as

$$Y = 1 - e^{-Kt^n} \qquad \text{Equation 2.2}$$

Which can be rewritten as

$$\ln \ln \left(\frac{1}{1-Y} \right) = \ln K + n \ln(t) \qquad \text{Equation 2.3}$$

Where Y is the extent of transformation or crystallization, K is the rate constant, n is the Avrami exponent and t is time.

Thus, the extent of transformation or crystallization followed over time, would be expected to follow an "S" shaped curve such that when integrated, a plot of $\ln \ln \left(\frac{1}{1-Y} \right)$ versus time should yield a straight line with slope of n and y-intercept of ln K.

As can be seen by Equation 2 and Equation 3, the Avrami equation contains two parameters: the rate constant and the Avrami exponent. The rate constant depends on the crystals growth constant and on the crystals nucleation constant, while the Avrami exponent depends on the type of crystal nucleation and the dimensions in which the growth takes place (Del Nobile and others 2003).

Amylopectin recrystallization can occur via nucleation and growth of new crystals or via growth of starch crystals already present in the bread, though this latter scenario is typically neglected when applying the Avrami equation to amylopectin retrogradation (Del Nobile and others 2003). Thus, the Avrami exponent depends on the type of crystal nucleation, sporadic or instantaneous, and the dimensions in which the growth takes places, implying that the Avrami exponent can assume an integer value ranging from 4 to 1 dimension. In three dimension, spherulitic crystals are formed, whereas disc-like crystals form in two dimension and rod-like crystals form in one dimension (Del Nobile and others 2003).

Using Avrami kinetics, the Avrami exponent has previously been determined to be n = 1 for both gelatinized starch (McIver and others 1968) and for bread (Kim and Dappolonia 1977c; Kim and Dappolonia 1977a), implying rod-like growth and instantaneous nucleation. Morgan (1954) noted that the nucleation sites probably corresponded to the regions of chain entanglement formed during gelation with crystallization then proceeding between two adjacent chains to re-form double helices. Good fit to the data for the staling of bread by constraining the

Avrami exponent to 1 has also been found by Fearn and Russell (1982), Russell (1983a) and Wilson and others (1991), though in these studies, the best data fit, though not significantly better, was found for integer values less than one.

Seow and Teo (1996) have also found Avrami exponents of less than one for corn starch gels, bread and rice cupcakes though Avrami exponents less than one have no physical meaning. However, non-integral Avrami exponents may arise if two separate processes, which may individually have Avrami exponents of 1, occur simultaneously. For examples, the kinetics of bread staling has previously been described in terms of two parallel first-order processes, one occurring within the first 24 hours after baking, and one observed for all later changes occurring during storage (Willhoft 1971a; Willhoft 1971b). It was suggested that certain changes were a result of the starch fraction while changes occurring from the gluten fraction in the bread loaf were superimposed on the starch fraction.

One of the implicit assumptions in applying the Avrami equation to the kinetics of bread staling, is that any enthalpy changes occurring during staling are a direct measure of the quantity of recrystallized starch produced. If the degree of order of the starch (i.e. amorphous, complete recrystallization or partial recrystallization) is different depending upon when the recrystallization occurs during staling, then varying changes in both enthalpy and entropy may account for a given decrease in free energy resulting in Avrami exponents less than one (Fearn and Russell 1982).

Even though breads tend to firm to the same ultimate firmness value regardless of storage temperature, the rate at which that ultimate firmness value is obtained is dependent on storage temperature and moisture content (Kulp and Ponte 1981).The rate constants of bread staling as well as the aging of starch gels tend to increase as the storage temperature is decreased, which is characteristic of crystallization processes (Fearn and Russell 1982). Recrystallization of starch occurs between the glass transition temperature and the melting temperature of the amylopectin as nucleation is fastest around the glass transition and crystal propagation is fastest around the melting temperature. Thus, bread staling has been found to be fastest around refrigeration conditions of 0 to 4°C (Aguirre and others 2011; Slade and Levine 1991).

Similar to starch retrogradation, bread staling has also been found to be optimum near 50% moisture content, with the rate increasing in the range of 27 to 50% moisture content due to an increasingly effective mobility of the starch chains while decreasing above 50% due to the

dilution factor (Le-Bail and others 2011). Furthermore, (Del Nobile and others 2003) proposed that starch crystal growth rate remains substantially unchanged while nucleation rate increases with reducing moisture content or reducing water activity. Thus, decreasing the water activity from 1 to 0.877 resulted in an increase in staling associated with the increased degree of undercooling.

2.3.5 Staling and the glass transition

Staling is generally considered to be a phenomenon that occurs above the glass transition of the food material, though the glass transition is not necessarily a static value. Slade and Levine (1991) described an increase in the Tg of bread during staling as a result of annealing and networking of amorphous chains in the starch. If stored long enough, the amorphous network was described as maturing, leading to an increase in Tg, as was observed by Hallberg and Chinachoti (1992) in bread during long-term storage. An increase in Tg during the staling of bread was also correlated with firming as measured by Instron, attributed to an increase in crosslink density in the starch granules due to formation of crystallites. It could then be used to calculate the extent of staling in bread, knowing that in fresh bread the Tg is at subzero temperature, but Tg increases to room temperature as a low level of starch network is reformed, and Tg then continues to increase to well above room temperature as the network matures and the bread becomes completely stale (Jagannath and others 1999).

However, the molecular mobility in low-moisture (<9% wet basis) white bread was studied as a function of temperature using pulsed-proton nuclear magnetic resonance (NMR), and dielectric and dynamic mechanical spectroscopies, finding that the water was mobile, even in glassy samples (Roudaut and others 1999a; Roudaut and others 1999b). These results were interpreted and extrapolated to suggest that the Tg is not a universal predictive parameter for the physical stability of glassy or rubbery food. Indeed, because bread firming, measured as a change in its dielectric properties, was observed at −53°C, located far below the reported Tg for both dry gelatinized starch and white bread, it was assumed that the relaxation observed corresponded to more localized motions, possibly associated with the local motion of a side group or short segment of the main chain. For example, in phenylene polymers, the low activation value (near zero) of the beta relaxations reflects limited cooperativity, which reflects the number of atoms involved in the movement of the relaxing unit (Starkweather and Avakian 1989). Furthermore,

several cereal-based products have exhibited changes in both mechanical properties and texture associated with a loss of crispness, even when still in the glassy state (Attenburrow and others 1992; Li and others 1998; Nicholls and others 1995; Roudaut and others 1999a; Roudaut and others 1999b; Roudaut and others 2004), again implying that staling cannot be solely characterized by changes in Tg.

2.3.6 Other potential mechanisms of staling

If changes in starch and amylopectin structure and subsequent changes in its glass transition do not solely describe changes encountered during staling, then other potential explanations and mechanisms need to be examined, particularly owing to the complex nature of food systems like bread. For example, Magnetic Resonance Imaging (MRI) revealed a spatial distribution of water in bread during storage in which, as storage time increased, the less mobile water fraction decreased whereas the mobility of the more mobile fraction increased, suggesting a relationship between water mobility and staling (Ruan and others 1996). In fact, bread stored in hermetically sealed pouches to prevent moisture loss (Hallberg and Chinachoti 2002) or breads produced with a higher initial moisture content (He and Hoseney 1990) or breads with added hydrocolloids (Davidou and others 1996) were found to have a slower firming rate and lower equilibrium firmness, indicating that bread firming can be strongly influenced by factors other than amylopectin recrystallization. Schiraldi, Piazza and Riva (1996) described this phenomenon as an interchain zipper in which the water molecules are displaced along the polymer chains acting as the slides on the zipper. The consequent direct interchain crosslinks would allow formation of a network that would justify the increasing firmness of the crumb and would also sustain the growth of amylopectin crystals.

However, the redistribution of moisture occurring during staling may not be just associated with the starch fraction but may also be associated with other components in the bread system, such as interactions between the starch and protein fractions. In fact, according to Willhoft (1971b), the natural ratio of starch to gluten (6:1) in bread crumb ensures that moisture transfer to the starch would result in firming of the continuous gluten phase, and in a model system starting from a typical baker's dough, Willhoft (1971a) estimated that up to 30 % of the moisture associated with the gluten fraction migrated to the starch during 120 hours of storage of the baked system at 25°C with the rate of migration decreasing approximately exponentially with

time. Since the gluten formed the continuous matrix of the crumb, drying out of the gluten fraction resulted in crumb firming. Dragsdorf and Varriano-Marston (1980) expanded on this conclusion to note that if starch crystallization did occur completely, little space would be available in the crystal structure for transfer of water from the gluten, thus preserving the flexibility of the gluten fraction and thereby reducing bread firming during storage.

Martin, Zeleznak and Hoseney (1991) proposed a model for bread staling as a result of starch/gluten interactions in which bread is represented by a continuous network of gluten interrupted by a discontinuous phase consisting of starch granule remnants and partially leached amylose. During baking, interactions (cross-links) occur between gluten and starch that then increase in strength and number during staling. Furthermore, during baking, monoglycerides and shortening may interact with starch granules, reducing granule swelling and thereby granule surface area, which in turn, leads to fewer or weaker interactions with gluten and reduced firming. Using NMR techniques, expanded on the role of starch swelling in starch/gluten interactions in bread by observing that the presence of gluten itself decreased starch swelling during baking, presumably since less water is available to the starch in the presence of gluten (Wang and others 2004). Thus, moisture redistribution between gluten and starch during storage could result in crumb firming.

2.3.7 Factors affecting the rate of staling

Several classes of ingredients have been used in cereal foods to improve quality, such as hydrocolloids, surfactants and enzymes. Hydrocolloids such as xanthan and locust bean gum, among others, are known to retard retrogradation, perhaps through an increase or stabilization of water content, or perhaps by inhibiting starch-gluten interactions or the development of macromolecular entanglement (Davidou and others 1996). Similarly, dextrins, whether added as an ingredient in the breadmaking, or produced by the action of added enzymes such as those in malted barley flour or pullulanase, have been shown to slow staling (Gerrard and others 1997; Jagannath and others 1998; Martin and Hoseney 1991). Jagarnnath et al. (1998) described the antistaling effect as being related to the miscibility (or lack thereof) of polymers by noting that maltodextrin had the most effect on reducing staling, most likely due to its good solubility and compatibility with starch and gluten polymers, whereas gelatin had less of an effect, since it was primarily only compatible with gluten. On the other hand, Martin and Hoseney (1991) contended

that maltodextrins of a certain size class reduced firming by interfering with the hydrogen-bonded crosslinks between the protein fibrils and the starch remnants. This conclusion was supported by the fact that bread can be refreshened with mild heating owing to the heat-liable nature of hydrogen bonds and the effect of heat on polymer entanglements.

Addition of surfactants to bread has also been well established to affect bread staling, though the mode of action has been debated. Surfactants are generally considered as surface active lipids and are well-known to form insoluble helical complexes with amylose, but that does not necessarily mean that amylose complexation is responsible for the decrease in staling (Gray and Bemiller 2003; Kulp and Ponte 1981). Rather, surfactants such as sodium stearyl lactylate (SSL), glycerol monostearate (GMS) and mono- and diglycerides, may adsorb to the starch granule surface, preventing moisture migration from the gluten to the starch fraction (Pisesookbunterng and Dappolonia 1983; Pisesookbunterng and others 1983; Xu and others 1992). Alternatively, the role of surfactants may be to function as a plasticizer and lower the amount of crosslinks in retrograded starch (Jagannath and others 1998) or lower the Tg such that the structure is not in the glassy state at room temperature (Gray and Bemiller 2003).

As previously discussed, dextrins, possibly produced by enzyme action on bread, may retard staling, but it has been suggested that, although dextrins can be correlated with antistaling, they do not directly inhibit the staling process, but may merely reflect the extent of starch modification (Duedahl-Olesen and others 1999; Gerrard and others 1997). Alternatively, enzymes may act to cleave the hydrogen bonds involved in the crosslinks formed between the starch and gluten, as postulated by Martin and Hoseney (1991). Yet still, Hug-Iten et al (2001) concluded that the antistaling effect of a maltogenic α-amylase was due to its ability to produce a partially degraded amylopectin that was less prone to crystallize as well as its ability to produce partially degraded amylose that was then responsible for rapid formation of a partially crystalline polymer network that later resisted rearrangements. For instance, an enzyme may reduce the connectivity between crystallites in the continuous starch phase, or, in contrast, an enzyme may induce the fast formation of a starch network and, by this, contribute to kinetic texture stabilization (Hug-Iten and others 2003). The debate over the mode of action of enzymes on their antistaling properties just underscores the complexity of the staling phenomenon itself.

2.3.8 Summary and conclusions

Bread staling is unquestionably a complex process, and as such, many mechanisms have been proposed to account for this universally observed phenomenon. Bread crust staling is generally considered to be the result of moisture redistribution from crumb to crust, whereas bread crumb staling is primarily attributed to amylopectin recrystallization post baking. As such, the Avrami equation, which was developed to model the kinetics of polymer crystallization, is often applied when describing the rate of bread staling. However, solely as a recrystallization process, staling would only be expected to occur for products in the rubbery state and not those in the glassy state, where molecular immobility may inhibit the interactions necessary to promote a crystallization process. However, the texture of low moisture baked food products, such as crackers, biscuits and breakfast cereals, have been shown to be dependent on many of the same factors that influence bread staling, and it has been suggested that staling corresponds with an increase in the glass transition. However, changes in the glass transition are not sufficient to fully explain the staling phenomenon in these systems and other mechanisms need to be explored, such as moisture redistribution within the components of the bread crumb or complex interactions between the starch and gluten fractions. The complexity continues when considering other factors that affect the staling rate, such as hydrocolloids, surfactants and enzymes, and their mechanistic action, whether on the starch fraction, the gluten fraction, or both. Thus, while amylopectin recrystallization can be used when simplistically describing changes associated with staling of bread, and perhaps other low moisture cereal-based food products, the entire system should be considered in relation to how all of the components interact individually and in their combined presence.

2.4 Tables

Table 2.1. Literature accounts of the sub-Tg endotherm and the proposed origin

System	Peak temperature (approximate), °C	Moisture content or RH (approximate), %	Suggested Origin	Reasoning	Comments	Reference
Agar, Alginate, Dextran, Guar gum, Konjac gum, Locust bean gum, Pectin, Pullulan, Pregelatinzed waxy starch, Xanthan	50 to 80 (depending on system)	Relative humidities of 10, 33, 57, 75, and 86%	Water-carbohydrate interactions	1) Peak observed for samples that do not experience a glass transition	1) Peak not evident on immediate rescan 2) Peak slowly recovered after room temperature storage 3) ΔH increased with increasing moisture content	Appelqvist et al., 1993
Gelatin	62 to 70	7 to14 (wet basis)	Enthalpy relaxation	1) System was below Tg	1) Tg and melting endotherms shifted to lower temperatrues at higher moisture 2) Relaxation endotherm was most pronounced at higher moisture 3) Peak became more pronounced as aging time increased	Badii et al., 2005
Syndiotactic polystyrene	70 to 95	Not given	Enthalpy relaxation	1) Assumptions based on referenced studies		Beckman et al., 1997

Table 2.1 Continued

System	Peak temperature (approximate), °C	Moisture content or RH (approximate), %	Suggested Origin	Reasoning	Comments	Reference
Rice starch, native and gelatinized	46.0°C at 15% moisture	8 to 18% for low moisture, 40 to 60% for high moisture	Enthalpy relaxation	1) Peak did not occur at moisture content >20% 2) Peak temperature showed no dependency with moisture	1) Peak occurred regardless of gelatinizion at moisture <20% 2) At moisture >12%, peak was superimposed with Tg peak 3) At moisture >12%, sub-Tg endotherm peak independent of Tg peak	Chung, Lee and Lim, 2002
Rice starch (normal and waxy, pregelatinized and granular)	55 to 65	14.5	Enthalpy relaxation	1) Relaxation enthalpy increased with aging time until equilibrium reached 2) Peak temperature of relaxation enthalpy peak linearly increased with logarithm of aging time		Chung, Chang and Lim, 2004; Chung and Lim, 2004;
Native and cross-linked (STPP) corn starch	35 to 55	15%, 67%	Enthalpy relaxation		1) Cross-linking resulted in greater extent of relaxation. Presumably, large phosphate groups increased free volume, allowing for more mobility 2) Similar trend experienced with Tg	Chung, Woo and Lim, 2004

Table 2.1 Continued

System	Peak temperature (approximate), °C	Moisture content or RH (approximate), %	Suggested Origin	Reasoning	Comments	Reference
Normal corn starch (pregelatinized)	57 to 62	13.5	Enthalpy relaxation	1) Starch sample had dual Tg's (57.3 and 73.4°C), which could suggest presence of two structurally different amorphous regions	1) Upper Tg increased as aging time increased (lower Tg overlapped relaxation peak) 2) Relaxation enthalpy increased with aging time, while the rate of change decreased	Chung, Yoo and Lim, 2005
Waxy corn starch (gelatinized and freeze-dried)	60	24	Retrogradation	1) Assumption based on data from MDSC, DSC, DMA, X-ray diffraction and Raman spectroscopy 2) Sample between Tg and Tm, the range in which recrystallization can take place		DeMeuter et al., 1999
Maltodextrin (21 DE), spray-dried	40 to 60	11, 23, 33, 43 and 53% relative humidities	Enthalpy relaxation	1) Peak occurs below Tg		Descamps et al., 2009

Table 2.1 Continued

System	Peak temperature (approximate), °C	Moisture content or RH (approximate), %	Suggested Origin	Reasoning	Comments	Reference
Corn flakes with different degrees of starch fragmentation	55 to 60	2 to 4	Enthalpy relaxation	1) Peak independent of aging time and moisture content 2) ΔH increased as moisture content and aging time increased	1) Increasing starch fragmentation required longer aging time before peak detected and had greater rate of increase in enthalpy	Gonzalez et al., 2010
Wheat starch	40 to 70	25 to 80	Retrogradation	1) Storage at 4 to 32°C for up to 4 weeks	1) Retrogradation endotherm temperature increased as storage temperature increased 2) ΔH higher at lower temperatures	Jang and Pyun, 1997
Waxy maize starch	50	10 to 22	Unknown	1) Peak first thought to be lipid melting, but starch contains very little lipid (0.14%) and peak size was proportional to water content (opposite of expected for lipid melting)	1) Peak not seen on rescan, but was seen again after storage	Kalichevsky et al., 1992

Table 2.1 Continued

System	Peak temperature (approximate), °C	Moisture content or RH (approximate), %	Suggested Origin	Reasoning	Comments	Reference
Maltodextrin (DE 6, 12, 21 and 33)	60 to 80	11, 22, 33, 43, 54 and 75% relative humidity	Water-carbohydrate interactions	1) Using thermodyanic clustering models, proposed a mechanism by which water dynamically disrupts hydrogen bonding between carbohydrate chains, leading to an expansion at the nanolevel, increasing the degrees of freedom of the carbohydrate chains. This uptake of water leads to increase rates of relaxations and greater mobility.		Kilburn et al., 2005

Table 2.1 Continued

System	Peak temperature (approximate), °C	Moisture content or RH (approximate), %	Suggested Origin	Reasoning	Comments	Reference
Ball-milled potato starch (amorphous)	60	16	Enthalpy relaxation	2) Peak increased as storage time increased 3) Cannot be a melting peak as sample was shown to be entirely amorphous by X-ray diffraction	1) Starch was not gelatinized, though crystallinity was lost	Kim et al., 2001
Cornflakes	50 to 66	2 to 8 (dry basis)	Unknown			Li, 2010
Waxy cornstarch	50 to 65	52	Retrogradation	1) Starch was gelatinized 2) Starch was above Tg		Liu et al., 2010b

Table 2.1 Continued

System	Peak temperature (approximate), °C	Moisture content or RH (approximate), %	Suggested Origin	Reasoning	Comments	Reference
Confectionary wafers (wheat-based)	60	Not given; Typical moisture content of wafers	Enthalpy relaxation	1) Peak not due to retrogradation since wafer was below Tg 2) When DSC profile for different scan rates was extrapolated to the intersection at the x-axis, the intersection occurred at ~0 (i.e. zero scan rate), no peak was observed, which implies that for a sufficiently slow heating rate, the sample has sufficient time to relax to its equilibrium position	1) X-ray diffraction indicated that the endothermic peak correspnded with a pattern characteristic of a 6-fold helical strcuture	Livings et al., 1997
Maltose monohydrate and sorbitol plasticized potato starch	45	5	Enthalpy relaxation	1) Volume change was linear with log time	1) Used Tool-Narayanaswamy equation to describe the observed calorimetric behavior during aging	Lourdin et al., 2002

Table 2.1 Continued

System	Peak temperature (approximate), °C	Moisture content or RH (approximate), %	Suggested Origin	Reasoning	Comments	Reference
Normal cornstarch, gelatinized and dried	36 to 52	10 to 50	Enthalpy relaxation	1) Peak only occurred in samples having less than 20% moisture 2) Enthalpy and peak temperature correlated with log time		Shogren, 1992
Potato starch (ungelatinized)	50	16	Enthalpy relaxation	1) Starch below Tg		Steeneken and Woortman, 2009
Semicrystalline polymers (synthetic)	Varies	Varies	Enthalpy relaxation	1) Samples subjected to high temperature and then quenched and aged	1) Peak occurs above and below conventional glass transition	Struik, 1987
Native and amorphous potato starch	22 to 57	16	Enthalpy relaxation	1) Absence of peak at storage temperatures far below Tg 2) Increase in peak size and temperature as aging temperature increased		Thiewes and Steeneken, 1997

Table 2.1 Continued

System	Peak temperature (approximate), °C	Moisture content or RH (approximate), %	Suggested Origin	Reasoning	Comments	Reference
Amorphous waxy starch, β-limit dextrin, amylopectin triacetate	50	5 to 25	Water-carbohydrate interactions	1) Peak appears for β-limit dextrin, which has reduced tendency to from double helices 2) Peak disappears for complete acetylation of waxy starch; suggests that hydroxyl groups play a role 3) ΔH increases as moisture content increases	1) Enthalpy of peak higher for β-limit dextrin than waxy starch; suggests that reduced chain length of amylopectin may enhance the formation	Yuan and Thompson, 1994

Table 2.2. Summary of arguments for and against proposed mechanisms for the origin of the sub-Tg endotherm

Origin	Supporting arguments	Opposing arguments
Melting of water-carbohydrate interactions	1) Endothermic peak found to occur for materials that do not exhibit a glass transition 2) Material softening, as measured by DMTA, was independent of frequency, which is more characteristic of melting rather than a relaxation process 3) Complete acetylation of starch resulted in disappearance of the peak 4) Peak size increases as moisture content, temperature or aging time increase 5) Peak temperature is independent of moisture content	1) Peak occurs above conventional Tg 2) Melting, particularly under low moisture conditions, typically occurs at much higher temerpatures
Physical aging (also referred to as enthalpy relaxation)	1) Common phenomenom of amorphous and semicrystalline polymers 2) Peak formation correlates with aging time 3) As DSC scan rate approaches zero, the peak disappears since the material has sufficient time to reach its equilibrium state 4) Peak correlated with double helical formation/reordering in starch 5) Peak size increases as moisture, temperature or aging time increases	1) Peak occurs above conventional Tg

2.5 References

Aguirre JF, Osella CA, Carrara CR, Sanchez HD, Buera MDP. 2011. Effect of storage temperature on starch retrogradation of bread staling. Starch/Staerke 63(9):587-93.

Appelqvist IAM, Cooke D, Gidley MJ, Lane SJ. 1993. Thermal-properties of polysaccharides at low moisture .1. An endothermic melting process and water-carbohydrate interactions. Carbohydr. Polym. 20(4):291-9.

Attenburrow GE, Davies AP, Goodband RM, Ingman SJ. 1992. The fracture behaviour of starch and gluten in the glassy state. J. Cereal Sci. 16(1):1-12.

Atwell WA, Hood LF, Lineback DR, Varriano-Marston E, Zobel HF. 1988. The terminology and methodology associated with basic starch phenomena. Cereal Foods World 33:306-11.

Avrami M. 1939. Kinetics of phase change. 1 General theory. Journal of Chemical Physics 7(12):1103-12.

Avrami M. 1940. Kinetics of phase change. II Transformation time relations for random distirbution of nuclei. Journal of Chemical Physics 8(2):212-24.

Avrami M. 1941. Granulation, phase change, and microstructure kinetics of phase change. III. Journal of Chemical Physics 9(2):177-84.

Badii F, MacNaughtan W, Farhat IA. 2005. Enthalpy relaxation of gelatin in the glassy state. Int. J. Biol. Macromol. 36(4):263-9.

Baik MY, Chinachoti P. 2000. Moisture redistribution and phase transitions during bread staling. Cereal Chem. 77(4):484-8.

Bechtel WG, Meisner DF, Bradley WB. 1953. The effect of crust on the staling of bread. Cereal Chem. 30:160-8.

Beckmann J, McKenna GB, Landes BG, Bank DH, Bubeck RA. 1997. Physical aging kinetics of syndiotactic polystyrene as determined from creep behavior. Polym. Eng. Sci. 37(9):1459-68.

Bhatt CM, Nagaraju J. 2009. Studies on glass transition and starch re-crystallization in wheat bread during staling using electrical impedance spectroscopy. Innov. Food Sci. Emerg. Technol. 10(2):241-5.

Biliaderis CG, Prokopowich DJ, Jacobson MR, BeMiller JN. 1996. Effect of n-alkyl glucosides on waxy maize and wheat starch retrogradation. Carbohydr. Res. 280(1):157-69.

Biliaderis CG, Zawistowski J. 1990. Viscoelastic behavior of aging starch gels - effects of
concentration, temperature, and starch hydrolysates on network properties Cereal Chem.
67(3):240-6.

Bulkin BJ, Kwak Y, Dea ICM. 1987. Retrogradation kinetics of waxy-corn and potato starches;
A rapid, Raman-spectroscopic study. Carbohydr. Res. 160:95-112.

Cairns P, I'Anson KJ, Morris VJ. 1991. The effect of added sugars on the retrogradation of wheat
starch gels by X-ray diffraction. Food Hydrocolloids 5(1-2):151-3.

Cameron RE, Donald AM. 1993. A small-angle X-ray scattering study of starch gelatinization in
excess and limiting water. Journal of Polymer Science, B. Polymer Physics 31:1197-203.

Chang SM, Liu LC. 1991. Retrogradation of rice starches studied by differential scanning
calorimetry and influence of sugars, NaCl and lipids. J. Food Sci. 56(2):564-&.

Chang YH, Lin JH. 2007. Effects of molecular size and structure of amylopectin on the
retrogradation thermal properties of waxy rice and waxy cornstarches. Food
Hydrocolloids 21(4):645-53.

Chen PL, Long Z, Ruan R, Labuza TP. 1997. Nuclear magnetic resonance studies of water
mobility in bread during storage. Lebensmittel-Wissenschaft und -Technologie
30(2):178-83.

Chung HJ, Chang HI, Lim ST. 2004a. Physical aging of glassy normal and waxy rice starches:
Effect of crystallinity on glass transition and enthalpy relaxation. Carbohydr. Polym.
58(2):101-7.

Chung HJ, Lee EJ, Lim ST. 2002. Comparison in glass transition and enthalpy relaxation
between native and gelatinized rice starches. Carbohydr. Polym. 48(3):287-98.

Chung HJ, Lim ST. 2004. Physical aging of glassy normal and waxy rice starches: thermal and
mechanical characterization. Carbohydr. Polym. 57(1):15-21.

Chung HJ, Woo KS, Lim ST. 2004b. Glass transition and enthalpy relaxation of cross-linked
corn starches. Carbohydr. Polym. 55(1):9-15.

Chung HJ, Yoo B, Lim ST. 2005. Effects of physical aging on thermal and mechanical a
properties of glassy normal corn starch. Starch-Starke 57(8):354-62.

Chung JH, Han JA, Yoo B, Seib PA, Lim ST. 2008. Effects of molecular size and chain profile
of waxy cereal amylopectins on paste rheology during retrogradation. Carbohydr. Polym.
71(3):365-71.

Cooke D, Gidley MJ. 1992. Loss of crystalline and molecular order during starch gelatinization: origin of the enthalpic transition. Carbohydr. Res. 227:103-12.

Czuchajowska Z, Pomeranz Y. 1989. Differential scanning calorimetry, water activity, and moisture contents in crumb center and near-crust zones of bread during storage. Cereal Chem. 66:305-9.

Davidou S, LeMeste M, Debever E, Bekaert D. 1996. A contribution to the study of staling of white bread: Effect of water and hydrocolloid. Food Hydrocolloids 10(4):375-83.

De Meuter P, Amelrijckx J, Rahier H, Van Mele B. 1999. Isothermal crystallization of concentrated amorphous starch systems measured by modulated differential scanning calorimetry. J. Polym. Sci. Pt. B-Polym. Phys. 37(20):2881-92.

Del Nobile MA, Martoriello T, Mocci G, La Notte E. 2003. Modeling the starch retrogradation kinetic of durum wheat bread. J. Food Eng. 59(2-3):123-8.

Descamps N, Palzer S, Zuercher U. 2009. The amorphous state of spray-dried maltodextrin: sub-sub-T-g enthalpy relaxation and impact of temperature and water annealing. Carbohydr. Res. 344(1):85-90.

Donovan JW. 1979. Phase transitions of the starch-water system. Biopolymers 18:263-75.

Doublier JL, Choplin L. 1989. A rheological description of amylose gelation. Carbohydr. Res. 193:215-26.

Dragsdorf RD, Varriano-Marston E. 1980. Bread staling: X-ray diffraction studies on bread supplemented with alpha-amylases from different sources. Cereal Chem. 57(5):310-4.

Duedahl-Olesen L, Zimmermann W, Delcour JA. 1999. Effects of Low Molecular Weight Carbohydrates on Farinograph Characteristics and Staling Endotherms of Wheat Flour-Water Doughs. Cereal Chemistry Journal 76(2):227-30.

Durrani CM, Donald AM. 1995. Physical characterization of amylopectin gels. Polym. Gels Netw. 3(1):1-27.

Elfstrand L, Frigard T, Andersson R, Eliasson AC, Jonsson M, Reslow M, Wahlgren M. 2004. Recrystallisation behaviour of native and processed waxy maize starch in relation to the molecular characteristics. Carbohydr. Polym. 57(4):389-400.

Eliasson AC, Ljunger G. 1988. Interactions between amylopectin and lipid additives during retrogradation in a model system. Journal of the Science of Food and Agriculture: 44 (4) 353-361 44(4):353-61.

Farhat IA, Blanshard JMV, Descamps M, Mitchell JR. 2000a. Effect of sugars on retrogradation of waxy maize starch-sugar extrudates. Cereal Chem. 77(2):202-8.

Farhat IA, Blanshard JMV, Mitchell JR. 2000b. The retrogradation of waxy maize starch extrudates: Effects of storage temperature and water content. Biopolymers 53(5):411-22.

Fearn T, Russell PL. 1982. A kinetic study of bread staling by differential scanning calorimetry - the effect of loaf specific volume J. Sci. Food Agric. 33(6):537-48.

Fisher DK, Thompson DB. 1997. Retrogradation of maize starch after thermal treatment within and above the gelatinization temperature range. Cereal Chem. 74(3):344-51.

Fredriksson H, Silverio J, Andersson R, Eliasson AC, Aman P. 1998. The influence of amylose and amylopectin characteristics on gelatinization and retrogradation properties of different starches. Carbohydr. Polym. 35(3-4):119-34.

Gerrard JA, Every D, Sutton KH, Gilpin MJ. 1997. The role of maltodextrins in the staling of bread. J. Cereal Sci. 26(2):201-9.

Gidley MJ. 1987. Factors affecting the crystalline type (A-C) of native starches and model compounds: a rationalisation of observed effects in terms of polymorphic structures. Carbohydr. Res. 161:301-4.

Gidley MJ, Cooke D, Wardsmith S. 1993. Low moisture polysaccharide systems: Thermal and spectroscopic aspects. In: Blanshard JMV, Lillford PJ, editors. Glassy State in Foods. Loughborough: Nottingham University Press. p. 303-16.

Goldstein A, Nantanga KKM, Seetharaman K. 2010. Molecular interactions in starch-water systems: effect of increasing starch concentration. Cereal Chem. 87(4):370-5.

Gonzalez DC, Khalef N, Wright K, Okos MR, Hamaker BR, Campanella OH. 2010. Physical aging of processed fragmented biopolymers. J. Food Eng. 100(2):187-93.

Goodfellow BJ, Wilson RH. 1990. A Fourier-Transform IR studgy of the gelation of amylose and amylopectin Biopolymers 30(13-14):1183-9.

Gray JA, Bemiller JN. 2003. Bread staling: molecular basis and control. Comprehensive Reviews in Food Science and Food Safety 2.

Gudmundsson M. 1994. Retrogradation of starch and the role of its components Thermochim. Acta 246(2):329-41.

Gudmundsson M, Eliasson AC. 1990. Retrogradation of amylopectin and the effects of amylose and added surfactants/emulsifiers Carbohydr. Polym. 13(3):295-315.

Hallberg LM, Chinachoti P. 1992. Dynamic Mechanical Analysis for Glass Transitions in Long Shelf-Life Bread. Journal of Food Science 57(5):1201-29.

Hallberg LM, Chinachoti P. 2002. A fresh perspective on staling: The significance of starch recrystallization on the firming of bread. Journal of Food Science 67(3):1092-6.

He H, Hoseney RC. 1990. Changes in bread firmness and moisture during long-term storage Cereal Chem. 67(6):603-5.

Hibi Y. 2001. Effect of retrograded waxy corn starch on bread staling. Starch-Starke 53(5):227-34.

Hizukuri S. 1985. Relationship between the distribution of the chain length of amylopectin and the crystalline structure of starch granules. Carbohydr. Res. 141:295-306.

Hoover R. 1995. Starch retrogradation. Food Rev. Int. 11(2):331-46.

Hug-Iten S, Escher F, Conde-Petit B. 2001. Structural Properties of Starch in Bread and Bread Model Systems: Influence of an Antistaling α-Amylase. Cereal Chemistry Journal 78(4):421-8.

Hug-Iten S, Escher F, Conde-Petit B. 2003. Staling of bread: Role of amylose and amylopectin and influence of starch-degrading enzymes. Cereal Chem. 80(6):654-61.

Hug-Iten S, Handschin S, Conde-Petit B, Escher F. 1999. Changes in starch microstructure on baking and staling of wheat bread. Food Sci. Technol.-Lebensm.-Wiss. Technol. 32(5):255-60.

Hutchinson JM. 1995. Physical aging of polymers. Prog. Polym. Sci. 20(4):703-60.

Ianson KJ, Miles MJ, Morris VJ, Besford LS, Jarvis DA, Marsh RA. 1990. The effects of added sugars on the retrogradation of wheat-starch gels. J. Cereal Sci. 11(3):243-8.

Imberty A, Chanzy H, Perez S, Buléon A, Tran V. 1988. The double-helical nature of the crystalline part of A-starch. Journal of Molecular Biology 201:365-78.

Jacobson MR, BeMiller JN. 1998. Method for determining the rate and extent of accelerated starch retrogradation. Cereal Chem. 75(1):22-9.

Jacobson MR, Obanni M, Bemiller JN. 1997. Retrogradation of starches from different botanical sources. Cereal Chem. 74(5):511-8.

Jagannath JH, Jayaraman KS, Arya SS. 1999. Studies on glass transition temperature during staling of bread containing different monomeric and polymeric additives. J. Appl. Polym. Sci. 71(7):1147-52.

Jagannath JH, Jayaraman KS, Arya SS, Somashekar R. 1998. Differential scanning calorimetry and wide-angle X-ray scattering studies of bread staling. J. Appl. Polym. Sci. 67(9):1597-603.

Jane JL, Chen YY, Lee LF, McPherson AE, Wong KS, Radosavljevic M, Kasemsuwan T. 1999. Effects of amylopectin branch chain length and amylose content on the gelatinization and pasting properties of starch. Cereal Chem. 76(5):629-37.

Jane JL, Robyt JF, Huang DH. 1985. 13C-NMR study of the conformation of helical complexes of amylopectin and of amylose in solution. Carbohydr. Res. 140:21-35.

Jang JK, Pyun YR. 1997. Effect of moisture level on the crystallinity of wheat starch aged at different temperatures. Starch-Starke 49(7-8):272-7.

Jenkins PJ, Donald AM. 1998. Gelatinization of starch: a combined SAXS/WAXS/DSC and SANS study. Carbohydr. Res. 308:133-47.

Jouppila K, Kansikas J, Roos YH. 1998. Factors affecting crystallization and crystallization kinetics in amorphous corn starch. Carbohydr. Polym. 36(2-3):143-9.

Jouppila K, Roos YH. 1997. The physical state of amorphous corn starch and its impact on crystallization. Carbohydr. Polym. 32(2):95-104.

Kalichevsky MT, Jaroszkiewicz EM, Ablett S, Blanshard JMV, Lillford PJ. 1992. The glass-transition of amylopectin measured by DSC, DMTA and NMR. Carbohydr. Polym. 18(2):77-88.

Kalichevsky MT, Orford PD, Ring SG. 1990. The retrogradation and gelation of amylopectins from various botanical sources. Carbohydr. Res. 198(1):49-55.

Karim AA, Norziah MH, Seow CC. 2000. Methods for the study of starch retrogradation. Food Chem. 71:9-36.

Keetels C, Oostergetel GT, vanVliet T. 1996a. Recrystallization of amylopectin in concentrated starch gels. Carbohydr. Polym. 30(1):61-4.

Keetels C, vanVliet T, Walstra P. 1996b. Gelation and retrogradation of concentrated starch systems .3. Effect of concentration and heating temperature. Food Hydrocolloids 10(3):363-8.

Kilburn D, Claude J, Schweizer T, Alam A, Ubbink J. 2005. Carbohydrate polymers in amorphous states: An integrated thermodynamic and nanostructural investigation. Biomacromolecules 6(2):864-79.

Kim HS, Huber KC. 2010. Physiochemical properties and amylopectin fine structures of A- and B- type granules of waxy and normal soft wheat starch. J. Cereal Sci. 51:256-64.

Kim SK, Dappolonia BL. 1977a. Bread staling studies 1. Effect of protein content on staling rate and bread crumb pasting properties Cereal Chem. 54(2):207-15.

Kim SK, Dappolonia BL. 1977b. Bread staling studies 2. Effect of protein content and storage temperqaute on role of starch Cereal Chem. 54(2):216-24.

Kim SK, Dappolonia BL. 1977c. Bread staling studies 3. Effect of pentosans on dough, bread and bread staling rate Cereal Chem. 54(2):225-9.

Kim YJ, Suzuki T, Hagiwara T, Yamaji I, Takai R. 2001. Enthalpy relaxation and glass to rubber transition of amorphous potato starch formed by ball-milling. Carbohydr. Polym. 46(1):1-6.

Kimshin MS, Mari F, Rao PA, Stengle TR, Chinachoti P. 1991. O-17 nuclear magnetic resonance studies of water mobility during bread staling Journal of Agricultural and Food Chemistry 39(11):1915-20.

Kohyama K, Matsuki J, Yasui T, Sasaki T. 2004. A differential thermal analysis of the gelatinization and retrogradation of wheat starches with different amylopectin chain lengths. Carbohydr. Polym. 58(1):71-7.

Kulp K, Ponte JG. 1981. Staling of white pan bread - fundamental causes Crc Critical Reviews in Food Science and Nutrition 15(1):1-48.

Lauritzen JI, Hoffman JD. 1973. Extension of theory of growth of chain-folded polymer crystals to large undercoolings. Journal of Applied Physics 44(10):4340-52.

Le-Bail A, Leray G, Perronnet A, Roelens G. 2011. Impact of the chilling conditions on the kinetics of staling of bread. J. Cereal Sci. 54(1):13-9.

le Botlan D, Desbois P. 1995. Starch retrogradation study in presence of sucrose by low-resolution nuclear magnetic resonance. Cereal Chemistry: 72 (2) 191-193 72(2):191-3.

Leloup VM, Colonna P, Ring SG, Roberts K, Wells B. 1992. Microstructure of amylose gels Carbohydr. Polym. 18(3):189-97.

Lewen KS, Paeschke T, Reid J, Molitor P, Schmidt SJ. 2003. Analysis of the retrogradation of low starch concentration gels using differential scanning calorimetry, rheology, and nuclear magnetic resonance spectroscopy. J. Agric. Food Chem. 51(8):2348-58.

Li Q. 2010. Investigating the glassy to rubber transition of polydextrose and cornflakes using automatic water vapor sorption instruments, DSC, and texture analysis. [Master of Science]. Urbana, IL: University of Illinois at Urbana-Champaign. 77-117 p.

Li Y, Kloeppel KM, Hsieh F. 1998. Texture of glassy corn cakes as a function of moisture content. Journal of Food Science 63(5):869-72.

Lim H, Sester CS, Paukstelis JV, Sobczynska D. 1992. O-17 nuclear magnetic resonance studies on wheat starch-sucrose-water interactions with increasing temperature. Cereal Chem. 69(382-386).

Lin W, Lineback OR. 1990. Changes in carbohydrate fractions in enzyme-supplemented bread and the potential relationship to staling. Starch/Staerke 42(10):385-94.

Liu H, Lelievre J, Ayoung-Chee W. 1991. A study of starch gelatinization using differential scanning calorimetry, X-ray, and birefringence measurements. Carbohydr. Res. 210:79-87.

Liu HS, Yu L, Chen L, Li L. 2007. Retrogradation of corn starch after thermal treatment at different temperatures. Carbohydr. Polym. 69(4):756-62.

Liu HS, Yu L, Tong Z, Chen L. 2010a. Retrogradation of waxy cornstarch studied by DSC. Starch-Starke 62(10):524-9.

Liu P, Yu L, Wang XY, Li D, Chen L, Li XX. 2010b. Glass transition temperature of starches with different amylose/amylopectin ratios. J. Cereal Sci. 51(3):388-91.

Liu Q, Thompson DB. 1998. Effects of moisture content and different gelatinization heating temperatures on retrogradation of waxy-type maize starches. Carbohydr. Res. 314(3-4):221-35.

Liu YY, Shi YC. 2006. Phase and state transitions in granular starches studied by dynamic differential scanning calorimetry. Starch-Starke 58(9):433-42.

Livings SJ, Breach C, Donald AM, Smith AC. 1997. Physical ageing of wheat flour-based confectionery wafers. Carbohydr. Polym. 34(4):347-55.

Lourdin D, Colonna P, Brownsey GJ, Noel TR, Ring SG. 2002. Structural relaxation and physical ageing of starchy materials. Carbohydr. Res. 337(9):827-33.

Lv XW, Wu L, Wang J, Li JG, Qin YC. 2011. Characterization of water binding and dehydration in gelatinized starch. J. Agric. Food Chem. 59(1):256-62.

Maga J, Ponte JG. 1975. Bread staling. CRC Critical Reviews in Food Technology 5(4):443-86.

Marsh RDL, Blanshard JMV. 1988. The application of polymer crystal growth theory to the kinetics of formation of the B-amylose polymorph in a 50% wheat starch gel. Carbohydr. Polym. 9:301-17.

Martin ML, Hoseney RC. 1991. A mechanism of bread firming. II. Role of starch hydrolyzing enzymes. Cereal Chem. 68(5):503-7.

Martin ML, Zeleznak KJ, Hoseney RC. 1991. A mechanism of bread firming. I. Role of starch swelling. Cereal Chem. 68(5):498-503.

Matalanis AM, Campanella OH, Hamaker BR. 2009. Storage retrogradation behavior of sorghum, maize and rice starch pastes related to amylopectin fine structure. J. Cereal Sci. 50(1):74-81.

McIver RG, Axford DWE, Colwell KH, Elton GAH. 1968. Kinetic study of the retrogradation of gelatinised starch. J. Sci. Food Agric. 19:560-3.

Mestres C, Colonna P, Buleon A. 1988. Gelation and crystallisation of maize starch after pasting, drum-drying or extrusion cooking. Journal of Cereal Science: 7 (2) 123-134 7(2):123-34.

Mihhalevski A, Heinmaa I, Traksmaa R, Pehk T, Mere A, Paalme T. 2012. Structural Changes of Starch during Baking and Staling of Rye Bread. Journal of Agricultural and Food Chemistry 60(34):8492-500.

Miles MJ, Morris VJ, Orford PD, Ring SG. 1985. The role of amylose and amylopectin in the gelation and retrogradation of starch. Carbohydr. Res. 135:271-81.

Mita T. 1992. Structure of potato starch pastes in the aging process by the measurement of their dynamic moduli Carbohydr. Polym. 17(4):269-76.

Mizuno A, Mitsuiki M, Motoki M. 1998. Effect of crystallinity on the glass transition temperature of starch. J. Agric. Food Chem. 46(1):98-103.

Morgan LB. 1954. Crystallization phenomenon in polymers II. The course of the crystallization. Philosphoical Transcations of the Royal Society of London. Series A, Mathematical and Physical Sciences 247(921):13-22.

Morris VJ. 1990. Starch gelation and retrogradation. Trends in Food Science & Technology: 1 (1) 2-6 1(1):2-6.

Mua JP, Jackson DS. 1998. Retrogradation and gel textural attributes of corn starch amylose and amylopectin fractions. J. Cereal Sci. 27(2):157-66.

Nicholls RJ, Appelqvist IAM, Davies AP, Ingman SJ, Lillford PJ. 1995. Glass transitions and the fracture behaviour of gluten and starches within the glassy state. J. Cereal Sci. 21(1):25-36.

Noel TR, Parker R, Brownsey GJ, Farhat IA, MacNaughtan W, Ring SG. 2005. Physical aging of starch, maltodextrin, and maltose. J. Agric. Food Chem. 53(22):8580-5.

Orford PD, Ring SG, Carroll V, Miles MJ, Morris VJ. 1987. The effect of concentration and botanical source on the gelation and retrogradation of starch. Journal of the Science of Food and Agriculture: 39 (2) 169-177 39(2):169-77.

Paredes-lopez L, Bello-Perez LA, Lopez MG. 1994. Amylopectin: structural, gelatinization and retrogradation studies. Food Chem. 50:411-7.

Patel BK, Seetharaman K. 2010. Effect of heating rate at different moisture contents on starch retrogradation and starch-water interactions during gelatinization. Starch-Starke 62(10):538-46.

Perera DY. 2003. Physical aging of organic coatings. Progress in Organic Coatings 47:61-76.

Perez S, Bertoft E. 2010. The molecular structures of starch components and their contribution to the architecture of starch granules: A comprehensive review. Starch-Starke 62(8):389-420.

Piazza L, Masi P. 1995. Moisture redistribution throughout the bread loaf during staling and its effect on mechanical properties Cereal Chem. 72(3):320-5.

Pisesookbunterng W, Dappolonia BL. 1983. Bread staling studies 1. Effect of surfactants on moisture migration from crumb to crust and firmness values of bread crumb Cereal Chem. 60(4):298-300.

Pisesookbunterng W, Dappolonia BL, Kulp K. 1983. Bread staling studies 2. The role of refreshening Cereal Chem. 60(4):301-5.

Primo-Martin C, Nieuwenhuijzen NHv, Hamer RJ, Vliet Tv. 2007. Crystallinity changes in wheat starch during the bread-making process: starch crystallinity in the bread crust. J. Cereal Sci. 45(2):219-26.

Putaux JL, Buleon A, Chanzy H. 2000. Network formation in dilute amylose and amylopectin studied by TEM. Macromolecules 33:6416-22.

Qi X, Tester RF, Snape CE, Ansell R. 2003. Molecular basis of the gelatinization and swelling characteristics of waxy rice starches grown in the same location during the same season. J. Cereal Sci. 37:363-76.

Randzio SL, Flis-Kabulska I, Grolier J-PE. 2002. Reexamination of phase transformations in the starch-water system. Macromolecules 35:8852-9.

Ratnayake WS, Jackson DS. 2007. A new insight into the gelatinization process of native starches. Carbohydr. Polym. 67:511-29.

Ribotta PD, Cuffini S, Leon AE, Anon MC. 2004. The staling of bread: an X-ray diffraction study. European Food Research and Technology 218(3):219-23.

Ribotta PD, Le Bail A. 2007. Thermo-physical assessment of bread during staling. LWT-Food Sci. Technol. 40(5):879-84.

Ring SG, Colonna P, Ianson KJ, Kalichevsky MT, Miles MJ, Morris VJ, Orford PD. 1987. The gelation and crystallization of amylopectin. Carbohydr. Res. 162:277-93.

Roudaut G, Maglione M, Le Meste M. 1999a. Relaxations below glass transition temperature in bread and its components. Cereal Chem. 76(1):78-81.

Roudaut G, Maglione M, van Dusschoten D, Le Meste M. 1999b. Molecular mobility in glassy bread: a multispectroscopy approach. Cereal Chem. 76(1):70-7.

Roudaut G, Simatos D, Champion D, Contreras-Lopez E, Meste Ml. 2004. Molecular mobility around the glass transition temperature: a mini review. Innovative Food Science and Emerging Technologies 5(2):127-34.

Roulet P, MacInnes WM, Wursch P, Sanchez RM, Raemy A. 1988. A comparative study of the retrogradation kinetics of gelatinized wheat starch in gel and powder form using X-rays, differential scanning calorimetry and dynamic mechanical analysis. Food Hydrocolloids 2(5):381-96.

Ruan R, Almaer S, Huang VT, Perkins P, Chen P, Fulcher RG. 1996. Relationship between firming and water mobility in starch-based food systems during storage. Cereal Chem. 73(3):328-32.

Russell PL. 1983a. A kinetic study of bread staling by differential scanning calorimetry and compressibility measurements - the effect of added monoglyceride J. Cereal Sci. 1(4):297-303.

Russell PL. 1983b. A kinetic study of bread staling by differential scanning calorimetry and compressibility measurements. The effect of added monoglyceride. J. Cereal Sci. 1:297-303.

Russell PL. 1987. Gelatinization of starches of different amylose/amylopectin content. A study by differential scanning calorimetry. J. Cereal Sci. 6:133-45.

Russell PL, Oliver G. 1989. The effect of pH and NaCl content on starch gel ageing. A study by differential scanning calorimetry and rheology. J. Cereal Sci. 10:123-38.

Sarko A, Wu HCH. 1978. The crystal structures of A-, B- and C- polymorphs of amylose and starch. Starch-Starke 30:73-8.

Schiraldi A, Piazza L, Riva M. 1996. Bread staling: A calorimetric approach. Cereal Chem. 73(1):32-9.

Seow CC, Teo CH. 1996. Staling of starch-based products: A comparative study by firmness and pulsed NMR measurements. Starch-Starke 48(3):90-3.

Shi YC, Seib PA. 1992. The structure of four waxy starches related to gelatinization and retrogradation. Carbohydr. Res. 227:131-45.

Shogren RL. 1992. Effect of moisture content on the melting and subsequent physical aging of corn starch. Carbohydr. Polym. 19(2):83-90.

Silverio J, Fredriksson H, Andersson R, Eliasson AC, Aman P. 2000. The effect of temperature cycling on the amylopectin retrogradation of starches with different amylopectin unit-chain lenght distribution. Carbohydr. Polym. 42:175-84.

Singh S, Singh N, Isono N, Noda T. 2010. Relationship of granule shize distribution and amylopectin structure with pasting, thermal, and retrogradation properties in wheat starch. J. Agric. Food Chem. 58:1180-8.

Slade L, Levine H. 1988. Non-equilibrium melting of native granular starch. I. Temperature location of the glass transition associated with gelatinization of A-type cereal starches. Carbohydr. Polym. 8:183-208.

Slade L, Levine H. 1991. Beyond water activity - Recent advances based on an alternative approach to the assessment of food quality and safety. Crit. Rev. Food Sci. Nutr. 30(2-3):115-360.

Smits ALM, Ruhnau FC, Vliegenthart JFG, van Soest JJG. 1998. Ageing of starch based systems as observed with FT-IR and solid state NMR spectroscopy. Starch-Starke 50:478-83.

Spies RD, Hoseney RC. 1982. Effect of sugars on starch gelatinization. Cereal Chem. 59:128-31.

Srichuwong S, Sunarti TC, Mishima T. 2005. Starches from different botanical sources I: contribution of amylopectin fine structure to thermal properties and enzyme digestibility. Carbohydr. Polym. 60:529-38.

Starkweather HW, Avakian P. 1989. .beta.-Relaxations in phenylene polymers. Macromolecules 22(10):4060-2.

Steeneken PAM, Woortman AJJ. 2009. Identification of the thermal transitions in potato starch at a low water content as studied by preparative DSC. Carbohydr. Polym. 77(2):288-92.

Struik LCE. 1987. The mechanical and physical ageing of semicrystalline polymers: 1. Polymer 28:1521-33.

Struik LCE. 1989a. Mechanical behaviour and physical ageing of semicrystalline polymers: 3. Prediction of long-term creep from short time tests. Polymer 30:799-814.

Struik LCE. 1989b. Mehcanical behaviour and physical ageing of semicrystalline polymers: 4. Polymer 30:815-30.

Tananuwong K, Reid DS. 2004. DSC and NMR relaxation studies of starch-water interactions during gelatinization. Carbohydr. Polym. 58:345-58.

Thiewes HJ, Steeneken PAM. 1997. The glass transition and the sub-T-g endotherm of amorphous and native potato starch at low moisture content. Carbohydr. Polym. 32(2):123-30.

Thomas LC, Schmidt SJ. 2010. Thermal analysis. In: Nielsen SS, editor. Food Analysis: Springer Science. p. 555-71.

Tian Y, Li Y, Xu X, Jin Z. 2011. Starch retrogradation studied by thermogravimetric analysis (TGA). Carbohydr. Polym. 84:1165-8.

van Soest JJG, de Wit D, Tournois H, Vliegenthart JFG. 1994. The influence of glycerol on structural changes in waxy maize starch as studied by Fourier transform infra-red spectroscopy. Polymer 35(22):4722-7.

Vandeputte GE, Vermeylen R, Geeroms J, Delcour JA. 2003. Rice starches. III. Structural aspects provide insight in amylopectin retrogradation properties and gel texture. J. Cereal Sci. 38:61-8.

Waigh TA, Gidley MJ, Komanshek BU, Donald AM. 2000. The phase transformations in starch during gelatinization: a liquid crystalline approach. Carbohydr. Res. 328:165-76.

Wang X, Choi S-G, Kerr WL. 2004. Water dynamics in white bread and starch gels as affected by water and gluten content. Lebensmittel-Wissenschaft und -Technologie 37:377-84.

Ward KEJ, Hoseney RC, Seib PA. 1994. Retrogradation of amylopectin from maize and wheat starches. Cereal Chem. 71(2):150-5.

Willhoft EM. 1971a. Bread staling 1. Experimental study J. Sci. Food Agric. 22(4):176-&.

Willhoft EM. 1971b. Bread staling 2. Theoretical study J. Sci. Food Agric. 22(4):180-&.

Wilson RH, Goodfellow BJ, Belton PS, Osborne BG, Oliver G, Russell PL. 1991. Comparison of fourier-transorm mid infrared spectroscopy and near infrared reflectance spectroscopy with differential scanning calorimetry for the study of the staling of bread J. Sci. Food Agric. 54(3):471-83.

Wilson RH, Kalichevsky MT, Ring SG, Belton PS. 1987. A Fourier-transform infrared study of the gelation and retrogradation of waxy-maize starch. Carbohydr. Res. 166:162-5.

Wu JY, Eads TM. 1993. Evolution of polymer mobility during ageing of gelatinized waxy maize starch: a magnetization transfer 1H NMR study. Carbohydr. Polym. 20:51-60.

Wynne-Jones S, Blanshard JMV. 1986. Hydration studies of wheat starch, amylopectin, amylose gels and bread by proton magnetic resonance. Carbohydr. Polym. 6(4):289-306.

Xu A, Chung K, Ponte JG. 1992. Bread crumb amylograph studies. I. Effect of storage time, shortening, flour lipids, and surfactants. Cereal Chem. 69:495-501.

Yao Y, Ding X. 2002. Pulsed nuclear magnetic resonance (PNMR) study of rice starch retrogradation. Cereal Chem. 79(6):751-6.

Yu L, Christie G. 2005. Microstructure and mechanical properties of orientated thermoplastic starches. J. Mater. Sci. 40(1):111-6.

Yu S, Ma Y, Sun DW. 2010. Effects of freezing rates on starch retrogradation and textural properties of cooked rice during storage. LWT - Food Science and Technology 43:1138-43.

Yuan RC, Thompson DB. 1994. Sub-Tg thermal properties of amorphous waxy starch and its derivatives. Carbohydr. Polym. 25(1):1-6.

Zeleznak KJ, Hoseney RC. 1986. The role of water in the retrogradation of wheat starch gels and bread crumb. Cereal Chem. 63(5):407-11.

Zhang W, Jackson DS. 1992. Retrogradation behavior of wheat starch gels with differing molecular profiles. Journal of Food Science 57(6):1428-32.

Zhou X, Baik BK, Wang R, Lim ST. 2010. Retrogradation of waxy and normal corn starch gels by temperature cycling. J. Cereal Sci. 51:57-65.

CHAPTER 3
MDSC INVESTIGATION OF THE SUB-TG ENDOTHERM IN PREGELATINIZED WAXY MAIZE STARCH AT LOW MOISTURE CONTENTS AND ITS SIMILARITIES TO ENDOTHERMS OBSERVED IN COMMERCIAL LOW MOISTURE STARCH BASED FOOD SYSTEMS

3.1 Abstract

A sub-Tg endotherm was observed in several varieties of commercial crackers, a low moisture starch-based food system. In order to elucidate the origin of this sub-Tg endotherm, pregelatinized waxy maize starch was studied using MDSC as a function of moisture content and storage temperature. A sub-Tg endotherm was observed between 45 to 65°C in the non-reversing signal for pregelatinized waxy maize starch granules stored between 0 and 72% RH and over a storage temperature range from 5 to 35°C. The enthalpy of this transition was independent of storage temperature, but exhibited an exponential relationship with increasing moisture content. The sub-Tg endotherm disappears upon immediate rescan but does reappear after 4 weeks of storage, though the enthalpy of transition is decreased. It is hypothesized that the sub-Tg endotherm represents the reformation of double helical structure within amylopectin chains, which is the first step in the amylopectin retrogradation process.

3.2 Introduction

In aqueous starch systems, 4 types of thermal events are generally encountered: (1) a so-called sub-Tg endotherm, (2) a glass transition, (3) various crystal melting processes and (4) a high-temperature endotherm which marks the transition into a thermoplastic melt (Thiewes and Steeneken 1997). The occurrence of an endothermic event, typically observed below the conventional glass transition, is a common feature of many semicrystalline polymers, including starch, which develops semi-crystalline shells termed "growth rings" through the organization of amylopectin molecules (Perez and Bertoft 2010). This sub-Tg thermal event has been reported for synthetic semicrystalline polymers (Beckmann and others 1997; Struik 1987), starch (Chung and others 2002; Kalichevsky and others 1992a; Kim and others 2001; Shogren 1992; Yuan and Thompson 1994), maltodextrin (Descamps and others 2009), confectionary wafers (Livings and others 1997), and cornflakes (Gonzalez and others 2010; Li 2010). While the origin of this sub-

Tg thermal event remains controversial, the most prevalent theories involve (1) "melting" of water-carbohydrate interactions and (2) physical aging.

The endothermic peak has been attributed to the melting of water-carbohydrate interactions, in particular, the disruption of the hydrogen-bond network involving water and polysaccharides (Appelqvist and others 1993; Yuan and Thompson 1994). This hypothesis relies on the assumption that large molecular weight carbohydrates, such as starch, are effectively immobile below the glass transition, preventing carbohydrate-carbohydrate interactions, whereas water-carbohydrate interactions between residues can still be formed or disrupted (Appelqvist and others 1993).

Alternatively, physical aging, also referred to as enthalpy relaxation, occurs for a glassy material as a result of the non-equilibrium state spontaneously relaxing to a more energetically favorable state. Physical aging is a general, thermoreversible phenonmenon, occurring for any glassy material as a result of its non-equilibrium state attempting to regain equilibrium (Perera 2003).

Furthermore, the sub-Tg endotherm in these systems occurs around 60°C, which is similar to that of the retrogradation of amylopectin under high moisture conditions. Retrogradation is a multistage process, similar to the crystallization of other semicrystalline polymers. The recrystallization process can be descirbed in 3 phases: (1) nucleation, or the initiation of oriented chain segments, (2) propagation (crystal growth), and (3), maturation during which crystal perfection and growth continue. However, in principle, retrogradation should not occur below Tg where molecular mobility is limited but its similarity to this sub-Tg peak warrants further investigation as amylopectin retrogradation is often attributed as the cause of a variety of physical and textural changes in a wide range of high moisture food systems. In particular, the recrystallization of the outer chains of amylopectin has been linked to the staling endotherm of bread (Jang and Pyun 1997).

Thus, the presence of this sub-Tg endothermic event has practical implications for low moisture carbohydrate and starchy food systems in that it may also be accompanied by physical changes directly impacting the texture and quality of the food system. In particular, foods that are classified as being in the "glassy" state may be affected, although the prevailing assumption has been that the physical characteristics of such food systems are kinetically stable. However, recently, Li (2010) observed the presence of an endothermic event with a peak temperature near

60°C during DSC analysis of cornflakes that was independent of moisture content over a relative humidity range from 11.3 to 68.9%. The features of this thermal event were similar to what has been described with the exception that the event was observed both below and above the glass transition of the cornflakes.

Prior to gaining insight into the textural implications of this phase transition, an understanding of the conditions that lead to its occurrence must be investigated. Therefore, the aim of this study is to investigate how this sub-Tg endotherm is affected by moisture content and storage temperature in pregelatinized waxy maize starch. Furthermore, similarities between the sub-Tg endotherm in the starch and any observed sub-Tg endotherms in various commercial crackers, as examples of low moisture starch based food products, will be described.

3.3 Materials and methods

Commercial, pregelatinized, drum-dried (X'PandR 612, Tate & Lyle; initial Aw = 0.42 at 25.02°C, initial moisture content = 9.32% wet basis) and pregelatinized, spray-cooked (X'PandR SC, Tate & Lyle; initial Aw = 0.15 at 24.99°C, initial moisture content = 5.88% wet basis) unmodified waxy cornstarch was obtained. Pregelatinized, drum-dried starch contains non-intact starch granule fragments, whereas pregelatinized, spray-cooked starch granules remain largely intact (Figure 3.1). The initial moisture contents of the starches were determined via quick drying with a halogen oven (CompuTrac Max 1000, Arizona Instruments, Chandler, Arizona), calibrated to vacuum oven drying for 4 hours at 25-100 mmHg and 105°C. The initial water activity values of the starches were determined using an Aqualab 4TE water activity meter (Decagon Devices, Pullman, Washington).

Starch samples were equilibrated over saturated salt solutions encompassing a range of %RH values (Table 3.1). Saturated salt slurries were made by adding an excess amount of salt into deionized water according to the known solubility values at 40°C, heating the slurry to ~50°C for about 2 hours, while stirring on a standard stir plate and then cooling to room temperature. Additionally, both starch samples were hydrated in room temperature excess deionized water to provide 50% moisture w/w, with the addition of 0.1% potassium sorbate and 0.1% sodium propionate to prevent mold growth. Moisture contents were confirmed via quick drying with a CompuTrac halogen oven. According to Zeleznak and Hoseney (1986), the staling/retrogradation endotherm reaches a maximum at moisture content between 50 to 60%.

A sufficient amount of saturated salt slurry was added to storage containers (airtight and water proof plastic containers commercially known as "Lock & Lock") to completely cover the bottom of the container. About 4 grams of "as is" intact or non-intact waxy maize starch granules was weighed into a small plastic cup and transferred to the "Lock & Lock" container with the saturated salt slurry. Containers were kept in incubators at storage temperatures of 5, 15, 25 and 35°C, and samples were weighed at 7-day intervals until each sample weight changed by less than 2mg/g dry weight between successive weight measurements (Bell and Labuza 2000), at which time the equilibrium moisture content was determined using the initial sample weight, the initial moisture content and the equilibrium weight.

3.3.1 Determination of pregelatinized starch phase transitions using MDSC

The presence of, onset and peak temperature and enthalpy of thermal transition in the equilibrated starch samples was determined using Modulated Differential Scanning Calorimetry (MDSC) with Q2000 Differential Scanning Calorimeter instrument (TA Instruments, New Castle, Delaware). MDSC allows for the separation of the heat flow into the reversing heat flow (heat capacity component) and non-reversing heat flow (kinetic component). Equilibrated samples were taken from the "Lock & Lock" containers and transferred to DSC aluminum hermetic pans, in duplicate, and sealed with internal hermetic lids immediately after transferring out of the "Lock & Lock" containers. Samples were pressed and sealed with hermetic pans and lids in order to maintain the appropriate moisture content and %RH within the sample throughout the study. Samples were equilibrated at -20°C and scanned using a modulated heating profile with a rate of 5°C/min, oscillation period of 40 seconds and amplitude of 0.5°C from -20°C to 120°C (MDSC first scan). Applying a sinusoidal heat rate superimposed on the linear rate allows for the separation of the measured total heat flow signal into the reversing heat flow and non-reversing heat flow. The samples were then immediately subjected to a second scan (MDSC rescan) using the same profile. Following MDSC analysis, the samples were transferred back to the same "Lock & Lock" container and stored at the same temperature and relative humidity for 4 weeks, after which the same MDSC analysis was repeated. Resulting heat flows were separated into the non-reversing and reversing flows (for example, Figure 3.2) and the onset temperature, peak temperature and enthalpy of the transitions of observed peaks were determined, in triplicate, through peak integration using the sigmoid tangent method as part of the Universal Analysis

software (TA Instruments 2009). Observed glass transitions were also analyzed for onset temperature, midpoint temperature and enthalpy change using glass transition analysis option and tangent selection at the inflection point with the Universal Analysis software (TA Instruments 2009).

3.3.2 Determination of phase transitions in commercial crackers

Five varieties of low-moisture cereal-based food products, covering a range of cracker processing methods, were obtained from a local grocery (Table 3.2). A single production lot of each product was selected. Products were ground in a coffee grinder, and the initial moisture content of the products was determined via quick drying with a halogen oven (CompuTrac Max 1000, Arizona Instruments), calibrated to vacuum oven drying at 105°.Ground samples were equilibrated over saturated salt solutions encompassing a range of %RH (Table 3.3).

The crackers were then stored at 25°C above the various saturated salt slurries in the same manner as described for the pregelatinized waxy maize starches. After constant weight is reached, defined as when the sample weight changed by less than 2mg/g dry weight between successive weighings (Bell and Labuza 2000), the equilibrium moisture content was determined using the initial sample weight, the initial moisture content and the equilibrium weight. The crackers were then held in storage for an additional 24 weeks to ensure that any thermal transitions had sufficient time to develop.

The presence of, onset and peak temperature and enthalpy of thermal transition in the equilibrated cracker samples was then determined using Modulated Differential Scanning Calorimetry (MDSC). Aged, equilibrated cracker samples were taken from the "Lock & Lock" containers and transferred to DSC T-zero aluminum hermetic pans in duplicate and sealed with internal hermetic lids immediately after transferring out of the "Lock & Lock" containers in order to maintain the appropriate moisture content and %RH within the sample throughout the study. Samples were equilibrated at 0°C and scanned using a modulated heating profile with a rate of 1°C/min, oscillation period of 80 seconds, and amplitude of 0.5°C from 0°C to 120°C using the Q2000 Differential Scanning Calorimeter instrument (TA Instruments, New Castle, Delaware). The onset temperature, peak temperature, and enthalpy of the transitions of observed peaks were determined through peak integration using the TRIOS Software version 2.3.4. 1613 from TA Instruments (2011). Each scan was analyzed in triplicate.

3.4 Results and discussion

3.4.1 Sub-Tg endothermic peak characterization

An endotherm with a peak temperature between 45 and 65°C was observed at all %RH and storage temperatures and for both intact and fragmented waxy starch granules in the non-reversing heat flow of the MDSC scan, indicating that this peak is related to a kinetic event occurring in the starch granule. The enthalpy of this thermal transition was independent of storage temperature, but exhibited an exponential relationship with %RH (Figure 3.3 and Figure 3.4). Literature reports of the sub-Tg endotherm have also indicated that, in general, as moisture content increased, enthalpy of the peak increased, while the onset and midpoint peak temperatures were independent of moisture content (Badii and others 2005; Chung and others 2002; Shogren 1992; Thiewes and Steeneken 1997).

The temperature range at which the sub-Tg transition occurred was dependent on the %RH and storage temperature. At the lowest storage temperature (5°C), the peak midpoint temperature, T_m, decreased as %RH increased, whereas T_m was relatively constant at 15°C and T_m increased with %RH for storage temperatures of 25 and 35°C (Figure 3.5). Additionally, at lower %RH (<40%), T_m was independent of storage temperature, and the sub-Tg transition peak only shifted temperature (higher or lower) at higher relative humidity values. At the higher storage temperatures (25 and 35°C) and higher %RH, sufficient mobility existed in the system to increase structure and possibly crystallinity so as to increase the temperature at which this structure is lost during an MDSC thermal scan. While the exact reason for the changes in amylopectin structure and conformation as a function of storage temperature and %RH is unknown, one explanation for the structure loss is that at the higher %RH, the amylopectin chains possessed enough mobility to begin to dissociate, such as by the unwinding of the double helices, but lacked sufficient mobility to interact with neighboring amylopectin chains and form a crystalline network that would increase structure. Appelqvist and others (1993) observed no systemic dependence of the DSC peak temperature of the sub-Tg endotherm on water content for a multitude of polymers, including waxy maize starch, pullulan, dextran, xanthan, agar, and guar, among others, while Li (2010) also did not observe a relationship between moisture content and sub-Tg peak temperature in cornflakes. However, these studies examined the sub-Tg endotherm

at room temperature only, and other reports have observed a shift to higher temperatures as relative humidity storage conditions increased (Thiewes and Steeneken 1997).

The temperature differential over which the sub-Tg peak occurred, characterized by ΔT ($T_m - T_{onset}$), varied over 4 to 12°C temperature span, and ΔT decreased with increasing %RH and was largely independent of storage temperature (Figure 3.6). This result indicates that as %RH increased, structure within the amylopectin network increased or became more "perfect," which agrees with the increase in T_m seen at the higher %RH and storage temperatures. At the lower temperatures and higher %RH, ΔT and T_m decreased, which could indicate the amylopectin structure was less stable (decreased T_m), though the range of structures within the amylopectin network contributing to the sub-Tg peak decreased (decreased ΔT).

After the initial MDSC scan, the starches were immediately rescanned using the same heating profile, and no peaks were detected. Following the rescan, the starches were stored at the same %RH and temperature for 4 weeks, after which, the MDSC characterization protocol was repeated. After 4 weeks, the sub-Tg endotherm reappeared, though the peak was generally broader (increased ΔT), while $T_{midpoint}$ was relatively unchanged (for example, Figure 3.5). Concurrently, a decrease in peak enthalpy by as much as 60-80%, depending on %RH and storage temperature, was observed (Figure 3.7 and Figure 3.8). The decrease in peak enthalpy generally increased as %RH increased, though this trend was more evident with the fragmented waxy cornstarch granules than with the intact granules. Similar observations of peak reappearance with a decrease in peak enthalpy were made by Appelqvist and others (1993).

3.4.2 Intact versus fragmented starch granules

The enthalpy of the thermal transition occurring in the non-reversing signal between 45 and 65°C exhibited an exponential relationship with respect to %RH and was independent of storage temperature. Additionally, that rate of exponential increase with increasing %RH was dependent on the condition of the starch granules (i.e. intact versus fragmented, see Figure 3.1). The rate of increase in peak enthalpy with increasing %RH was less with intact starch granules than with fragmented as evidenced by the smaller exponent value (b) in the equation of best fit for $y = me^{bx}$ (Figure 3.4). The value m describes the enthalpy of this peak at 0% RH, which implies that intact starch granules exhibit a greater thermal transition than fragmented starch granules at low relative humidity where essentially chain mobility and reassociation does not

exist, most likely owing to the presence of more and larger amylopectin chains. Thus, the process of drum-drying starch, which leads to starch granule fragmentation, destroys some of the structure within the starch granule that cannot be regained under typical storage conditions of the pure, dry starch (intact starch granules had initial A_w of 0.15 and the fragmented starch had initial A_w of 0.42). However, as relative humidity increases, the amylopectin within the fragmented starch granules may gain mobility faster than within intact starch granules and can then more easily reassociate and realign amylopectin chains and thereby increase peak enthalpy. Amylopectin within a fragmented starch granule may also interact with chains of neighboring starch granules, giving more opportunities for chain reassociation and realignment, whereas within an intact granule, amylopectin reassociation is constrained to that granule. Similarly, the rate at which conformational rearrangements are occurring in the enthalpy relaxation (i.e. physical aging) process is dependent on aging time and moisture content of the material (Badii and others 2005; Kilburn and others 2005; Livings and others 1997). The fragmented waxy corn starch granules, with a higher moisture content at a constant relative humidity, would be expected to undergo conformational rearrangements faster, as seen in this study, and Gonzalez and others (2010) also concluded that molecular relaxation occurred faster as starch became more fragmented during the shearing process for cornflakes.

At low %RH, the peak temperature for this sub-Tg transition is lower for fragmented granules than for intact granules, but this trend reverses as %RH increases (Figure 3.9). The peak temperature at low %RH is determined by the structural integrity of the amylopectin chains normally present in the starch after production and stored under typical conditions. But, if %RH increases, then the amylopectin chains associated with fragmented starch granules can more easily reassociate and increase structure due to the greater mobility than is possible within an intact granule, which serves to increase the peak temperature.

3.4.3 Comparison of the sub-Tg endotherm at low moisture content to the amylopectin retrogradation endotherm at high moisture content

Amylopectin retrogradation, defined as the processes in which the molecules in gelatinzed starch reassociate in an ordered structure (Atwell and others 1988) through the re-adoption of double helical structures and chain aggregation. The sub-Tg endotherm at low moisture content occurs around 60°C, which is similar to that of the retrogradation endotherm of

amylopectin under high moisture conditions. However, retrogradation, which is a recrystallization process, should not occur below Tg, but its similarity to this sub-Tg peak warrants further investigation as amylopectin retrogradation is often attributed as the cause of a variety of physical and textural changes in a wide range of food systems. In particular, the recrystallization of the outer chains of amylopectin has been linked to the staling endotherm of baked foods (Jang and Pyun 1997).

Similar to the sub-Tg peak observed at 45-65°C, a retrogradation peak in the non-reversing heat flow was observed within this temperature range for intact and fragmented starch granules stored at 50% solids (in the concentration range where maximum retrogradation endotherm is typically observed). At high storage temperature (35°C), the enthalpy associated with the retrogradation endotherm was within the range and temperature encountered for the sub-Tg endotherm observed at higher %RH (>50% RH).

Unlike the sub-Tg endotherm in which the observed enthalpy was independent of storage temperature, the enthalpy of the retrogradation endotherm exhibited a negative relationship with storage temperature (Figure 3.10). In freshly gelatinized starch, the amylopectin is completely amorphous, and the water within the granule is nearly uniformly distributed. The degree to which the amylopectin will retrograde or recrystallize depends on the temperature as it relates to the mobility of the amylopectin chains and their ability to reassociate. When retrogradation is considered as a crystallization process, then the degree of retrogradation should be maximum somewhere between Tg and Tm (melting temperature), as nucleation rate increases exponentially with decreasing temperature down to the glass transition temperature, while the propagation rate increases exponentially with increasing temperature up to the melting temperature (Silverio and others 2000). Thus, retrogradation is often at a maximum near refrigeraton temperatures (e.g., 4°C) since, at 50% moisture, Tg is below zero and Tm approaches 100°C. Slade and Levine (1988b) reported Tg of -5°C and Tm of 95°C for waxy cornstarch at 55% moisture. The enthalpy of the retrogradation endotherm decreases as the storage temperature increases above 5°C as the storage temperature approaches Tm, and in theory, the enthalpy would decrease if storage temperatures less than 5°C were investigated owing to the fact that propagation would be limited due to limited mobility at or near freezing conditions.

3.4.4 Characterization of other phase transitions occurring at low moisture contents

Amylopectin, as a semicrystalline polymer containing both partially amorphous and partially crystalline regions, exhibits a glass transition associated with the amorphous material. The glass transition temperature is an important characteristic in terms of its implications on storage stability and retention of crispiness, particularly for baked products, as retrogradation can theoretically only occur in the temperature region between Tg and the onset of gelatinization/melting of crystallites. The glass transition temperature depends on the moisture content and was observed to increase with decreasing moisture content for both intact and fragmented waxy corn starch granules stored under various relative humidities and temperatures (Figure 3.11). Within the moisture content range studied, the glass transition temperature exhibited a negative linear dependence with moisture content that was independent of fragmentation of the starch granule (Figure 3.12) and within the temperature range reported in the literature (Biladeris 2009).

An amylopectin glass transition was only observed for waxy corn starch stored at certain %RH and temperature conditions, particularly those conditions resulting in starch moisture contents of 13 to 20% dry basis. A glass transition was also observed for waxy corn starch at extremely low moisture (roughly 1% moisture content, dry basis), though this transition was not observed for every replicate tested. The glass transition temperature of amylopectin is not always well-defined, owing to the heterogeneous nature of the amorphous portion of amylopectin. The presence of crystallinity can also make the observance of Tg more difficult, and Tg in a native starch granule is often easier to observe than for retrograded starch since the amylopectin in native starch is heterogeneous in a relatively organized fashion, at least when compared with retrograded amylopectin (Kalichevsky and others 1992b). A glass transition was not detected in this study in the immediate rescan or after 4 weeks storage.

As the name implies, the sub-Tg endotherm studied is defined as such since it occurs below the observed glass transition. However, in some instances, the sub-Tg endotherm occurred simultaneously with the glass transition. For example, intact waxy corn starch stored at 72.1% RH and 5°C exhibited a sub-Tg endotherm at 43.06°C and glass transition with Tg_o at 41.95°C and Tg_m at 44.11°C (Figure 3.13). Amylopectin can be described as a semicrystalline polymer consisting of a mobile amorphous phase, a rigid amorphous phase and a crystalline phase. The mobile amorphous phase contributes to the phase transitions occurring in the bulk amorphous

phase and would be the primary contributor to the observed glass transition. The rigid amorphous phase is linked to thermal transitions occurring in the amorphous region directly connected to the crystalline lamellae and structural rearrangements could still occur within this region above the observed Tg. Below Tg, crystallization or the propagation of the order of neighboring amylopectin chains is inhibited, but the formation of double helices within an amylopectin chain would be possible (Liu and Shi, 2006). The double helices could then serve as the nuclei that would propagate amylopectin order during retrogradation. Nucleation should be optimal as the glass transition is approached, which is in agreement with the increase in enthalpy of the sub-Tg endotherm seen as %RH increased and the glass transition temperature decreased (Figure 3.4).

Those samples in which a glass transition was observed (except for the samples at about ~1% moisture content, dry basis) also exhibited a second endothermic peak immediately following the sub-Tg endothermic peak (Figure 3.14). Peak enthalpy and peak temperature increased as the storage temperature increased for samples stored over potassium iodide saturated salt solution (~70% RH; moisture content varied from 14-17% depending on storage temperature) (Figure 3.15). One explanation for this second endothermic peak is that this transition represents the second phase of the retrogradation phenomenon, if retrogradation is considered as consisting of 2 phases, the first being the re-formation of double helical structure within an amylopectin chain, and the second being the alignment of double helices into an ordered array. Below the glass transition, the first phase can still occur, and this is what has commonly been referred to as physical aging. During the relaxation process, X-ray diffraction data of aged, wheat-based confectionary wafers indicated the presence of a small, but well-defined peak at 2θ angle of 20° superimposed on the broad amorphous halo, typical of gelatinized starch products, which was not found in freshly prepared wafers. The position and d-spacing of this peak was characteristic of a 6-fold helical structure that corresponded to the 310 reflection of V-type amylose, which is typically observed when amylose complexes with lipids (Livings and others 1997). However, amylose-lipid melting typically occurs at much higher temperatures (95-130°C in excess water and higher for limited water conditions) than the temperature range of the sub-Tg endotherm. Rather, the authors proposed that on aging below Tg, short chain amylopectin domains with helical ordering form but without the aggregation of these to form crystals.

Above the glass transition, both events, formation of double helices and aggregation of helices, have sufficient mobility to take place and at temperatures well above the observed glass transition, the processes occur simultaneously so that only 1 endothermic peak is observed. At temperatures near the glass transition, the peak separates so that 2 distinct transitions are observed. Furthermore, if the second phase in the retrogradation process is considered as propagation in crystalline structure, then it would be expected for the enthalpy of transition to increase as temperature moved further away from the glass transition, as was seen here for the second endothermic peak with the enthalpy increasing as storage temperature increased (and consequently, glass transition temperature at that moisture content, decreased).

3.4.5 Characterization of the sub-Tg endotherm in commercial crackers

Crackers are generally defined as cereal based food products baked to a moisture content of <5% (Manley 2011). As such, crackers represent a commercially relevant low moisture application in which starch is at least partially gelatinized in processing and may subsequently undergo physical changes leading to the development of a sug-Tg endotherm. In fact, a sub-Tg endotherm with peak temperature between 40 and 55°C was observed in several commercially available crackers covering a range of processing methods and technologies (e.g water crackers; Figure 3.16).

Similarly, the enthalpy of the sub-Tg endotherm for all of the commercial crackers tested exhibited an exponential relationship with moisture content analogous to that seen in the pregelatinized waxy maize starch samples (Figure 3.17). Thus, the sub-Tg endotherm in commercial crackers can be attributed to the pregelatinized starch fraction present in the application. Furthermore, the sub-Tg endotherm occurs around 50°C, which is similar to that of the retrogradation of amylopectin under high moisture conditions. Amylopectin retrogradation is a ecrystallization process that can be descirbed in 3 phases: (1) nucleation, or the initiation of oriented chain segments through reformation of double helical structure, (2) propagation (crystal growth), occuring through aggregation of the double helices into ordered arraysand (3), maturation during which crystal perfection and growth continue.However, due to limited mobility, retrogradation should not occur below Tg, but its similarity to this sub-Tg peak warrants further investigation as amylopectin retrogradation is often attributed as the cause of a variety of physical and textural changes in a wide range of food systems. In particular, the

88

recrystallization of the outer chains of amylopectin has been linked to the staling endotherm of baked foods (Jang and Pyun 1997). The similarities between amylopectin retrogradation and the sub-Tg endotherm in low moisture pregelatinized starch and starch-based food applications is explored furhter in upcoming chapters.

3.5 Summary and conclusions

A sub-Tg endotherm was observed between 45-65°C in the non-reversing signal for intact and waxy corn starch granules stored between 0 and 72% RH and over a temperature range from 5 to 35°C. The enthalpy of this transition was independent of storage temperature but exhibited an exponential relationship with increasing %RH. The endotherm temperature is independent of %RH and storage temperature for %RH less than 40%, but as %RH increases above 40%, the peak temperature shifts to higher temperatures for starches stored at 25 and 35°C and stays the same or decreases to lower temperatures for starches stored at 5 and 15°C. As %RH increased, the width of the endotherm decreased. The sub-Tg endotherm disappears upon immediate rescan but does reappear after 4 weeks storage, though the enthalpy of transition is decreased.

Intact waxy corn starch granules initially required more energy (higher ΔH) to disrupt the amylopectin network at lower %RH than fragmented waxy corn starch granules, but the rate of increase in enthalpy versus %RH was greater for fragmented waxy corn starch granules than for intact granules. Similarly, at low %RH, the sub-Tg endotherm temperature was lower for fragmented starch granules than for intact granules, but at higher %RH, that trend was reversed. At higher %RH, the fragmented granules may develop sufficient mobility to allow additional interaction with amylopectin networks of neighboring granules that is not possible within an intact granule, giving more structure and energy to the resulting network.

Similar to the observed sub-Tg endotherm, amylopectin retrogradation was observed to occur in the non-reversing phase over the temperature span of 45 to 65°C. Unlike the sub-Tg endotherm, the enthalpy of the retrogradation endotherm was dependent on the storage temperature. However, under certain storage conditions, notably storage at higher %RH (66-71%), a second endotherm was observed in the non-reversing phase that was dependent on the storage temperature. This second endotherm was observed when the sub-Tg endotherm was found to occur simultaneously with the glass transition. It is hypothesized that the sub-Tg

89

endotherm represents the reformation of double helical structure within amylopectin chains, commonly referred to as physical aging, as reported by Livings and others (1997). The second endotherm represents the alignment of the double helices into an ordered array. Below the glass transition, only the first event, the formation of double helical structure, can occur, but, above the glass transition, both events have sufficient mobility to take place. At temperatures well above the observed glass transition, the processes occur simultaneously so that only 1 endothermic peak is observed, and at temperatures near the glass transition, the peak separates so that 2 distinct transitions are observed.

Furthermore, commercial crackers, a low moisture starch-based food system, exhibit a similar sub-Tg endotherm occurring over the same temperature span with the similar exponential dependence on moisture content. Thus, the sub-Tg endotherm can be attributed to the pregelatinized starch fraction. If that sub-Tg endotherm is further linked to the reformation of double helices as might occur during the first step of amylopectin retrogradation, then this sub-Tg endotherm may explain texture changes or staling that can occur in crackers as might occur in bread at higher moisture contents. This connection will be explored further in upcoming chapters.

3.6 Figures and tables

(a)

(b)
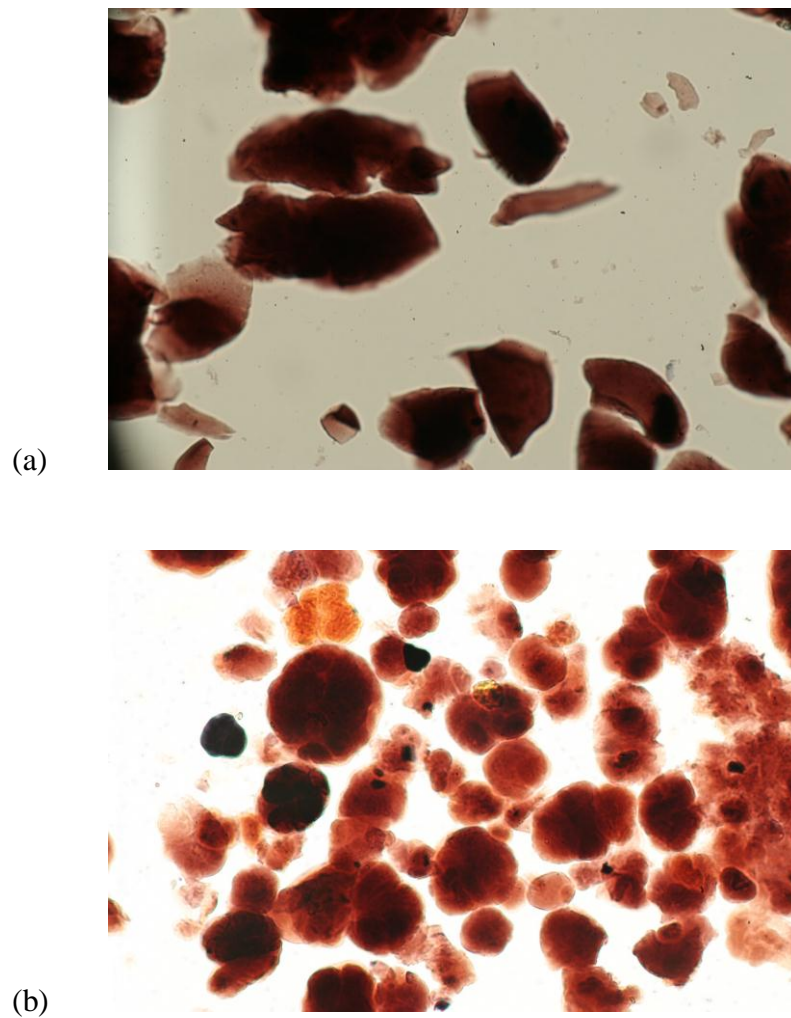
Figure 3.1. Microscope image of (a) drum dried and (b) spray cooked pregelatinized waxy maize starches at 200X magnification after iodine staining, depicting the presence of fragmented or intact granules, respectively.
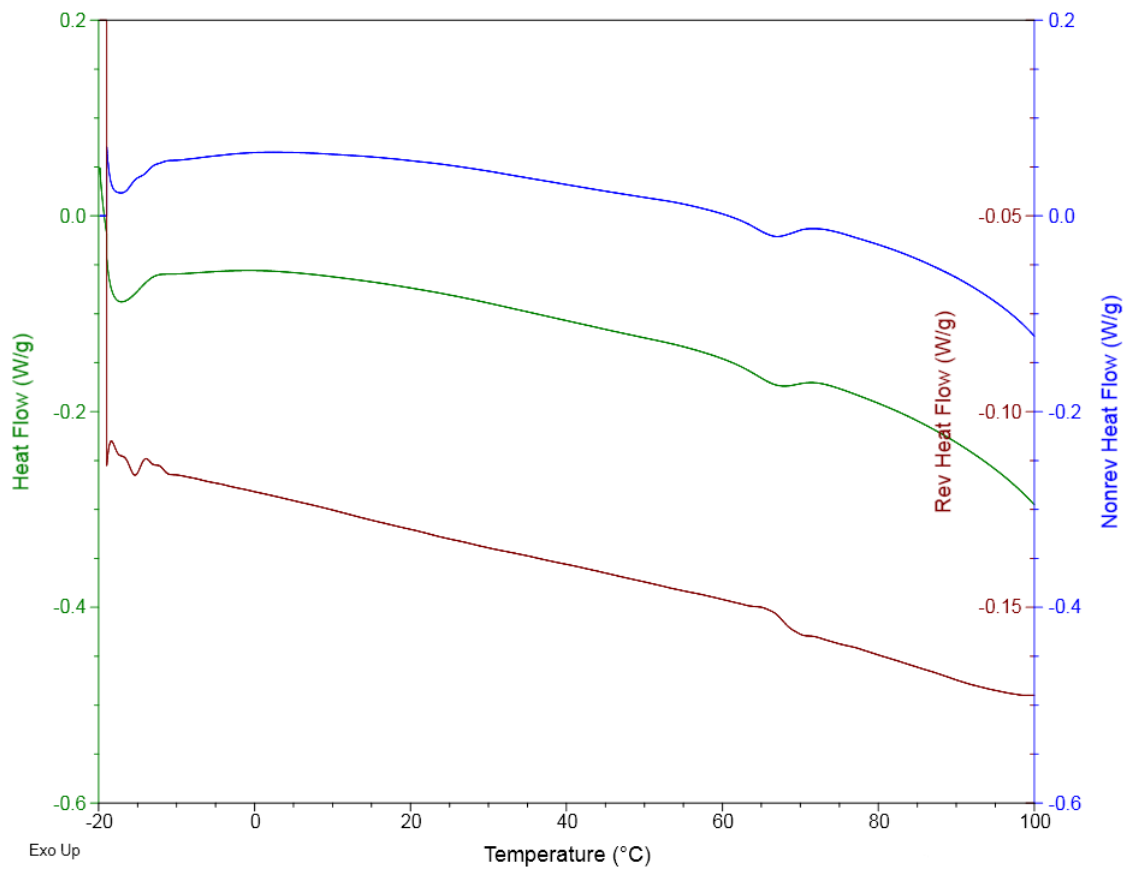
Figure 3.2. MDSC plot of fragmented pregelatinized waxy maize starch held at 5°C over KI saturated salt slurry.
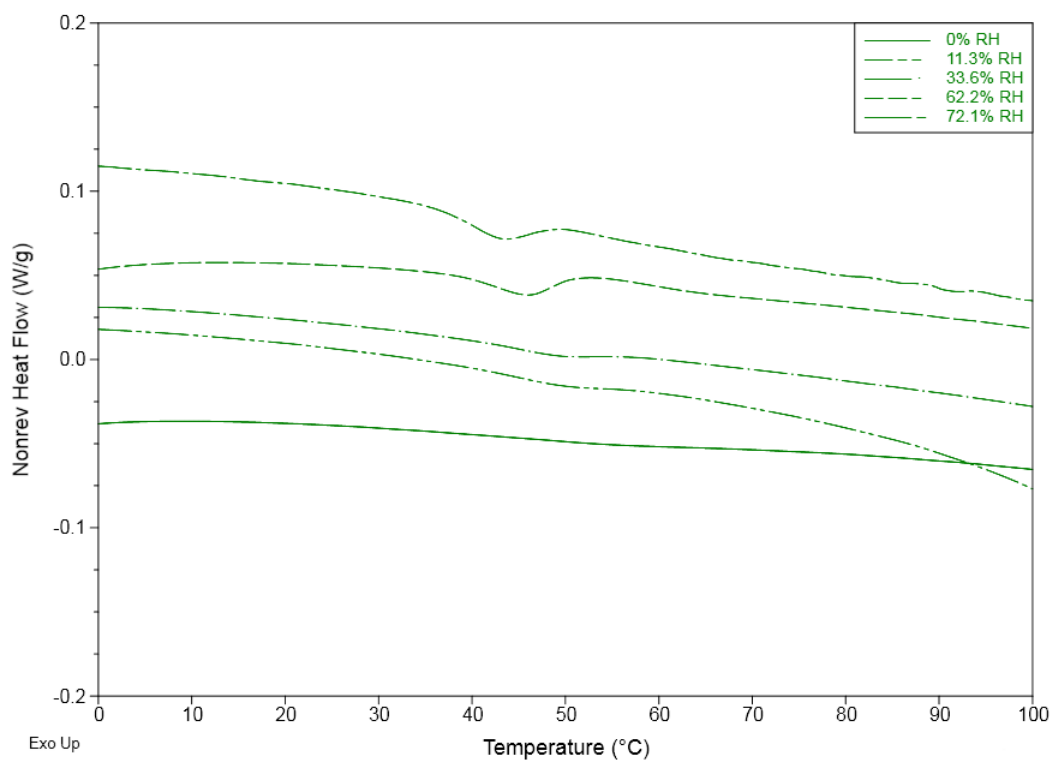
Figure 3.3. MDSC-observed sub-Tg endotherms for intact pregelatinized waxy maize starch held at 5°C and 0, 11.3, 33.6, 62.2 and 72.1% RH.
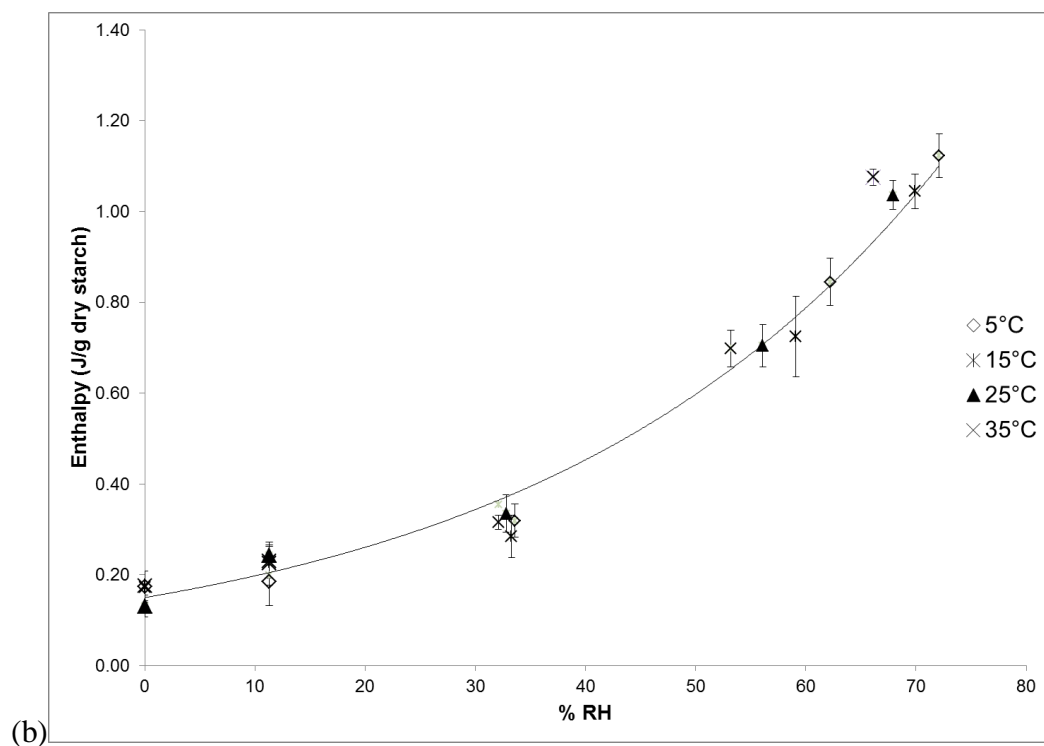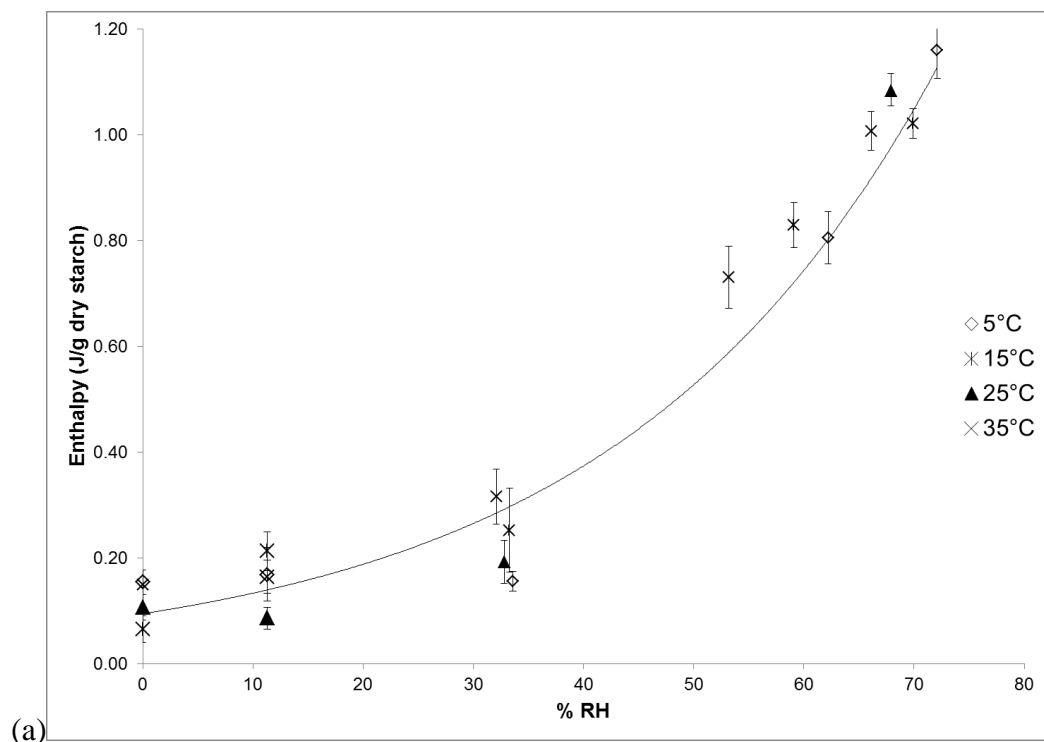
Figure 3.4. Enthalpy associated with sub-Tg endotherm in the non-reversing heat flow characterized by %RH and storage temperature for (a) fragmented pregelatinized waxy maize starch and (b) intact pregelatinized waxy maize starch. Error bars represent one standard deviation.

(a)

(b)
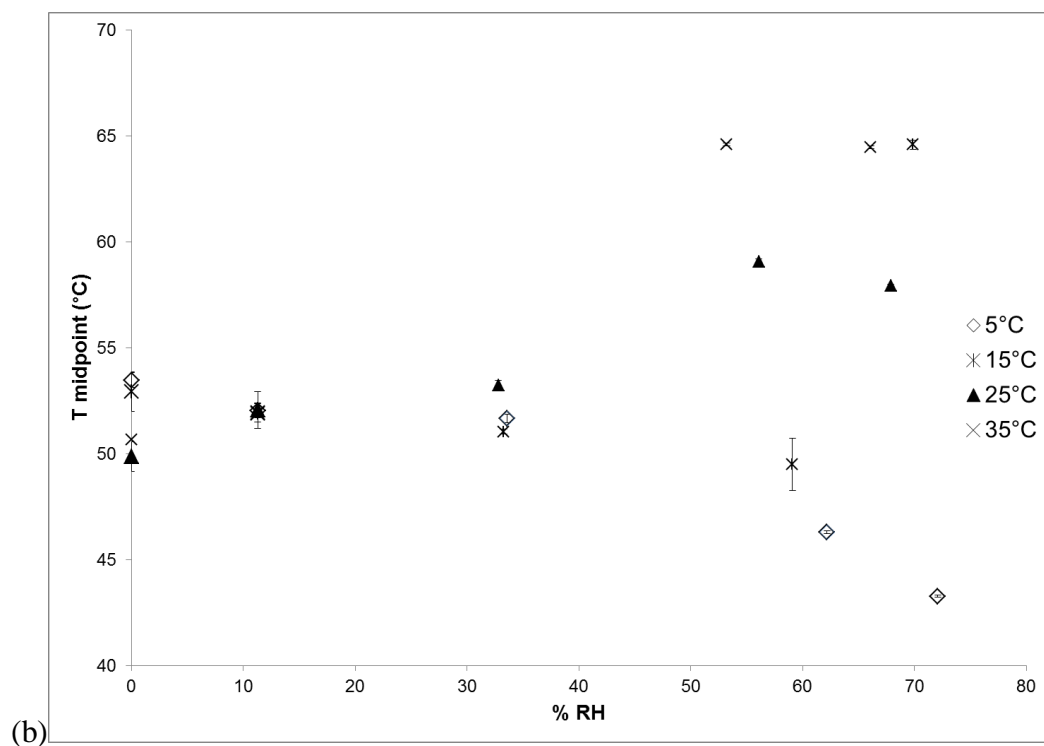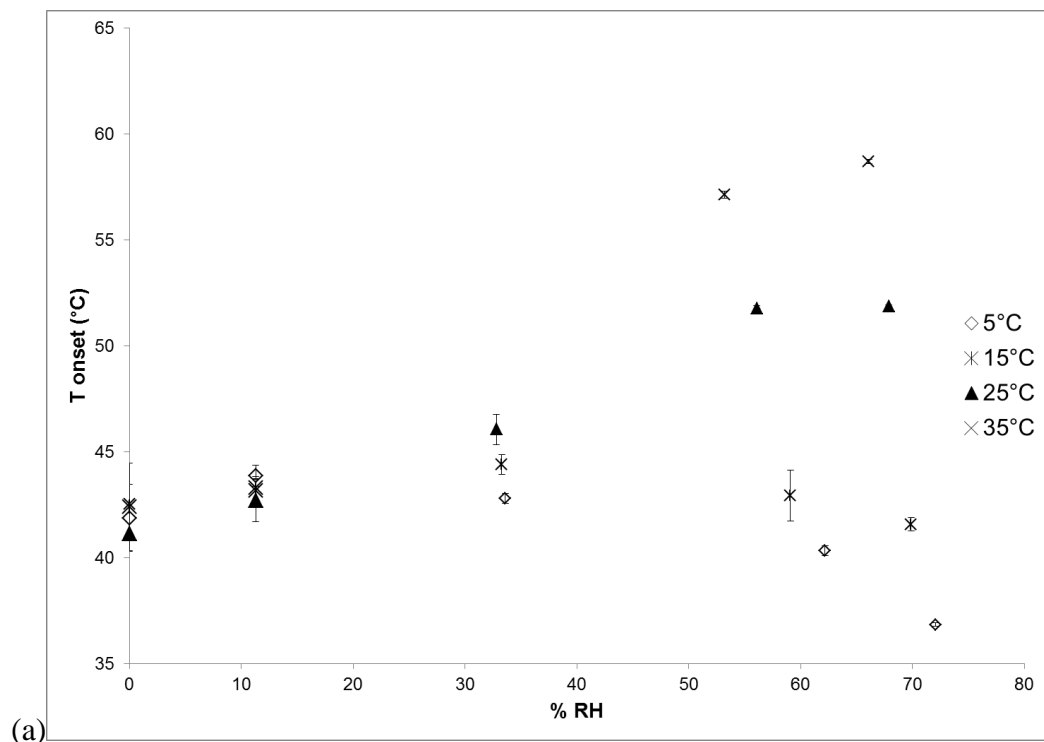
Figure 3.5. Dependence of sub-Tg endotherm peak temperature (a) T_{onset} and (b) $T_{midpoint}$ on %RH and storage temperature for intact pregelatinized waxy maize starch in the non-reversing signal. Error bars represent one standard deviation.
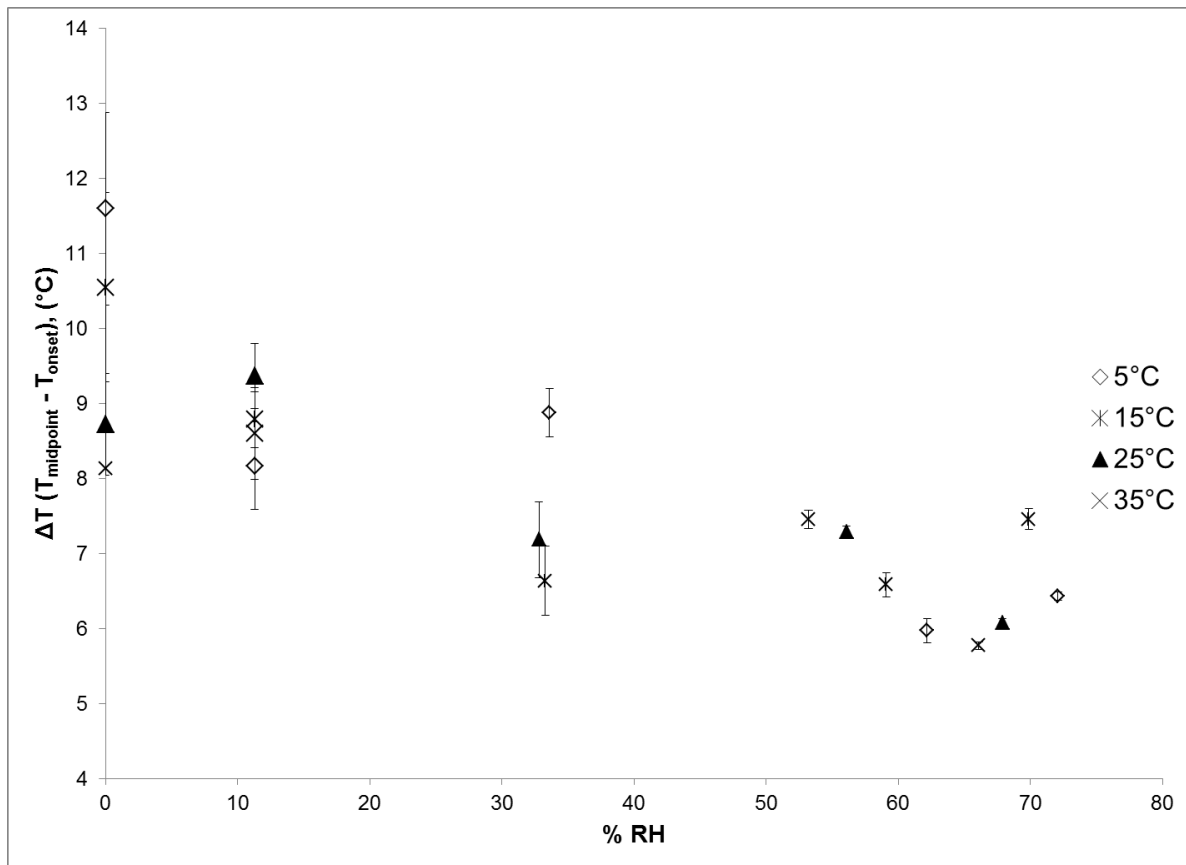
Figure 3.6. Dependence of sub-Tg ΔT ($T_{midpoint} - T_{onset}$) on %RH and storage temperature for intact pregelatinized waxy maize starch in the non-reversing signal. Error bars represent one standard deviation.
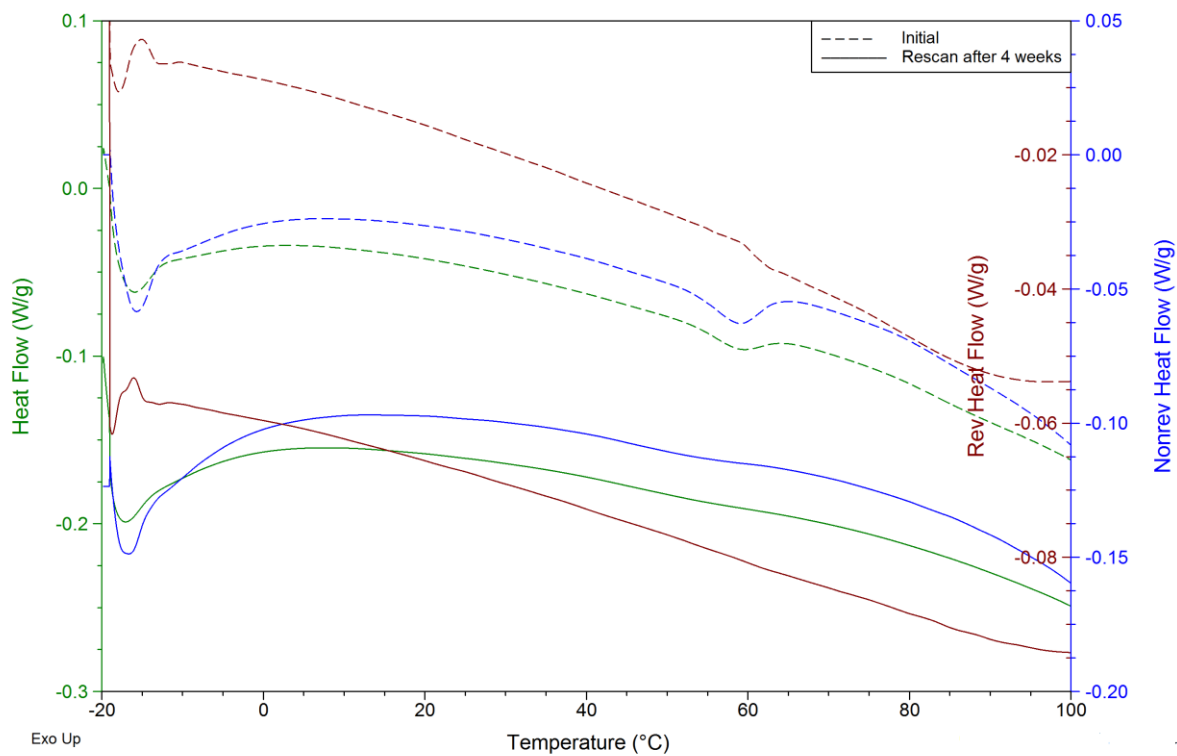
Figure 3.7. MDSC scan of fragmented pregelatinized waxy maize starch stored at 25°C over KI saturated salt solution initially and rescan after 4 weeks of storage.
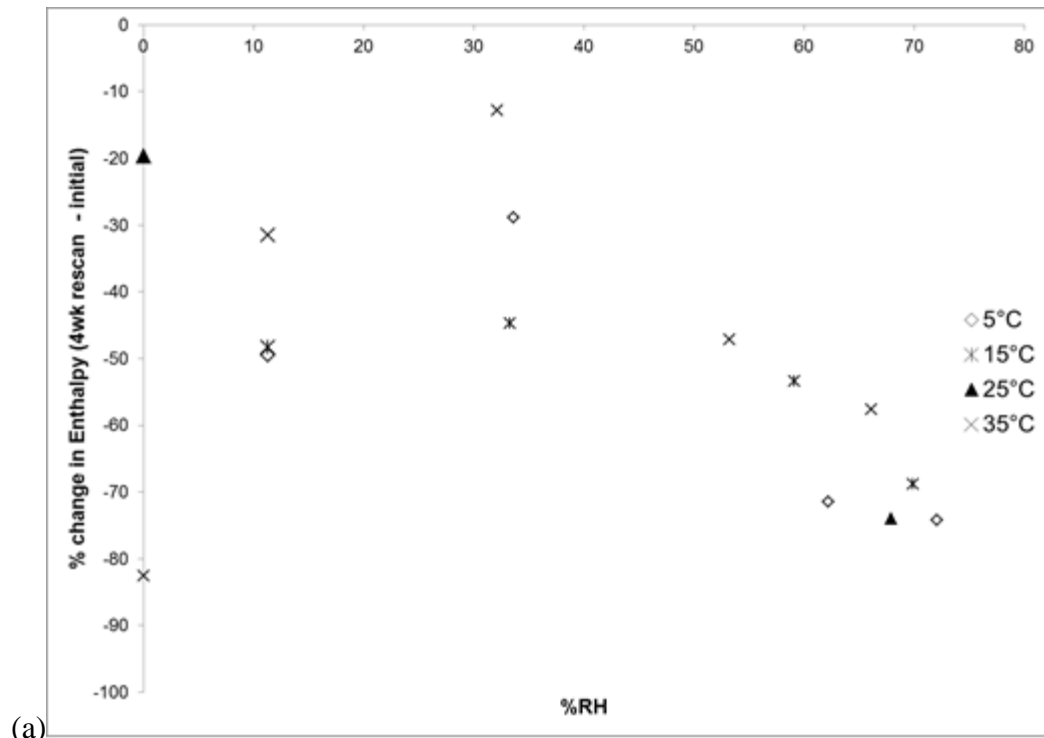
(a)
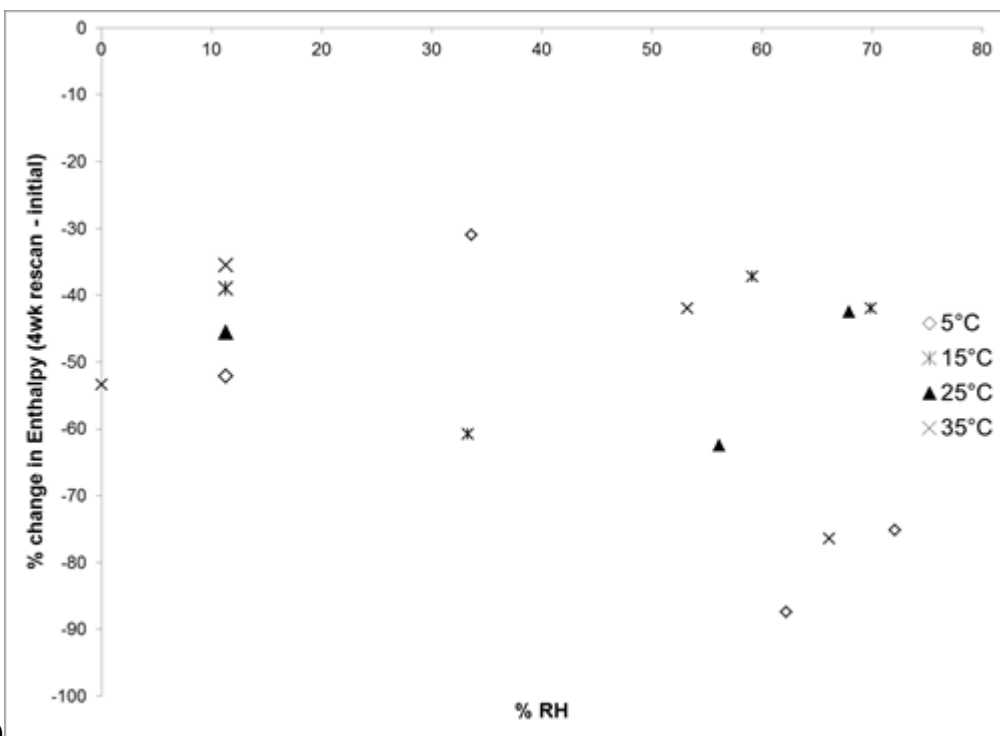
(b)

Figure 3.8. Percent decrease in sub-Tg enthalpy in the non-reversing signal after 4 week storage for (a) fragmented pregelatinized waxy maize starch and (b) intact pregelatinized waxy maize starch.
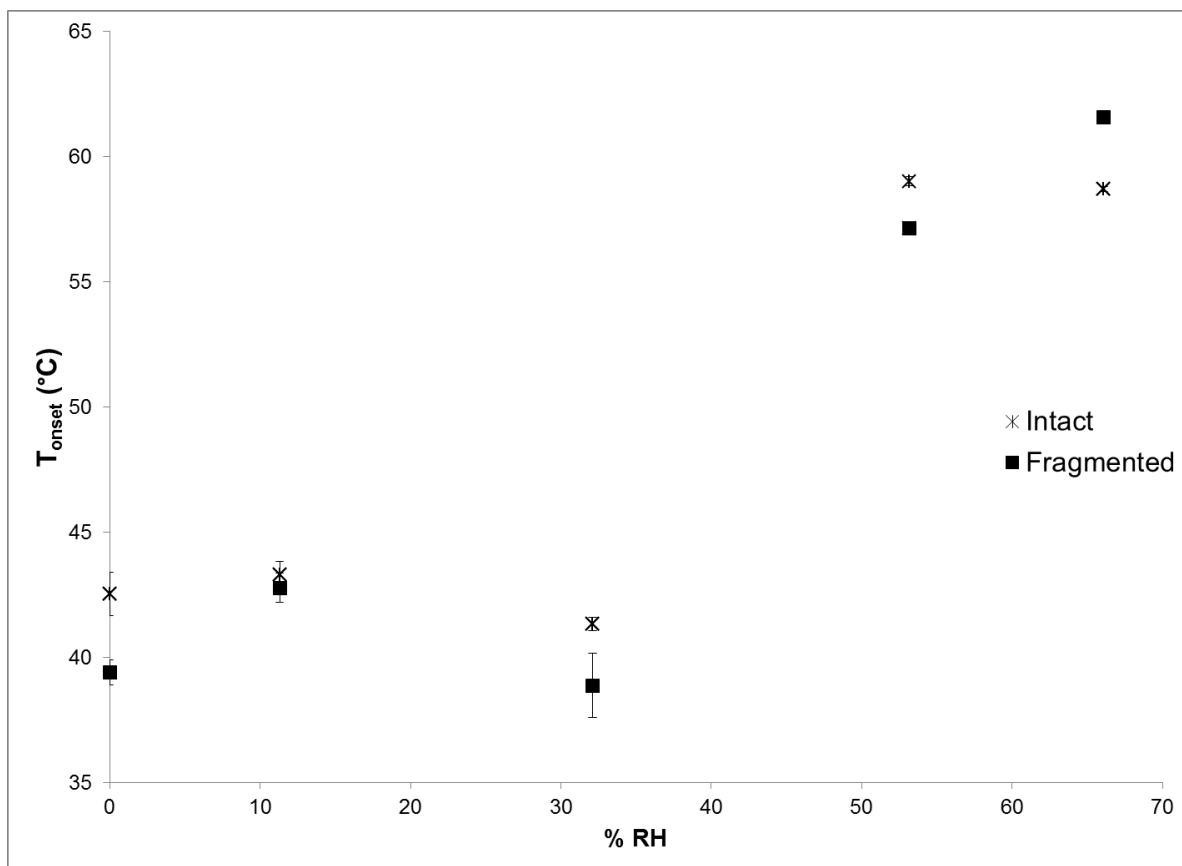
Figure 3.9. Sub-Tg endotherm peak temperature dependence on %RH for intact and fragmented pregelatinized waxy maize starches stored at 35°C. Error bars represent one standard deviation.
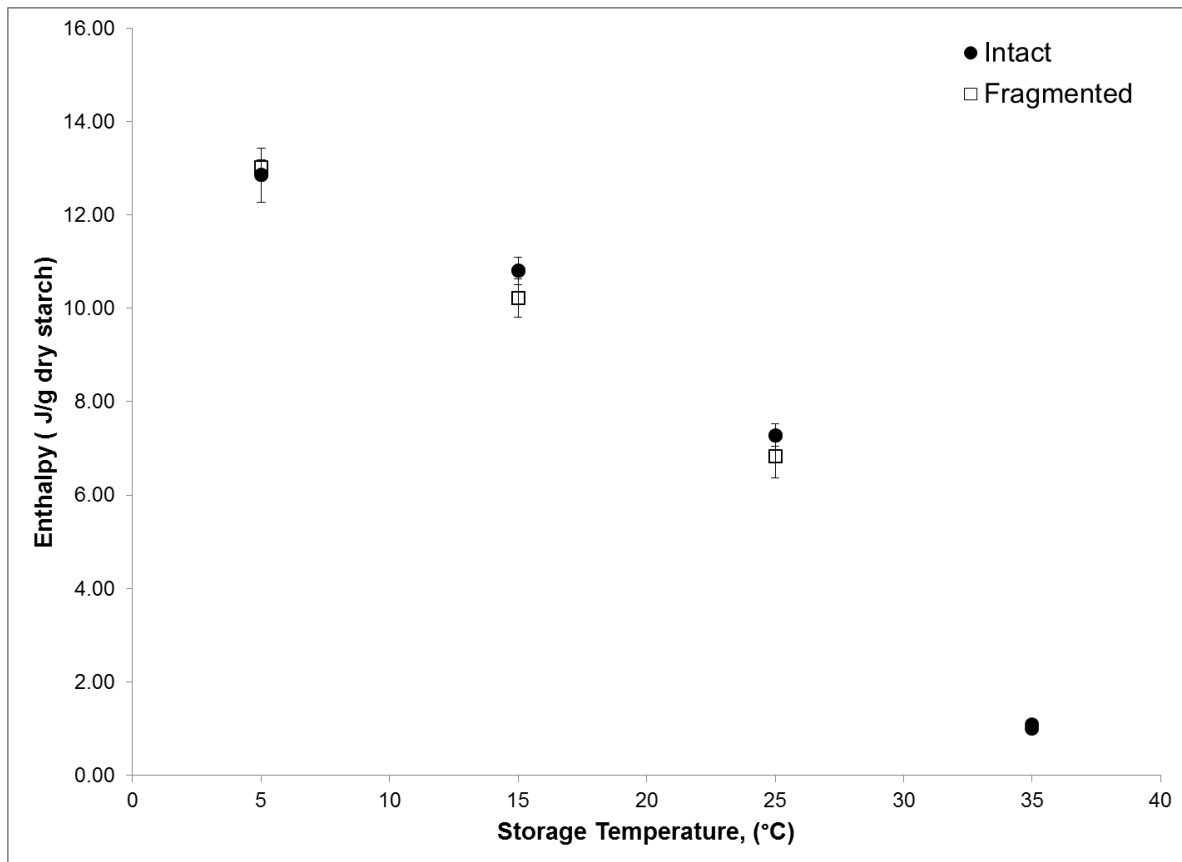
Figure 3.10. Enthalpy associated with MDSC retrogradation endotherm occurring in the non-reversing heat flow between 45 and 65°C for 50% moisture (wet basis) retrograded starch, intact granules and fragmented granules. Error bars represent one standard deviation.
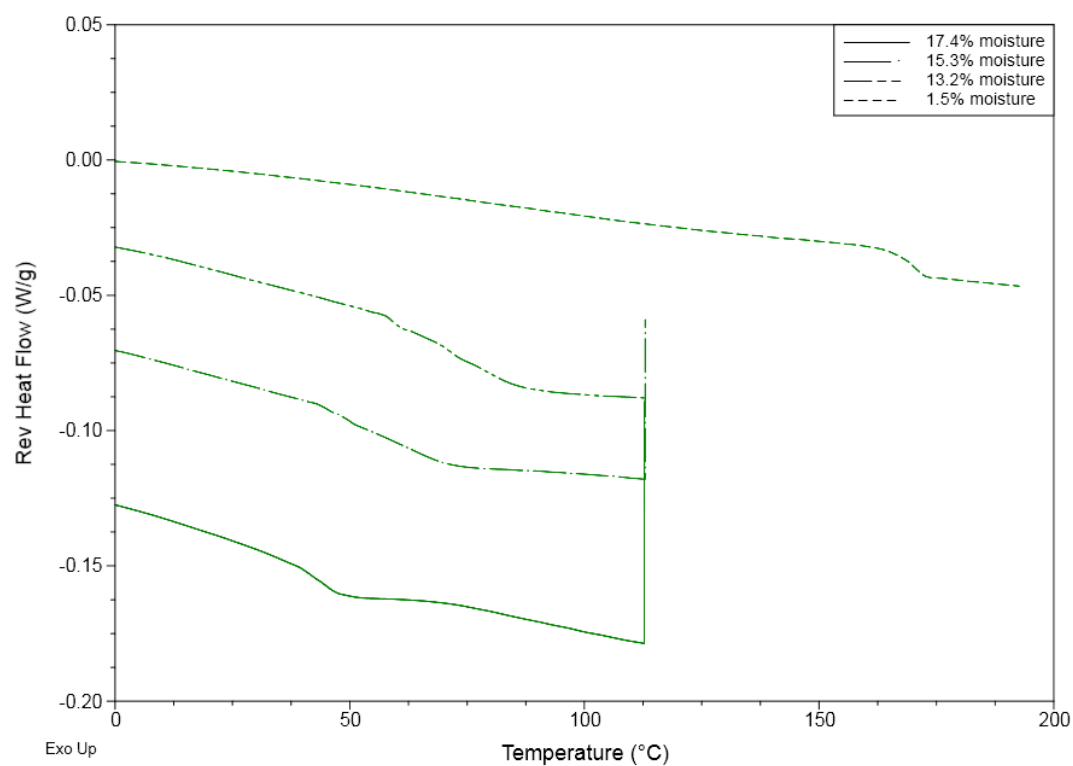
Figure 3.11. MDSC observed glass transition in the reversing heat flow for intact pregelatinized waxy maize starch stored at 5°C.
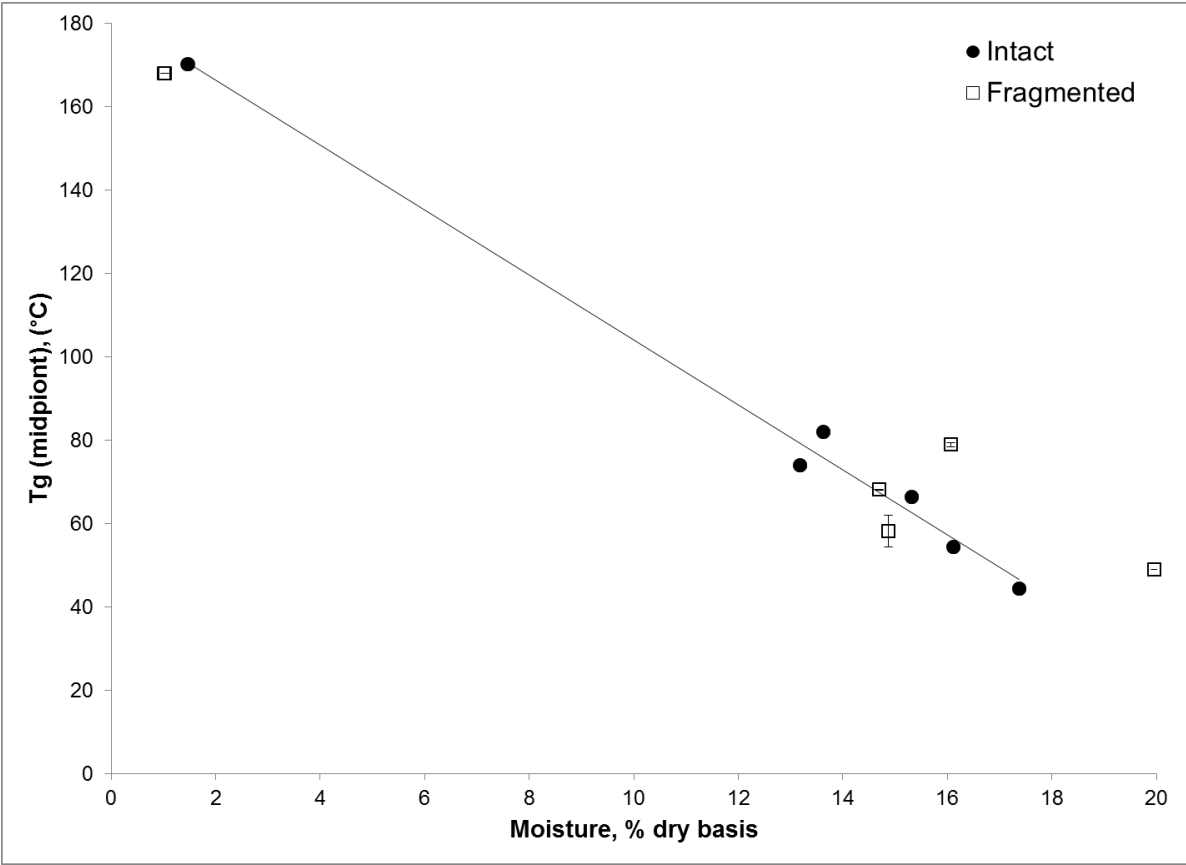
Figure 3.12. Dependence of amylopectin Tg on moisture content for intact and fragmented pregelatinized waxy maize starches. Error bars represent one standard deviation.
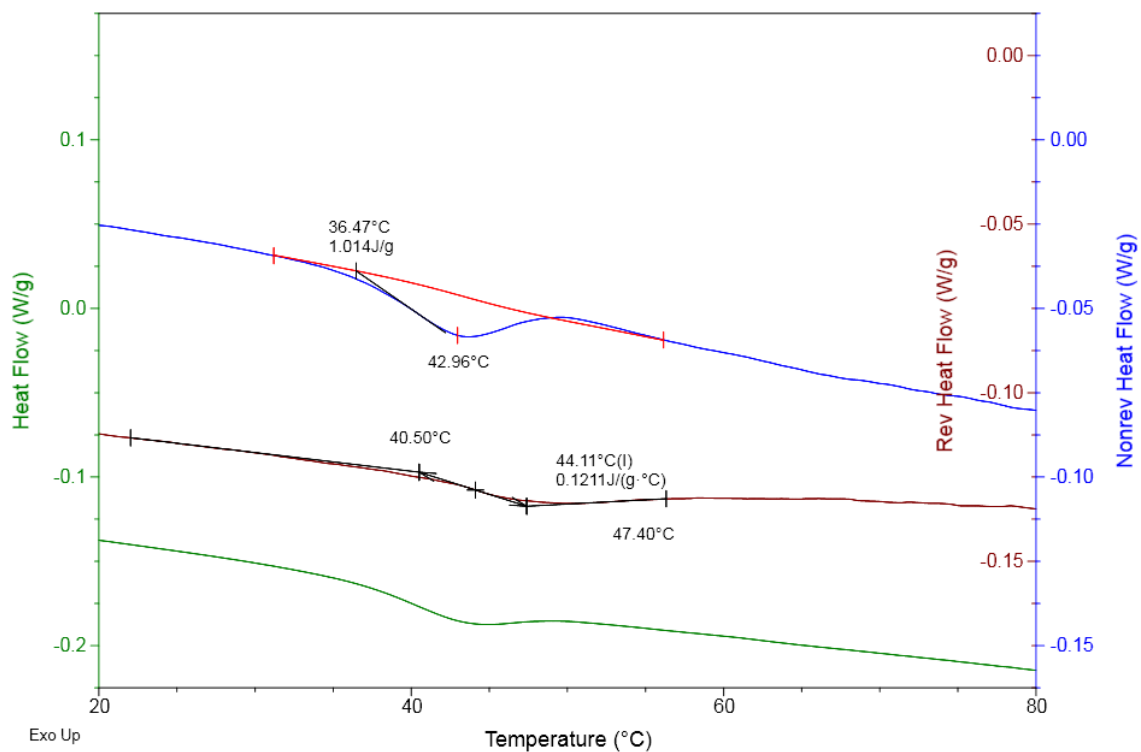
Figure 3.13. MDSC-observed sub-Tg endotherm in the non-reversing phase and glass transition in the reversing heat flow for intact pregelatinized waxy maize starch stored at 72.1% RH and 5°C.
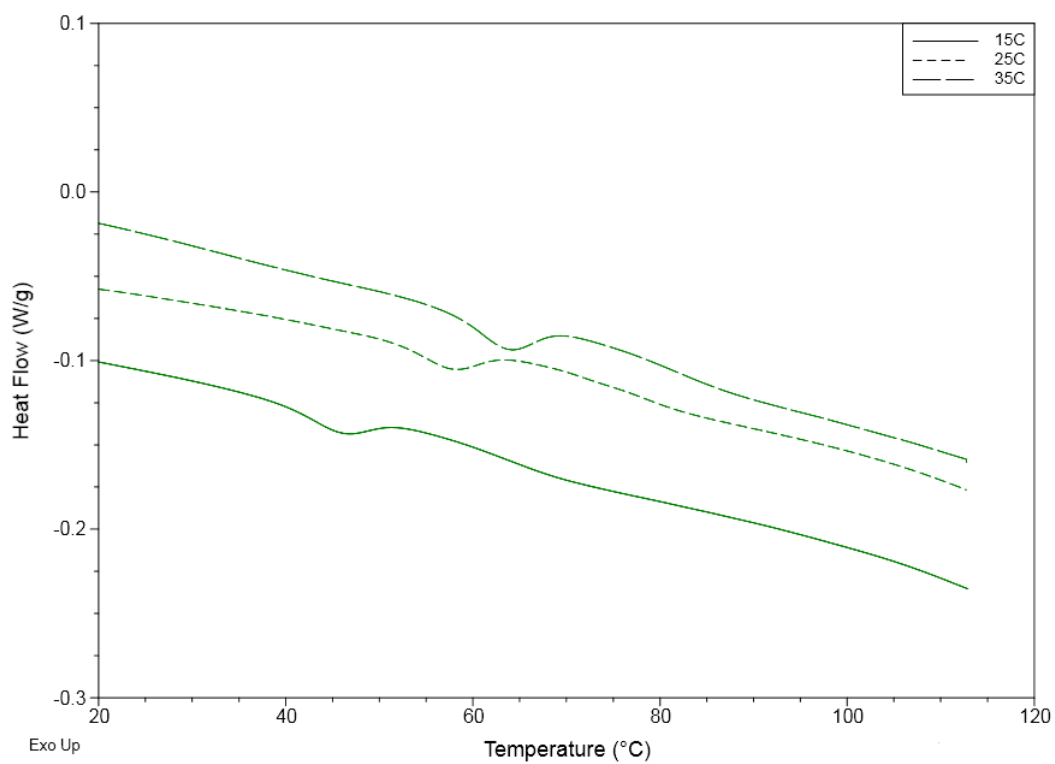
Figure 3.14. MDSC observed sub-Tg and secondary endothermic peak for intact pregelatinized waxy maize starch stored over KI saturated salt slurry at 15, 25 and 35°C.
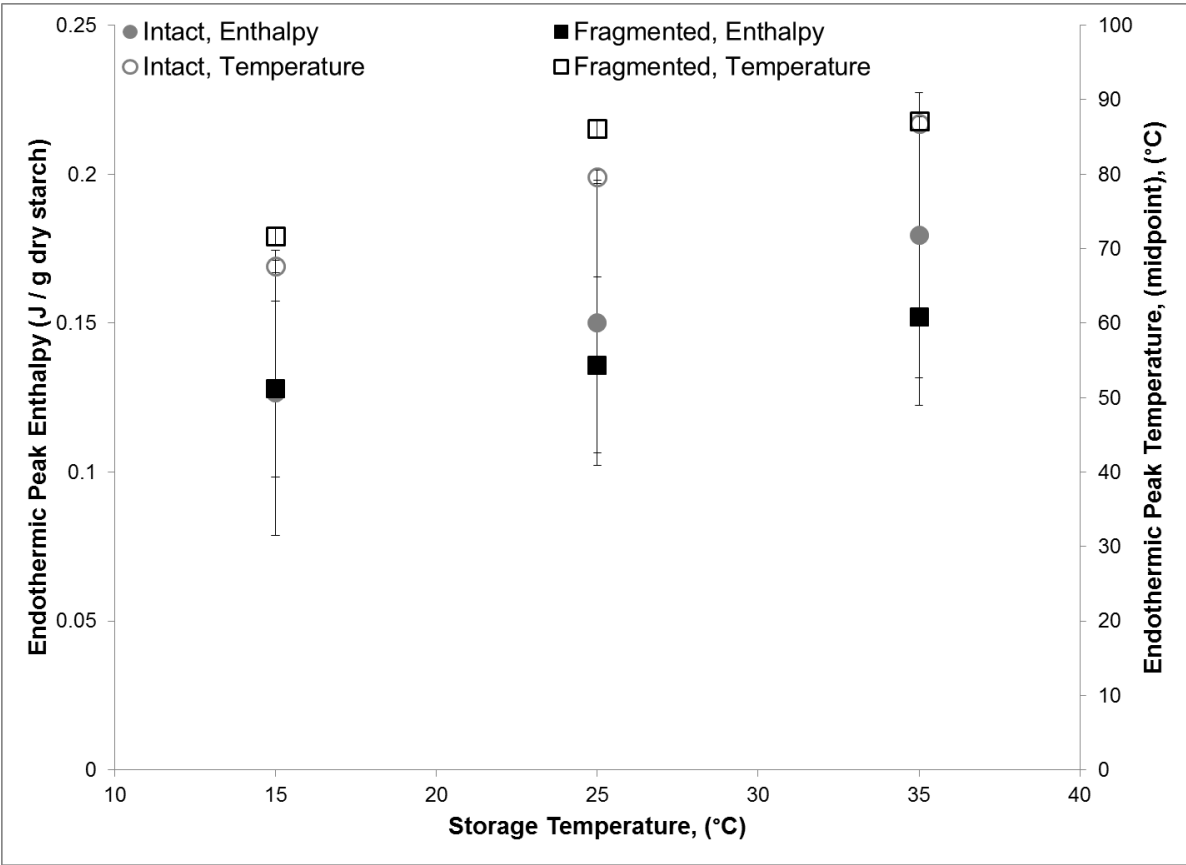
Figure 3.15. Storage temperature effect on second endothermic peak enthalpy and peak temperature for intact and fragmented pregelatinized waxy maize starches stored at ~70% RH. Error bars represent one standard deviation.
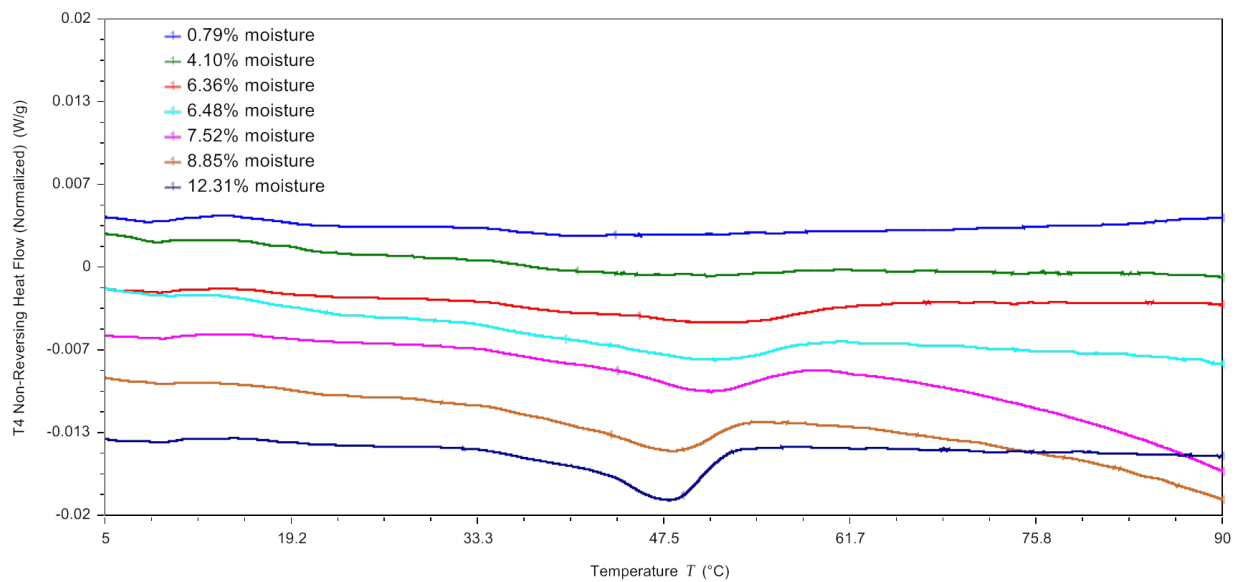
Figure 3.16. MDSC sub-Tg endotherms in the non-reversing heat flow for Carr's water crackers at different moisture contents.
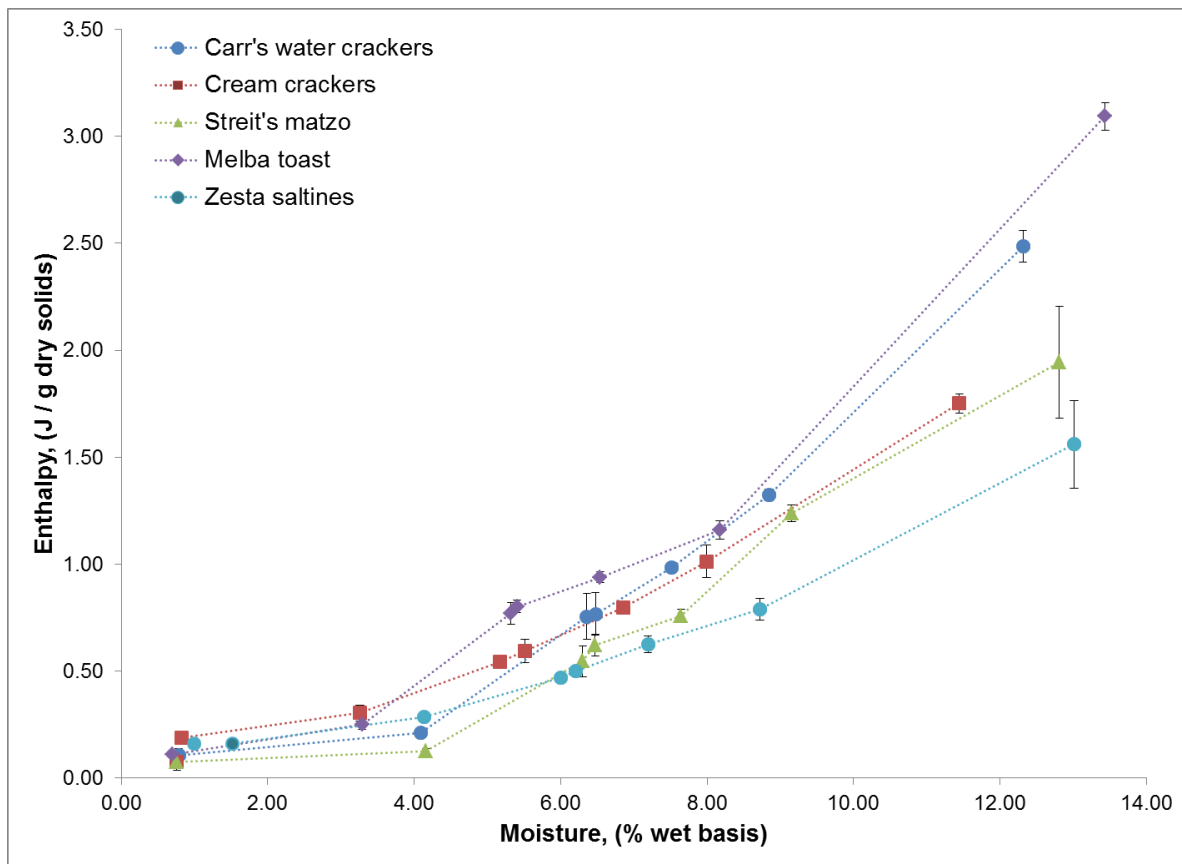
Figure 3.17. MDSC-observed enthalpies of the sub-Tg endotherm in the non-reversing heat flow for commercial crackers at different moisture contents. Error bars represent one standard deviation.

Table 3.1. Dessicant and saturated salt slurries used for pregelatinized waxy maize starch investigation

Salt	%RH[1]				Solubility (g/100g H_2O)[2]			
	5°C	15°C	25°C	35°C	0°C	10°C	20°C	40°C
Desiccant (calcium sulfate)	0.0	0.0	0.0	0.0	--	--	--	--
LiCl	11.3	11.3	11.3	11.3	69.2	74.5	83.5	89.8
$MgCl_2$	33.6	33.3	32.8	32.1	52.9	68.1	73.9	88.5
NaBr	62.2	59.1	56.1	53.2	80.2	85.2	90.8	107
KI	72.1	69.9	67.9	66.1	128	136	144	162

[1]%RH data obtained from Greenspan (1977)

[2]solubility data obtained from Haynes (2012)

Table 3.2. Low moisture cereal-based food products evaluated

Product		Manufacturer	Lot	Manufacturing process	Ingredient statement
Carr's Table Water Crackers		United Biscuits	JUL1615CW 1	Unleavened, baked	Wheat Flour, Vegetable Oil (Palm), Salt
Keeblers Zesta Original Saltine Crackers		Kellogg's	JUN2615 TC1	Sponge/fermented, baked	Enriched Flour, Soybean Oil, Salt, Corn Syrup, Yeast, Baking Soda, Soy Lecithin
Streit's Matzos 100% Whole Wheat		Aron Streit Inc	JAN 15 2016	Unleavened, baked	Unbleached whole wheat flour, Water
S&F Cream Crackers Craquelins		S&F Foods	4156	Yeast leavened, baked	Wheat Flour, Palm Oil, Barley Malt Extract, Salt, Yeast, Sodium Bicarbonate and Sulphites.
Old London Melba Toasts Classic		B&G Foods	05 AUG 15 3	Yeast leavened, baked & toasted	Wheat Flour, Salt, Yeast, Molasses, Distilled Vinegar, Dextrose

Table 3.3. **Dessicant and saturated salt slurries used for commercial cracker investigation**

Salt	%RH[a] at 25°C	Solubility[b] (g/100g H_2O) at 20°C
Desiccant (calcium sulfate)	0	n/a
LiCl	11.3	83.5
KCH_3COO	22.5	256
$MgCl_2$	32.8	73.9
K_2CO_3	43.2	111
$Mg(NO_3)_2$	52.9	90.8
KI	67.9	144

[a] %RH data obtained from Greenspan (1977)

[b] solubility data obtained from Haynes (2012)

n/a - not applicable

3.7 References

Appelqvist IAM, Cooke D, Gidley MJ, Lane SJ. 1993. Thermal-properties of polysaccharides at low moisture .1. An endothermic melting process and water-carbohydrate interactions. Carbohydr. Polym. 20(4):291-9.

Atwell WA, Hood LF, Lineback DR, Varriano-Marston E, Zobel HF. 1988. The terminology and methodology associated with basic starch phenomena. Cereal Foods World 33:306-11.

Badii F, MacNaughtan W, Farhat IA. 2005. Enthalpy relaxation of gelatin in the glassy state. Int. J. Biol. Macromol. 36(4):263-9.

Beckmann J, McKenna GB, Landes BG, Bank DH, Bubeck RA. 1997. Physical aging kinetics of syndiotactic polystyrene as determined from creep behavior. Polym. Eng. Sci. 37(9):1459-68.

Bell LN, Labuza TP. 2000. Moisture Sorption – Practical Aspects of Isotherm Measurement and Use 2nd ed. St. Paul, MN: American Association of Cereal Chemists, Inc.

Biladeris CG. 2009. Structural transitions and related physical properties of starch. In: BeMiller J, Whistler R, editors. Starch: Chemistry and Technology. Burlington, MA: Academic Press.

Chung HJ, Lee EJ, Lim ST. 2002. Comparison in glass transition and enthalpy relaxation between native and gelatinized rice starches. Carbohydr. Polym. 48(3):287-98.

Descamps N, Palzer S, Zuercher U. 2009. The amorphous state of spray-dried maltodextrin: sub-sub-T-g enthalpy relaxation and impact of temperature and water annealing. Carbohydr. Res. 344(1):85-90.

Gonzalez DC, Khalef N, Wright K, Okos MR, Hamaker BR, Campanella OH. 2010. Physical aging of processed fragmented biopolymers. J. Food Eng. 100(2):187-93.

Greenspan L. 1977. Humidity fixed points of binary saturated aqueous solutions. Journal of Research of the National Bureau of Standards - A, Physics and Chemistry 81A(1):89-96.

Haynes WM. 2012. CRC Handbook of Chemistry and Physics. 92nd (internet version 2012) ed. Boca Raton, FL: CRC Press/Taylor and Francis.

Instruments T. 2009. Universal Analysis 2000. In: Instruments T, editor. 4.7A ed: TA Instruments.

Jang JK, Pyun YR. 1997. Effect of moisture level on the crystallinity of wheat starch aged at different temperatures. Starch-Starke 49(7-8):272-7.

Kalichevsky MT, Jaroszkiewicz EM, Ablett S, Blanshard JMV, Lillford PJ. 1992a. The glass-transition of amylopectin measured by DSC, DMTA and NMR. Carbohydr. Polym. 18(2):77-88.

Kalichevsky MT, Jaroszkiewicz EM, Ablett S, Blanshard JMV, Lillford PJ. 1992b. The glass transition of amylopectin measured by DSC, DMTA and NMR. Carbohydrate Polymers 18(2):77-88.

Kilburn D, Claude J, Schweizer T, Alam A, Ubbink J. 2005. Carbohydrate polymers in amorphous states: An integrated thermodynamic and nanostructural investigation. Biomacromolecules 6(2):864-79.

Kim YJ, Suzuki T, Hagiwara T, Yamaji I, Takai R. 2001. Enthalpy relaxation and glass to rubber transition of amorphous potato starch formed by ball-milling. Carbohydr. Polym. 46(1):1-6.

Li Q. 2010. Investigating the glassy to rubber transition of polydextrose and cornflakes using automatic water vapor sorption instruments, DSC, and texture analysis. [Master of Science]. Urbana, IL: University of Illinois at Urbana-Champaign. 77-117 p.

Livings SJ, Breach C, Donald AM, Smith AC. 1997. Physical ageing of wheat flour-based confectionery wafers. Carbohydr. Polym. 34(4):347-55.

Manley D. 2011. Manley's Technology of Biscuits, Crackers and Cookies 4th ed: Woodhead Publishing.

Perera DY. 2003. Physical aging of organic coatings. Progress in Organic Coatings 47:61-76.

Perez S, Bertoft E. 2010. The molecular structures of starch components and their contribution to the architecture of starch granules: A comprehensive review. Starch-Starke 62(8):389-420.

Shogren RL. 1992. Effect of moisture content on the melting and subsequent physical aging of corn starch. Carbohydr. Polym. 19(2):83-90.

Silverio J, Fredriksson H, Andersson R, Eliasson AC, Aman P. 2000. The effect of temperature cycling on the amylopectin retrogradation of starches with different amylopectin unit-chain lenght distribution. Carbohydr. Polym. 42:175-84.

Slade L, Levine H. 1988. Non-equilibrium melting of native granular starch: part I. temperature location of the glass transition associated with gelatinization of A-type cereal starches. Carbohydrate Polymers 8:183-208.

Struik LCE. 1987. The mechanical and physical ageing of semicrystalline polymers: 1. Polymer 28:1521-33.

TA Instruments - Waters L. 2011. TRIOS version 2.3.4 1613. 2.3.4 ed. New Castle, Delaware, USA.

Thiewes HJ, Steeneken PAM. 1997. The glass transition and the sub-T-g endotherm of amorphous and native potato starch at low moisture content. Carbohydr. Polym. 32(2):123-30.

Yuan RC, Thompson DB. 1994. Sub-Tg thermal properties of amorphous waxy starch and its derivatives. Carbohydr. Polym. 25(1):1-6.

Zeleznak KJ, Hoseney RC. 1986. The role of water in the retrogradation of wheat starch gels and bread crumb. Cereal Chem. 63(5):407-11.

CHAPTER 4

CHARACTERIZATION OF THE SUB-TG ENDOTHERM BY MDSC AND ITS RELATION TO STRUCTURAL PROPERTIES OF PREGELATINIZED GRANULAR WAXY MAIZE STARCH AT LOW MOISTURE CONTENTS OBSERVED BY X-RAY DIFFRACTION, FTIR-ATR and ^{13}C CP/MAS NMR

4.1 Abstract

The occurrence of an endothermic event, typically observed below the conventional glass transition, is a common feature of many polymer systems, including starch amylopectin and other polysaccharides. This sub-Tg endotherm was characterized for pregelatinized waxy maize starch at low moisture contents (1 to14% wet basis) by MDSC and associated with structural conformations observed by FTIR-ATR and powder x-ray diffraction in relation to retrograded pregelatinized waxy maize starch at 50% moisture content and non-gelatinized waxy maize starch. An endotherm with a peak temperature between 55 and 65°C was observed for all starch moisture contents in the non-reversing heat flow of the MDSC scan for all pregelatinized waxy maize starches. Peak enthalpy was exponentially related with increasing starch moisture content. A similar endotherm was observed for the retrograded starch; however, as measured by x-ray powder diffraction, the retrograded starch exhibited the typical B-type crystalline pattern, while only an amorphous halo was observed for the pregelatinized starches at low moisture contents. FTIR-ATR spectra revealed strong absorbances at 995 and 1022 cm^{-1} for all samples. Intensity at 1022 cm^{-1}, the peak commonly associated with the amorphous starch fraction, substantially decreased following the DSC scan from 0 to 120°C at 10°C/minute, indicating that short-range structural order had increased in the pregelatinized starch samples, though that order was not correlated with crystallinity, as evidenced by low peak absorbance intensities at 1045 cm^{-1}. However, the peak at 1080 cm^{-1}, also commonly attributed to amylopectin order, was observed to increase with increasing moisture content of the pregelatinized waxy maize starches. Increasing order through increasing amylopectin double helical content as moisture content increased in pregelatinized waxy maize starches was confirmed by solid-state ^{13}C CP/MAS NMR. Thus, monitoring FTIR-ATR spectra in confirmation with NMR, may be a useful tool for understanding the structural state of amylopectin at low moisture contents, in particular, as

related to the kinetic development of structural ordering and increased molecular mobility below the measured glass transition.

4.2 Introduction

In aqueous starch systems, 4 types of thermal events are generally encountered: (1) a so-called sub-Tg endotherm, (2) a glass transition, (3) various crystal melting processes and (4) a high-temperature endotherm which marks the transition into a thermoplastic melt (Thiewes and Steeneken 1997). The occurrence of an endothermic event, typically observed below the conventional glass transition, is a common feature of many semicrystalline polymers, including starch, which develops semi-crystalline shells termed "growth rings" through the organization of amylopectin molecules (Perez and Bertoft 2010). For example, Chung and others (2002) reported a sub-Tg endotherm peak temperature for gelatinized rice starch at 12% moisture as approximately 55°C and Tg as approximately 65°C. Similarly, Zeleznak and Hoseney (1987) reported the glass tranisition of pregelatinized wheat starch as 65°C and higher for moisture contents of 12% and below. This sub-Tg endotherm has been observed for other semicrystalline polymers (Beckmann and others 1997; Struik 1987), starch (Chung and others 2002; Kalichevsky and others 1992a; Kim and others 2001; Shogren 1992; Yuan and Thompson 1994), maltodextrin (Descamps and others 2009), confectionary wafers (Livings and others 1997), and cornflakes (Gonzalez and others 2010; Li 2010), among others.

While the origin of this sub-Tg thermal event remains controversial, physical aging is the most prevalent explanation. Physical aging, also referred to as enthalpy relaxation, occurs for a glassy material as a result of the non-equilibrium state spontaneously relaxing toward a more energetically favorable state. Physical aging is a general, thermoreversible phenonmenon, occurring for any glassy material as a result of its non-equilibrium state attempting to regain equilibrium (Perera 2003). In particular, Shogren (1992) characterized the physical aging of gelatinized maize starch at moisture contents <20% through the observance of an endotherm peak between 36 to 52°C measured by DSC. By definition, physical aging is a phenomenon that occurs below Tg, however, Li (2010) recently observed the presence of a similar endothermic event in cornflakes at different moisture contents, with the exception that the event was observed both below and above the glass transition of the cornflakes.

Regardless of its origin, the presence of this sub-Tg endothermic event has practical implications for low moisture starchy food systems in that it is remarkably similar to amylopectin retrogradtion, which is commonly considered to only occur at higher moisture contents, above the system glass transition. Amylopectin retrogradation is a non-equilibrium thermoreversible recrystallization process which is governed by a consecutive three step mechanism of nucleation, propagation and maturation (Kalichevsky and others 1990; Keetels and others 1996; Slade and Levine 1988). After gelatinization, the reordering of the amylopectin molecules results in heterogeneous recrystallization that is responsible for the broad endotherm observed by DSC in which the least stable crystals melt at lower temperatures and the remaining crystallites, of higher quality, melt at higher temperatures (Elfstrand and others 2004).

A range of physical and chemical techniques, including viscometry and rheological measurements, turbidity measurements, FTIR, NMR , X-ray diffraction, and differential scanning calorimetry, have been used to study the retrogradation of amylopectin. These methods differ in the level to which the starch is probed, from the macroscopic to the molecular level, and as such, each can give a different view as to changes occurring during and after retrogradation. In general, using a combination of 2 to 3 methods allows for cross comparison and provide a more complete understanding of the retrogradation process (Karim and others 2000). For example, X-ray diffraction is commonly used together with DSC to assess starch retrogradation. Starch granules, being partially crystalline, give distinct X-ray diffraction patterns (Sarko and Wu 1978) that are lost during gelatinization and subsequently partially reformed during retrogradation. Additionally, the Fourier-transform infrared (FTIR) spectra of starch solutions in the 1300-800 cm^{-1} region are sensitive to the structural conformation. Most bands in this region arise from highly coupled C-C and C-O stretching modes, that while difficult to assign, changes in these modes can be measured over time as a means to assess the extent of retrogradation (Goodfellow and Wilson, 1990; Wilson and others, 1987). Beyond measurements of crystalline order, solid-state ^{13}C CP/MAS NMR has been successfully used to quantify the amylopectin double helical order in starch, both independent of and within crystalline arrays (Atichokudomchai and others 2004; Bogracheva and others 2001; Gidley and Bociek 1988; Lewen and others 2003; Paris and others 1999; Tan and others 2007).

Amylopectin retrogradation is generally considered to be directly responsible for bread staling, in which the bread product is characterized by considerable firming and texture changes.

As such, the similarity between the sub-Tg endotherm in amylopectin at low moisture contents to conventional amylopectin retrogradation at higher moisture contents, suggests that texture changes of low moisture starch based food products, such as crackers and snack foods, may be similarly correlated with staling. Characterization of the sub-Tg endotherm in relation to amylopectin structural changes that may occur at low moisture contents is critical for understanding texture and physical changes that may occur in low moisture starch-based food applications. Thus, the objective of this work is to characterize the sub-Tg endotherm of pregelatinized waxy maize starch at low moisture contents by MDSC in relation to any structural differences that may be observed by x-ray diffraction, FTIR-ATR and ^{13}C CP/MAS NMR.

4.3 Materials and methods

Commercial, pregelatinized, spray-cooked unmodified waxy maize starch was obtained (X'PandR SC, Tate & Lyle, Hoffman Estates, Illinois) , and the initial moisture content of the starch was determined via quick drying with a halogen oven (CompuTrac Max 1000, Arizona Instruments, Chandler, Arizona), calibrated to vacuum oven drying for 4 hours at 25-100 mmHg and 105°C. The initial water activity of the starches was determined using an Aqualab 4TE water activity meter (Decagon Devices, Pullman, Washington). The pregelatinized, spray-cooked waxy maize starch was equilibrated over saturated salt solutions encompassing a range of %RH values (Table 4.1). Saturated salt slurries were prepared by adding an excess amount of salt into deionized water according to the known solubility values at 40°C, heating the slurry to approximately 50°C for about 2 hours, while stirring on a standard stir plate and then cooling to room temperature.

A sufficient amount of saturated salt slurry was added to storage containers (airtight and water proof plastic containers commercially known as "Lock & Lock") to completely cover the bottom of the container. About 4 grams of "as is" pregelatinized waxy maize starch granules were weighed into a small plastic cup and transferred to the "Lock & Lock" container with the saturated salt slurry. Containers were kept in an incubator at a storage temperature of 25°C. After constant weight was reached, defined as when the sample weight changed by less than 2mg/g dry weight between successive weight measurements (Bell and Labuza 2000), the equilibrium moisture content was determined using the initial sample weight, the initial moisture content and the equilibrium weight.

The onset and peak temperature, and enthalpy of thermal transition in the equilibrated starch samples were determined using Modulated Differential Scanning Calorimetry (MDSC) with the DISCOVERY Differential Scanning Calorimeter instrument (TA Instruments, New Castle, Delaware). MDSC allows for the separation of the heat flow into the reversing heat flow (heat capacity component) and non-reversing heat flow (kinetic component). Equilibrated samples, in duplicate, were taken from the "Lock & Lock" containers and transferred to DSC T-zero aluminum hermetic pans and sealed with internal hermetic lids immediately after transferring out of the "Lock & Lock" containers in order to maintain the appropriate moisture content and %RH within the sample throughout the study. Samples were equilibrated at 0°C and scanned using a modulated heating profile with a rate of 1°C/min, oscillation period of 80 seconds, and amplitude of 0.5°C from 0°C to 120°C (MDSC first scan). The onset temperature, peak temperature, and enthalpy of the transitions of observed peaks were determined, in triplicate, through peak integration using the TRIOS Software version 2.3.4. 1613 from TA Instruments (2011). Observed glass transitions were also analyzed for onset temperature, midpoint temperature, and enthalpy change using the glass transition by tangent analysis option in the TRIOS software. Each scan was analyzed in triplicate.

Wide-angle x-ray scattering (WAXS) diffactograms were acquired over the range of 5 to 65° 2θ (0.05°) using a Bruker D5000 diffractometer (Bruker AXS, Inc., Madison, Wisconsin) equipped with a copper tube operating at 40kV and 30 mA, producing 0.154 nm CuK_α radiation. Experiments were carried out in the Frederick Seitz Materials Research Laboratory Central Research Facilities, University of Illinois at Urbana-Champaign.

Fourier-transform infrared, attenuated total reflectance (FTIR-ATR) spectra of the equilibrated starch samples were acquired using a Thermo Nicolet iS™10 FT-IR with the Scientific Smart iTR™ diamond attenuated total reflectance (ATR) accessory with nitrogen purge (Thermo Scientific, Waltham, Massachusetts). Spectra were obtained at a resolution of $4cm^{-1}$ from 4000 to 400 cm^{-1} and averaged over 100 scans, recorded against an empty cell as background. Deconvoluted spectra were baseline corrected in the 1200 to 800 cm^{-1} region and peak heights were analyzed at 995, 1022, 1044, 1078 and 1151 cm^{-1} using the OMNIC 9.1.27 software (Thermo Fisher Scientific 2012) . Duplicate FTIR-ATR spectra were obtained of each sample, and each spectrum was analyzed in triplicate.

^{13}C cross-polarization MAS (CPMAS) NMR experiments of the equilibrated pregelatinized starch samples and native, ungelatinized waxy maize starch were conducted at 7.04 T on a Varian Unity Inovaspectrometer at the SCS NMR Facility of the University of Illinois at Urbana-Champaign, operating at 75.4 MHz at room temperature. The samples were ground into a fine powder to make the sample homogeneous, and then packed into 4 mm o.d. zirconia rotors. A 4 mm APEX HX Chemagneticsprobe was used for all MAS experiments under a magic-angle spinning rate of 10 kHz and proton decoupling. The ^{13}C chemical shifts were referenced to an external standard sample of hexamethylbenzene (HMB, δiso= 17.3 ppm for the methyl peak, relative to TMS at 0 ppm). The ^{1}H selective 90 degree pulse length determined on the above-mentioned compound was 2.25 μs. A recycle delay of 2s and a contact time of 1ms were used for all experiments (optimized on the native maize starch sample), with a number of transients between 10,000 to 12,000 scans acquired. The MNOVA software (Mestrelab Research 2013) was used to peak fit all resulting spectra. The low a_w (0% RH) and high a_w (67.9% RH) starch samples were run in duplicate, and all spectra were analyzed in triplicate.

4.4 Results and discussion

4.4.1 Characterization of sub-Tg endothermic transition by MDSC

A sub-Tg endotherm with a peak temperature between 55 and 65°C was observed at all starch moisture contents in the non-reversing heat flow of the MDSC scan for the pregelatinized waxy maize starch (Figure 4.1), indicating that this peak is related to a kinetic event occurring in the starch granule. A similar peak with substantially higher enthalpy was also observed for the 50% moisture retrograded starch sample. At this higher moisture content, the retrograded sample at room temperature is above Tg, which is well below 0°C, while the pregelatinized waxy maize starch samples were below Tg, which is approximately 65°C and above for moisture contents of 12% and below (Zeleznak and Hoseney 1987). The starch retrogradation peak for the 50% moisture sample is due to the readoption of double helical chain structures and subsequent aggregation and crystallization of those chains. Thus, the similarity to the sub-Tg peak warrants closer investigation as retrogradation is generally considered negligible for samples below their Tg.

The enthalpy of the sub-Tg thermal transition exhibited an exponential relationship with increasing starch moisture content (Figure 4.2), while onset and peak temperature were not influenced by starch moisture content. Literature reports of the sub-Tg endotherm have also indicated that, in general, as moisture content increased, enthalpy of the peak increased, while the onset and midpoint peak temperatures were independent of moisture content (Badii and others 2005; Chung and others 2002; Shogren 1992; Thiewes and Steeneken 1997).

The temperature range over which the sub-Tg peak occurred, characterized by ΔT ($T_{midpont} - T_{onset}$), varied from a 6 to 15°C temperature span, and ΔT decreased with increasing starch moisture content (Figure 4.3). This result indicates that as starch moisture content increased, structure within the amylopectin network increased or became more "perfect," presumably due to greater chain mobility allowing better realignment. At lower starch moisture contents, amylopectin chains have less mobility and a greater variety of chain structures is reformed, leading to a wider temperature span in the sub-Tg transition. Interestingly, ΔT for the retrograded starch sample at 50% moisture content was approximately 24°C, much broader than for the sub-Tg though the peak itself was also significantly larger. In addition, the retrogradation peak encompasses both double helical structure formation and chain aggregation, whereas at the lower moisture contents, sufficient mobility may not exist to promote all structure reformation associated with retrogradation and the sub-Tg may presumably arise from partial structure reformation.

For starch containing 12.16% and 13.91% moisture, a glass transition was also observed in the reversing heat flow with Tg_{mid} at 82.2 and 99.2°C respectively (Figure 4.4). In both instances, the glass transition immediately followed the sub-Tg endotherm and was within the temperature range of the amylopectin glass transition temperature for similar starch moisture contents previously reported in the literature (Biladeris 2009). A glass transition was not observed for the retrograded starch sample at 50% moisture, but, as Kalichevsky and others (1992b) reports, Tg in a native starch granule is often easier to observe than for retrograded starch since the amylopectin in native starch is heterogeneous in a relatively organized fashion, at least when compared with retrograded amylopectin. At 50% moisture content, the literature reported glass transition temperature of amylopectin is well below 0°C, outside of the temperature range investigated here.

Amylopectin can be described as a semicrystalline polymer consisting of a mobile amorphous phase, a rigid amorphous phase and a crystalline phase. The mobile amorphous phase contributes to the phase transitions occurring in the bulk amorphous phase and would be the primary contributor to the observed glass transition. The rigid amorphous phase is linked to thermal transitions occurring in the amorphous region directly connected to the crystalline lamellae and structural rearrangements could still occur within this region above the observed Tg. Below Tg, crystallization or the propagation of the order of neighboring amylopectin chains is inhibited, but the formation of double helices within an amylopectin chain may be possible. The double helices could then serve as the nuclei that would propagate amylopectin order during retrogradation.

Thus, the sub-Tg endotherm may be attributed to double helical reformation, but without crystalline order occurring before the glass transition. Retrogradation, as occurring above Tg, would encompass both double helical reformation and crystallization concurrently. This hypothesis is further supported by the observance of a second endotherm for these samples in the MDSC non-reversing heat flow concurrent to or immediately following the glass transition (Figure 4.5). This second endotherm was only observed for those samples that also exhibited a glass transition and would presumably be attributed to the reordering of the double helices above Tg.

4.4.2 Characterization of starch crystallinity by X-ray diffraction

Starch granules, being partially crystalline, give distinct X-ray diffraction patterns (Sarko and Wu 1978). Powder diffraction patterns of starch show relatively broad peaks superimposed on an amorphous "halo." The relative intensity of these two features can be used to estimate the level of crystalline order; for example, broad diffraction peaks indicate either imperfect or relatively small crystallites (Cooke and Gidley 1992). Thus, X-ray diffraction patterns of the low moisture pregelatinized waxy maize starch samples were acquired allowing for detection of crystallinity, if any.

Native, non-gelatinized waxy maize starch exhibited the typical A-type diffraction pattern typically associated with cereal starches, whereas the starch at 50% moisture exhibited the typical B-type structure common for retrograded starch, though at lower intensity due to dilution with a higher concentration of water in the sample (Figure 4.6). B-type crystallinity

generally arises from retrograded starch that undergoes "fast" recrystallization, particularly when retrogradation occurs at lower temperatures. The more tightly packed A-type polymorph, though more thermodynamically stable, requires a higher energy barrier for formation, and only forms for retrograded starch that recrystallizes slowly (Gidley 1987). The pregelatinized waxy maize starches at moisture contents from 1 to 14% exhibited no discernible diffraction pattern amidst the amorphous "halo." Thus, the starch samples did not contain any detectable level of crystallinity in the inherent structure, which aligns with the hypothesis that double helical structures may reform, but the helices do not realign and recrystallize when the starch is below its glass transition.

4.4.3 Characterization of amylopectin short-range order by FTIR-ATR

FTIR-ATR has been used as a tool to investigate short-range order of starch and describe its structure, particularly as it relates to the gelatinization and retrogradation processes (Capron and others 2007; Warren and others 2013; Goodfellow and Wilson 1990; Wilson and others 1987; van Soest and others 1995; Sevenou and others 2002). The FTIR-ATR spectra of the equilibrated pregelatinized waxy maize starches were dominated by bands in the regions of 3700 to 3000 cm^{-1} and 1300 to 800 cm^{-1} (Figure 4.7). Absorbance bands in the 3700 to 3000 cm^{-1} region are known to arise from OH bond stretching associated with water (Brubach and others 2005), and have little relevance here other than as an indication of the relative moisture content in each sample.

The most important absorption bands for starch are due to C−C and C−O stretching modes and C−O−H bending modes and are observed in the region of 1300 to 800 cm^{-1}. While difficult to assign given that each band is linked to another as a result of highly coupled vibrational modes that create differences in assignment, comparative changes in these modes can be measured as a means to assess the extent of structural changes or crystallinity of starch (Goodfellow and Wilson 1990; Wilson and others 1987; Capron and others 2007). Broadly speaking, the principal band associated with amorphous starch has previously been assigned to absorbance at 1022 cm^{-1}, while shoulders around 1045 and 995 cm^{-1} have been assigned to crystalline starch (Capron and others 2007; van Soest and others 1995).

The spectra in the region of interest for the pregelatinized, spray-cooked waxy maize starch samples at various relative humidity conditions are shown in detail in Figure 4.8. Clearly,

a substantial increase in absorbance intensity occurs between relative humidity conditions of 56.1 and 67.9% (12.16% to 13.91% moisture content, wb), so for ease of viewing at the relative humidity conditions <67.9%, these spectra are again shown in Figure 4.9. The substantial increase in absorbance by the starch stored at 67.9% RH may be due to the transition from the glassy to the rubbery state.

All spectra show a large peak around 995 cm^{-1} with overlapping shoulders around 1022 and 1045 cm^{-1}. As stated earlier, the absorbances at 1022 and 1045 cm^{-1} are commonly attributed to the amorphous and crystalline starch fractions, respectively, and the ratio of these intensities is commonly used to describe the relative the amount of starch crystallinity. However, X-ray diffraction of these samples has shown that no detectable crystallinity existed within these starch structures (Figure 4.6) despite the observance of a clear shoulder at 1045 cm^{-1} in these samples. Regardless, to determine if the peaks at 995, 1022 and 1045 cm^{-1} were related to the amorphous or crystalline fraction of amylopectin, the pregelatinized starches were subjected to a DSC scan from 0 to 120°C to remove all thermal history, and consequently create a completely amorphous structure, and then immediately reanalyzed by FTIR-ATR. The spectra obtained immediately post DSC scan are shown in Figure 4.10, which shows that the shoulder at 1022 cm^{-1} became more pronounced immediately after the DSC scan. This finding agrees with van Soest and others (1995) and Capron and others (2007) that the 1022 cm^{-1} peak is related to the amorphous starch fraction.

Thus, some ordered, but non-crystalline, structure must exist within the pregelatinized waxy maize starches that develops over time, leading to the differences in the FTIR-ATR absorbance patterns observed for starches equilibrated at different %RH values. Furthermore, decreases in peak intensity at 1022 cm^{-1} may be useful in following the transition from amorphous to more ordered amylopectin structures.

In addition to peaks at 995 and 1022 cm^{-1}, the starch sample at 13.91% moisture, stored at 67.9% RH, also exhibited a second shoulder at 1045 cm^{-1} that was not observed for the other low moisture samples. Interestingly, the peak at 1045 cm^{-1} was also observed for 50% moisture retrograded starch and for non-gelatinized native starch (Figure 4.11). Also of note, the main peak at 995 cm^{-1} shifted to a higher wavelength at 1000 cm^{-1} for the retrograded starch, typical of the B-type polymorph. The development of a third peak in the 1045 to 995 cm^{-1} wavelength range indicates separation of amylopectin chains into more distinct and organized structures. The

peak at 1045 cm^{-1} has been previously correlated with the crystalline starch fraction (Capron and others 2007; van Soest and others 1995) even though no crystallinity was observed in these samples by x-ray diffraction.

As such, Figure 4.12 depicts the ratio of the absorbances at 1022/1045 cm^{-1} for the pregelatinized waxy maize starch samples at different moisture contents in relation to the 50% moisture pregelatinized, retrograded starch and non-gelatinized starch. Pregelatinzed starches with moisture contents from 6.09 to 12.16% had a ratio of approximately 4.5, while pregelatinized starch at 13.91% moisture content, retrograded starch and non-gelatinized starch have a ratio of 3 or less. Very low moisture pregelatinized starch (1.1% moisture) also had a ratio less than 3, but due to the very low absorbance intensities across the entire measured range and its broad, diffuse profile, peaks were difficult to separate and quantify intensity. As this ratio decreases, the crystalline starch fraction of the starch would be assumed to be increasing, meaning that double helices are stacking into ordered arrays. In fact, the native, non-gelatinized starch exhibited the smallest ratio and would be expected to contain the largest degree of crystallinity. Thus, at 13.91% moisture content, in which the glass transition was observed by MDSC nearly simultaneous with the sub-T_g endotherm, sufficient mobility existed to promote crystalline order, but at a level not yet detectable by x-ray diffraction. Thus, the absorbance ratio of 1022/1045 cm^{-1} may be a useful tool in monitoring the development of short-range molecular order in amylopectin and the kinetic development of sub-T_g retrogradation.

While the 1022/1045 cm^{-1} peak ratio has been commonly used to describe the relative amount of crystallinity in starch (Capron and others 2007; van Soest and others 1995), changes in peak absorbances at 1080 cm^{-1} have also been observed to be related to starch crystallinity (Rubens and Heremans 2000; Rubens and others 1999; Warren and others 2013). In fact, the absorbance ratio 1080/1151 cm^{-1} was also found to be dependent on the starch moisture content for the pregelatinized waxy maize starch samples (Figure 4.13). Immediately following DSC, this ratio was independent of moisture content, but prior to removing the thermal history, starch moisture content exhibited an increasing relationship with the 1080/1151 cm^{-1} ratio.

Given that the 1080 cm^{-1} observance has previously been related to starch crystalline order, the increase in this ratio with moisture may also indicate an increase in starch structural order. In fact, given that starch order and crystallinity is comprised of both amylopectin double helical order and subsequent crystalline arrangement of the double helices, the observances of

multiple peaks related to amylopectin ordered fraction is not surprising. As significant absorbance at 1045 cm^{-1} was only observed for the 12.16 and 13.91% moisture content pregelatinized starch samples, this peak may be related to the arrangement of double helices, while the 1080 cm^{-1} peak may be related to the initial formation of those double helices.

4.4.4 Characterization of amylopectin short-range order by ^{13}C CP/MAS NMR spectroscopy

The use of ^{13}C CP/MAS NMR spectroscopy in starch characterization provides information on the molecular organization at shorter distance scales than those probed by X-ray diffraction. As such, NMR spectroscopy can provide useful insights into starch order corresponding to double helix content beyond the double helices that are packed in regular arrays that can be detected by X-ray diffraction (Cooke and Gidley 1992; Gidley and Bociek 1985; Jane and others 1985; Tan and others 2007). For example, the different crystalline polymorphic forms of starch (A-, B-, and V-type), as well as amorphous starch, have been reported to exhibit different ^{13}C NMR spectral features (Gidley 1987; Gidley and Bociek 1988; Vergin and others 1987; Vergin and others 1986), and analysis of the NMR spectra as a composite of spectra from the amorphous and ordered components can provide estimates of the percentage of amylopectin double helices in the starch.

All ^{13}C CP/MAS spectra showed resolved resonances in the ranges 102 to103, 81 to 84, and 60 to 62 ppm (Figure 4.14), which have previously been assigned to C-1, C-4, and C-6 sites of glucose, respectively (Bogracheva and others 2001; Gidley and Bociek 1988). The spectra also contain a large peak at 73-75 ppm, which has been assigned to the C-2, 3, 4 and 5 sites. The broad shoulder that appears at 103 ppm was found to arise from the amorphous domains for C-1 and the broad resonance at 82 ppm from amorphous domains for C-4 based on the fact that these broad resonances were absent in the A- and B-type spherulitic crystal spectra, but had a dominant presence in the amorphous samples (Gidley and Bociek 1985; Vergin and others 1986). While the C-6 site also provides useful structural information, this resonance has been found to be dependent on experimental contact time unlike the C-1 and C-4 peaks, presumably because it is more efficiently cross-polarized than other resonances as C-6 is a methylene carbon, whereas all other sites are methine (Gidley and Bociek 1985).

125

The C-1 peak at 101 to 103 ppm has also been used to assess amylopectin double helical content. Resonances in this region can also give rise to doublets (for B-type crystallites) or triplets (for A-type crystallites) as was seen with the 50% moisture pregelatinized waxy maize starch and the non-gelatinized waxy maize starch. However, the overlapping of peaks in this region made separation of the peak linked to double helical content difficult, and as such, the peaks in this region were found to have no correlation with moisture content of the pregelatinized waxy maize starches.

While the C-1 and C-4 resonances have been associated with the amorphous domains, changes in the shape and area of these peaks has been consistently used to characterize and quantify amylopectin double helical content (Atichokudomchai and others 2004; Bogracheva and others 2001; Flores-Morales and others 2012; Paris and others 1999; Tan and others 2007), and for the pregelatinized waxy maize starches studied herein, the C-4 resonance at 82.6 ppm became markedly more defined between the non-gelatinized native starch plus 50% high moisture pregelatinized starch and all of the low moisture pregelatinized starches (Figure 4.14). As such, narrowing of the peak width corresponds with an increase in amorphous content, or conversely, broadening of the peak is related to an increase in starch double helical content. In fact, increasing peak width for the 82.6 ppm peak correlated with an increase in moisture content for the pregelatinized waxy maize starches (Figure 4.15), and, consequently, double helical content increases with increasing moisture content. Interestingly, the increase in double helical content is non-linear and shows a similar exponential dependence on moisture content as previously described for the sub-Tg enthalpic transition observed by MDSC (Figure 4.2). Additionally, solid-state ^{13}C CP/MAS NMR spectrum of amorphous starch only arise from amylopectin in the glassy state, further confirming the glassy state of these pregelatinized waxy maize starches.

Both the peak absorbance ratio 1080/1151 measured via FTIR-ATR and the peak width at 82.6 ppm measured by ^{13}C CP/MAS NMR are positively correlated with the sub-Tg peak enthalpy measured by MDSC (Figure 4.16). The relationship between the NMR and MDSC data is steeper than the FTIR-MDSC relationship, most likely since NMR is a direct measure of the change in double helical content of starch whereas FTIR measures related changes that correspond with the double helical content. Regardless, MDSC, FTIR-ATR and ^{13}C CP/MAS NMR are useful tools for investigating the sub-Tg endotherm on a quantitative and structural level.

4.5 Summary and conclusions

A sub-Tg endotherm with a peak temperature between 55 and 65°C was observed at all starch moisture contents in the non-reversing heat flow of the MDSC scan for the pregelatinized waxy maize starch. A similar peak with substantially higher enthalpy was also observed for the 50% moisture content retrograded starch sample; such peak is well above the Tg for this system. The enthalpy of this transition exhibited an exponential relationship with increasing moisture content, but the peak temperature was independent of moisture content.

Using FTIR-ATR, pregelatinized waxy maize starches stored at various relative humidity conditions exhibited a large absorbance at 995 cm^{-1} with overlapping shoulders at 1022 and 1045 cm^{-1}; the shoulder peak observed at 1022 cm^{-1}, which has previously been attributed to the amorphous fraction of starch, was found to significantly increase after a DSC thermal scan, supporting this conclusion. Since the post DSC samples all had higher absorbance intensities at 1022 cm^{-1} after DSC compared to before DSC scan, the amylopectin structure is assumed to have become more ordered, even though no crystalline order was observed by x-ray diffraction. Non-gelatinized starch, 50% moisture content retrograded starch and pregelatinized starch at 13.91% moisture content also exhibited absorbance at 1045 cm^{-1}, related to the crystalline starch fraction, in addition to all samples exhibiting absorbance at 1080 and 1150 cm^{-1}. The absorbance ratio 1080/1151 cm^{-1} was found to increase with moisture content of pregelatinized waxy maize starch while this ratio was independent of moisture content immediately following DSC scan. Thus, the 1045 cm^{-1} peak may be related to double helical crystallinity, while the 1080 peak may be a result of the reformation of those double helices post gelatinization. Increasing amylopectin double helical content with increasing moisture in pregelatinized waxy maize starches was confirmed by solid-state ^{13}C CP/MAS NMR. Thus, monitoring FTIR-ATR spectra in confirmation with NMR, may be a useful tool for understanding the structural state of amylopectin at low moisture contents, in particular, as related to the kinetic development of structural ordering and increased molecular mobility below the measured glass transition.

4.6 Acknowledgements

the x-ray diffraction work and to Dr. Andre Sutrisno and the School of Chemical Sciences NMR Facility at the University of Illinois for assistance with the ^{13}C CPMAS NMR work.

4.7 Figures and tables
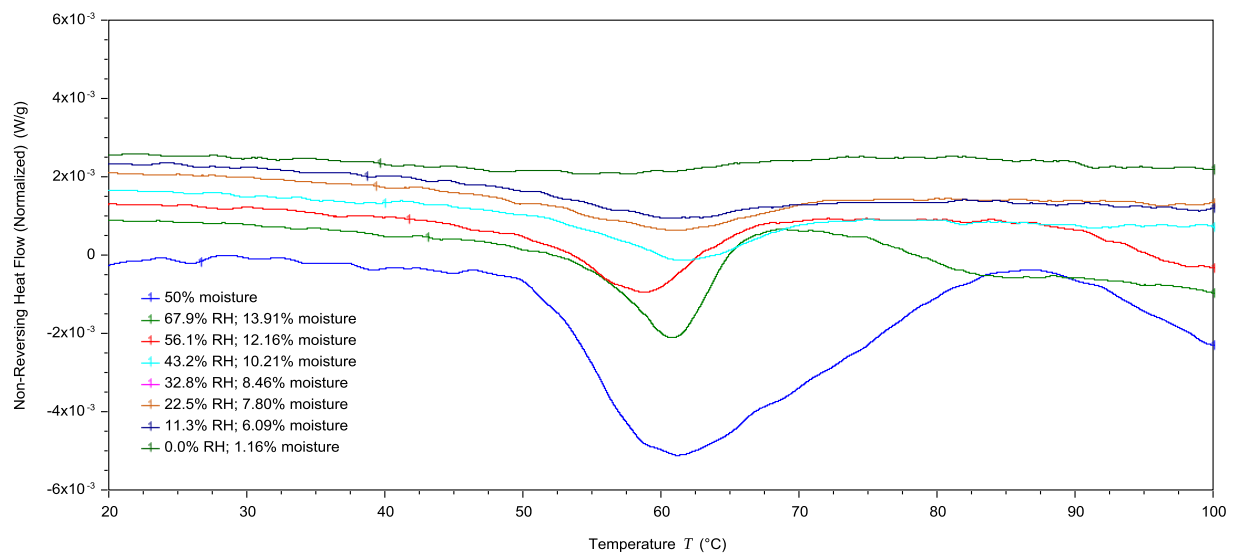
Figure 4.1. MDSC-observed sub-Tg endotherm for pregelatinized waxy maize starch at different moisture contents
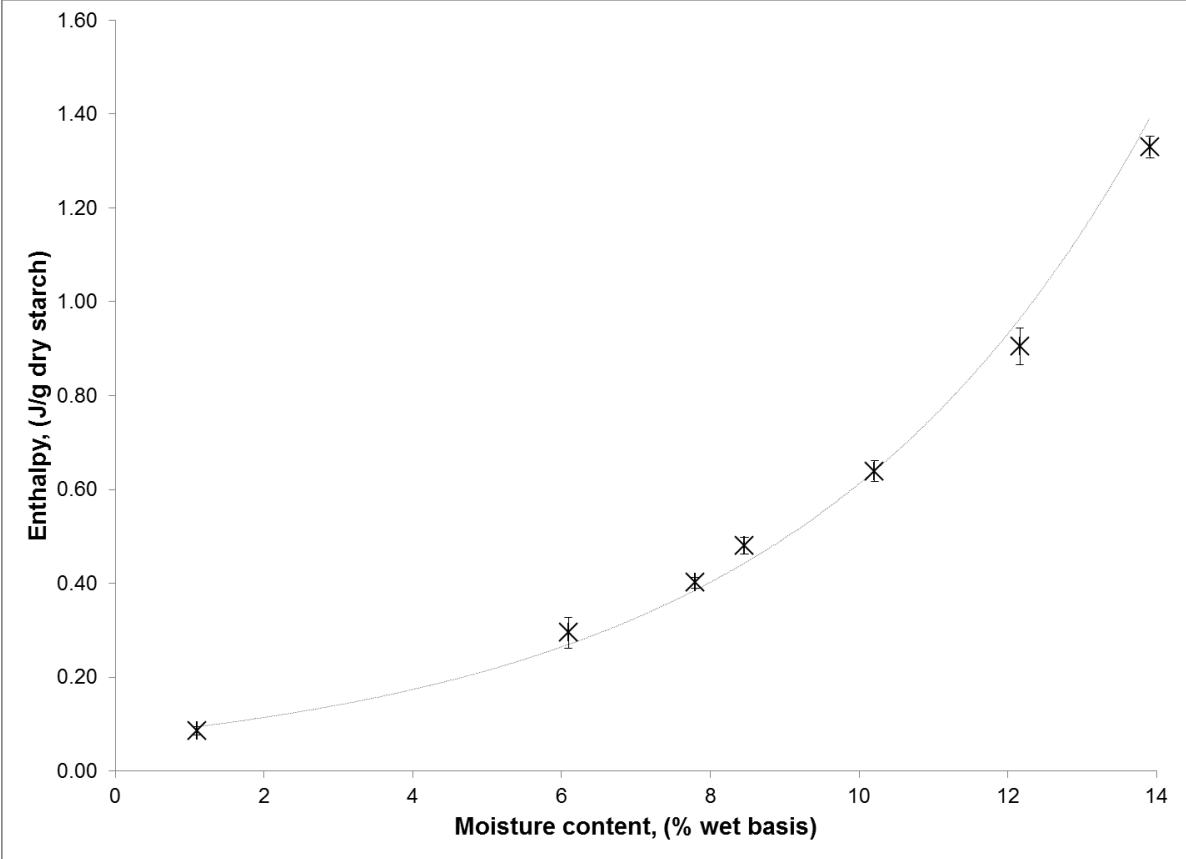
Figure 4.2. Enthalpy associated with sub-Tg endotherm in the non-reversing heat flow characterized as a function of starch moisture content. Error bars represent one standard deviation.
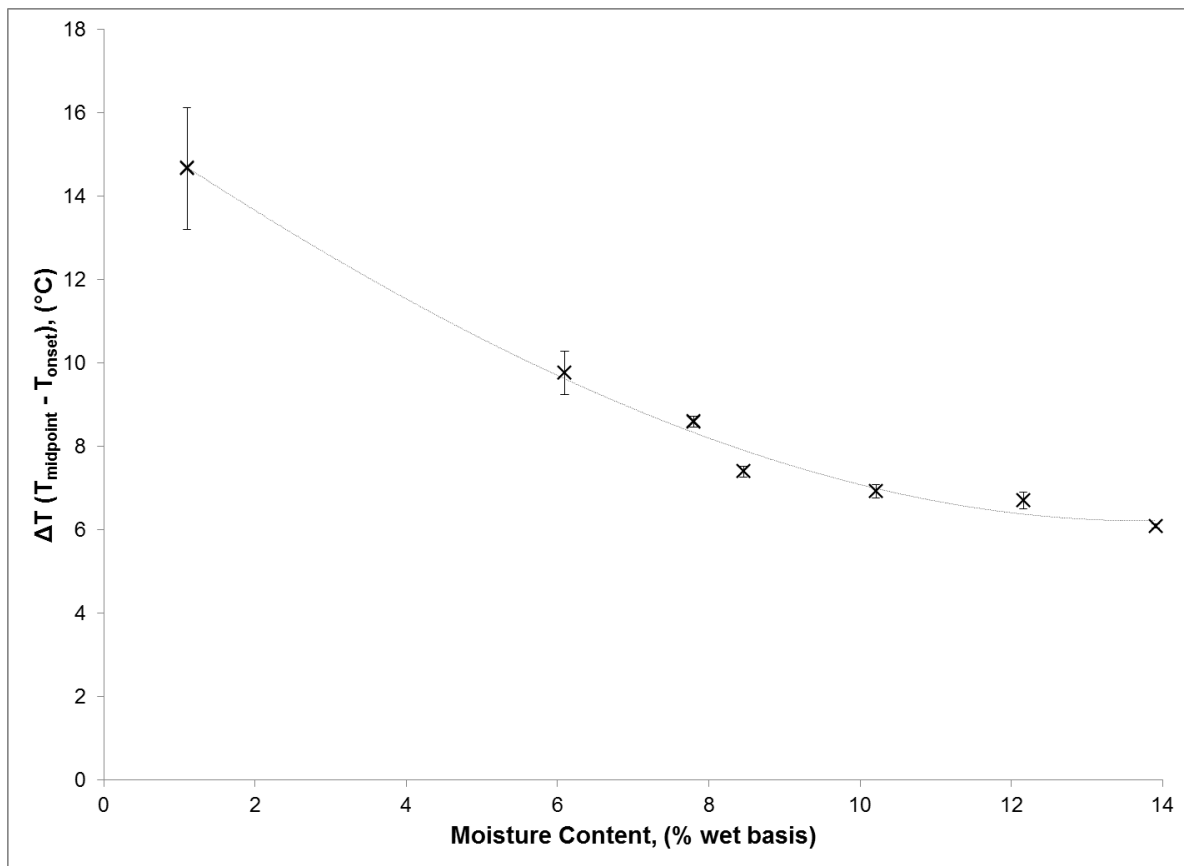
Figure 4.3. Dependence of sub Tg endotherm ΔT ($T_{midpoint} - T_{onset}$) on starch moisture content. Error bars represent one standard deviation.
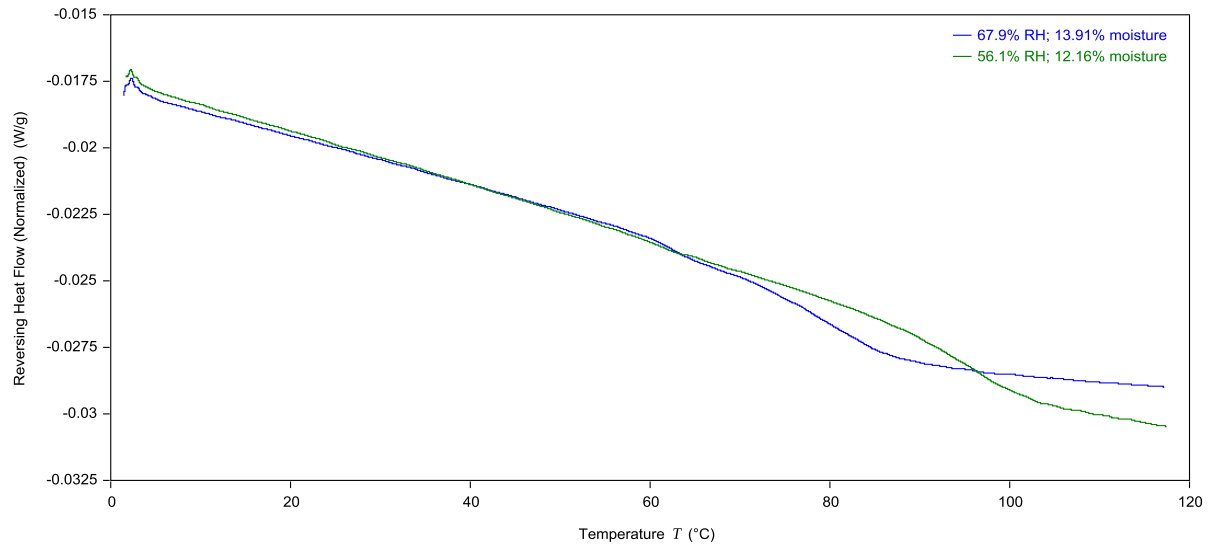
Figure 4.4. MDSC observed glass transition in the reversing heat flow for pregelatinized waxy maize starch samples at 12.16 and 13.91% moisture content.
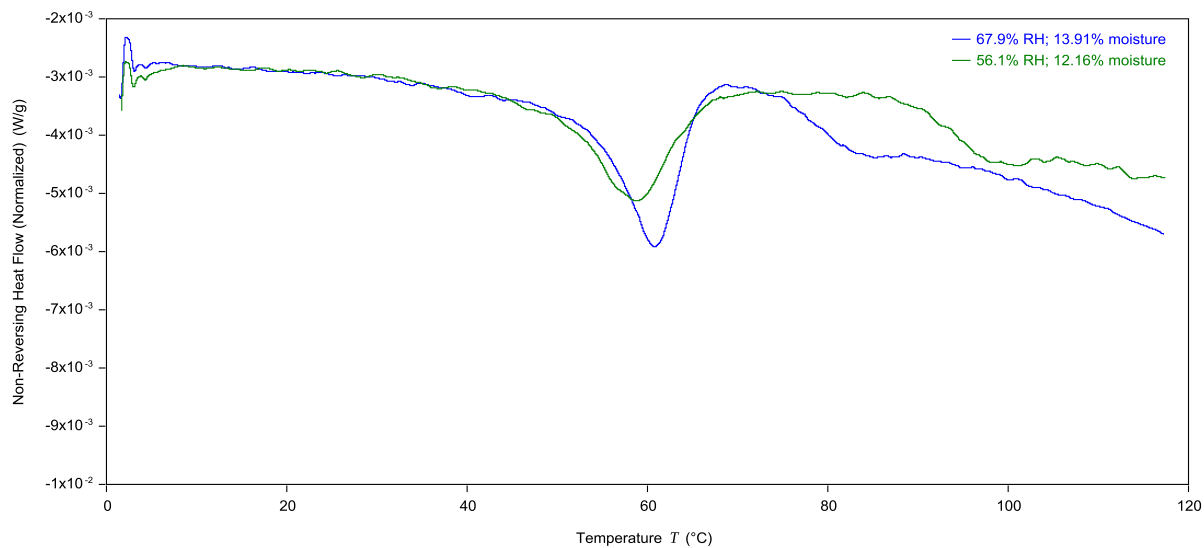
Figure 4.5. MDSC observed sub-Tg and post-Tg endotherms in the non-reversing heat flow for pregelatinized waxy maize starch samples at 12.16 and 13.91% moisture content.
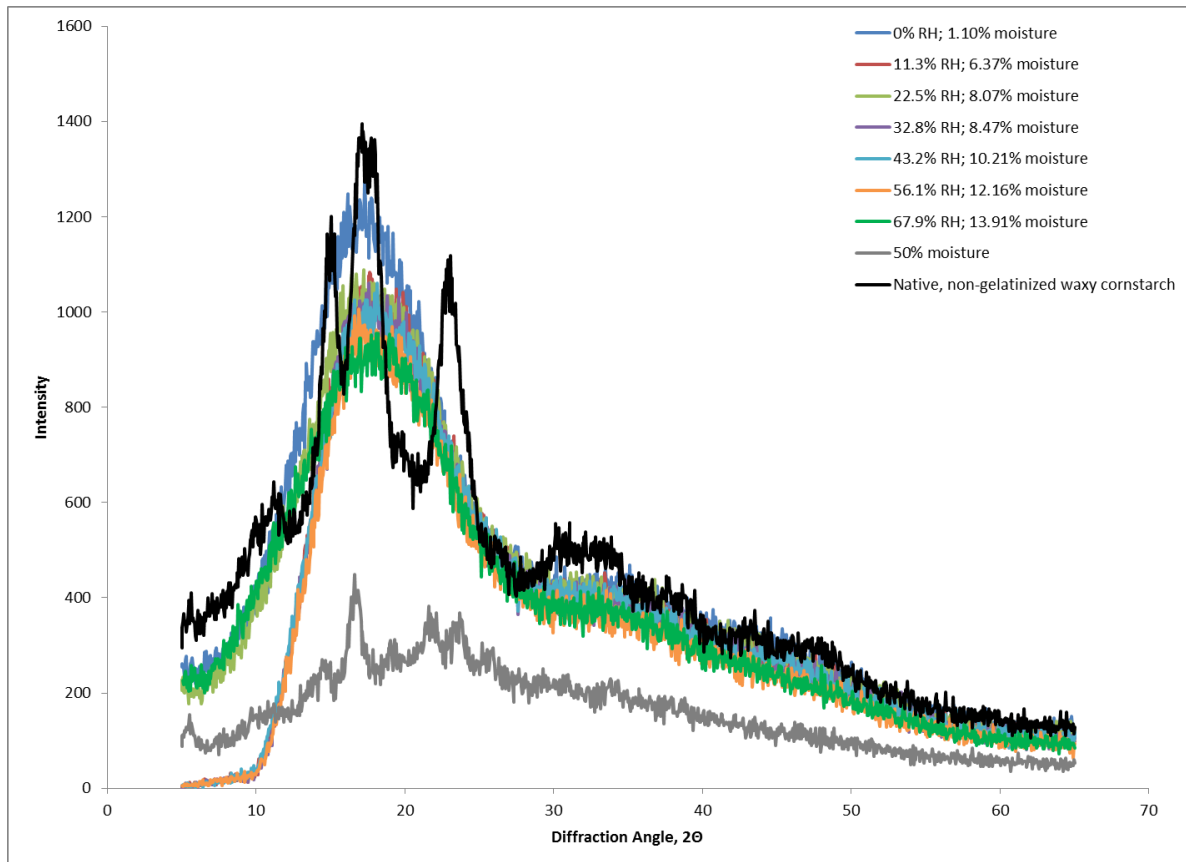
Figure 4.6. X-ray diffraction patterns for pregelatinized waxy maize starch stored at different moisture contents, in comparison to pregelatinized, retrograded starch at 50% moisture content and native, non-gelatinized waxy maize starch.
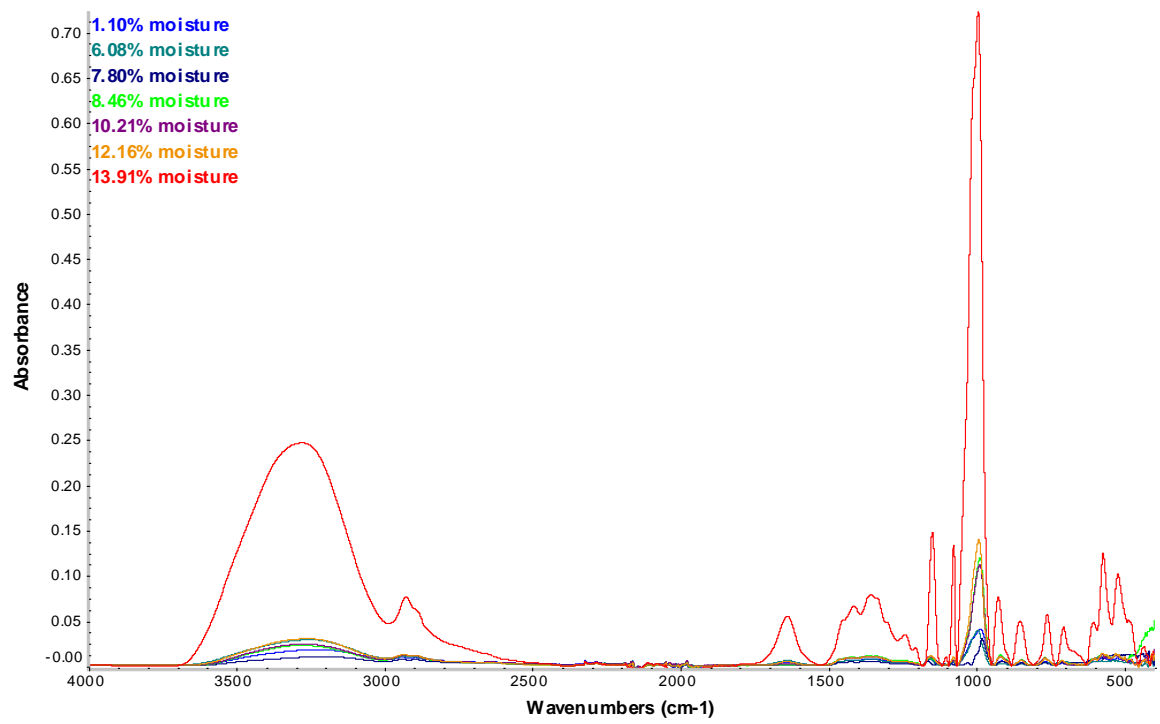
Figure 4.7. FTIR-ATR spectra of pregelatinized, waxy maize starch samples at low moisture contents.
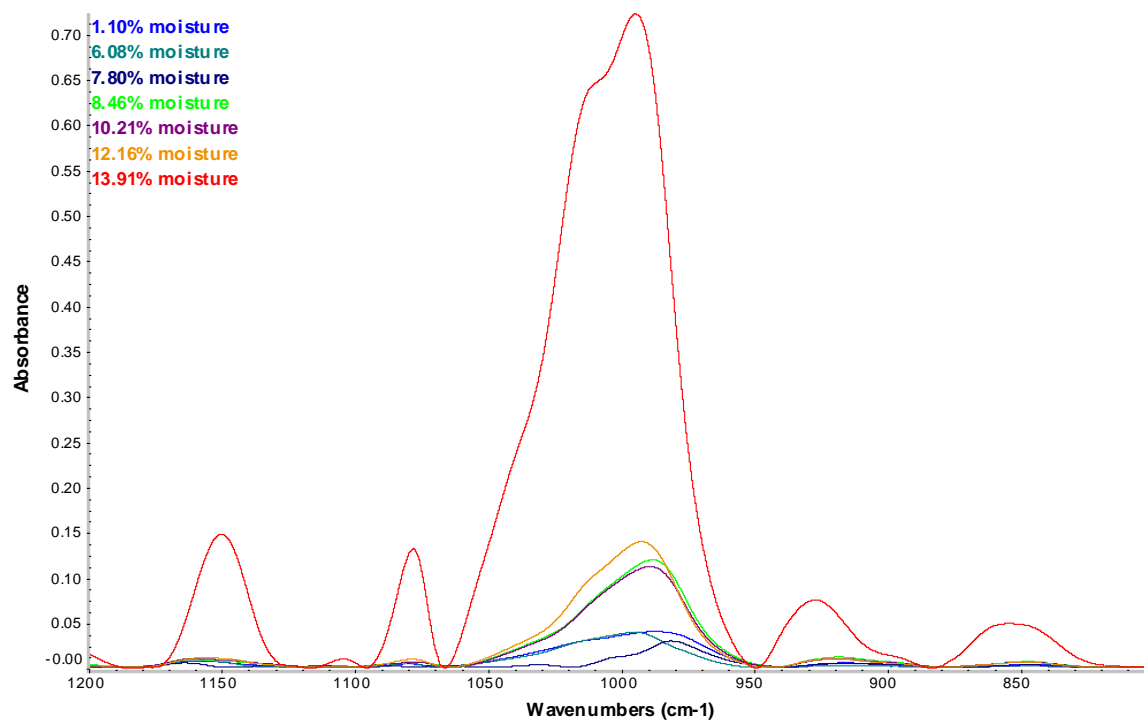
Figure 4.8. FTIR-ATR spectra in the region of 1200 to 800 cm^{-1} of pregelatinized, waxy maize starch at low moisture contents.
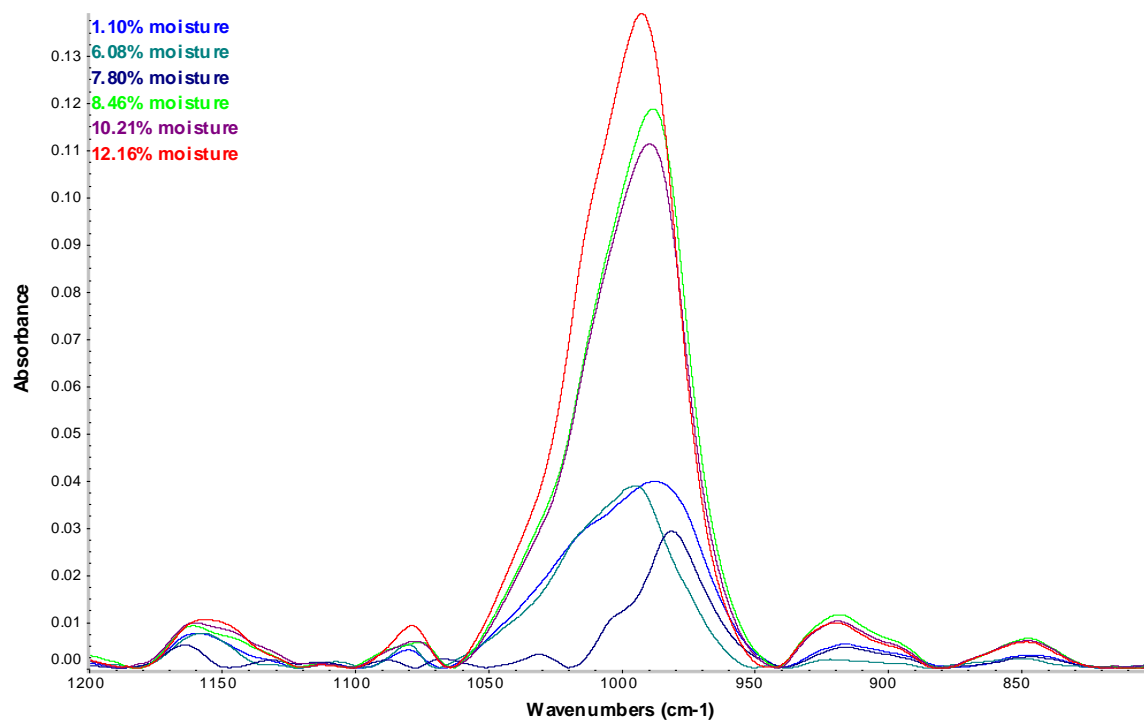
Figure 4.9. FTIR-ATR spectra in the region of 1200 to 800 cm^{-1} of pregelatinized, waxy maize starch at low moisture contents.
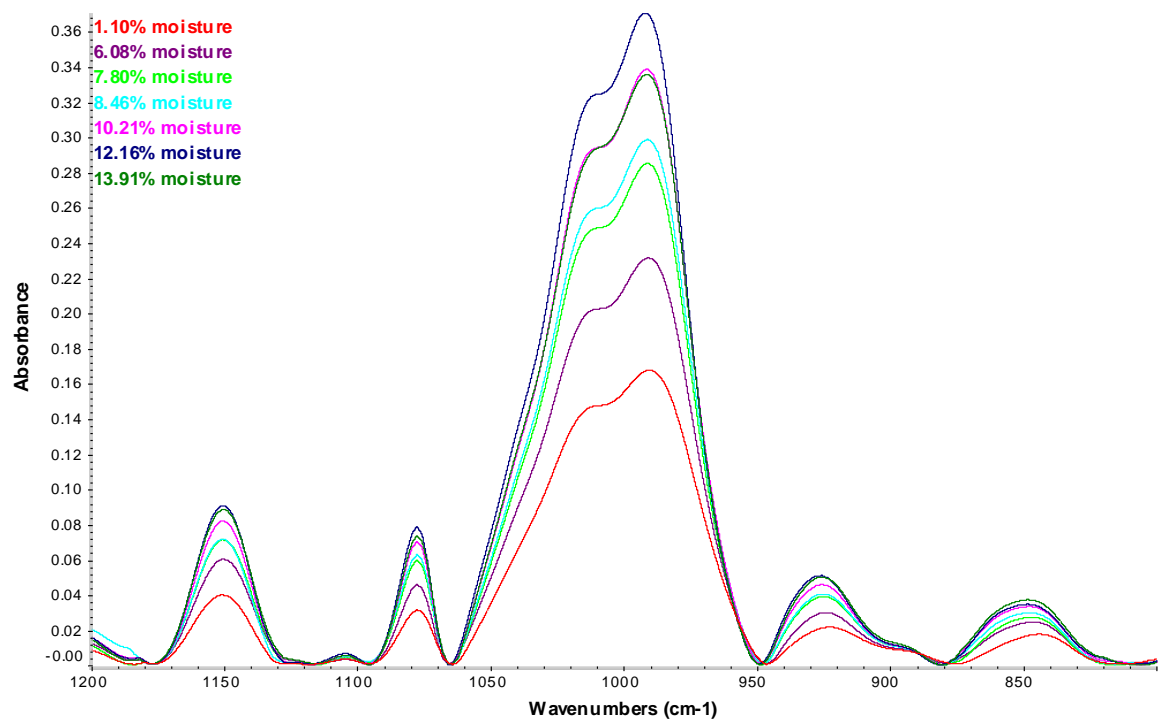
Figure 4.10. FTIR-ATR spectra in the region of 1200 to 800 cm^{-1} of pregelatinized, waxy maize starch at low moisture contents, immediately after DSC thermal scan from 0 to 120°C.
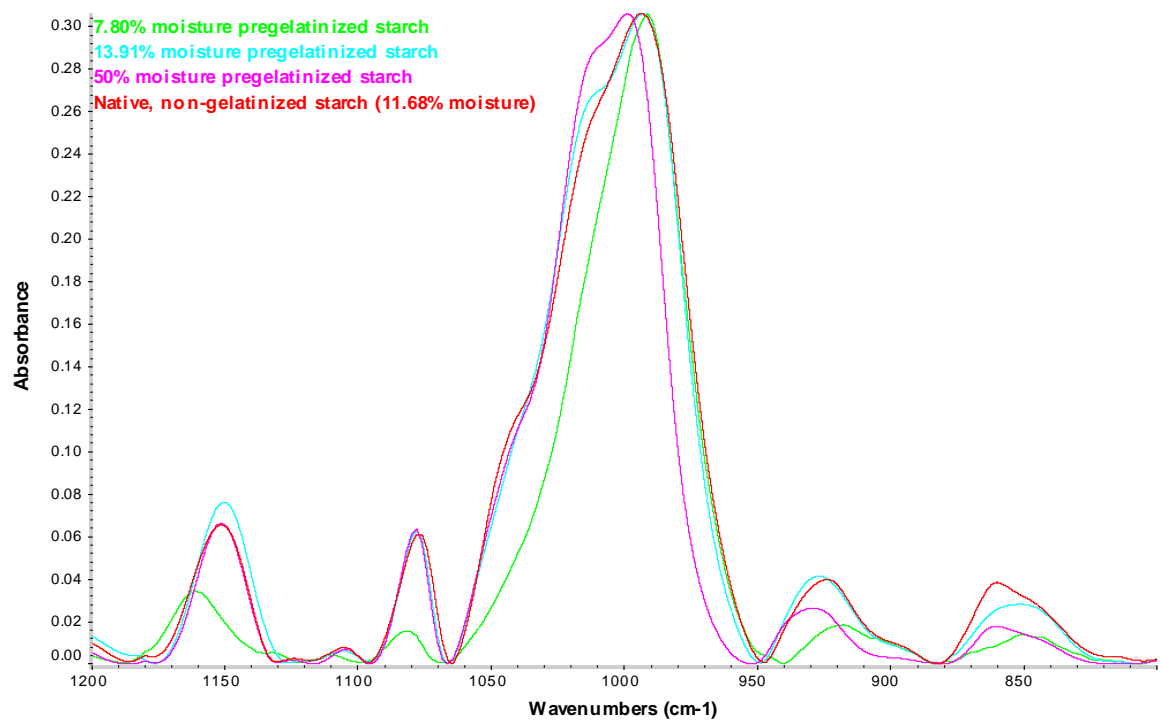
Figure 4.11. FTIR-ATR spectra in the region of 1200 to 800 cm^{-1} of pregelatinized waxy maize starch at 7.80%, 13.90% and 50% moisture content and non-gelatinized native waxy maize starch (11.68% moisture content).
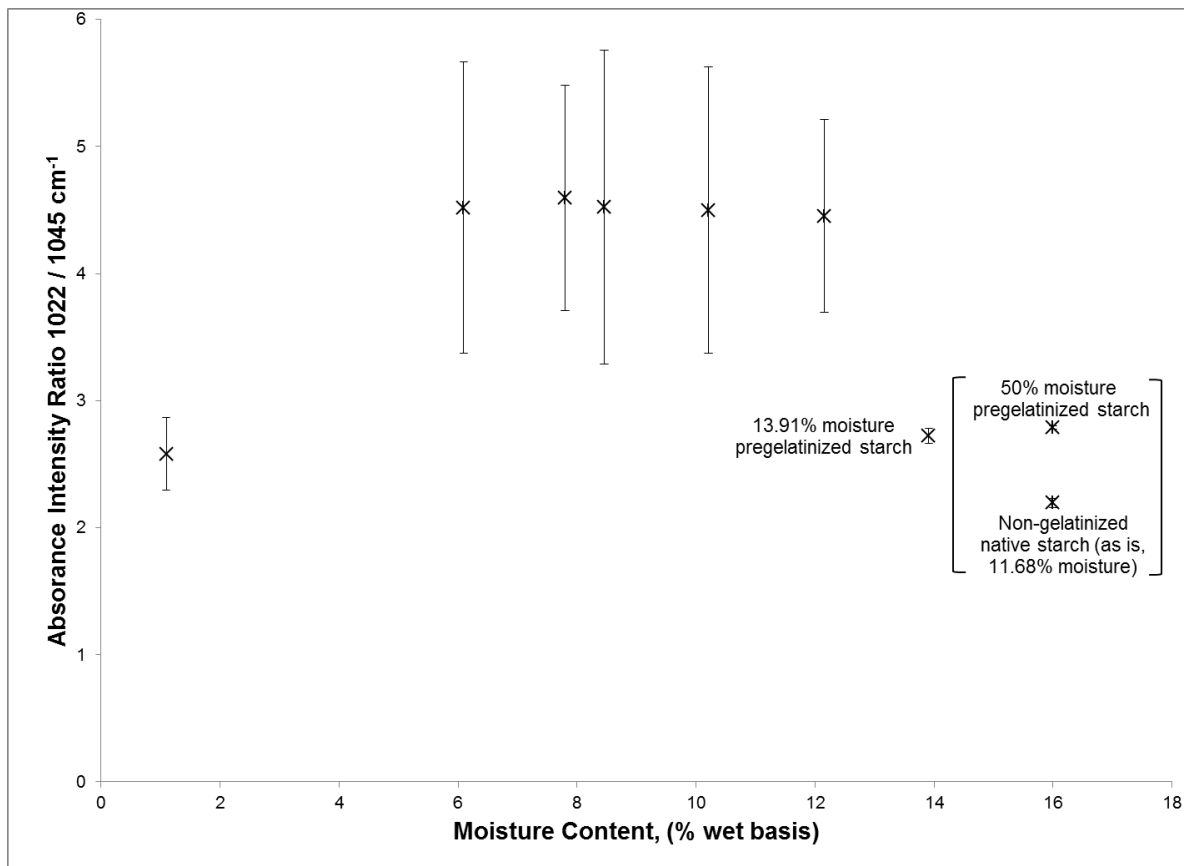
Figure 4.12. FTIR-ATR ratio of the absorbances 1022 / 1045 cm⁻¹ for pregelatinized waxy maize starches stored at various relative humidities and for 50% moisture content retrograded starch and non-gelatinized starch. Error bars represent one standard deviation.
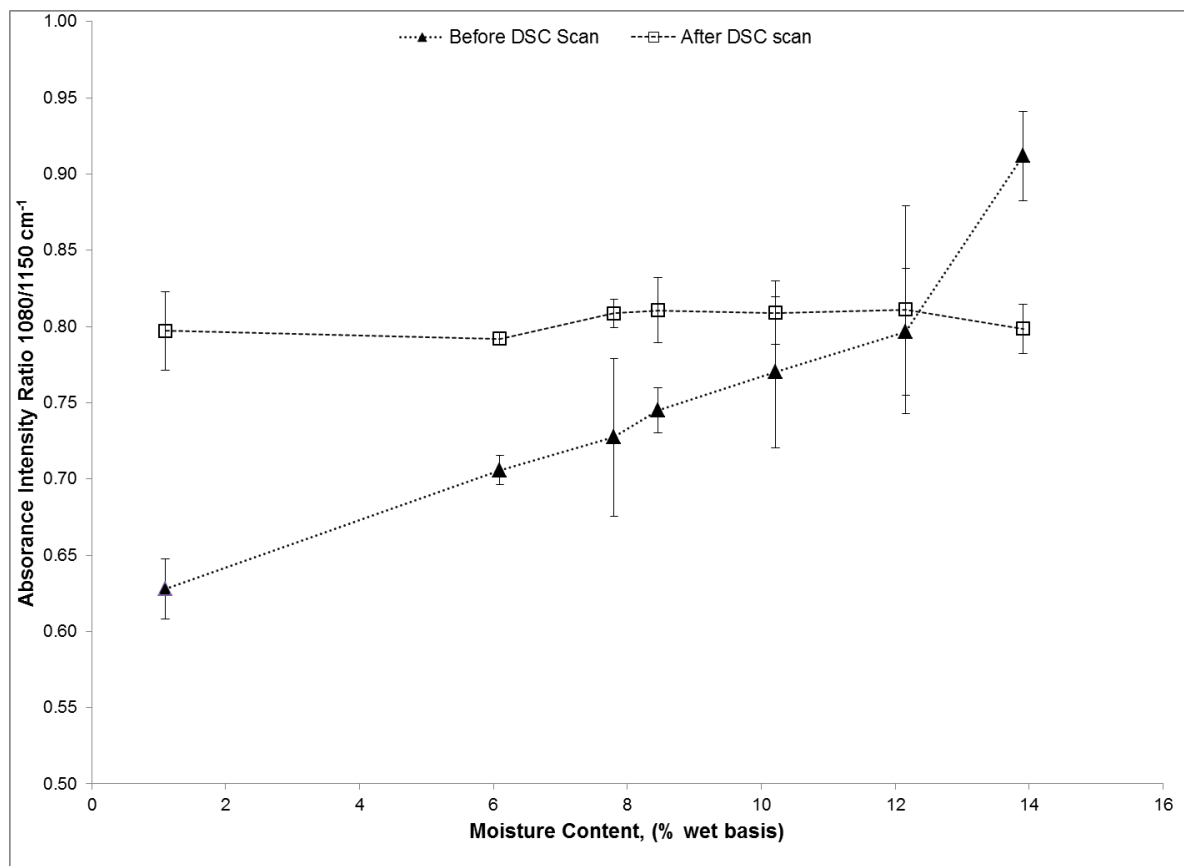
Figure 4.13. FTIR-ATR ratio of the absorbances 1080 / 1150 cm^{-1} for pregelatinized waxy maize starches stored at various relative humidity values before and immediately after DSC scan. Error bars represent one standard deviation.
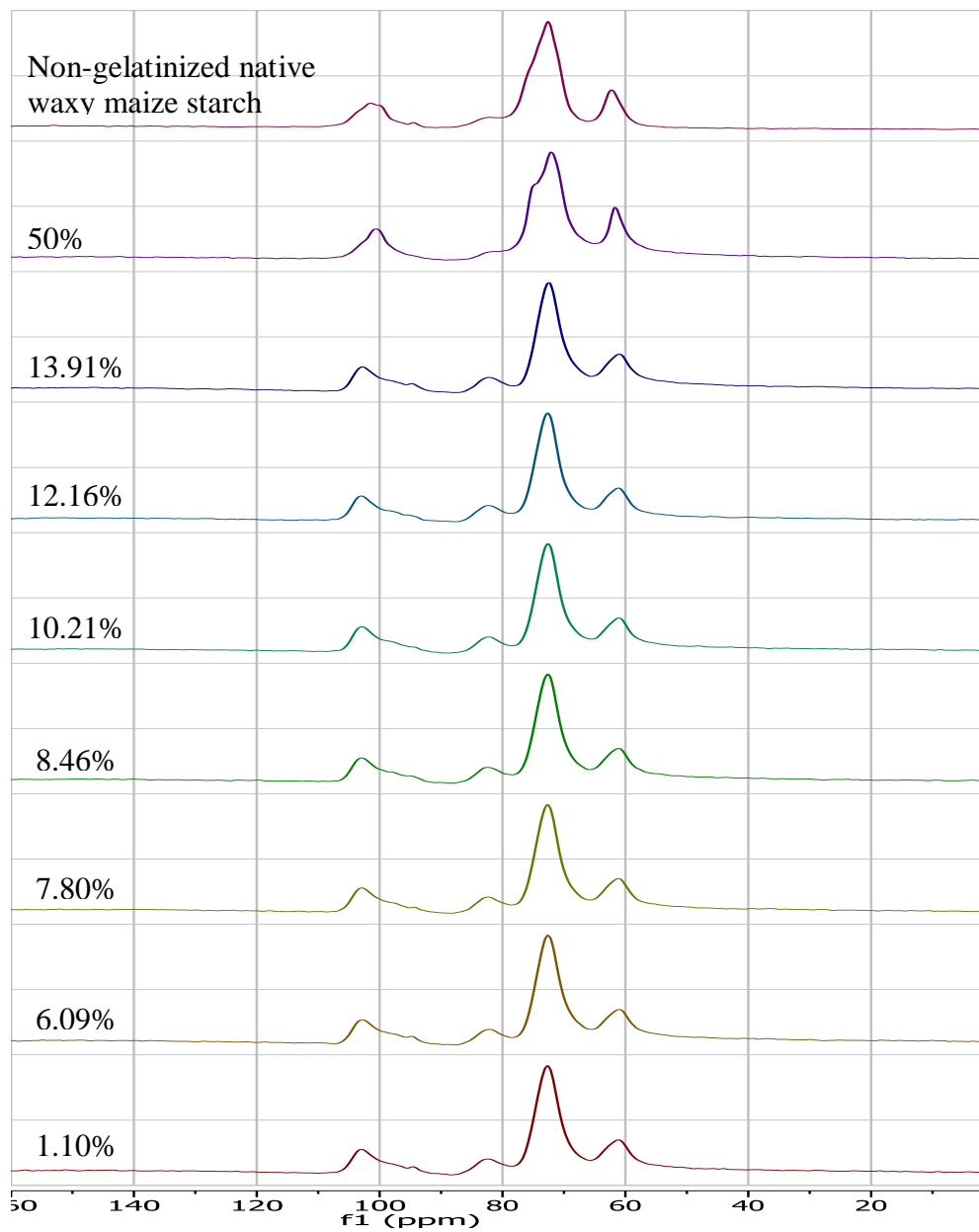
Figure 4.14. ^{13}C CP/MAS NMR spectra for non-gelatinized waxy maize starch and pregelatinized waxy maize starches at different moisture contents.
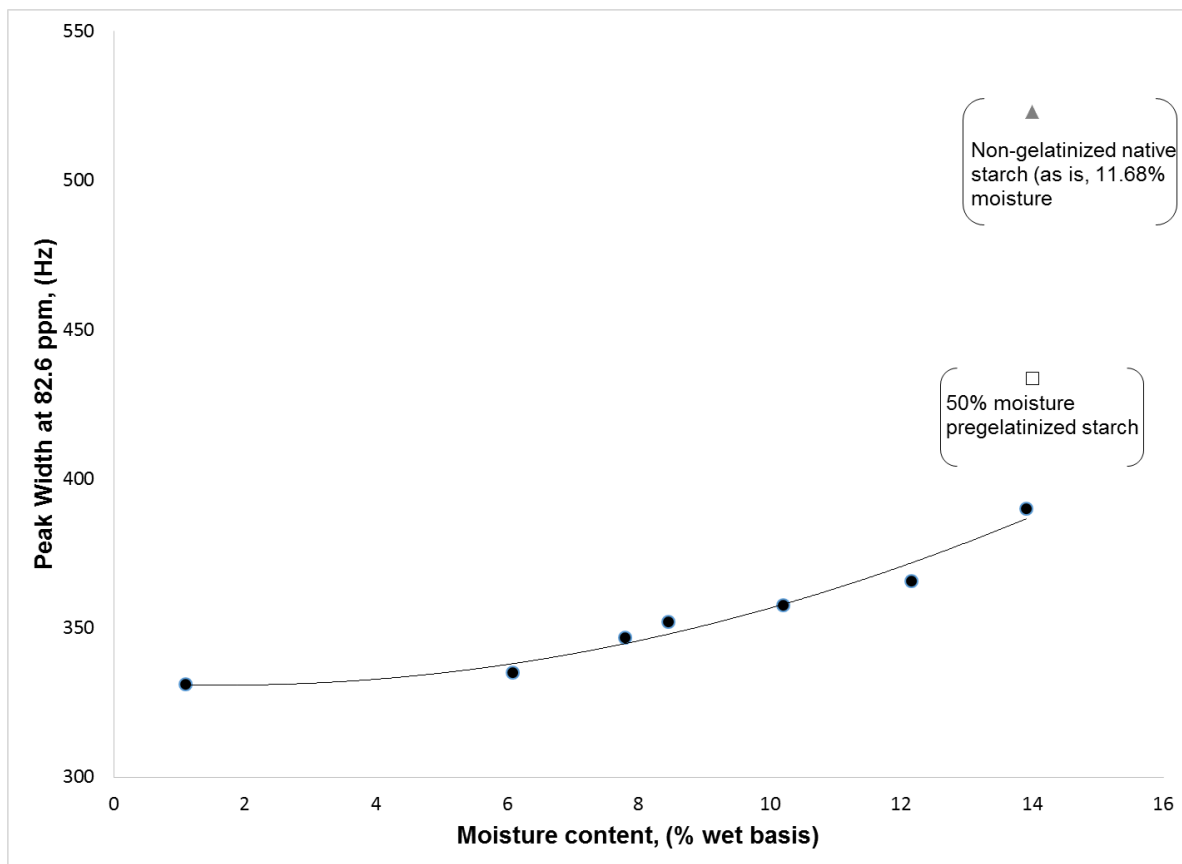
Figure 4.15. ^{13}C CP/MAS NMR peak width at 82.6 ppm for pregelatinized waxy maize starches at different moisture contents.
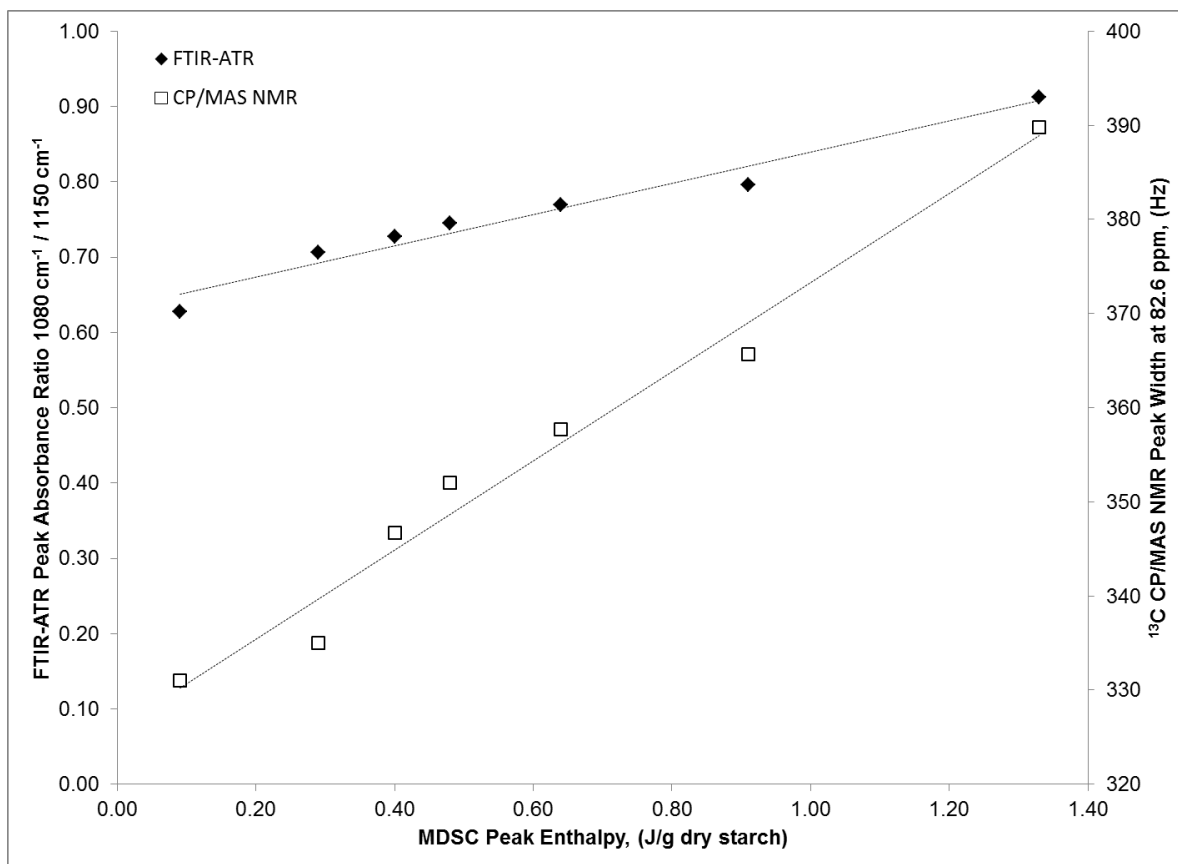
Figure 4.16. Correlation of FTIR-ATR peak absorbance ratio 1080 cm^{-1} /1151 cm^{-1} and ^{13}C CP/MAS NMR peak width at 82.6 ppm with MDSC peak enthalpy.

Table 4.1. Dessicant and saturated salt slurries providing %RH values from 11.3 to 72.1%

Salt	%RH[a]				Solubility (g/100g H_2O)[b]			
	5°C	15°C	25°C	35°C	0°C	10°C	20°C	40°C
Desiccant (calcium sulfate)	0	0	0	0	n/a	n/a	n/a	n/a
LiCl	11.3	11.3	11.3	11.3	69.2	74.5	83.5	89.8
KCH_3COO	24.2	23.4	22.5	21.5	216	233	256	324
$MgCl_2$	33.6	33.3	32.8	32.1	52.9	68.1	73.9	88.5
K_2CO_3	43.2	43.2	43.2	43.2	105	109	111	117
NaBr	62.2	59.1	56.1	53.2	80.2	85.2	90.8	107
KI	72.1	69.9	67.9	66.1	128	136	144	162

[a] %RH data obtained from Greenspan (1977)

[b] solubility data obtained from Haynes (2012)

n/a – not applicable

4.8 References

Atichokudomchai N, Varavinit S, Chinachoti P. 2004. A study of ordered structure in acid-modified tapioca starch by 13C CP/MAS NMR. Carbohydr. Polym. 58:383-9.

Badii F, MacNaughtan W, Farhat IA. 2005. Enthalpy relaxation of gelatin in the glassy state. Int. J. Biol. Macromol. 36(4):263-9.

Beckmann J, McKenna GB, Landes BG, Bank DH, Bubeck RA. 1997. Physical aging kinetics of syndiotactic polystyrene as determined from creep behavior. Polym. Eng. Sci. 37(9):1459-68.

Bell LN, Labuza TP. 2000. Moisture Sorption – Practical Aspects of Isotherm Measurement and Use 2nd ed. St. Paul, MN: American Association of Cereal Chemists, Inc.

Biladeris CG. 2009. Structural transitions and related physical properties of starch. In: BeMiller J, Whistler R, editors. Starch: Chemistry and Technology. Burlington, MA: Academic Press.

Bogracheva TY, Wang YL, Hedley CL. 2001. The effect of water content on the ordered/disordered structures in starch. Biopolymers 58:247-59.

Brubach JB, Mermet A, Filabozzi A, Gerschel A, Roy P. 2005. Signatures of the hydrogen bonding in the infrared bands of water. Journal of Chemical Physics 122(18):7.

Capron I, Robert P, Colonna P, Brogly M, Planchot V. 2007. Starch in rubbery and glassy states by FTIR spectroscopy. Carbohydrate Polymers 68(2):249-59.

Chung HJ, Lee EJ, Lim ST. 2002. Comparison in glass transition and enthalpy relaxation between native and gelatinized rice starches. Carbohydr. Polym. 48(3):287-98.

Cooke D, Gidley MJ. 1992. Loss of crystalline and molecular order during starch gelatinization: origin of the enthalpic transition. Carbohydr. Res. 227:103-12.

Descamps N, Palzer S, Zuercher U. 2009. The amorphous state of spray-dried maltodextrin: sub-sub-T-g enthalpy relaxation and impact of temperature and water annealing. Carbohydr. Res. 344(1):85-90.

Elfstrand L, Frigard T, Andersson R, Eliasson AC, Jonsson M, Reslow M, Wahlgren M. 2004. Recrystallisation behaviour of native and processed waxy maize starch in relation to the molecular characteristics. Carbohydr. Polym. 57(4):389-400.

Flores-Morales A, Jiménez-Estrada M, Mora-Escobedo R. 2012. Determination of the structural changes by FT-IR, Raman, and CP/MAS 13C NMR spectroscopy on retrograded starch of maize tortillas. Carbohydr. Polym. 87:61-8.

Gidley MJ. 1987. Factors affecting the crystalline type (A-C) of native starches and model compounds: a rationalisation of observed effects in terms of polymorphic structures. Carbohydr. Res. 161:301-4.

Gidley MJ, Bociek SM. 1985. Molecular organization in starch: A 13C CP/MAS NMR study. Journal of the American Chemical Society 107:7040-4.

Gidley MJ, Bociek SM. 1988. 13C CP/MAS NMR studies of amylose inclusion complexes, cyclodextrins, and the amorphous phase of starch granules: Relationships between glycosidic linkage conformation and solid-state 13C chemical shifts. Journal of the American Chemical Society 110:3820-9.

Gonzalez DC, Khalef N, Wright K, Okos MR, Hamaker BR, Campanella OH. 2010. Physical aging of processed fragmented biopolymers. J. Food Eng. 100(2):187-93.

Goodfellow BJ, Wilson RH. 1990. A Fourier-Transform IR studgy of the gelation of amylose and amylopectin Biopolymers 30(13-14):1183-9.

Greenspan L. 1977. Humidity fixed points of binary saturated aqueous solutions. Journal of Research of the National Bureau of Standards - A, Physics and Chemistry 81A(1):89-96.

Haynes WM. 2012. CRC Handbook of Chemistry and Physics. 92nd (internet version 2012) ed. Boca Raton, FL: CRC Press/Taylor and Francis.

Jane JL, Robyt JF, Huang DH. 1985. 13C-NMR study of the conformation of helical complexes of amylopectin and of amylose in solution. Carbohydr. Res. 140:21-35.

Kalichevsky MT, Jaroszkiewicz EM, Ablett S, Blanshard JMV, Lillford PJ. 1992a. The glass-transition of amylopectin measured by DSC, DMTA and NMR. Carbohydr. Polym. 18(2):77-88.

Kalichevsky MT, Jaroszkiewicz EM, Ablett S, Blanshard JMV, Lillford PJ. 1992b. The glass transition of amylopectin measured by DSC, DMTA and NMR. Carbohydrate Polymers 18(2):77-88.

Kalichevsky MT, Orford PD, Ring SG. 1990. The retrogradation and gelation of amylopectins from various botanical sources. Carbohydr. Res. 198(1):49-55.

Karim AA, Norziah MH, Seow CC. 2000. Methods for the study of starch retrogradation. Food Chem. 71:9-36.

Keetels C, vanVliet T, Walstra P. 1996. Gelation and retrogradation of concentrated starch systems .2. Retrogradation. Food Hydrocolloids 10(3):355-62.

Kim YJ, Suzuki T, Hagiwara T, Yamaji I, Takai R. 2001. Enthalpy relaxation and glass to rubber transition of amorphous potato starch formed by ball-milling. Carbohydr. Polym. 46(1):1-6.

Lewen KS, Paeschke T, Reid J, Molitor P, Schmidt SJ. 2003. Analysis of the retrogradation of low starch concentration gels using differential scanning calorimetry, rheology, and nuclear magnetic resonance spectroscopy. J. Agric. Food Chem. 51(8):2348-58.

Li Q. 2010. Investigating the glassy to rubber transition of polydextrose and cornflakes using automatic water vapor sorption instruments, DSC, and texture analysis. [Master of Science]. Urbana, IL: University of Illinois at Urbana-Champaign. 77-117 p.

Livings SJ, Breach C, Donald AM, Smith AC. 1997. Physical ageing of wheat flour-based confectionery wafers. Carbohydr. Polym. 34(4):347-55.

Mestrelab Research SL. 2013. Mnova version 8.1.1. 8.1.1 ed. Santiago de Compostela, Spain.

Paris M, Bizot H, Emery J, Buzare´ JY, Bule´on A. 1999. Crystallinity and structuring role of water in native and recrystallized starches by 13C CP-MAS NMR spectroscopy 1: Spectral decomposition. Carbohydr. Polym. 39:327-39.

Perera DY. 2003. Physical aging of organic coatings. Progress in Organic Coatings 47:61-76.

Perez S, Bertoft E. 2010. The molecular structures of starch components and their contribution to the architecture of starch granules: A comprehensive review. Starch-Starke 62(8):389-420.

Rubens P, Heremans K. 2000. Pressure-temperature gelatinizatin of phase diagram of starch: an in situ Fourier Transform Infrared study. Biopolymers 54(7):524-30.

Rubens P, Snauwaert J, Heremans K, Stute R. 1999. In situ observation of pressure-induced gelation of starches studied with FTIR in the diamond anvil cell. Carbohydrate Polymers 39(3):231-5.

Sarko A, Wu HCH. 1978. The crystal structures of A-, B- and C- polymorphs of amylose and starch. Starch-Starke 30:73-8.

Sevenou O, Hill SE, Farhat IA, Mitchell JR. 2002. Organisation of the external region of the starch granule as determined by infrared spectroscopy. International Journal of Biological Macromolecules 31(1–3):79-85.

Shogren RL. 1992. Effect of moisture content on the melting and subsequent physical aging of corn starch. Carbohydr. Polym. 19(2):83-90.

Slade L, Levine H. 1988. Non-equilibrium melting of native granular starch. I. Temperature location of the glass transition associated with gelatinization of A-type cereal starches. Carbohydr. Polym. 8:183-208.

Struik LCE. 1987. The mechanical and physical ageing of semicrystalline polymers: 1. Polymer 28:1521-33.

TA Instruments - Waters L. 2011. TRIOS version 2.3.4 1613. 2.3.4 ed. New Castle, Delaware, USA.

Tan I, Flanagan BM, Halley PJ, Whittaker AK, Gidley MJ. 2007. A method for estimating the nature and relative proportions of amorphous, single, and double-helical components in starch granules by 13C CP/MAS NMR. Biomacromolecules 8:885-91.

Thermo Fisher Scientific I. 2012. OMNIC version 9.1.27. 9.1.27 ed. Waltham, Massachussetts, USA.

Thiewes HJ, Steeneken PAM. 1997. The glass transition and the sub-T-g endotherm of amorphous and native potato starch at low moisture content. Carbohydr. Polym. 32(2):123-30.

van Soest JJG, Tournois H, de Wit D, Vliegenthart JFG. 1995. Short-range structure in (partially) crystalline potato starch determined with attenuated total reflectance Fourier-transform IR spectroscopy. Carbohydrate Research 279(0):201-14.

Vergin VP, Fyfe CA, Marchessault RH. 1987. Investigation of the crystalline "V" amylose complexes by high-resolution 13C CP/MAS NMR spectroscopy. Macromolecules 20:3007-12.

Vergin VP, Fyfe CA, Marchessault RH, Taylor MG. 1986. Characterization of the crystalline A and B starch polymorphs and investigation of starch crystallization by high-resolution 13C CP/MAS NMR. Macromolecules 19:1030-4.

Warren FJ, Perston BB, Royall PG, Butterworth PJ, Ellis PR. 2013. Infrared spectroscopy with heated attenuated total internal reflectance enabling precise measurement of thermally

149

induced transitions in complex biological polymers. Analytical Chemistry 85(8):3999-4006.

Wilson RH, Kalichevsky MT, Ring SG, Belton PS. 1987. A Fourier-transform infrared study of the gelation and retrogradation of waxy-maize starch. Carbohydr. Res. 166:162-5.

Yuan RC, Thompson DB. 1994. Sub-Tg thermal properties of amorphous waxy starch and its derivatives. Carbohydr. Polym. 25(1):1-6.

Zeleznak KJ, Hoseney RC. 1987. The glass transition in starch. Cereal Chem. 64(2):121-4.

CHAPTER 5

KINETIC INVESTIGATION OF THE SUB-TG ENDOTHERM IN PREGELATINIZED WAXY MAIZE STARCHES AT LOW MOISTURE CONTENTS

5.1 Abstract

The occurrence of a sub-Tg endotherm in low moisture pregelatinized waxy maize starches has been previously linked with the reformation of amylopectin double helices, but without the observance of measurable crystallinity. The objective of this study was to follow the kinetic development of the sub-Tg endotherm in low moisture (1 to 14%) waxy maize starches over 24 weeks as related to 50% moisture content retrograded starch. The sub-Tg endotherm, measured by MDSC and the FTIR-ATR absorbance ratio at 1080 cm^{-1}/1151 cm^{-1}, was observed to increase with time according to Avrami kinetics. The Avrami exponent n was estimated at 0.24 and was found to be independent of moisture content for the low moisture pregelatinized waxy maize starches. An Avrami exponent value less than one was not surprising considering that Avrami kinetics are used to describe crystallization processes and these low moisture starches are assumed to only proceed through the nucleation step characterized by the reformation of double helical ordered structure in the amylopectin. The Avrami rate constant, K, was exponentially correlated with starch moisture content as was the enthalpy of the sub-Tg endotherm given that greater mobility exists at the higher moisture contents to increase the amount and rate of double helical nucleation. The Avrami equation and its relationship with moisture content provides a useful means of predicting the kinetic formation of the sub-Tg endotherm and its potential impact on the stability and textural shelf-life of low-moisture starchy foods.

5.2 Introduction

The occurrence of an endothermic event, typically observed below the conventional glass transition, is a common feature of many polymer systems, including starch, amylopectin and other polysaccharides. For example, Chung and others (2002) reported a sub-Tg endotherm peak temperature for gelatinized rice starch at 12% moisture as approximately 55°C and Tg as approximately 65°C. Similarly, Zeleznak and Hoseney (1987) reported the glass tranisition of pregelatinized wheat starch as 65C and higher for moisture contents of 12% and below. This sub-

Tg endotherm has been described for other semicrystalline polymers (Beckmann and others 1997; Struik 1987), starch (Chung and others 2002; Kalichevsky and others 1992; Kim and others 2001; Shogren 1992; Yuan and Thompson 1994), maltodextrin (Descamps and others 2009), confectionary wafers (Livings and others 1997), and cornflakes (Gonzalez and others 2010; Li 2010), among others.

The presence of this sub-Tg endothermic event has practical implications for carbohydrate and starchy food systems since it is also typically accompanied by physical changes directly impacting the texture and quality of the food system. In particular, foods that are classified as being in the "glassy" state may be affected, although the prevailing assumption has been that the physical characteristics of such food systems are kinetically stable. Furthermore, this sub-Tg endothermic event has remarkable similarities to amylopectin retrogradation, which is commonly considered to only occur at higher moisture contents, above the system glass transition. Amylopectin retrogradation is a non-equilibrium thermoreversible recrystallization process which is governed by a consecutive three step mechanism of nucleation, propagation and maturation (Kalichevsky and others 1990; Keetels and others 1996; Slade and Levine 1988) . After gelatinization, the reordering of the amylopectin molecules results in heterogeneous recrystallization that is responsible for the broad endotherm observed by DSC in which the least stable crystals melt at lower temperatures and the remaining crystallites, of higher quality, melt at higher temperatures (Elfstrand and others 2004).

The kinetics describing the retrogradation and recrystallization behavior of amylopectin are often modeled using classical Avrami kinetics for polymer crystallization (Avrami 1939; Avrami 1940; Avrami 1941) even though the Avrami equation assumes thermodynamic equilibrium and the retrogradation process is known to be non-equilibrium (Marsh and Blanshard 1988; Zhang and Jackson 1992). Nevertheless, Avrami kinetics have been successfully used to describe retrogradation of both gelatinized starch (Farhat and others 2000; Jouppila and others 1998; McIver and others 1968; Seow and Teo 1996) and amylopectin associated bread staling (Del Nobile and others 2003; Fearn and Russell 1982; Russell 1983).

Because amylopectin retrogradation requires orientational mobility of the polymer chains in the granule, the crystallization process is assumed to occur only in the temperature range between the glass transition temperature and the melting temperature, e.g. in the range of approximately 25.0 and 60°C for a starch gel containing 50% water (Silverio and others 2000).

However, retrogradation as a crystallization process proceeds through the mechanism of nuleation, propagration and maturation, and in terms of nucleation, the double helices of amylopectin can act as nuclei and increase the rate of nucleation (Elfstrand and others 2004; Morgan 1954). Interestingly, the development of the sub-Tg endotherm of pregelatinized waxy maize starches has been linked to increased amylopectin double helical content without a measurable increase in crystallinity. Thus, such a system may potentially have proceeded through the first step of retrogradation, and as such, similarities between the sub-Tg endotherm and retrogration, in terms of mechanism and kinetics, could arise. The objective of this work is to characterize the kinetic development of the sub-Tg endotherm in pregelatinized waxy maize starches at low moisture contents, particularly as it relates to amylopectin recrystallization and retrogradation.

5.3 Materials and methods

Commercial, pregelatinized, spray-cooked (X'PandR SC, Tate & Lyle; initial a_w = 0.15 at 24.99°C, initial moisture content = 5.88% wet basis) unmodified waxy maize starch, with intact starch granules, was obtained, and the initial moisture content of the starch was determined via quick drying with a halogen oven (CompuTrac Max 1000, Arizona Instruments, Chandler, Arizona), calibrated to vacuum oven drying for 4 hours at 25 to 100 mmHg and 105°C. The initial water activity of the starches was determined using an Aqualab 4TE water activity meter (Decagon Devices, Pullman, Washington). The pregelatinized, spray-cooked waxy maize starch was equilibrated over saturated salt solutions encompassing a range of %RH values (Table 5.1). Saturated salt slurries were prepared by adding an excess amount of salt into deionized water according to the known solubility values at 40°C, heating the slurry to approximately 50°C for about 2 hours, while stirring on a standard stir plate and then cooling to room temperature.

A sufficient amount of saturated salt slurry was added to storage containers (airtight and water proof plastic containers commercially known as "Lock & Lock") to completely cover the bottom of the container. About 4 grams of "as is" pregelatinized waxy maize starch granules was weighed into a small plastic cup and transferred to the "Lock & Lock" container with the saturated salt slurry. Containers were kept in an incubator at a storage temperature of 25°C. After constant weight was reached, defined as when the sample weight changed by less than 2mg/g dry weight between successive weight measurements (Bell and Labuza 2000), the equilibrium

153

moisture content was determined using the initial sample weight, the initial moisture content and the equilibrium weight.

For each %RH storage condition, thermal history of the equilibrated starch was removed by heating the sample from 0 to 120°C at 10°C/min using Differential Scanning Calorimetry (DSC) with the Q2000 Differential Scanning Calorimeter instrument (TA Instruments, New Castle, Delaware). Equilibrated samples were taken from the "Lock & Lock" containers and transferred to DSC T-zero aluminum hermetic pans and sealed with internal hermetic lids immediately after transferring out of the "Lock & Lock" containers in order to maintain the appropriate moisture content and %RH within the sample throughout the study. Samples, in the hermetically sealed DSC pan, were scanned and then returned to the incubator at 25°C and stored for up to 24 weeks. At time intervals of 1, 2, 3, 4, 8, 12, 16, 20 and 24 weeks, aged starch samples, in triplicate, were rescanned using Modulated Differential Scanning Calorimetry (MDSC). MDSC allows for the separation of the heat flow into the reversing heat flow (heat capacity component) and non-reversing heat flow (kinetic component). Samples were equilibrated at 0°C and scanned using a modulated heating profile with a rate of 1°C/min, oscillation period of 80 seconds, and amplitude of 0.5°C from 0°C to 120°C (MDSC first scan). The onset temperature, peak temperature, and enthalpy of the transitions of observed peaks were determined through peak integration using the TRIOS Software version 2.3.4..1613 from TA Instruments (2011). Each scan was analyzed in triplicate.

Similarly, the pregelatinized waxy maize starch was hydrated in room temperature excess deionized water to provide 50% moisture w/w, with the addition of 0.1% sodium azide to prevent mold growth. According to Zeleznak and Hoseney (1986), the staling/retrogradation endotherm reaches a maximum at 50-60% moisture content. Thermal history was removed via scanning in the DSC, and samples were stored in the incubator at 25°C and then rescanned using the MDSC profile given at time intervals of 1, 2, 3, 6, 7, 14, 21 and 28 days. The time intervals for the higher moisture sample were much shorter than for the low moisture content samples as amylopectin recrystallization is expected to occur much more quickly under these higher moisture conditions.

Concurrent with MDSC analysis, Fourier-transform infrared, attenuated total reflectance (FTIR-ATR) spectra of the aged starch samples were acquired using a Thermo Nicolet iS™10 FT-IR with the Scientific Smart iTR™ diamond attenuated total reflectance (ATR) accessory

with nitrogen purge (Thermo Scientific, Waltham, Massachusetts). Spectra were obtained at a resolution of 4cm^{-1} from 4000 to 400 cm^{-1} and averaged over 100 scans, recorded against an empty cell as background. Deconvoluted spectra were baseline corrected in the 1200 to 800 cm^{-1} region and peak height was analyzed at 995, 1022, 1044, 1078 and 1151 cm^{-1} using the OMNIC 9.1.27 software (Thermo Fisher Scientific 2012) . Duplicate FTIR-ATR spectra were obtained of each sample, and each spectrum was analyzed in triplicate.

5.4 Results and discussion

A sub-Tg endotherm with a peak temperature between 45 and 55°C was observed at all %RH and starch moisture contents in the non-reversing heat flow of the MDSC scan for the pregelatinized waxy maize starches, which proportionally increased in intensity over the 24 week storage period (Figure 5.1 and Figure 5.2). Onset and peak temperature were unaffected by starch moisture content or time.

Over the same 24-week time period, FTIR-ATR spectra revealed similar profiles in the 1200 to 800 cm^{-1} region (Figure 5.3), where the most important absorption bands for starch occur, due to C−C and C−O stretching modes and C−O−H bending modes. While difficult to assign given that each band is linked to another as a result of highly coupled vibrational modes that create differences in assignment, comparative changes in these modes can be measured as a means to assess the extent of structural changes and/or crystallinity of starch (Goodfellow and Wilson 1990; Wilson and others 1987; Capron and others 2007). Previously, the ratio of the absorbances at 1022 and 1045 cm^{-1} has been used to follow starch transitions through gelatinization and retrogradation (Capron and others 2007; Sevenou and others 2002; van Soest and others 1995; Warren and others 2013; Wilson and others 1991) and changes in this ratio were also detected for non-crystalline low moisture pregelatinized waxy maize starches (described in Chapter 4). . However, over the time-scale studied herein, no changes in this absorbance ratio were encountered over any of the starch moisture contents investigated in this study.

While the 1022/1045 cm^{-1} peak ratio has been commonly used to assess starch phase transitions, changes in peak absorbance at 1080 cm^{-1} have also been observed to be related to structured order in starch (Rubens and Heremans 2000; Rubens and others 1999; Warren and others 2013). In fact, the absorbance ratio 1080/1151 cm^{-1} was also found to be correlated with

155

the sub-Tg endotherm and the reformation of double helices as measured by ^{13}C CP/MAS NMR spectroscopy and described in Chapter 3. Closer examination of the 1080 and 1151 cm^{-1} peaks over storage time reveals that the ratio 1080/1151 increases with time for each moisture content studied in the pregelatinized waxy maize starch (Figure 5.4 and Figure 5.5). Thus, these results suggest that the sub-Tg endotherm measured by DSC over time is correlated with the reformation of amylopectin double helical structure as measured by FTIR-ATR.

Most of the proposed models used to predict the kinetics of retrogradation and amylopectin recrystallization are based on the Avrami equation, originally derived to describe polymer crystallization from the melt (Avrami 1939; Avrami 1940; Avrami 1941). The Avrami equation can be represented as:

$$Y = 1 - e^{-Kt^n}$$
Equation 5.4

Which can be rewritten as

$$\ln \ln(\frac{1}{1-Y}) = \ln K + n \ln(t)$$
Equation 5.5

Where Y is the extent of transformation or crystallization, K is the rate constant, n is the Avrami exponent and t is time.

Thus, the extent of transformation or crystallization followed over time, would be expected to follow an "S" shaped curve such that when integrated, a plot of $\ln \ln(\frac{1}{1-Y})$ versus time should yield a straight line with slope of n and y-intercept of ln K. When the MDSC-measured enthalpies of the sub-Tg endotherm for the low moisture pregelatinized waxy maize starches are expressed in this manner, straight lines are observed (Figure 5.6). In fact, the low moisture pregelatinized waxy maize starches yield parallel lines with approximately the same slope (n = 0.24) but different y-intercepts. At 50% moisture, a straight line is also observed but with a substantially steeper slope (n = 0.55).

As can be seen by Equation 5.1 and Equation 5.2, the Avrami equation contains two parameters: the rate constant K and the Avrami exponent n. The rate constant depends on the crystals growth constant and on the crystals nucleation constant, while the Avrami exponent depends on the type of crystal nucleation and the dimensions in which the growth takes place, implying that the Avrami exponent can assume an integer value ranging from 4 to 1 dimensions.

In three dimensions, spherulitic crystals are formed, whereas disc-like crystals form in two dimension and rod-like crystals form in one dimension (Del Nobile and others 2003).

The Avrami exponent has previously been determined to be n = 1 for both gelatinized starch (McIver and others 1968) and for bread (Kim and Dappolonia 1977b; Kim and Dappolonia 1977a), implying rod-like growth and instantaneous nucleation. Morgan (1954) noted that the nucleation sites probably corresponded to the regions of chain entanglement formed during gelation with crystallization then proceeding between two adjacent chains to re-form double helices. Good fit to the data for the staling of bread by constraining the Avrami exponent to 1 has also been reported by Fearn and Russell (1982), Russell (1983) and Wilson and others (1991), though in these studies, the best data fit, though not significantly better, was found for integer values less than one.

In the MDSC study herein, the Avrami exponent n averaged to n = 0.24 over the low moisture pregelatinized waxy maize starches even though Avrami exponents less than one have no physical meaning. However, these low moisture starches do not undergo full crystallization as no crystallinity has been previously observed (described in Chapter 4); although, the 50% moisture starch, in which retrogradtion and amylopectin recrystallization is assumed to have occurred, was also found to have an Avrami exponent of less than one (n = 0.55). In the FTIR-ATR study, the Avrami exponent n averaged to n = 0.25 for the low moisture starches and n = 0.37 for the 50% moisture starch though the FTIR data was more highly variable than the MDSC data as can be seen in Figure 5.2 and Figure 5.5, as MDSC is a more sensitive tool for measuring the sub-Tg endotherm.

Avrami exponents of less than one have been reported previously for corn starch gels, bread and rice cupcakes (Seow and Teo 1996). Accordingly, one of the implicit assumptions in applying the Avrami equation to the kinetics of amylopectin recrystallization is that any enthalpy changes occurring during staling are a direct measure of the quantity of recrystallized starch produced. If the degree of order of the starch (i.e. amorphous, complete recrystallization or partial recrystallization) is different, then varying changes in both enthalpy and entropy may account for a given decrease in free energy resulting in Avrami exponents less than one (Fearn and Russell 1982). For the low moisture pregelatinized starches, the enthalpy change is known to only represent reformation of double helices and partial ordered structure and thus, only the

nucleation step of the recrystallization process. As such, an Avrami exponent of less than one is not surprising.

As the Avrami plots for the low moisture starches yielded parallel lines based on moisture content, their y-intercepts, ln K, are linearly correlated with moisture content and K, the rate constant, is exponentially correlated with moisture content (Figure 5.7). The Avrami rate constant K depends on the crystals growth constant and on the crystals nucleation constant, (Del Nobile and others 2003). As the low moisture starches do not experience crystal growth, in this case, K is assumed to depend on the nucleation constant, and increasing moisture content leads to enhanced nucleation as more mobility would exist in the amylopectin chains allowing for reformation of double helices. Interestingly, the rate constant K exhibits a similar relationship with starch moisture content as the MDSC enthalpy of the sub-Tg endotherm, further corroborating that the sub-Tg endotherm is a measure of the nucleation, or reformation of double helices, in amylopectin over time, even at low moisture contents. At 50% moisture content, the rate constant K was found to be K = 1.00, which would be expected to be higher as significantly more mobility exists for this sample above the glass transition that both nucleation and crystal growth can occur. Regardless, the Avrami equation provides a useful means of predicting the kinetic formation of the sub-Tg endotherm and its potential impact on the stability of low-moisture starchy foods. Knowing the relationship between the rate constant K and starch moisture content allows for understanding of the effect of moisture content on the shelf-life and texture of such products.

5.5 Summary and conclusions

Using MSDC and FTIR-ATR, the kinetic development of the sub-Tg endotherm in low moisture waxy maize starches was followed over 24 weeks and measured as it related to the retrogradation and amylopectin recrystallization endotherm for 50% moisture content starch. Enthalpy of the sub-Tg endotherm and the FTIR-ATR absorbance ratio at 1080 cm^{-1}/1151 cm^{-1} increased with time according to Avrami kinetics. The Avrami exponent n was found to be n = 0.24 and was independent of moisture content for the low moisture pregelatinized waxy maize starches. An Avrami exponent value less than one was not surprising considering that Avrami kinetics are used to describe crystallization processes and these low moisture starches are assumed to only proceed through the nucleation step with the reformation of double helical

ordered structure in the amylopectin. The Avrami rate constant, K, was exponentially correlated with starch moisture content as was the enthalpy of the sub-Tg endotherm given that greater mobility exists at the higher moisture contents to increase the amount and rate of double helical nucleation. The Avrami equation and its relationship with moisture content provides a useful means of predicting the kinetic formation of the sub-Tg endotherm and its potential impact on the stability and textural shelf-life of low-moisture starchy foods.

5.6 Figures and tables
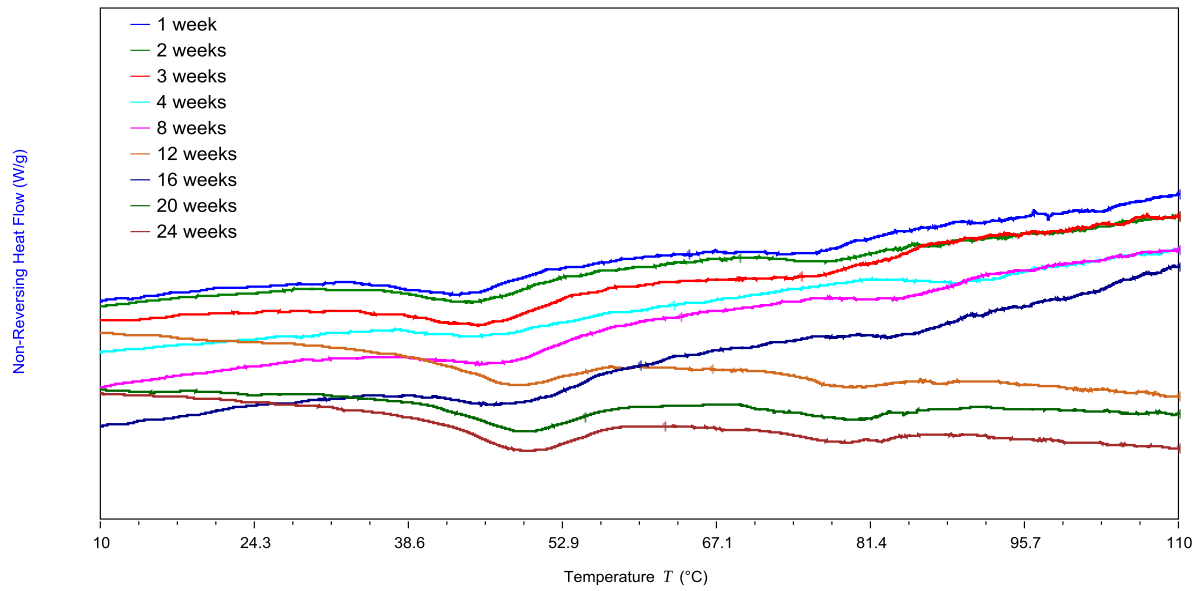
Figure 5.1. MDSC-observed sub-Tg endotherm for 13.91% moisture content (wet basis) pregelatinized waxy maize starch at over 24 weeks.
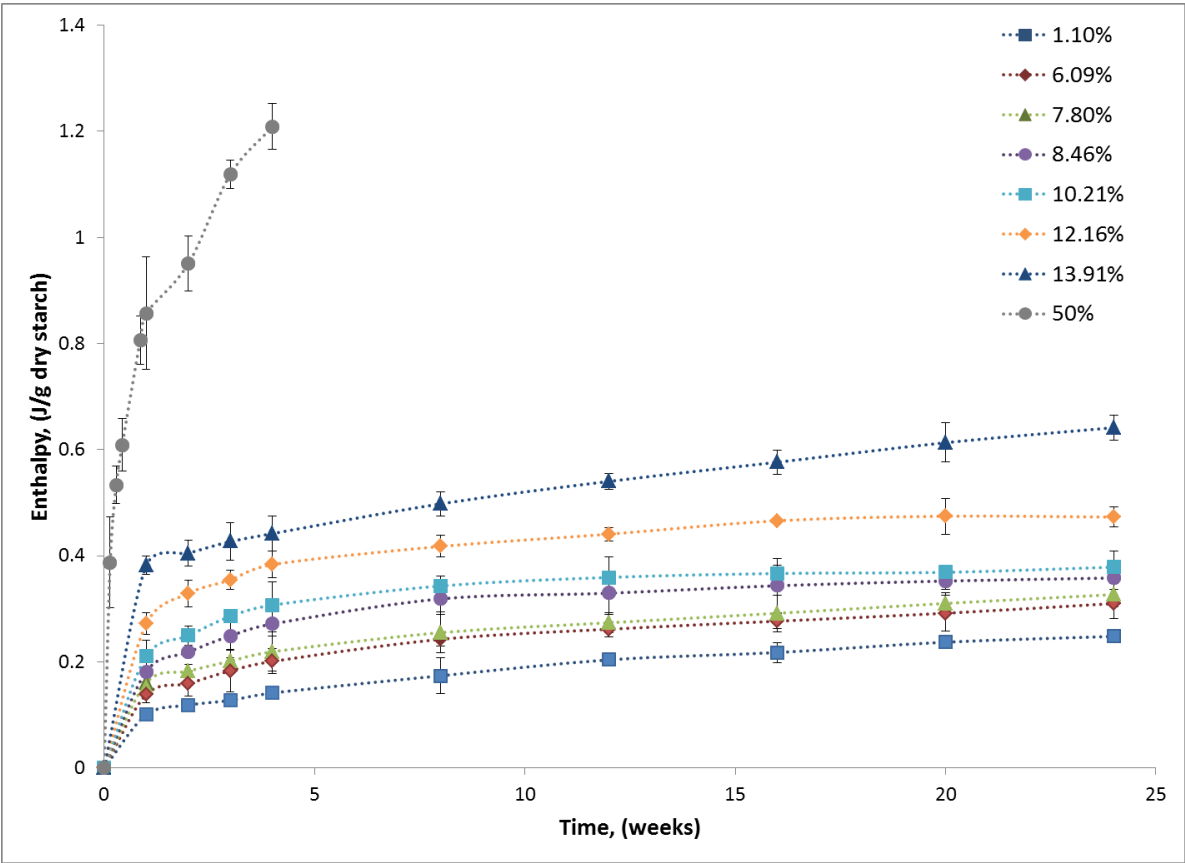
Figure 5.2. Enthalpy values of the sub-Tg endotherm for low moisture content pregelatinized waxy maize starch over 24 weeks. Error bars represent one standard deviation.
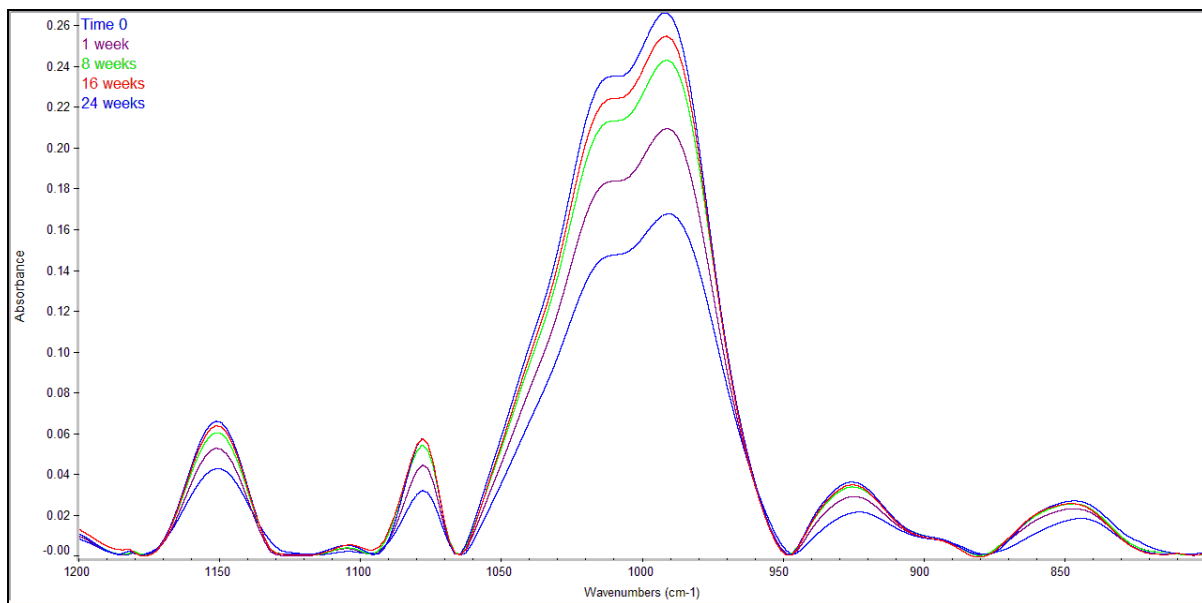
Figure 5.3. FTIR-ATR spectra from 1200 to 800 cm^{-1} of 13.91% moisture content pregelatinized waxy maize starch over 24 weeks.
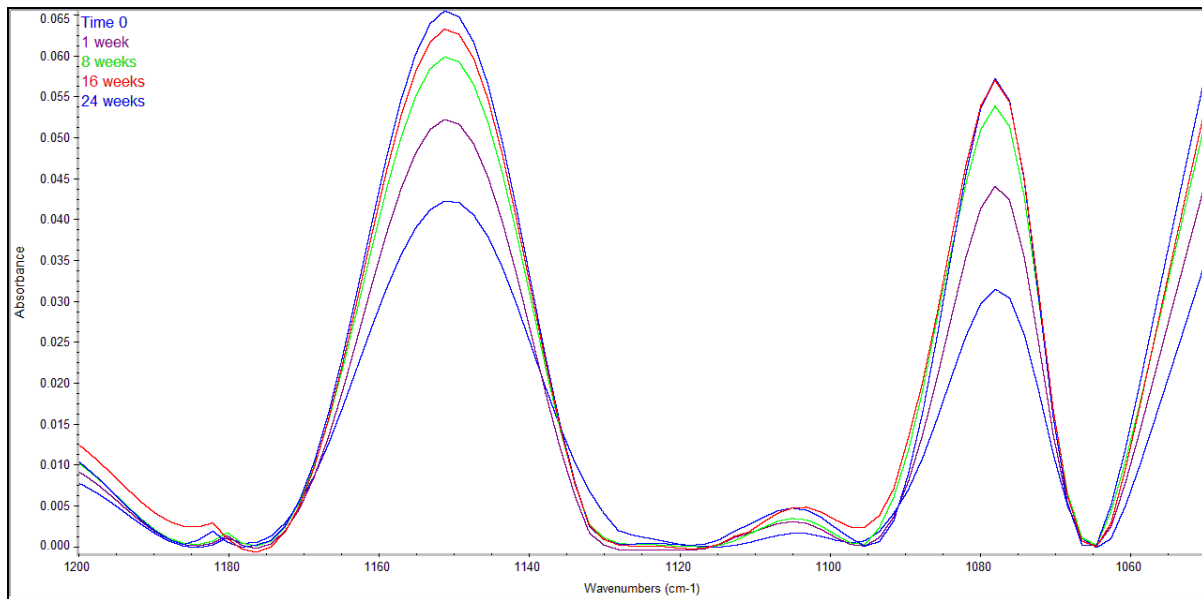
Figure 5.4. FTIR-ATR spectra from 1200 to 1050 cm^{-1} of 13.91% moisture content pregelatinized waxy maize starch over 24 weeks.
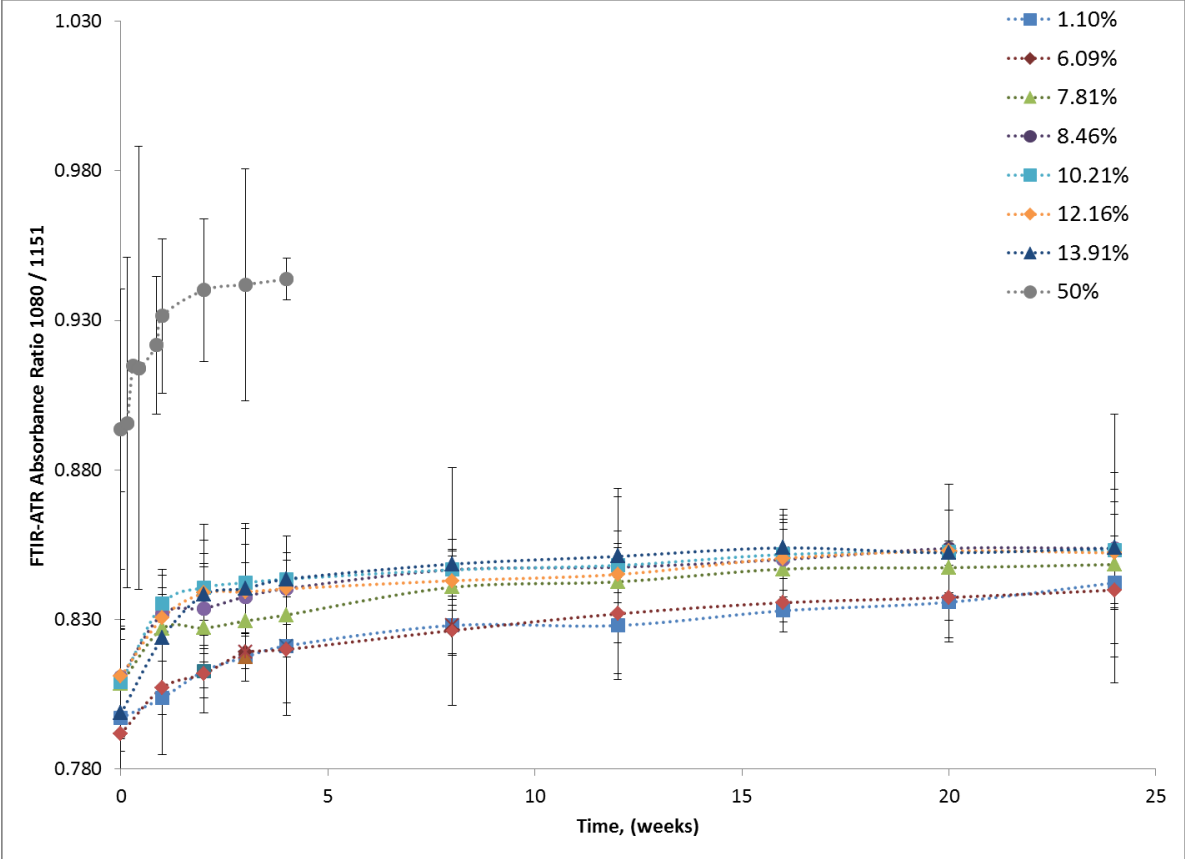
Figure 5.5. FTIR-ATR absorbance ratio 1080/1151 for low moisture content pregelatinized waxy maize starches over 24 weeks. Error bars represent one standard deviation.
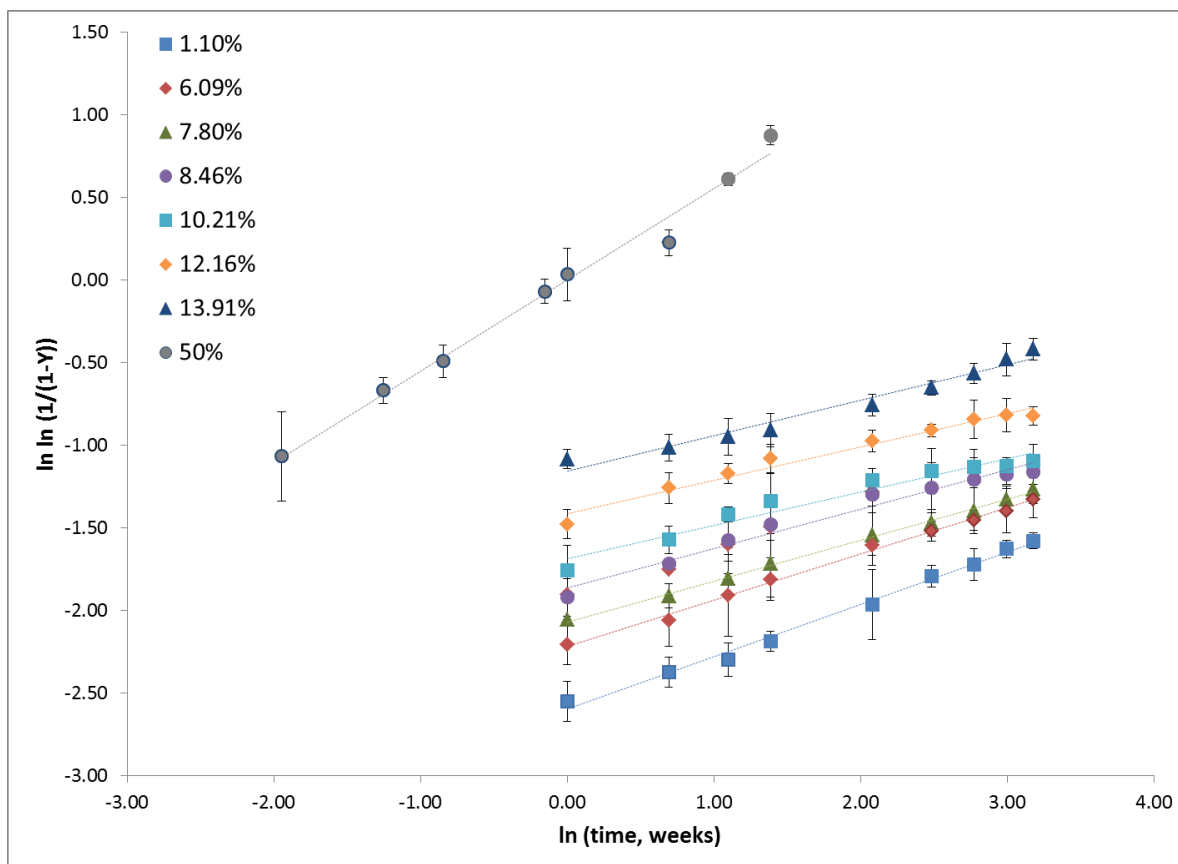
Figure 5.6. $\ln\ln(\dfrac{1}{1-Y})$ **versus ln (time) for low moisture content pregelatinized waxy maize starches over 24 weeks based on enthalpies of the sub-Tg endotherm measured by MDSC. Error bars represent one standard deviation. Lines represent lines of best fit, all with correlation coefficients r > 0.95.**
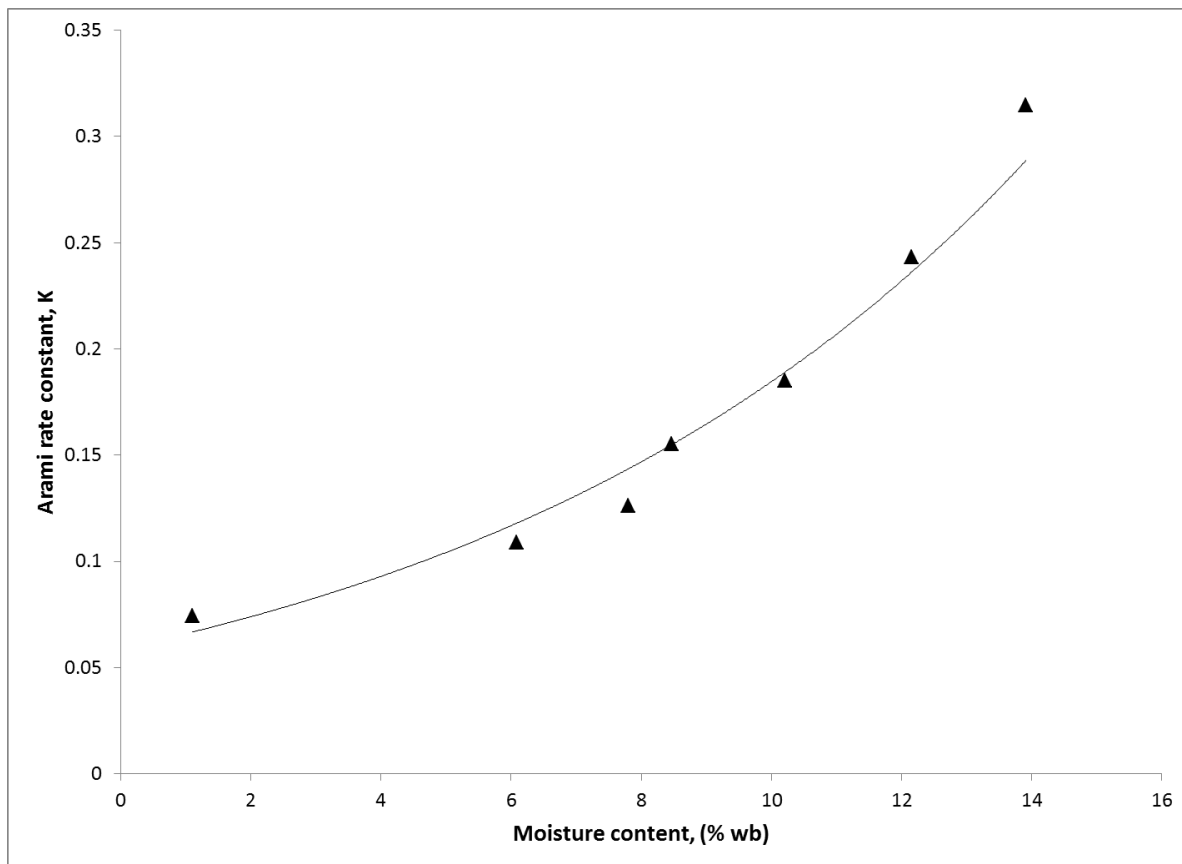
Figure 5.7. Avrami rate constant, K, for low moisture content pregelatinized waxy maize starches. Solid line represents line of best fit for exponential trend (r = 0.97).

Table 5.1. Dessicant and saturated salt slurries providing %RH from 0.0 to 72.1%

Salt	%RH[a]				Solubility (g/100g H_2O)[b]			
	5°C	15°C	25°C	35°C	0°C	10°C	20°C	40°C
Desiccant (calcium sulfate)	0	0	0	0	n/a	n/a	n/a	n/a
LiCl	11.3	11.3	11.3	11.3	69.2	74.5	83.5	89.8
KCH_3COO	24.2	23.4	22.5	21.5	216	233	256	324
$MgCl_2$	33.6	33.3	32.8	32.1	52.9	68.1	73.9	88.5
K_2CO_3	43.2	43.2	43.2	43.2	105	109	111	117
NaBr	62.2	59.1	56.1	53.2	80.2	85.2	90.8	107
KI	72.1	69.9	67.9	66.1	128	136	144	162

[a] %RH data obtained from Greenspan (1977)

[b] solubility data obtained from Haynes (2012)

n/a – not applicable

5.7 References

Avrami M. 1939. Kinetics of phase change. 1 General theory. Journal of Chemical Physics 7(12):1103-12.

Avrami M. 1940. Kinetics of phase change. II Transformation time relations for random distirbution of nuclei. Journal of Chemical Physics 8(2):212-24.

Avrami M. 1941. Granulation, phase change, and microstructure kinetics of phase change. III. Journal of Chemical Physics 9(2):177-84.

Beckmann J, McKenna GB, Landes BG, Bank DH, Bubeck RA. 1997. Physical aging kinetics of syndiotactic polystyrene as determined from creep behavior. Polym. Eng. Sci. 37(9):1459-68.

Bell LN, Labuza TP. 2000. Moisture Sorption – Practical Aspects of Isotherm Measurement and Use 2nd ed. St. Paul, MN: American Association of Cereal Chemists, Inc.

Capron I, Robert P, Colonna P, Brogly M, Planchot V. 2007. Starch in rubbery and glassy states by FTIR spectroscopy. Carbohydrate Polymers 68(2):249-59.

Chung HJ, Lee EJ, Lim ST. 2002. Comparison in glass transition and enthalpy relaxation between native and gelatinized rice starches. Carbohydr. Polym. 48(3):287-98.

Del Nobile MA, Martoriello T, Mocci G, La Notte E. 2003. Modeling the starch retrogradation kinetic of durum wheat bread. J. Food Eng. 59(2-3):123-8.

Descamps N, Palzer S, Zuercher U. 2009. The amorphous state of spray-dried maltodextrin: sub-sub-T-g enthalpy relaxation and impact of temperature and water annealing. Carbohydr. Res. 344(1):85-90.

Elfstrand L, Frigard T, Andersson R, Eliasson AC, Jonsson M, Reslow M, Wahlgren M. 2004. Recrystallisation behaviour of native and processed waxy maize starch in relation to the molecular characteristics. Carbohydr. Polym. 57(4):389-400.

Farhat IA, Blanshard JMV, Mitchell JR. 2000. The retrogradation of waxy maize starch extrudates: Effects of storage temperature and water content. Biopolymers 53(5):411-22.

Fearn T, Russell PL. 1982. A kinetic study of bread staling by differential scanning calorimetry - the effect of loaf specific volume J. Sci. Food Agric. 33(6):537-48.

Gonzalez DC, Khalef N, Wright K, Okos MR, Hamaker BR, Campanella OH. 2010. Physical aging of processed fragmented biopolymers. J. Food Eng. 100(2):187-93.

Goodfellow BJ, Wilson RH. 1990. A Fourier-Transform IR studgy of the gelation of amylose and amylopectin Biopolymers 30(13-14):1183-9.

Greenspan L. 1977. Humidity fixed points of binary saturated aqueous solutions. Journal of Research of the National Bureau of Standards - A, Physics and Chemistry 81A(1):89-96.

Haynes WM. 2012. CRC Handbook of Chemistry and Physics. 92nd (internet version 2012) ed. Boca Raton, FL: CRC Press/Taylor and Francis.

Jouppila K, Kansikas J, Roos YH. 1998. Factors affecting crystallization and crystallization kinetics in amorphous corn starch. Carbohydr. Polym. 36(2-3):143-9.

Kalichevsky MT, Jaroszkiewicz EM, Ablett S, Blanshard JMV, Lillford PJ. 1992. The glass-transition of amylopectin measured by DSC, DMTA and NMR. Carbohydr. Polym. 18(2):77-88.

Kalichevsky MT, Orford PD, Ring SG. 1990. The retrogradation and gelation of amylopectins from various botanical sources. Carbohydr. Res. 198(1):49-55.

Keetels C, vanVliet T, Walstra P. 1996. Gelation and retrogradation of concentrated starch systems .2. Retrogradation. Food Hydrocolloids 10(3):355-62.

Kim SK, Dappolonia BL. 1977a. Bread staling studies 1. Effect of protein content on staling rate and bread crumb pasting properties Cereal Chem. 54(2):207-15.

Kim SK, Dappolonia BL. 1977b. Bread staling studies 3. Effect of pentosans on dough, bread and bread staling rate Cereal Chem. 54(2):225-9.

Kim YJ, Suzuki T, Hagiwara T, Yamaji I, Takai R. 2001. Enthalpy relaxation and glass to rubber transition of amorphous potato starch formed by ball-milling. Carbohydr. Polym. 46(1):1-6.

Li Q. 2010. Investigating the glassy to rubber transition of polydextrose and cornflakes using automatic water vapor sorption instruments, DSC, and texture analysis. [Master of Science]. Urbana, IL: University of Illinois at Urbana-Champaign. 77-117 p.

Livings SJ, Breach C, Donald AM, Smith AC. 1997. Physical ageing of wheat flour-based confectionery wafers. Carbohydr. Polym. 34(4):347-55.

Marsh RDL, Blanshard JMV. 1988. The application of polymer crystal growth theory to the kinetics of formation of the B-amylose polymorph in a 50% wheat starch gel. Carbohydr. Polym. 9:301-17.

McIver RG, Axford DWE, Colwell KH, Elton GAH. 1968. Kinetic study of the retrogradation of gelatinised starch. J. Sci. Food Agric. 19:560-3.

Morgan LB. 1954. Crystallization phenomenon in polymers II. The course of the crystallization. Philosphoical Transcations of the Royal Society of London. Series A, Mathematical and Physical Sciences 247(921):13-22.

Rubens P, Heremans K. 2000. Pressure-temperature gelatinizatin of phase diagram of starch: an in situ Fourier Transform Infrared study. Biopolymers 54(7):524-30.

Rubens P, Snauwaert J, Heremans K, Stute R. 1999. In situ observation of pressure-induced gelation of starches studied with FTIR in the diamond anvil cell. Carbohydrate Polymers 39(3):231-5.

Russell PL. 1983. A kinetic study of bread staling by differential scanning calorimetry and compressibility measurements - the effect of added monoglyceride J. Cereal Sci. 1(4):297-303.

Seow CC, Teo CH. 1996. Staling of starch-based products: A comparative study by firmness and pulsed NMR measurements. Starch-Starke 48(3):90-3.

Sevenou O, Hill SE, Farhat IA, Mitchell JR. 2002. Organisation of the external region of the starch granule as determined by infrared spectroscopy. International Journal of Biological Macromolecules 31(1–3):79-85.

Shogren RL. 1992. Effect of moisture content on the melting and subsequent physical aging of corn starch. Carbohydr. Polym. 19(2):83-90.

Silverio J, Fredriksson H, Andersson R, Eliasson AC, Aman P. 2000. The effect of temperature cycling on the amylopectin retrogradation of starches with different amylopectin unit-chain lenght distribution. Carbohydr. Polym. 42:175-84.

Slade L, Levine H. 1988. Non-equilibrium melting of native granular starch. I. Temperature location of the glass transition associated with gelatinization of A-type cereal starches. Carbohydr. Polym. 8:183-208.

Struik LCE. 1987. The mechanical and physical ageing of semicrystalline polymers: 1. Polymer 28:1521-33.

TA Instruments - Waters L. 2011. TRIOS version 2.3.4 1613. 2.3.4 ed. New Castle, Delaware, USA.

Thermo Fisher Scientific I. 2012. OMNIC version 9.1.27. 9.1.27 ed. Waltham, Massachussetts, USA.

van Soest JJG, Tournois H, de Wit D, Vliegenthart JFG. 1995. Short-range structure in (partially) crystalline potato starch determined with attenuated total reflectance Fourier-transform IR spectroscopy. Carbohydrate Research 279(0):201-14.

Warren FJ, Perston BB, Royall PG, Butterworth PJ, Ellis PR. 2013. Infrared spectroscopy with heated attenuated total internal reflectance enabling precise measurement of thermally induced transitions in complex biological polymers. Analytical Chemistry 85(8):3999-4006.

Wilson RH, Goodfellow BJ, Belton PS, Osborne BG, Oliver G, Russell PL. 1991. Comparison of fourier-transorm mid infrared spectroscopy and near infrared reflectance spectroscopy with differential scanning calorimetry for the study of the staling of bread J. Sci. Food Agric. 54(3):471-83.

Wilson RH, Kalichevsky MT, Ring SG, Belton PS. 1987. A Fourier-transform infrared study of the gelation and retrogradation of waxy-maize starch. Carbohydr. Res. 166:162-5.

Yuan RC, Thompson DB. 1994. Sub-Tg thermal properties of amorphous waxy starch and its derivatives. Carbohydr. Polym. 25(1):1-6.

Zeleznak KJ, Hoseney RC. 1986. The role of water in the retrogradation of wheat starch gels and bread crumb. Cereal Chem. 63(5):407-11.

Zeleznak KJ, Hoseney RC. 1987. The glass transition in starch. Cereal Chem. 64(2):121-4.

Zhang W, Jackson DS. 1992. Retrogradation behavior of wheat starch gels with differing molecular profiles. Journal of Food Science 57(6):1428-32.

CHAPTER 6

DEVELOPMENT OF THE SUB-TG ENDOTHERM AND ASSOCIATED TEXTURAL CHANGES IN A MODEL CRACKER SYSTEM

6.1 Abstract

Previous work has reported that, in pregelatinized starch at low moisture contents, amylopectin can reform double helices, giving rise to a sub-Tg endotherm. This development is similar to the first step of the amylopectin retrogradation process that has been linked with bread staling at higher moisture contents. As such, the aim of this work was to characterize the development of the sub-Tg endotherm in baked waxy maize starch and a model low moisture cracker system, and link the development of the endotherm to corresponding textural changes in the crackers that can be described as "staling." In wheat-flour based crackers and baked waxy maize starch, the development of the sub-Tg endotherm was monitored using MDSC and starch structural changes were assessed using FTIR-ATR. Concurrently, the cracker texture was analyzed over time by 3-point bend analysis using a TA-XT Plus texture analyzer. The development of the sub-Tg endotherm in the model cracker system and baked waxy maize starch was found to be correlated with a decrease in the FTIR-ATR absorbance ratio 1080 cm^{-1} / 1151 cm^{-1}, which has been previously linked to the reformation of amylopectin double helices. Furthermore, the enthalpy of the endotherm developed over time according to Avrami kinetics, as is often used to describe starch retrogradation and bread staling. Over the same timeframe, the hardness of the crackers decreased, and the hardness was negatively correlated with the enthalpy of the sub-Tg endotherm measured by MDSC. This work confirms that staling and associated textural changes in low moisture starch-based food systems, such as crackers, is a result of reformation of amylopectin double helices without crystallization or aggregation of those helices that develops at higher moisture contents.

6.2 Introduction

While recognized and investigated for many years, bread staling still results in substantial economic losses to both the baking industry and the consumer. The generally accepted definition of staling is "a term which indicates decreasing consumer acceptance of bakery products caused by changes in crumb other than those resulting from the action of spoilage organisms" (Bechtel

172

and others 1953). At the macroscopic level, staling is characterized by a time-dependent firming of the crumb, flavor changes and loss of crispy crust. At the molecular level, moisture migration and redistribution, recrystallization of starch components and changes in interactions between the protein and starch fractions may contribute to the global processes known as staling.

The retrogradation of starch polymers was first proposed as a mechanism for staling based on evidence of the similarity in x-ray diffraction patterns between fresh bread and freshly gelatinized wheat starch as well as between stale bread and retrograded starch (Gray and Bemiller 2003). When starch granules are gelatinized, a portion of the amylose may diffuse into the interstitial environment, concentrate, and quickly undergo retrogradation upon cooling. Thus, even if amylose leaches from the starch granules during the baking process, by the time the bread has completely cooled, any interstitial amylose will have retrograded and become insoluble, and therefore, unlikely to play a role in any future staling events (Kim and Dappolonia 1977c; Kim and Dappolonia 1977a; Kim and Dappolonia 1977b). Starch is a 2-component polymer, composed of amylose and amylopectin, and if changes in starch structure are at least partly responsible for the staling phenomenon, then the amylopectin fraction must be the responsible polymer.

Wheat flour, the primary component of bread, contains approximately 84 to 88% (db) starch. During baking, the starch partially gelatinizes, leading to the formation of a continuous starch network. As a consequence of gelatinization, amylopectin crystallites are melted, leading to amylopectin in the amorphous plasticized state in the fresh bread crumb and phase separation of the amylopectin and amylose components (Hug-Iten and others 1999). The amylopectin is located primarily inside the starch granule, though some amylopectin side chains may protrude into the intergranular space, as well as into the amylose-rich granule center. Reorganization of the amylopectin results in reformation of its double helical structures, which can repack into crystallites upon aging. This reorganization imparts rigidity to both the swollen granule and the intergranular material by acting as physical crosslinks in the overall gel structure leading to staling of the bread. The reorganization of starch into even very low levels of crystallinity is magnified in its effect on crumb firmness (Hug-Iten and others 2003; Ribotta and others 2004). For example, Ribotta and Le Bail (2007) witnessed changes in the thermo-mechanical profile of aged bread crumb by dynamic mechanical analysis (DMA), and as the concentration of retrograded starch increased, the contraction capacity of bread crumb was significantly impacted.

Staling is generally considered to be a phenomenon that occurs above the glass transition of the material, though the glass transition is not necessarily a static value. Slade and Levine (1991) described an increase in the Tg of bread during staling as a result of annealing and networking of amorphous chains in the starch. If stored long enough, the amorphous network was described as maturing leading to an increase in Tg, as was observed by Hallberg and Chinachoti (1992) in meal, ready-to-eat (MRE) bread during long-term storage up to 3 years. An increase in Tg during the staling of bread was also correlated with firming as measured by Instron, attributed to an increase in crosslink density in the starch granules due to formation of crystallites. The Tg of the bread could then be used to calculate the extent of staling, knowing that in fresh bread the Tg is at subzero temperature, but Tg increases to room temperature as a low level of starch network is reformed, and Tg then continues to increase to well above room temperature as the network matures and the bread becomes completely stale (Jagannath and others 1999).

However, the molecular mobility in low-moisture (<9% wet basis) white bread was studied as a function of temperature using pulsed-proton nuclear magnetic resonance (NMR), and dielectric and dynamic mechanical spectroscopies, reporting that the water was transversely and longitudinally mobile, even in glassy samples (Roudaut and others 1999a; Roudaut and others 1999b). These results were interpreted and extrapolated to suggest that the Tg is not a universal predictive parameter for the physical stability of glassy or rubbery materials. Indeed, because bread firming, measured as a change in its dielectric properties, was observed at −53°C, located far below the reported Tg for both dry gelatinized starch and white bread, it was assumed that the relaxation observed corresponded to more localized motions, possibly associated with the local motion of a side group or short segment of the main chain, typically referred to as beta relaxations. For example, in phenylene polymers, the low activation value (near zero) of the beta relaxations reflects limited cooperativity, which reflects the number of atoms involved in the movement of the relaxing unit (Starkweather and Avakian 1989). Furthermore, several cereal-based products have exhibited changes in both mechanical properties and texture associated with a loss of crispness, even while in the glassy state (Attenburrow and others 1992; Li and others 1998; Nicholls and others 1995; Roudaut and others 1999a; Roudaut and others 1999b; Roudaut and others 2004), again implying that staling cannot be solely characterized by changes in Tg.

At room temperature, typical bread is considered to be above Tg, while commercial crackers, which generally have a moisture content of <3% wet basis, are well below the system Tg. Yet, the texture of low moisture baked food products such as crackers, biscuits and breakfast cereals have been shown to be dependent on many of the same factors that influence bread staling. Furthermore, work reported in previous chapters linked the development of the sub-Tg endotherm in amylopectin at low moisture contents to the reformation of double helices, which is the first step of the amylopectin retrogradation process. The rate of reformation of amylopectin double helical structure was further found to follow Avrami kinetics, which is also often used to describe the kinetics of bread staling. As such, the aim of this work is to characterize the development of the sub-Tg endotherm in a model low moisture cracker system as related to textural changes in the cracker system occurring during storage.

6.3 Materials and methods

6.3.1 Cracker model system

A model sheeted cracker, similar to a matzo cracker or water cracker, was prepared by mixing 100 parts pastry flour (White Spray, Conagra) with 45 parts of water and baked at 425°F for 4 minutes using the mixing and sheeting procedure described by the AACC benchtop method for chemically leavened crackers (Kweon and others 2011a; Kweon and others 2011b). The dough was prepared by mixing the flour and water for 10 minutes in the McDuffy laboratory pin mixer attachment for the Hobart mixer. Dough was sheeted to 1.1 mm thickness using the Rondo SS0 615 floor model sheeter (Rondo Inc., Moonachie, New Jersey) without folding and rotation of the dough sheet between successive passes. Dough was cut into 4.0 cm diameter round pieces with 7 docker pins and then baked in a Picard MT-4-8 revolutionary oven (Picard Ovens Inc., Victoraville, Quebec, Canada). Similarly, 100 parts unmodified native waxy maize starch (Waxy #1, Tate & Lyle) was mixed with 45 parts water and allowed to equilibrate for 2 hours before spreading in a thin layer on a baking sheet and baking at 425°F for 4 minutes. Initial moisture content of the crackers and the baked starch was determined by weight loss after baking.

6.3.2 Characterization of moisture dependence

After allowing the crackers to cool at ambient conditions, a portion of the crackers was ground using a laboratory coffee grinder, and then the ground crackers and a portion of the baked starch were equilibrated over saturated salt solutions encompassing a range of %RH values (Table 6.1). Saturated salt slurries were prepared by adding an excess amount of salt into deionized water according to the known solubility values, heating the slurry to approximately 50°C for about 2 hours, while stirring on a standard stir plate and then cooling to room temperature.

A sufficient amount of saturated salt slurry was added to storage containers (airtight and water proof plastic containers commercially known as "Lock & Lock") to completely cover the bottom of the container. About 4 grams of "as is" ground crackers and baked waxy maize starch were separately weighed into small plastic cups and transferred to the "Lock & Lock" container holding the saturated salt slurry. Containers were kept in an incubator at a storage temperature of 25°C. After constant weight was reached, defined as when the sample weight changed by less than 2mg/g dry weight between successive weight measurements (Bell and Labuza 2000), the equilibrium moisture content was determined using the initial sample weight, the initial moisture content and the equilibrium sample weight. The ground crackers and baked starch were subsequently held at their respective %RH and 25°C storage temperature for at least 6 months to allow for full development of any phase or structural transitions within the starch amylopectin.

After 6-month storage over the saturated salt solutions, the ground crackers and baked starch were analyzed for thermal transitions using Modulated Differential Scanning Claorimetry (MDSC). Samples were taken from the "Lock & Lock" containers and transferred to DSC T-zero aluminum hermetic pans in triplicate and sealed with internal hermetic lids immediately after transferring out of the "Lock & Lock" containers in order to maintain the appropriate moisture content and %RH within the sample throughout the study. Samples were equilibrated at 0°C and scanned using a modulated heating profile with a rate of 1°C/min, oscillation period of 80 seconds, and amplitude of 0.5°C from 0°C to 120°C using the Q2000 Differential Scanning Calorimeter instrument (TA Instruments, New Castle, Delaware). The onset temperature, peak temperature, and enthalpy of the transitions of observed peaks were determined through peak integration using the TRIOS Software version 2.3.4.1613 from TA Instruments (2011). Each scan was analyzed in triplicate.

In addition to MDSC analysis, Fourier-transform infrared, attenuated total reflectance (FTIR-ATR) spectra of the ground crackers and baked starch were acquired using a Thermo Nicolet iS™10 FT-IR with the Scientific Smart iTR™ diamond attenuated total reflectance (ATR) accessory with nitrogen purge (Thermo Scientific, Waltham, Massachusetts). Spectra were obtained at a resolution of 4cm^{-1} from 4000 to 400 cm^{-1} and averaged over 100 scans, recorded against an empty cell as background. Deconvoluted spectra were baseline corrected in the 1200 to 800 cm^{-1} region and peak height was analyzed at 995, 1022, 1044, 1078 and 1151 cm^{-1} using the OMNIC 9.1.27 software (Thermo Fisher Scientific 2012) . Triplicate FTIR-ATR spectra were obtained of each sample, and each spectrum was analyzed in triplicate.

6.3.3 Characterization of cracker texture over time

The remaining portion of crackers and baked waxy maize starch were stored in the incubator at 25°C and removed at weeks 0, 4, 8, 12, 16, 20, 24, 28 and 32 for texture testing. Crackers were analyzed for breakage force, distance to break and brittleness (resistance to bend or snap) using the 3-point bend procedure with the TA-XT Plus texture analyzer (Stable Microsystems, Surrey, United Kingdom) using a 25 kg load cell and the HDP/3PB 3-point bending rig apparatus. The test measures the force in compression after the trigger value of 5 grams force is obtained using a pre-test speed of 1.0 mm/s, test speed of 5.0 mm/s and post-test speed of 1.0 mm/s. Crackers are flexed to the moment of breakage on a fixture consisting of two parallel supporting bars placed 3.0 cm apart, over which the crackers were centered. Once the trigger force was attained, the force was observed to increase until such time as the cracker fractured and fell into two pieces. The maximum force needed to break the cracker was recorded as the break force (in g_f). The distance the probe traveled before the cracker broke (in mm) and the slope of the line created up to the moment of cracker breakage (in g_f/mm) were also recorded.

As previously described for tea biscuits by Baltsavias and others (1997) and Saleem (2005), those recorded parameters can then be used to determine the mechanical and fracture properties of the cracker according to the following expressions based on the theory of the flexure of short beams:

$$\sigma_{max} = \frac{3FL}{2bh^2}$$ Equation 6.1

177

$$\varepsilon = \frac{6tY}{L^2} \qquad \text{Equation 6.2}$$

$$E = \frac{L^3 m}{4bh^3} \qquad \text{Equation 6.3}$$

where σ is the failure stress (measured in kPa), ε is the failure strain (reported as % deformation), and E is Young's modulus (also referred to as the bending or flexure modulus of elasticity; measured in kPa). F is the break force (in Newtons), L is the span length or the distance between the two adjustable supports (in m), b is the width or diameter of the crackers (in m), h is the thickness of the crackers (in m), Y is the deformation at the beam center under the failure load measured as the distance the probe traveled before the cracker broke (in m), and m is the slope of the load-deflection curve, measured as the gradient/slope of the line from start to maximum force (in N / m). For each sample, 10 crackers were analyzed.

6.3.4 Characterization of cracker sub-Tg endotherm kinetic development

Following texture testing, crackers were ground using a laboratory coffee grinder and moisture content was determined via quick drying with a halogen oven (CompuTrac Max 1000, Arizona Instruments, Chandler, Arizona), calibrated to vacuum oven drying for 4 hours at 25-100 mmHg and 105°C.The moisture content of the remaining portion of baked waxy maize starch was determined similarly at each time point. The ground crackers and baked waxy maize starch were subsequently scanned for thermal transitions and FTIR-ATR spectra were acquired using the MDSC profile and FTIR conditions, respectively, as previously described.

6.4 Results and discussion

Wheat flour-based crackers and baked waxy maize starch were characterized at different moisture contents, from 1 to 14% wet basis, after minimum 6 month equilibration following baking. A sub-Tg endotherm with a peak temperature between 40 and 55°C was observed at all moisture contents in the non-reversing heat flow of the MDSC scan for both the crackers and baked starch (Figure 6.1 and Figure 6.2), indicating that this peak is related to a kinetic event occurring in the starch granule rather than as a result of interactions between the starch and

178

protein in the wheat flour. All observed endotherms occurred below Tg, which is approximately 65°C and above for starch moisture contents of 12% and below (Zeleznak and Hoseney 1987).

The enthalpy of the sub-Tg thermal transition in both the crackers and baked starch exhibited an exponential relationship with increasing moisture content (Figure 6.3). Literature reports of the sub-Tg endotherm have also indicated that, in general, as moisture content increased, enthalpy of the peak increased, while the onset and midpoint peak temperatures were independent of moisture content (Badii and others 2005; Chung and others 2002; Shogren 1992; Thiewes and Steeneken 1997). Similar trend with moisture content was also observed with pregelatinized waxy maize starch at low moisture contents reported in previous chapters. This endotherm was linked to the re-adoption of double helical structure by the starch amylopectin following gelatinization. The reformation of the double helical structure is the first step in the amylopectin retrogradation process, though at these low moisture contents, redevelopment of crystalline structure was not observed. During baking, the starch in the wheat flour of the crackers or the baked waxy maize starch is at least partially gelatinized, meaning that structural order in the starch granules is lost. Post-baking, this structural order through reformation of the amylopectin double helices can be regained, even at low moisture contents, giving rise to the observed endotherms.

Over a 32 week time period, the enthalpy of the sub-Tg endotherm in the crackers and baked waxy maize starch was observed to increase with time (Figure 6.4 and Figure 6.5). Over the same time period, the ratio of the FTIR-ATR absorbance peaks at 1080 cm^{-1} / 1151 cm^{-1} was found to decrease (Figure 6.6 and Figure 6.7). A decrease in this ratio was previously linked to the reformation of amylopectin double helices in pregelatinized waxy maize starch in an earlier chapter. Furthermore, literature also describes changes in peak absorbance at 1080 cm^{-1} as being related to starch ordered structure (Rubens and Heremans 2000; Rubens and others 1999; Warren and others 2013).

Most of the proposed models used to predict the kinetics of retrogradation and amylopectin recrystallization are based on the Avrami equation, originally derived to describe polymer crystallization from the melt (Avrami 1939; Avrami 1940; Avrami 1941). The Avrami equation can be represented as:

$$Y = 1 - e^{-Kt^n} \qquad\qquad\qquad \text{Equation 6.4}$$

Which can be rewritten as

$$\ln \ln(\frac{1}{1-Y}) = \ln K + n \ln(t)$$
<div align="right">Equation 6.5</div>

Where Y is the extent of transformation or crystallization, K is the rate constant, n is the Avrami exponent and t is time.

Thus, the extent of transformation or crystallization followed over time, would be expected to follow an "S" shaped curve such that when integrated, a plot of $\ln \ln(\frac{1}{1-Y})$ versus time should yield a straight line with slope of n and y-intercept of ln K. When the MDSC-measured enthalpies of the sub-Tg endotherm for the crackers and baked pregelatinized waxy maize starches are expressed in this manner, straight lines are observed with the same slope (n = 0.48) and y-intercept (ln K = -2.34; K = 0.096) (Figure 6.8). The congruence of the development of the sub-Tg endotherm in the crackers and baked waxy maize starch implies the same underlying mechanism such as the reformation of the double helices within the amylopectin after baking.

In the Avrami equation, the rate constant, K, depends on the crystals growth constant and on the crystals nucleation constant, while the Avrami exponent, n, depends on the type of crystal nucleation and the dimensions in which the growth takes place, implying that the Avrami exponent can assume an integer value ranging from 4 to 1 dimension. In three dimensions, spherulitic crystals are formed, whereas disc-like crystals form in two dimension and rod-like crystals form in one dimension (Del Nobile and others 2003). The Avrami exponent has previously been determined to be n = 1 for both gelatinized starch (McIver and others 1968) and for bread (Kim and Dappolonia 1977c; Kim and Dappolonia 1977a), implying rod-like growth and instantaneous nucleation. Morgan (1954) noted that the nucleation sites probably corresponded to the regions of chain entanglement formed during gelation with crystallization then proceeding between two adjacent chains to re-form double helices. Good fit to the data for the staling of bread by constraining the Avrami exponent to 1 has also been reported by Fearn

and Russell (1982), Russell (1983) and Wilson and others (1991), though in these studies, the best data fit, though not significantly better, was found for integer values less than one.

Avrami exponents of less than one have been found previously for corn starch gels, bread and rice cupcakes (Seow and Teo 1996). Accordingly, one of the implicit assumptions in applying the Avrami equation to the kinetics of amylopectin recrystallization is that any enthalpy changes occurring during staling are a direct measure of the quantity of recrystallized starch produced. If the degree of order of the starch (i.e. amorphous, complete recrystallization or partial recrystallization) is different, then varying changes in both enthalpy and entropy may account for a given decrease in free energy resulting in Avrami exponents less than one (Fearn and Russell 1982). For the crackers and baked waxy maize starch, the enthalpy change is known to only represent reformation of double helices and partial ordered structure and thus, only the nucleation step of the recrystallization process. Furthermore, both systems contain a mixture of gelatinized, ungelatinzed, and partially gelatinized starch due to the lower moisture conditions during baking. As such, an Avrami exponent of less than one is not surprising.

Over the 32-week storage period, the texture of the crackers measured by 3-point bend texture profile analysis was also observed to change (Figure 6.9). Failure stress, or the force required to break the crackers, and Young's Modulus, a measure of the "toughness" of the crackers, trended down over time, while failure strain was relatively unaffected by time (Figure 6.10, Figure 6.11, and Figure 6.12). In particular, the failure stress strongly correlated with the enthalpy of the sub-Tg endotherm as measured by MDSC (Figure 6.13 confirming that textural changes in the crackers related to staling are a result of the reformation of amylopectin double helices, similar to the first step of the retrogradation process that occurs in bread and other starch-based systems at higher moisture contents. Textural changes associated with bread staling have long been linked to amylopectin retrogradation, while several cereal-based products have exhibited changes in both mechanical properties and texture associated with a loss of crispness and staling, even while in the glassy state (Attenburrow and others 1992; Li and others 1998; Nicholls and others 1995; Roudaut and others 1999a; Roudaut and others 1999b; Roudaut and others 2004). This work confirms that staling and associated textural changes in low moisture starch-based food systems, such as crackers, is a result of reformation of amylopectin double helices without crystallization or aggregation of those helices that might develop at higher moisture contents.

6.5 Summary and conclusions

In wheat-flour based crackers and baked waxy maize starch, a sub-Tg endotherm was observed that was exponentially related to moisture content and similar to endotherms observed in commercial pregelatinized starches. The development of this endotherm was correlated with a decrease in the FTIR-ATR absorbance ratio 1080 cm^{-1}/1151 cm^{-1}, which has been previously liked to the reformation of amylopectin double helices. Furthermore, the enthalpy of the endotherm developed over time according to Avrami kinetics, as is often used to describe starch retrogradation and bread staling. Over the same timeframe, the failure stress or hardness of the crackers decreased, and the failure stress was negatively correlated with the enthalpy of the sub-Tg endotherm measured by MDSC. This work confirms that staling and associated textural changes in low moisture starch-based food systems like crackers is a result of reformation of amylopectin double helices without crystallization or aggregation of those helices that might develop at higher moisture contents.

6.6 Figures and tables
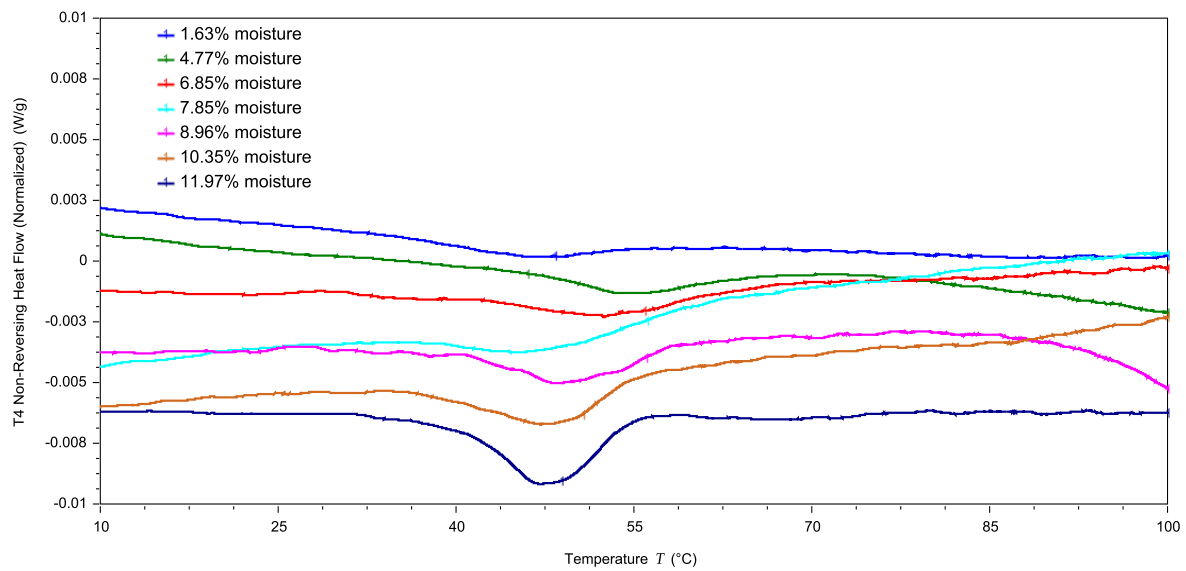
Figure 6.1. MDSC-observed sub-Tg endotherm for crackers at different moisture contents (% wet basis) after 6 month equilibration.
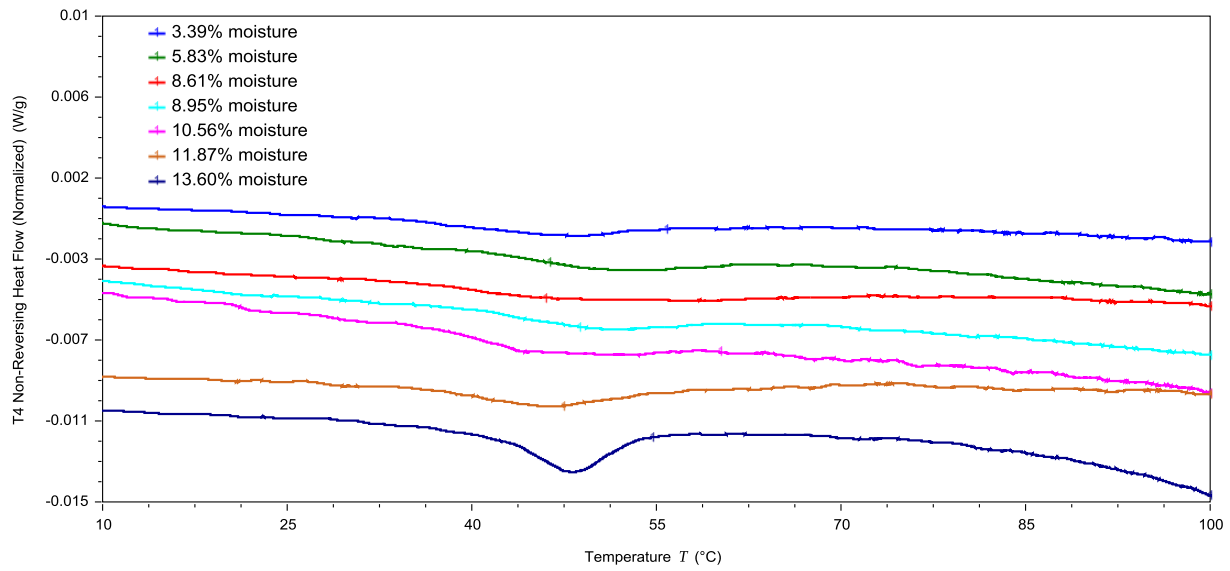
Figure 6.2. MDSC-observed sub-Tg endotherm for baked waxy maize starch at different moisture contents (% wet basis) after 6 month equilibration.
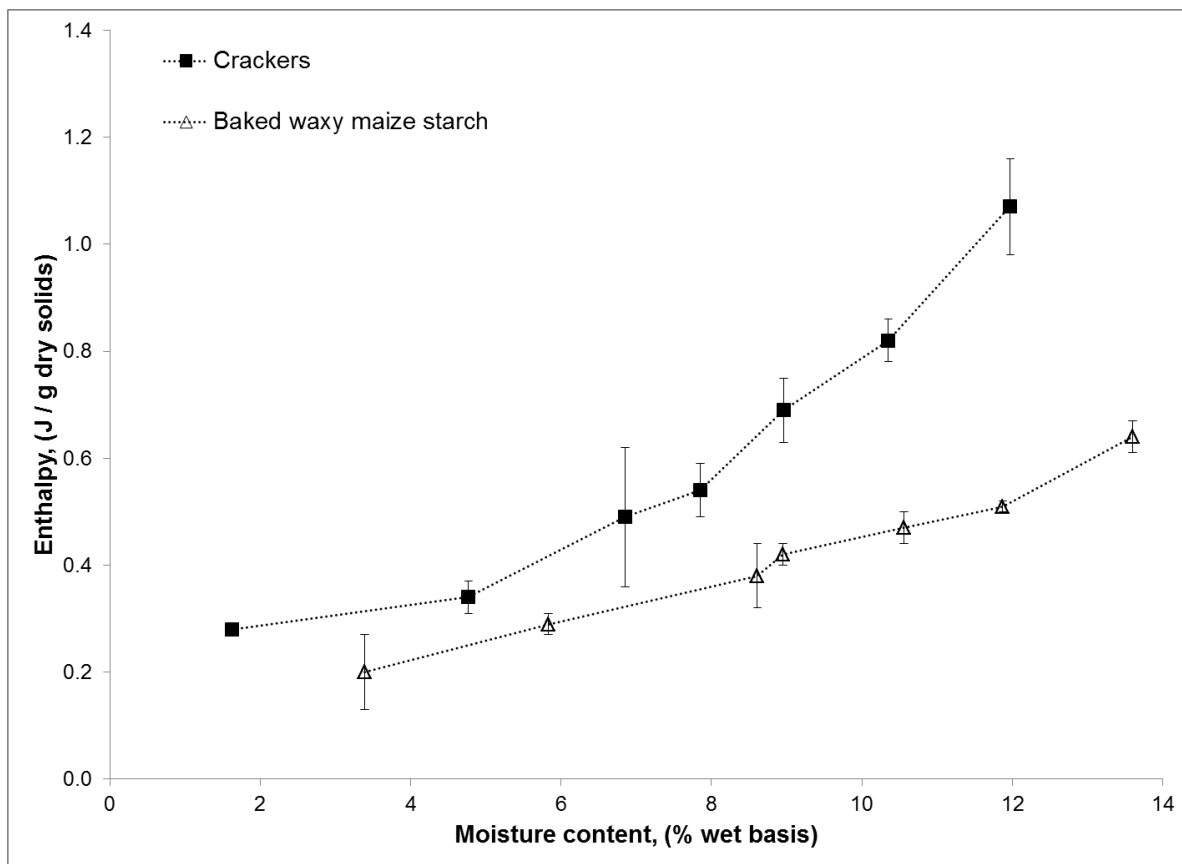
Figure 6.3. Enthalpy associated with the sub-Tg endotherm in the non-reversing heat flow characterized as a function of moisture content of the crackers or baked starch after 6 month equilibration. Error bars represent one standard deviation.
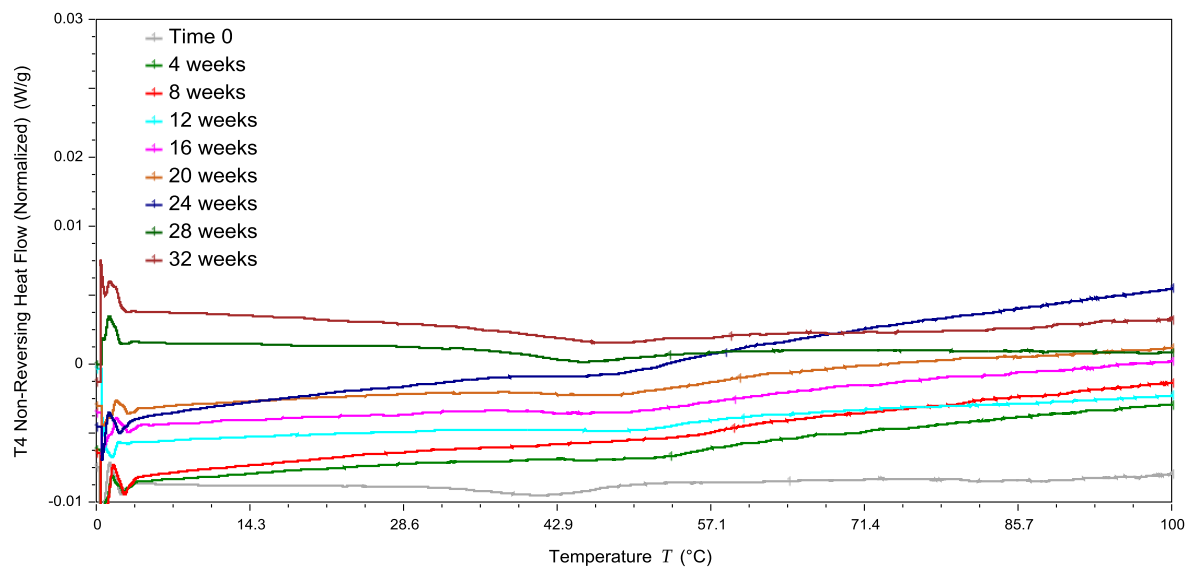
Figure 6.4. MDSC-observed sub-Tg endotherm for crackers stored at 25°C for 32 weeks.
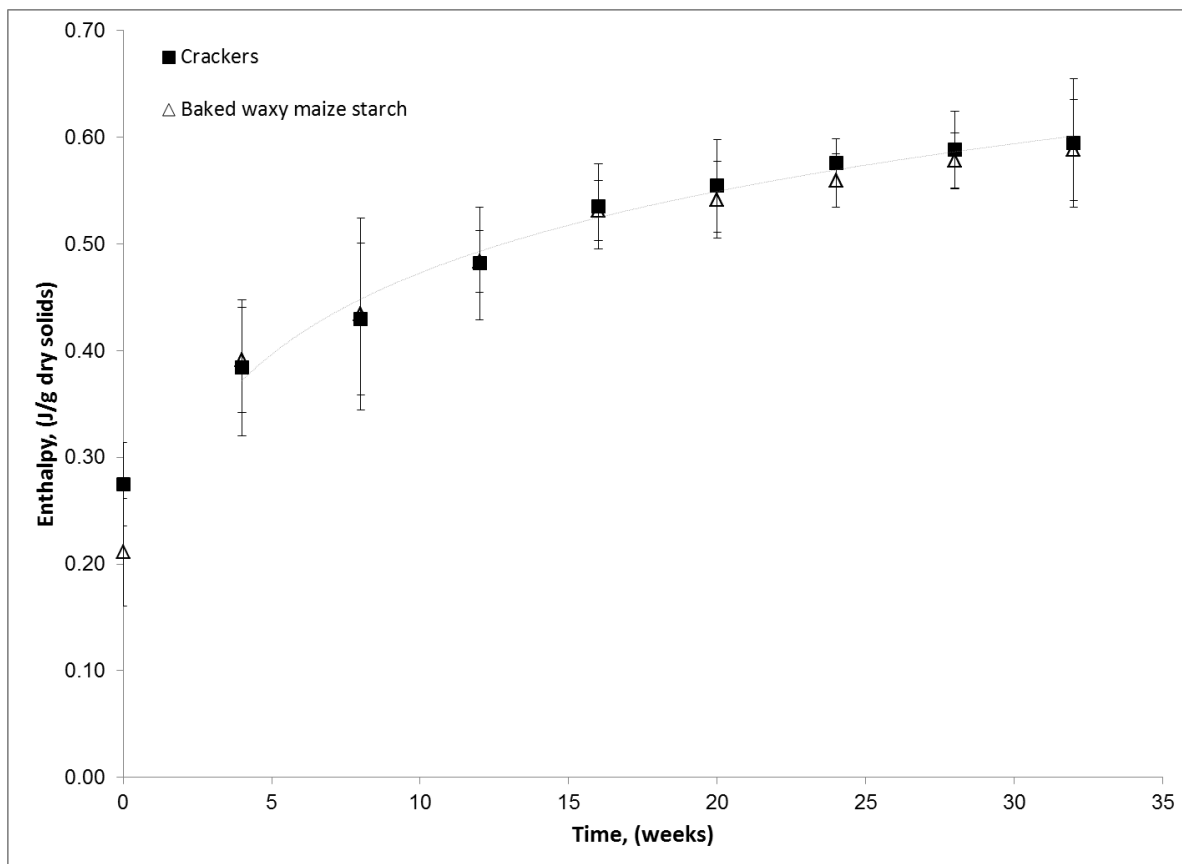
Figure 6.5. Enthalpy associated with the sub-Tg endotherm in the non-reversing heat flow for crackers and baked waxy maize starch stored at 25°C for 32 weeks. Error bars represent one standard deviation.
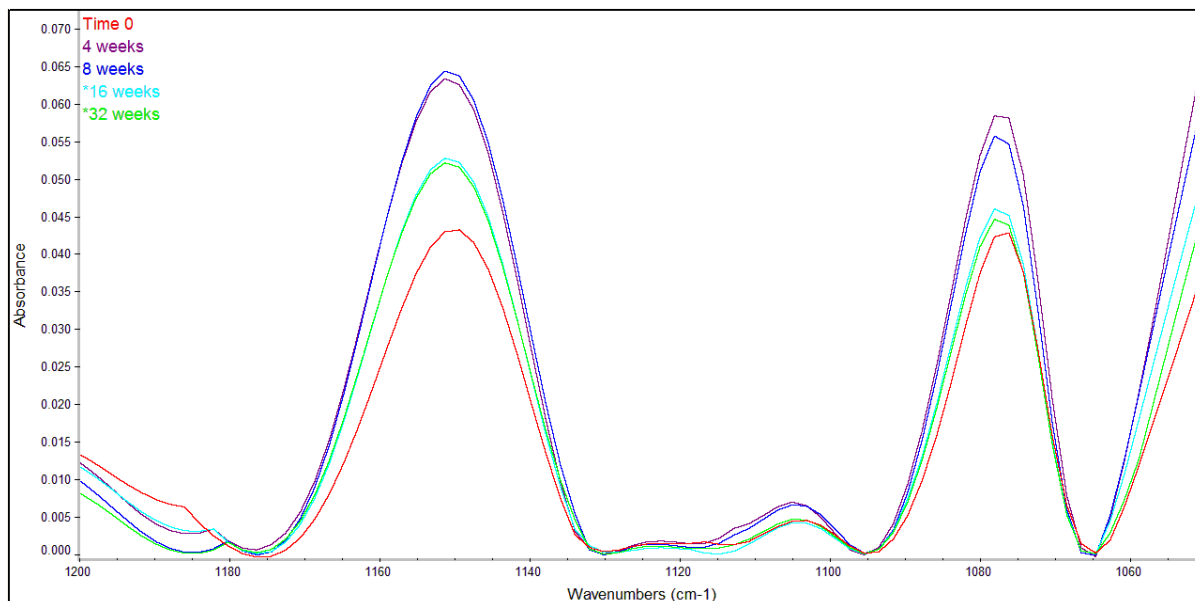
Figure 6.6. FTIR-ATR spectra from 1200 to 1050 cm^{-1} of crackers stored at 25°C for 32 weeks.
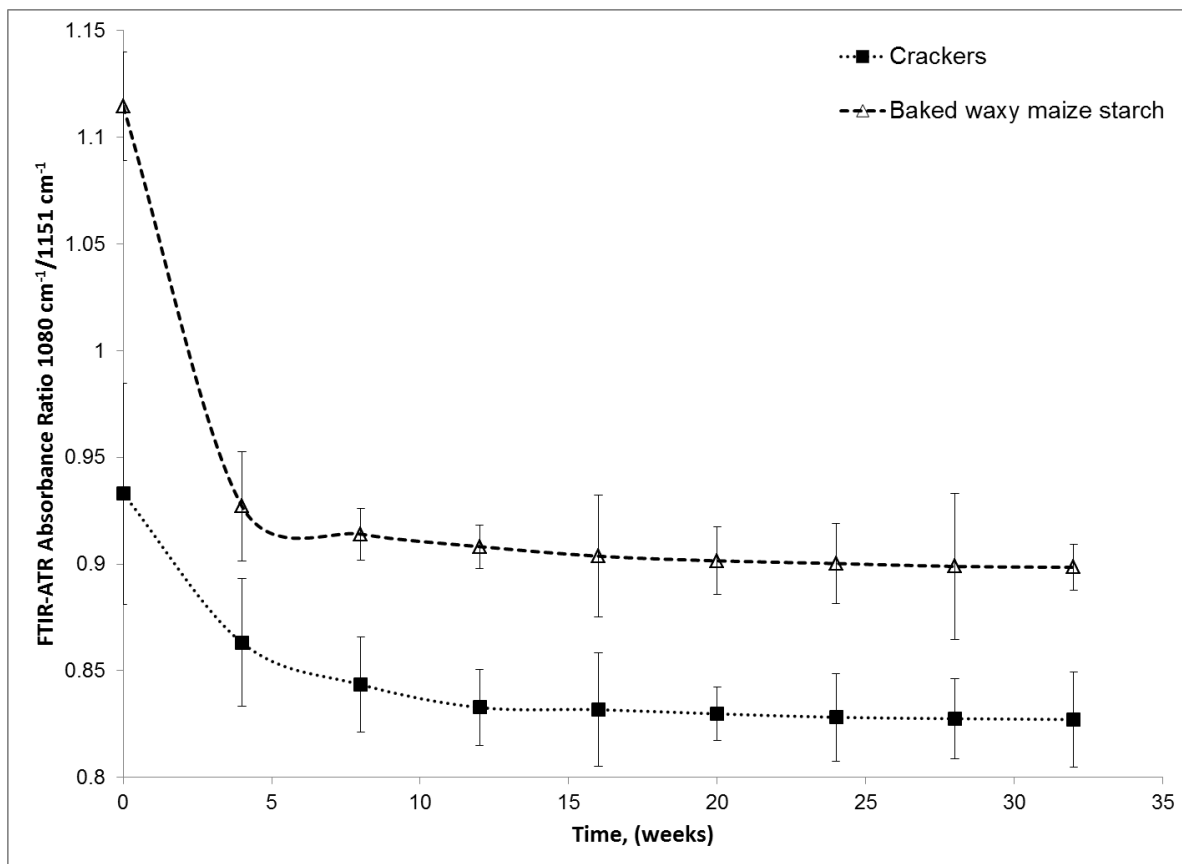
Figure 6.7. FTIR-ATR absorbance ratio 1080 cm^{-1}/1151 cm^{-1} for crackers and baked waxy maize starch stored at 25°C for 32 weeks. Error bars represent one standard deviation.
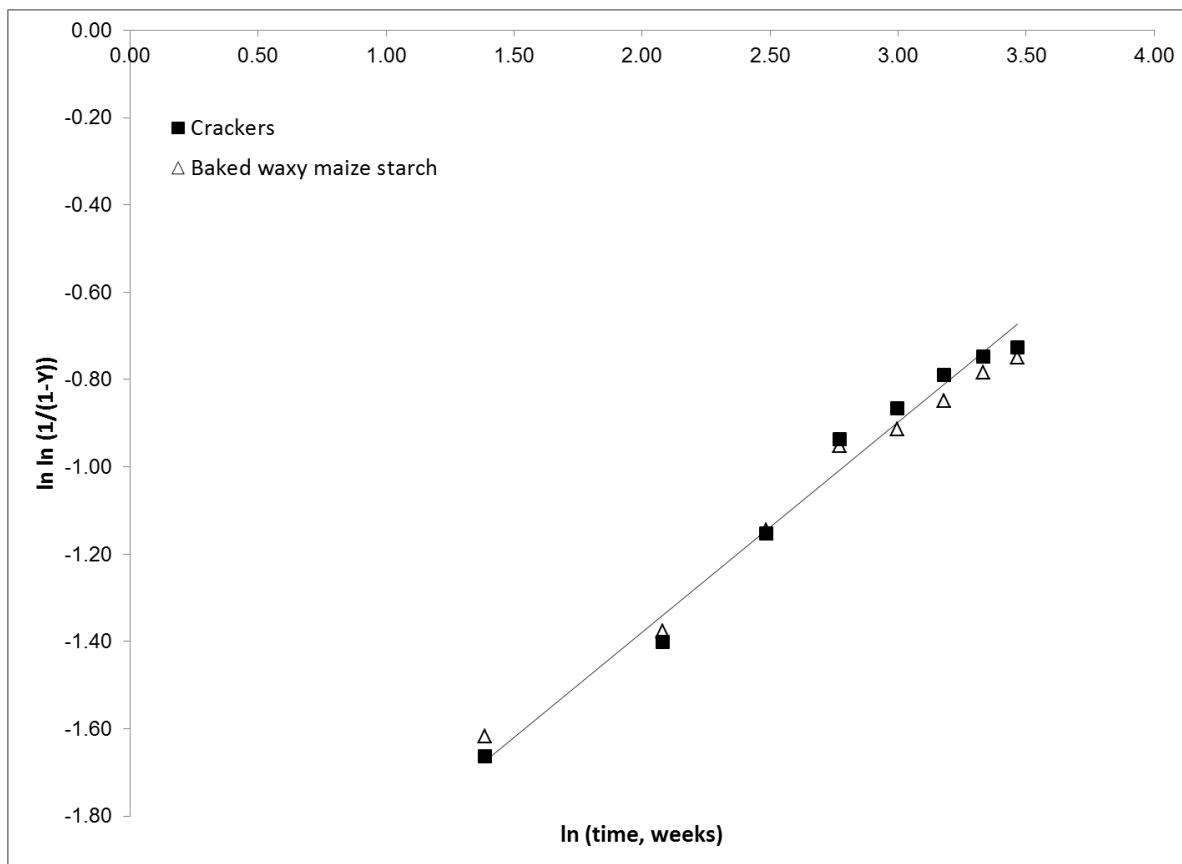
Figure 6.8. $\ln\ln(\dfrac{1}{1-Y})$ versus ln (time) for crackers and baked waxy maize starch over 32

weeks based on enthalpies of the sub-Tg endotherm measured by MDSC. Error bars

represent one standard deviation. Line represents the line of best fit with correlation

coefficient r = 0.98.
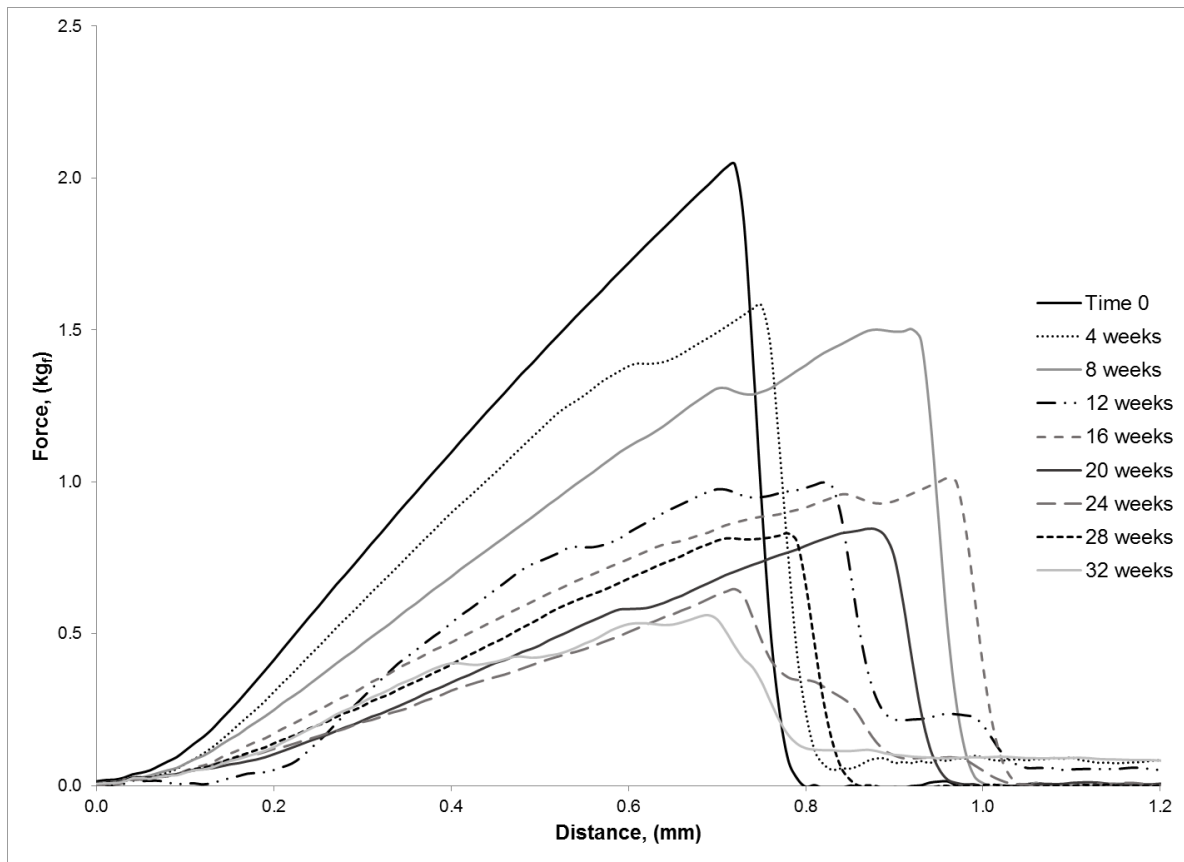
Figure 6.9. 3-point bend texture profile analysis of crackers stored at 25°C for 32 weeks.
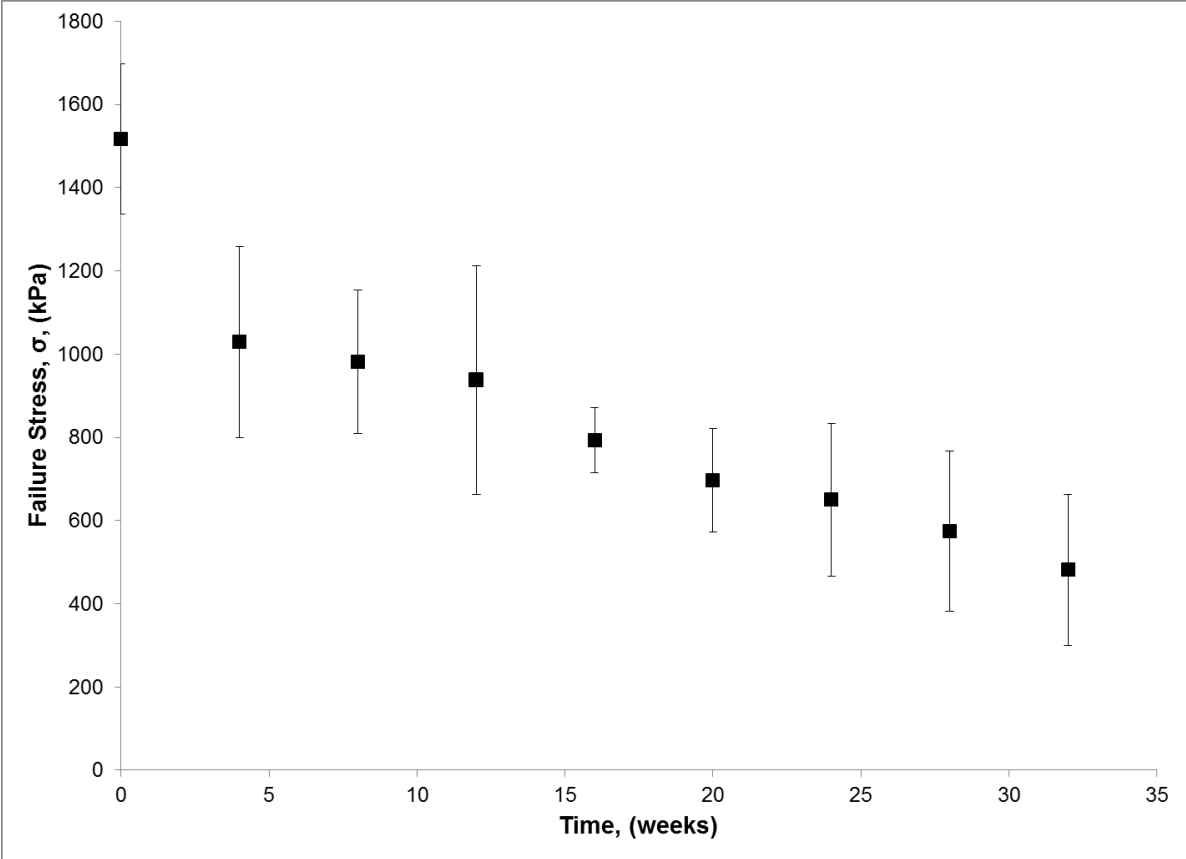
Figure 6.10. Failure stress of crackers stored at 25°C for 32 weeks. Error bars represent one standard deviation.
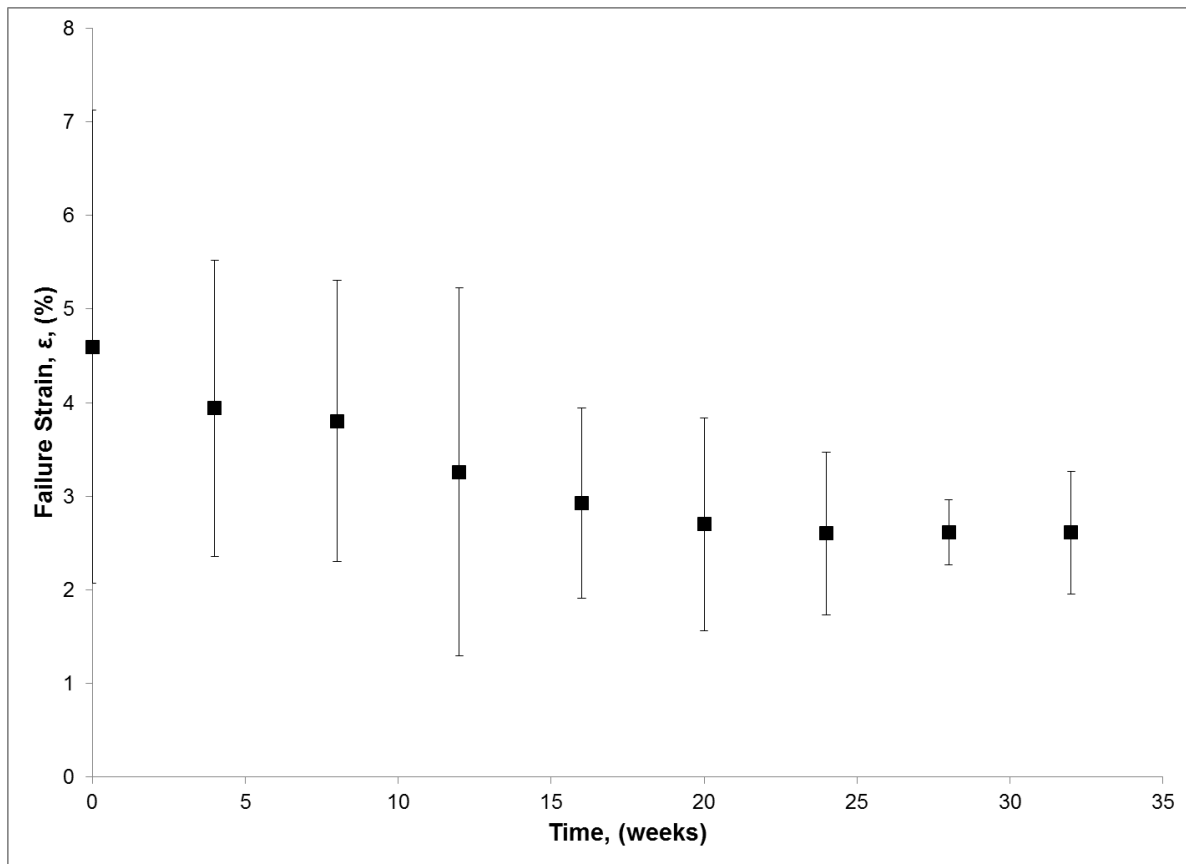
Figure 6.11. Failure strain of crackers stored at 25°C for 32 weeks. Error bars represent one standard deviation.
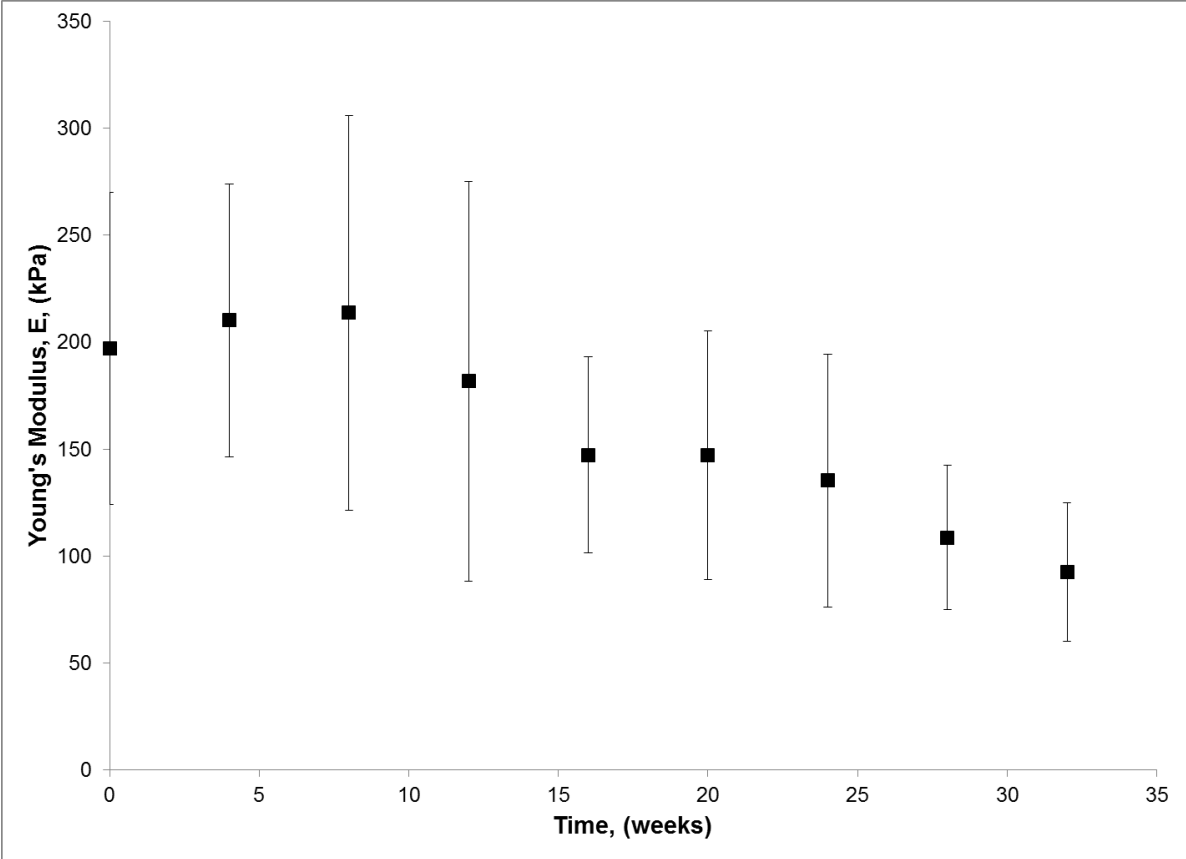
Figure 6.12. Young's Modulus of crackers stored at 25°C for 32 weeks. Error bars represent one standard deviation.
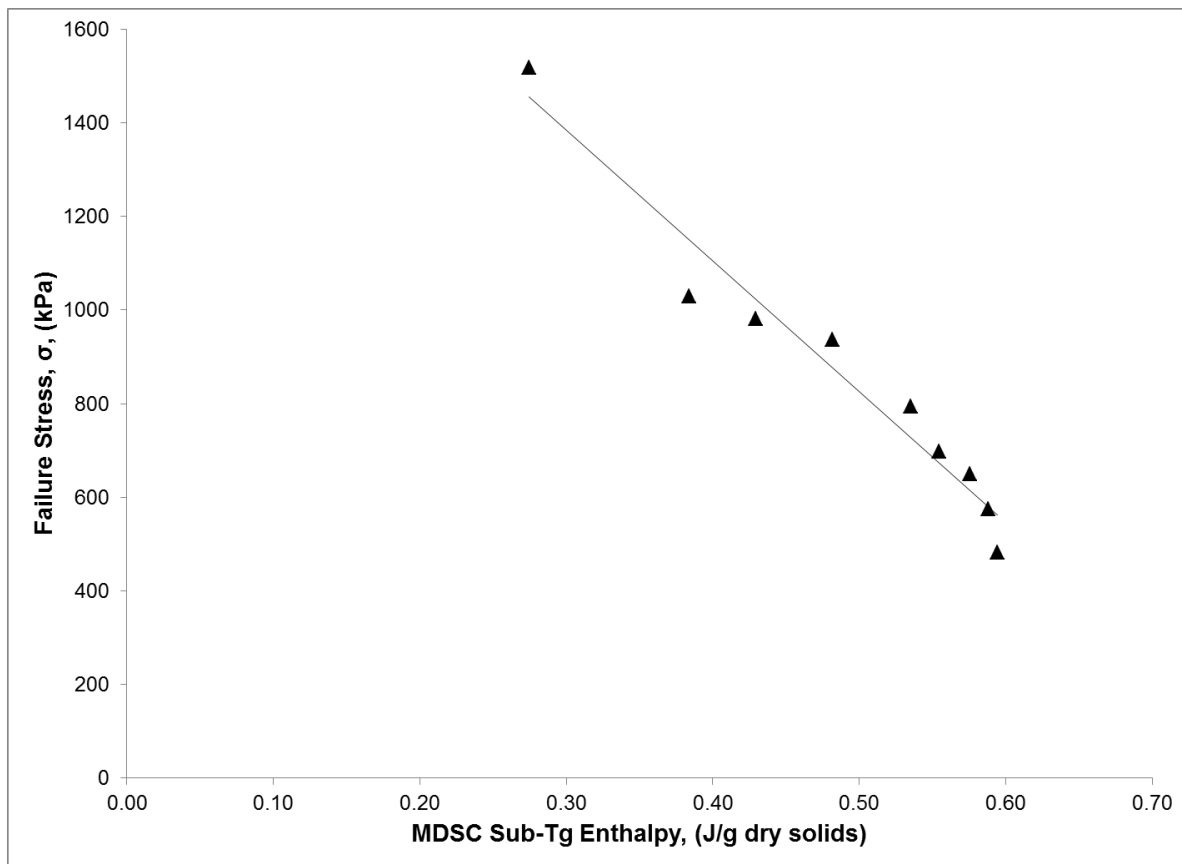
Figure 6.13. Correlation of failure stress and failure stress in crackers with enthalpy of the sub-Tg endotherm observed by MDSC. Line represents the line of best fit with correlation coefficient r = 0.95.

Table 6.1. Dessicant and saturated salt slurries providing %RH from 0 to 67.9%

Salt	%RH[a]	Solubility (g/100g H_2O)[b]
	25°C	20°C
Desiccant (calcium sulfate)	0	n/a
LiCl	11.3	83.5
KCH_3COO	22.5	256
$MgCl_2$	32.8	73.9
K_2CO_3	43.2	111
$Mg(NO_3)_2$	52.9	125
KI	67.9	144

[a] %RH data obtained from Greenspan (1977)

[b] solubility data obtained from Haynes (2012)

n/a – not applicable

6.7 References

Attenburrow GE, Davies AP, Goodband RM, Ingman SJ. 1992. The fracture behaviour of starch and gluten in the glassy state. J. Cereal Sci. 16(1):1-12.

Avrami M. 1939. Kinetics of phase change. 1 General theory. Journal of Chemical Physics 7(12):1103-12.

Avrami M. 1940. Kinetics of phase change. II Transformation time relations for random distirbution of nuclei. Journal of Chemical Physics 8(2):212-24.

Avrami M. 1941. Granulation, phase change, and microstructure kinetics of phase change. III. Journal of Chemical Physics 9(2):177-84.

Badii F, MacNaughtan W, Farhat IA. 2005. Enthalpy relaxation of gelatin in the glassy state. Int. J. Biol. Macromol. 36(4):263-9.

Baltsavias A, Jurgens A, Van Vliet T. 1997. Factors affecting fracture properties of short-dough biscuits. Journal of Texture Studies 28:205-19.

Bechtel WG, Meisner DF, Bradley WB. 1953. The effect of crust on the staling of bread. Cereal Chem. 30:160-8.

Bell LN, Labuza TP. 2000. Moisture Sorption – Practical Aspects of Isotherm Measurement and Use 2nd ed. St. Paul, MN: American Association of Cereal Chemists, Inc.

Chung HJ, Lee EJ, Lim ST. 2002. Comparison in glass transition and enthalpy relaxation between native and gelatinized rice starches. Carbohydr. Polym. 48(3):287-98.

Del Nobile MA, Martoriello T, Mocci G, La Notte E. 2003. Modeling the starch retrogradation kinetic of durum wheat bread. J. Food Eng. 59(2-3):123-8.

Fearn T, Russell PL. 1982. A kinetic study of bread staling by differential scanning calorimetry - the effect of loaf specific volume J. Sci. Food Agric. 33(6):537-48.

Gray JA, Bemiller JN. 2003. Bread staling: molecular basis and control. Comprehensive Reviews in Food Science and Food Safety 2.

Greenspan L. 1977. Humidity fixed points of binary saturated aqueous solutions. Journal of Research of the National Bureau of Standards - A, Physics and Chemistry 81A(1):89-96.

Hallberg LM, Chinachoti P. 1992. Dynamic Mechanical Analysis for Glass Transitions in Long Shelf-Life Bread. Journal of Food Science 57(5):1201-29.

Haynes WM. 2012. CRC Handbook of Chemistry and Physics. 92nd (internet version 2012) ed. Boca Raton, FL: CRC Press/Taylor and Francis.

Hug-Iten S, Escher F, Conde-Petit B. 2003. Staling of bread: Role of amylose and amylopectin and influence of starch-degrading enzymes. Cereal Chem. 80(6):654-61.

Hug-Iten S, Handschin S, Conde-Petit B, Escher F. 1999. Changes in starch microstructure on baking and staling of wheat bread. Food Sci. Technol.-Lebensm.-Wiss. Technol. 32(5):255-60.

Jagannath JH, Jayaraman KS, Arya SS. 1999. Studies on glass transition temperature during staling of bread containing different monomeric and polymeric additives. J. Appl. Polym. Sci. 71(7):1147-52.

Kim SK, Dappolonia BL. 1977a. Bread staling studies 1. Effect of protein content on staling rate and bread crumb pasting properties Cereal Chem. 54(2):207-15.

Kim SK, Dappolonia BL. 1977b. Bread staling studies 2. Effect of protein content and storage temperqaute on role of starch Cereal Chem. 54(2):216-24.

Kim SK, Dappolonia BL. 1977c. Bread staling studies 3. Effect of pentosans on dough, bread and bread staling rate Cereal Chem. 54(2):225-9.

Kweon M, Slade L, Levine H. 2011a. Development of a benchtop baking method for chemically leavened crackers. I. Identification of a diagnostic formula and procedure. Cereal Chem. 88(1):19-24.

Kweon M, Slade L, Levine H. 2011b. Development of a benchtop baking method for chemically leavened crackers. II. Validation of the method. Cereal Chem. 88(1):25-30.

Li Y, Kloeppel KM, Hsieh F. 1998. Texture of glassy corn cakes as a function of moisture content. Journal of Food Science 63(5):869-72.

McIver RG, Axford DWE, Colwell KH, Elton GAH. 1968. Kinetic study of the retrogradation of gelatinised starch. J. Sci. Food Agric. 19:560-3.

Morgan LB. 1954. Crystallization phenomenon in polymers II. The course of the crystallization. Philosphoical Transcations of the Royal Society of London. Series A, Mathematical and Physical Sciences 247(921):13-22.

Nicholls RJ, Appelqvist IAM, Davies AP, Ingman SJ, Lillford PJ. 1995. Glass transitions and the fracture behaviour of gluten and starches within the glassy state. J. Cereal Sci. 21(1):25-36.

Ribotta PD, Cuffini S, Leon AE, Anon MC. 2004. The staling of bread: an X-ray diffraction study. European Food Research and Technology 218(3):219-23.

Ribotta PD, Le Bail A. 2007. Thermo-physical assessment of bread during staling. LWT-Food Sci. Technol. 40(5):879-84.

Roudaut G, Maglione M, Le Meste M. 1999a. Relaxations below glass transition temperature in bread and its components. Cereal Chem. 76(1):78-81.

Roudaut G, Maglione M, van Dusschoten D, Le Meste M. 1999b. Molecular mobility in glassy bread: a multispectroscopy approach. Cereal Chem. 76(1):70-7.

Roudaut G, Simatos D, Champion D, Contreras-Lopez E, Meste Ml. 2004. Molecular mobility around the glass transition temperature: a mini review. Innovative Food Science and Emerging Technologies 5(2):127-34.

Rubens P, Heremans K. 2000. Pressure-temperature gelatinizatin of phase diagram of starch: an in situ Fourier Transform Infrared study. Biopolymers 54(7):524-30.

Rubens P, Snauwaert J, Heremans K, Stute R. 1999. In situ observation of pressure-induced gelation of starches studied with FTIR in the diamond anvil cell. Carbohydrate Polymers 39(3):231-5.

Russell PL. 1983. A kinetic study of bread staling by differential scanning calorimetry and compressibility measurements - the effect of added monoglyceride J. Cereal Sci. 1(4):297-303.

Saleem Q. 2005. Mechanical and fracture properties for predicting checking in semi-sweet biscuits. International Journal of Food Science and Technology 40:361-7.

Seow CC, Teo CH. 1996. Staling of starch-based products: A comparative study by firmness and pulsed NMR measurements. Starch-Starke 48(3):90-3.

Shogren RL. 1992. Effect of moisture content on the melting and subsequent physical aging of corn starch. Carbohydr. Polym. 19(2):83-90.

Slade L, Levine H. 1991. Beyond water activity - Recent advances based on an alternative approach to the assessment of food quality and safety. Crit. Rev. Food Sci. Nutr. 30(2-3):115-360.

Starkweather HW, Avakian P. 1989. .beta.-Relaxations in phenylene polymers. Macromolecules 22(10):4060-2.

TA Instruments - Waters L. 2011. TRIOS version 2.3.4 1613. 2.3.4 ed. New Castle, Delaware, USA.

Thermo Fisher Scientific I. 2012. OMNIC version 9.1.27. 9.1.27 ed. Waltham, Massachussetts, USA.

Thiewes HJ, Steeneken PAM. 1997. The glass transition and the sub-T-g endotherm of amorphous and native potato starch at low moisture content. Carbohydr. Polym. 32(2):123-30.

Warren FJ, Perston BB, Royall PG, Butterworth PJ, Ellis PR. 2013. Infrared spectroscopy with heated attenuated total internal reflectance enabling precise measurement of thermally induced transitions in complex biological polymers. Analytical Chemistry 85(8):3999-4006.

Wilson RH, Goodfellow BJ, Belton PS, Osborne BG, Oliver G, Russell PL. 1991. Comparison of fourier-transorm mid infrared spectroscopy and near infrared reflectance spectroscopy with differential scanning calorimetry for the study of the staling of bread J. Sci. Food Agric. 54(3):471-83.

Zeleznak KJ, Hoseney RC. 1987. The glass transition in starch. Cereal Chem. 64(2):121-4.

CHAPTER 7
CONCLUSIONS AND RECOMMENDATIONS

7.1 Summary and conclusions

Commercial crackers, a low moisture starch-based food system, exhibit a sub-Tg endotherm with an exponential dependence on moisture content. The presence of this sub-Tg endothermic event has practical implications for low moisture carbohydrate and starchy food systems in that it may also be accompanied by physical changes directly impacting the texture and quality of the food system. In particular, foods that are classified as being in the "glassy" state may be affected, although the prevailing assumption has been that the physical characteristics of such food systems are kinetically stable.

In order to elucidate the origin of this sub-Tg endotherm, pregelatinized waxy maize starch was studied as a function of moisture content and storage temperature using MDSC. A sub-Tg endotherm with a peak temperature between 55 and 65°C was observed at all starch moisture contents in the non-reversing heat flow of the MDSC scan. A similar peak with substantially higher enthalpy was also observed for the 50% moisture retrograded starch sample; however, this peak is well above the Tg for this system. The enthalpy of this transition was independent of storage temperature for the low moisture pregelatinized waxy maize starch samples, but was dependent on storage temperature at 50% moisture content.

As measured by x-ray powder diffraction, no crystallinity was observed for the low moisture pregelatinized waxy maize starches, but the retrograded starch exhibited the typical B-type crystalline pattern. FTIR-ATR spectra revealed an increase in the peak at 1080 cm^{-1} with increasing moisture content; this peak has been commonly attributed to amylopectin order. In fact, the low moisture pregelatinized waxy maize starches were found to have increasing amylopectin double helical content with increasing moisture content, as confirmed by solid-state ^{13}C CP/MAS NMR. Reformation of double helices is considered to be the first step in the amylopectin retrogradation process, followed by realignment of the helices into crystalline order, as occurs at higher moisture contents.

The sub-Tg endotherm, as measured by MDSC and the FTIR-ATR absorbance ratio at 1080 cm^{-1}/ 1151 cm^{-1}, was observed to increase with time according to Avrami kinetics. The Avrami exponent n was found to be n = 0.24 and was independent of moisture content for the

low moisture pregelatinized waxy maize starches. An Avrami exponent value less than one was not surprising, considering that Avrami kinetics are used to describe crystallization processes and these low moisture starches are assumed to only proceed through the nucleation step with the reformation of double helical ordered structure in the amylopectin. The Avrami rate constant, K, was exponentially correlated with starch moisture content as was the enthalpy of the sub-Tg endotherm given that greater mobility exists at the higher moisture contents to increase the amount and rate of double helical nucleation.

In wheat-flour based crackers and baked waxy maize starch, a sub-Tg endotherm was also observed that was exponentially related to moisture content and similar to endotherms observed in the pregelatinized starches. The development of this endotherm was correlated with the FTIR-ATR absorbance ratio 1080 cm^{-1} / 1151 cm^{-1}, and the enthalpy of the endotherm developed over time according to Avrami kinetics. Over the same timeframe, the failure stress or hardness of the crackers decreased, and the failure stress was negatively correlated with the enthalpy of the sub-Tg endotherm measured by MDSC. This work confirms that staling and associated textural changes in low moisture starch-based food systems, like crackers, is a result of reformation of amylopectin double helices without crystallization or aggregation of those helices that might develop at higher moisture contents.

7.2 Recommendations for future work

As most food products, especially those at lower moisture contents, have shelf-lifes on the order of months to year or more, it is vitally important to understand textural and quality changes that may be occurring during long-term storage. Undoubtedly, the most important phase transitions for starch in a food system, in terms of the impact on food texture and quality, are starch gelatinization and retrogradation.

In terms of direct impact on the food industry, starch retrogradation has long been associated with the staling of bread, the rate of which is often described by the Avrami equation. Similar to the starch amylopectin retrogradation endotherm at higher moisture contents, the presence of a sub-Tg endotherm in starch-based food systems at low moisture contents has also been identified and correlated with the reformation of amylopectin double helices, recognized to be the first step in the retrogradation process. However, several distinct differences can be observed between retrogradation at higher moisture and the sub-Tg endotherm: 1) retorgadation

202

is generally considered to only occur above the system Tg, 2) retrogradation is dependent on storage temperature and the sub-Tg endotherm is independent, and 3) retrogradation leads to the bread crumb firming whereas the sub-Tg endotherm was linked with a softening of crakers during storage, even as moisture content remained constant. Potentially, moisture redistribution within the cracker during storage, as a result of amylopectin double helices reforming, is leading to localized stresses in the cracker system that is weakening the overall system. More work would be needed to verify this hypothesis.

While the sub-Tg endotherm in low moisture pregelatinzed waxy maize starch and associated food products has been corrleated with the first step of the retrogradation process, this endotherm may also be linked with physical aging. Also termed enthalpy relaxation, physical aging describes the relaxation of a towards equilibrium, or the state that would have been reached if relaxation limits were not reached during cooling, resulting in a spontaneous decrese in enthalpy, specific volume, entropy and other physical properties. Physical aging is a general phenomenon that occurs for amorphous materials, including, but not limited to, pregelatinized starch. For low moisture amorphous amylopectin, physical aging may encompass reformation of double helices, but structural changes involved with other polymers undergoing physical aging may involve different processes. Further work would be needed to elucidate similarities or differences in the processes undertaken by other polymers, in particular, other carbohydrate based polymers, through physial aging, which may provide insights on common molecular mobilities that may be possible below a system glass transition. Regardless, this work confirms that amylopectin is capable of reforming double helices at low moisture contents and this reformation is associated with textural changes in low moisture starchy foods that may impact the product shelf-life.

Table A1. Initial MDSC characterization of sub-Tg endotherm for intact waxy corn starch granules

Saturated Salt Solution	%RH	Moisture, (grams H_2O / 100 grams dry starch)	Storage Temperature, (^{o}C)	Nonreversing Signal - Initial				Total heat flow - Initial			
				Tm onset, (^{o}C)	Tm peak, (^{o}C)	Enthalpy, (J/g)	Enthalpy, (J/g dry starch)	Tm onset, (^{o}C)	Tm peak, (^{o}C)	Enthalpy, (J/g)	Enthalpy, (J/g dry starch)
CaSO$_4$	0.00	1.48	5	41.88 ± 1.60	53.47 ± 0.35	0.17 ± 0.03	0.17 ± 0.03	41.56 ± 1.95	54.05 ± 0.87	0.17 ± 0.02	0.17 ± 0.02
CaSO$_4$	0.00	0.75	15	42.38 ± 2.07	52.93 ± 0.93	0.17 ± 0.03	0.18 ± 0.03	42.67 ± 2.45	51.30 ± 4.53	0.16 ± 0.04	0.16 ± 0.04
CaSO$_4$	0.00	0.21	25	41.14 ± 0.30	49.86 ± 0.70	0.13 ± 0.02	0.13 ± 0.02	40.13 ± 1.05	49.78 ± 0.71	0.16 ± 0.04	0.16 ± 0.04
CaSO$_4$	0.00	1.01	35	42.53 ± 0.87	50.67 ± 0.14	0.17 ± 0.01	0.17 ± 0.01	42.77 ± 0.98	51.09 ± 0.10	0.17 ± 0.03	0.17 ± 0.03
LiCl	11.30	7.32	5	43.87 ± 0.50	52.04 ± 0.33	0.18 ± 0.05	0.20 ± 0.05	43.21 ± 0.52	51.72 ± 0.06	0.18 ± 0.06	0.19 ± 0.06
LiCl	11.30	6.10	15	43.16 ± 0.57	51.94 ± 0.44	0.22 ± 0.03	0.23 ± 0.04	42.59 ± 1.24	52.32 ± 0.40	0.18 ± 0.07	0.20 ± 0.07
LiCl	11.30	5.29	25	42.69 ± 0.99	52.06 ± 0.87	0.23 ± 0.02	0.24 ± 0.02	42.76 ± 1.60	53.52 ± 2.45	0.22 ± 0.02	0.23 ± 0.02
LiCl	11.30	5.01	35	43.28 ± 0.54	51.88 ± 0.15	0.21 ± 0.05	0.22 ± 0.05	42.90 ± 1.32	52.46 ± 0.32	0.23 ± 0.03	0.24 ± 0.03
MgCl$_2$	33.60	10.54	5	42.79 ± 0.25	51.67 ± 0.20	0.29 ± 0.03	0.32 ± 0.04	43.85 ± 0.37	52.93 ± 0.29	0.24 ± 0.02	0.27 ± 0.02
MgCl$_2$	33.30	10.77	15	44.40 ± 0.46	51.04 ± 0.12	0.25 ± 0.04	0.28 ± 0.05	42.83 ± 0.31	51.23 ± 0.14	0.24 ± 0.05	0.27 ± 0.05
MgCl$_2$	32.80	8.40	25	46.05 ± 0.71	53.23 ± 0.24	0.31 ± 0.04	0.33 ± 0.04	46.15 ± 0.76	53.59 ± 0.36	0.29 ± 0.03	0.32 ± 0.03
MgCl$_2$	32.10	8.47	35	41.34 ± 0.27	49.36 ± 0.15	0.32 ± 0.01	0.35 ± 0.02	40.81 ± 0.35	49.73 ± 0.21	0.35 ± 0.03	0.38 ± 0.04
NaBr	62.20	19.21	5	40.32 ± 0.23	46.30 ± 0.06	0.68 ± 0.04	0.84 ± 0.05	40.30 ± 0.31	46.18 ± 0.20	0.63 ± 0.05	0.78 ± 0.06
NaBr	59.10	14.84	15	42.92 ± 1.21	49.50 ± 1.23	0.62 ± 0.08	0.72 ± 0.09	43.00 ± 0.27	50.10 ± 0.14	0.63 ± 0.06	0.74 ± 0.07
NaBr	56.10	12.77	25	51.76 ± 0.12	59.05 ± 0.13	0.61 ± 0.04	0.70 ± 0.05	51.64 ± 0.08	59.21 ± 0.07	0.61 ± 0.05	0.70 ± 0.06

Table A1 Continued

Saturated Salt Solution	%RH	Moisture, (grams H₂O / 100 grams dry starch)	Storage Temp-erature, (°C)	Nonreversing Signal - Initial				Total heat flow - Initial			
				Tm onset, (°C)	Tm peak, (°C)	Enthalpy, (J/g)	Enthalpy, (J/g dry starch)	Tm onset, (°C)	Tm peak, (°C)	Enthalpy, (J/g)	Enthalpy, (J/g dry starch)
NaBr	53.20	12.01	35	57.13 ± 0.18	64.59 ± 0.06	0.61 ± 0.04	0.70 ± 0.04	57.62 ± 0.14	64.34 ± 0.07	0.64 ± 0.05	0.73 ± 0.06
KI	72.10	21.04	5	36.84 ± 0.07	43.27 ± 0.04	0.89 ± 0.04	1.12 ± 0.05	36.75 ± 0.15	43.12 ± 0.06	0.88 ± 0.04	1.12 ± 0.05
KI	69.90	18.09	15	41.57 ± 0.31	48.79 ± 0.22	0.86 ± 0.03	1.04 ± 0.04	41.71 ± 0.21	49.15 ± 0.12	0.87 ± 0.02	1.06 ± 0.02
KI	67.90	15.19	25	51.87 ± 0.07	57.95 ± 0.04	0.88 ± 0.03	1.04 ± 0.03	51.98 ± 0.13	57.83 ± 0.07	0.86 ± 0.02	1.01 ± 0.02
KI	66.10	15.77	35	58.70 ± 0.11	64.47 ± 0.07	0.91 ± 0.02	1.08 ± 0.02	59.00 ± 0.14	64.47 ± 0.09	0.87 ± 0.04	1.03 ± 0.05
50% MC	100.00	100.00	5	45.64 ± 0.02	57.89 ± 0.47	6.43 ± 0.29	12.85 ± 0.59	46.15 ± 0.44	57.47 ± 0.30	5.63 ± 0.53	11.26 ± 1.06
50% MC	100.00	100.00	15	44.03 ± 0.05	57.48 ± 0.28	5.40 ± 0.14	10.80 ± 0.29	44.08 ± 0.03	56.63 ± 0.27	4.10 ± 0.22	8.20 ± 0.45
50% MC	100.00	100.00	25	52.36 ± 0.16	64.91 ± 0.00	3.64 ± 0.12	7.28 ± 0.24	52.87 ± 0.13	64.55 ± 0.11	3.06 ± 0.31	6.11 ± 0.62
50% MC	100.00	100.00	35	62.26 ± 0.19	70.42 ± 0.14	0.54 ± 0.03	1.08 ± 0.06	61.84 ± 0.09	70.47 ± 0.14	0.59 ± 0.05	1.17 ± 0.11

Table A2. MDSC characterization of sub-Tg endotherm, rescan after 4 week storage, for intact waxy corn starch granules

Saturated Salt Solution	%RH	Moisture, (grams H$_2$O / 100 grams dry starch)	Storage Temperature, (°C)	Nonreversing Signal – 4 week rescan				Total heat flow – 4 week rescan			
				Tm onset, (°C)	Tm peak, (°C)	Enthalpy, (J/g)	Enthalpy, (J/g dry starch)	Tm onset, (°C)	Tm peak, (°C)	Enthalpy, (J/g)	Enthalpy, (J/g dry starch)
CaSO$_4$	0.00	1.48	5	Not detected							
CaSO$_4$	0.00	0.75	15	Not detected							
CaSO$_4$	0.00	0.21	25	41.73 ± 0.54	48.92 ± 0.42	0.23 ± 0.04	0.23 ± 0.04	41.31 ± 0.46	48.87 ± 0.33	0.25 ± 0.06	0.25 ± 0.06
CaSO$_4$	0.00	1.01	35	58.14 ± 0.49	65.82 ± 0.60	0.08 ± 0.01	0.08 ± 0.01	56.94 ± 0.37	65.20 ± 0.07	0.09 ± 0.01	0.09 ± 0.01
LiCl	11.30	7.32	5	41.85 ± 0.52	50.41 ± 0.18	0.09 ± 0.01	0.10 ± 0.01	41.82 ± 0.61	51.14 ± 0.06	0.09 ± 0.02	0.10 ± 0.02
LiCl	11.30	6.10	15	43.34 ± 0.31	50.63 ± 0.00	0.13 ± 0.03	0.14 ± 0.03	41.98 ± 0.66	47.67 ± 0.02	0.13 ± 0.03	0.13 ± 0.03
LiCl	11.30	5.29	25	44.69 ± 0.57	55.24 ± 0.41	0.12 ± 0.02	0.13 ± 0.02	43.84 ± 0.91	52.92 ± 4.51	0.12 ± 0.02	0.12 ± 0.02
LiCl	11.30	5.01	35	55.85 ± 0.20	64.39 ± 0.00	0.14 ± 0.02	0.15 ± 0.02	56.16 ± 0.60	65.85 ± 0.60	0.16 ± 0.01	0.17 ± 0.01
MgCl$_2$	33.60	10.54	5	43.19 ± 0.20	51.18 ± 0.86	0.20 ± 0.03	0.22 ± 0.03	42.46 ± 0.10	50.87 ± 0.00	0.18 ± 0.01	0.20 ± 0.01
MgCl$_2$	33.30	10.77	15	40.46 ± 0.41	47.62 ± 0.32	0.10 ± 0.01	0.11 ± 0.01	39.78 ± 0.42	48.63 ± 0.27	0.16 ± 0.01	0.18 ±0.01
MgCl$_2$	32.80	8.40	25	49.08 ± 1.23	58.03 ± 0.92	0.40 ± 0.14	0.44 ± 0.16	48.37 ± 1.18	57.43 ± 0.41	0.37 ± 0.15	0.40 ± 0.17
MgCl$_2$	32.10	8.47	35	48.57 ± 1.85	60.00 ± 2.34	0.19 ± 0.07	0.21 ± 0.08	48.43 ± 1.81	59.73 ± 1.38	0.34 ± 0.33	0.38 ± 0.36
NaBr	62.20	19.21	5	41.16 ± 0.57	48.11 ± 0.97	0.09 ± 0.05	0.11 ± 0.06	41.31 ± 0.48	48.24 ± 0.25	0.19 ± 0.14	0.23 ± 0.18
NaBr	59.10	14.84	15	39.23 ± 1.14	49.82 ± 0.73	0.39 ± 0.10	0.45 ± 0.12	39.62 ± 0.15	49.88 ± 0.59	0.31 ± 0.09	0.36 ± 0.11
NaBr	56.10	12.77	25	43.55 ± 0.37	53.95 ± 1.47	0.23 ± 0.12	0.26 ± 0.13	41.49 ± 1.36	53.05 ± 0.54	0.31 ± 0.16	0.35 ± 0.18
NaBr	53.20	12.01	35	51.38 ± 0.70	63.23 ± 1.91	0.36 ± 0.11	0.41 ± 0.12	50.72 ± 2.25	64.13 ± 2.30	0.44 ± 0.26	0.51 ± 0.29
KI	72.10	21.04	5	39.48 ± 0.25	46.10 ± 1.25	0.22 ± 0.04	0.28 ± 0.05	40.50 ± 1.41	47.03 ± 0.20	0.17 ± 0.03	0.21 ± 0.04
KI	69.90	18.09	15	39.06 ± 0.41	48.53 ± 0.19	0.29 ± 0.07	0.35 ± 0.08	39.52 ± 0.35	48.50 ± 0.31	0.24 ± 0.04	0.29 ± 0.05

Table A2 Continued

Saturated Salt Solution	%RH	Moisture, (grams H$_2$O / 100 grams dry starch)	Storage Temp-erature, (ºC)	Nonreversing Signal – 4 week rescan				Total heat flow – 4 week rescan			
				Tm onset, (ºC)	Tm peak, (ºC)	Enthalpy, (J/g)	Enthalpy, (J/g dry starch)	Tm onset, (ºC)	Tm peak, (ºC)	Enthalpy, (J/g)	Enthalpy, (J/g dry starch)
KI	67.90	15.19	25	42.33 ± 0.78	54.41 ± 0.29	0.51 ± 0.14	0.60 ± 0.16	41.07 ± 0.60	54.31 ± 0.33	0.61 ± 0.08	0.72 ± 0.10
KI	66.10	15.77	35	54.84 ± 0.28	66.70 ± 0.25	0.21 ± 0.03	0.25 ± 0.03	54.70 ± 0.37	66.55 ± 0.34	0.20 ± 0.02	0.24 ± 0.03
50% MC	100.00	100.00	5	48.28 ± 0.18	58.79 ± 0.17	1.67 ± 0.13	3.34 ± 0.26	46.85 ± 0.20	57.19 ± 0.30	1.29 ± 0.03	2.59 ± 0.07
50% MC	100.00	100.00	15	40.39 ± 2.16	51.66 ± 1.04	3.14 ± 0.39	6.29 ± 0.77	39.76 ± 0.09	51.56 ± 0.20	3.09 ± 0.09	6.17 ± 0.18
50% MC	100.00	100.00	25	48.06 ± 0.80	56.96 ± 0.58	0.22 ± 0.05	0.45 ± 0.10	48.06 ± 1.04	51.88 ± 0.50	0.22 ± 0.06	0.45 ± 0.12
50% MC	100.00	100.00	35	55.59 ± 0.50	69.53 ± 0.61	1.51 ± 0.16	3.03 ± 0.33	58.62 ± 2.02	69.26 ± 0.72	1.28 ± 0.19	2.55 ± 0.38

Table A3. Initial MDSC characterization of sub-Tg endotherm for fragmented waxy corn starch granules

Saturated Salt Solution	%RH	Moisture, (grams H_2O / 100 grams dry starch)	Storage Temperature, (^{o}C)	Nonreversing Signal – Initial				Total heat flow – Initial			
				Tm onset, (^{o}C)	Tm peak, (^{o}C)	Enthalpy, (J/g)	Enthalpy, (J/g dry starch)	Tm onset, (^{o}C)	Tm peak, (^{o}C)	Enthalpy, (J/g)	Enthalpy, (J/g dry starch)
CaSO$_4$	0.00	1.02	5	44.22 ± 0.76	54.08 ± 0.57	0.15 ± 0.02	0.15 ± 0.02	42.57 ± 1.25	53.31 ± 0.44	0.17 ± 0.02	0.18 ± 0.02
CaSO$_4$	0.00	1.09	15	41.35 ± 1.44	45.72 ± 1.92	0.06 ± 0.03	0.06 ± 0.04	42.57 ± 0.72	47.41 ± 0.73	0.06 ± 0.03	0.06 ± 0.03
CaSO$_4$	0.00	4.08	25	42.16 ± 0.38	49.29 ± 0.70	0.10 ± 0.02	0.11 ± 0.02	41.58 ± 0.20	48.85 ± 0.50	0.11 ± 0.01	0.12 ± 0.01
CaSO$_4$	0.00	0.51	35	39.41 ± 0.50	46.51 ± 0.13	0.15 ± 0.02	0.15 ± 0.02	42.82 ± 0.33	50.89 ± 0.31	0.19 ± 0.01	0.19 ± 0.01
LiCl	11.30	7.96	5	43.71 ± 0.75	50.95 ± 0.40	0.17 ± 0.05	0.18 ± 0.05	42.94 ± 0.42	51.10 ± 0.47	0.17 ± 0.04	0.19 ± 0.05
LiCl	11.30	5.78	15	42.73 ± 0.64	50.78 ± 0.07	0.20 ± 0.04	0.21 ± 0.04	42.96 ± 0.75	51.63 ± 0.70	0.20 ± 0.05	0.21 ± 0.05
LiCl	11.30	8.53	25	49.96 ± 1.17	55.79 ± 1.61	0.08 ± 0.02	0.09 ± 0.02	50.27 ± 0.97	56.97 ± 1.42	0.12 ± 0.03	0.12 ± 0.04
LiCl	11.30	4.77	35	42.78 ± 0.60	49.84 ± 0.85	0.16 ± 0.03	0.16 ± 0.03	42.71 ± 1.02	49.51 ± 1.75	0.16 ± 0.02	0.17 ± 0.02
MgCl$_2$	33.60	10.15	5	43.63 ± 0.50	51.48 ± 0.23	0.14 ± 0.02	0.16 ± 0.02	43.83 ± 0.07	51.43 ± 0.33	0.11 ± 0.01	0.12 ± 0.02
MgCl$_2$	33.30	9.44	15	51.06 ± 0.87	57.58 ± 0.22	0.23 ± 0.07	0.25 ± 0.08	50.71 ± 0.88	57.77 ± 0.71	0.20 ± 0.04	0.22 ± 0.04
MgCl$_2$	32.80	11.46	25	55.83 ± 1.38	62.58 ± 1.28	0.19 ± 0.04	0.19 ± 0.04	53.23 ± 0.97	60.79 ± 0.83	0.26 ± 0.03	0.26 ± 0.03
MgCl$_2$	32.10	8.83	35	38.87 ± 1.27	48.76 ± 0.24	0.29 ± 0.05	0.32 ± 0.05	39.01 ± 1.78	49.25 ± 0.57	0.31 ± 0.03	0.35 ± 0.03
NaBr	62.20	17.47	5	43.70 ± 0.20	50.29 ± 0.08	0.66 ± 0.04	0.81 ± 0.05	43.75 ± 0.08	50.49 ± 0.08	0.63 ± 0.03	0.77 ± 0.04
NaBr	59.10	20.55	15	42.35 ± 0.35	51.07 ± 0.55	0.66 ± 0.03	0.83 ± 0.04	43.63 ± 0.30	51.56 ± 0.50	0.66 ± 0.04	0.84 ± 0.06
NaBr	56.10	16.07	25	55.35 ± 0.99	62.96 ± 1.39	0.23 ± 0.06	0.27 ± 0.07	55.35 ± 0.37	62.63 ± 0.60	0.22 ± 0.05	0.26 ± 0.06
NaBr	53.20	15.10	35	59.01 ± 0.16	65.66 ± 0.10	0.62 ± 0.05	0.73 ± 0.06	58.98 ± 0.21	65.69 ± 0.21	0.61 ± 0.03	0.72 ± 0.03
KI	72.10	24.95	5	52.68 ± 0.14	57.5 ± 0.06	0.87 ± 0.04	1.16 ± 0.05	52.30 ± 0.21	57.64 ± 0.12	0.87 ± 0.05	1.16 ± 0.07
KI	69.90	17.23	15	41.66 ± 0.15	49.70 ± 0.07	0.87 ± 0.02	1.02 ± 0.03	41.45 ± 0.18	50.00 ± 0.16	0.86 ± 0.02	1.02 ± 0.02

Table A3 Continued

Saturated Salt Solution	%RH	Moisture, (grams H$_2$O / 100 grams dry starch)	Storage Temp-erature, (°C)	Nonreversing Signal – Initial				Total heat flow – Initial			
				Tm onset, (°C)	Tm peak, (°C)	Enthalpy, (J/g)	Enthalpy, (J/g dry starch)	Tm onset, (°C)	Tm peak, (°C)	Enthalpy, (J/g)	Enthalpy, (J/g dry starch)
KI	67.90	19.14	25	52.76 ± 0.04	59.61 ± 0.02	0.88 ± 0.03	1.08 ± 0.03	52.98 ± 0.05	59.52 ± 0.01	0.86 ± 0.02	1.06 ± 0.03
KI	66.10	13.96	35	61.58 ± 0.14	66.56 ± 0.09	0.87 ± 0.03	1.01 ± 0.04	61.58 ± 0.08	67.00 ± 0.07	0.88 ± 0.02	1.02 ± 0.03
50% MC	100.00	100.00	5	46.98 ± 0.07	59.88 ± 0.12	6.51 ± 0.08	13.01 ± 0.16	47.00 ± 0.07	59.34 ± 0.63	5.56 ± 0.64	11.12 ± 1.27
50% MC	100.00	100.00	15	45.79 ± 0.10	58.57 ± 0.10	5.11 ± 0.20	10.22 ± 0.41	45.80 ± 0.18	58.35 ± 0.22	4.55 ± 0.33	9.11 ± 0.66
50% MC	100.00	100.00	25	51.85 ± 0.23	63.87 ± 0.21	3.42 ± 0.24	6.83 ± 0.47	51.84 ± 0.44	63.39 ± 0.26	2.83 ± 0.33	5.67 ± 0.67

Table A4. MDSC characterization of sub-Tg endotherm, rescan after 4 week storage, for fragmented waxy corn starch granules

Saturated Salt Solution	%RH	Moisture, (grams H_2O / 100 grams dry starch)	Storage Temp-erature, (°C)	Nonreversing Signal – 4 week rescan				Total heat flow – 4 week rescan			
				Tm onset, (°C)	Tm peak, (°C)	Enthalpy, (J/g)	Enthalpy, (J/g dry starch)	Tm onset, (°C)	Tm peak, (°C)	Enthalpy, (J/g)	Enthalpy, (J/g dry starch)
CaSO$_4$	0.00	1.02	5	Not detected							
CaSO$_4$	0.00	1.09	15	Not detected							
CaSO$_4$	0.00	4.08	25	43.07 ± 0.43	48.56 ± 0.57	0.08 ± 0.02	0.09 ± 0.02	43.36 ± 0.25	48.73 ± 0.30	0.07 ± 0.01	0.08 ± 0.01
CaSO$_4$	0.00	0.51	35	64.91 ± 1.91	67.18 ± 1.78	0.03 ± 0.02	0.03 ± 0.02	63.96 ± 0.43	67.28 ± 0.00	0.04 ± 0.01	0.04 ± 0.01
LiCl	11.30	7.96	5	46.71 ± 0.46	52.10 ± 0.26	0.08 ± 0.01	0.09 ± 0.01	46.27 ± 0.55	52.81 ± 0.62	0.09 ± 0.02	0.10 ± 0.02
LiCl	11.30	5.78	15	43.23 ± 0.22	48.00 ± 0.05	0.10 ± 0.01	0.11 ± 0.01	40.87 ± 0.12	47.67 ± 0.03	0.11 ± 0.01	0.11 ± 0.01
LiCl	11.30	8.53	25	52.94 ± 0.47	58.28 ± 0.79	0.09 ± 0.02	0.10 ± 0.02	53.42 ± 1.19	59.32 ± 1.69	0.10 ± 0.02	0.11 ± 0.03
LiCl	11.30	4.77	35	59.75 ± 0.22	65.51 ± 0.04	0.11 ± 0.01	0.11 ± 0.01	65.57 ± 0.03	69.22 ± 0.09	0.10 ± 0.01	0.10 ± 0.01
MgCl$_2$	33.60	10.15	5	45.38 ± 0.52	51.89 ± 0.67	0.10 ± 0.01	0.11 ± 0.01	45.70 ± 0.47	51.33 ± 1.04	0.12 ± 0.02	0.13 ± 0.02
MgCl$_2$	33.30	9.44	15	41.51 ± 0.66	48.75 ± 0.18	0.13 ± 0.02	0.14 ± 0.02	39.03 ± 0.34	47.67 ± 0.47	0.13 ± 0.01	0.15 ± 0.02
MgCl$_2$	32.80	11.46	25	50.37 ± 0.93	57.79 ± 1.08	0.29 ± 0.03	0.29 ± 0.03	50.76 ± 0.25	57.56 ± 0.58	0.22 ± 0.08	0.22 ± 0.08
MgCl$_2$	32.10	8.83	35	48.36 ± 0.98	59.68 ± 0.10	0.25 ± 0.07	0.27 ± 0.07	46.79 ± 1.70	59.88 ± 2.55	0.26 ± 0.11	0,.28 ± 0.12
NaBr	62.20	17.47	5	43.52 ± 0.16	52.24 ± 0.00	0.19 ± 0.02	0.23 ± 0.03	42.64 ± 0.73	51.95 ± 0.48	0.19 ± 0.07	0.23 ± 0.08
NaBr	59.10	20.55	15	42.72 ± 0.57	51.74 ± 0.31	0.31 ± 0.08	0.39 ± 0.10	42.72 ± 0.64	51.86 ± 0.64	0.27 ± 0.29	0.34 ± 0.09
NaBr	56.10	16.07	25	42.18 ± 0.92	52.82 ± 0.86	0.28 ± 0.11	0.33 ± 0.13	40.99 ± 0.58	51.43 ± 1.25	0.24 ± 0.10	0.28 ± 0.12
NaBr	53.20	15.10	35	48.12 ± 1.42	57.63 ± 0.89	0.33 ± 0.10	0.39 ± 0.12	47.69 ± 1.35	59.37 ± 1.55	0.51 ± 0.17	0.60 ± 0.19
KI	72.10	24.95	5	40.51 ± 0.18	49.01 ± 0.55	0.22 ± 0.06	0.30 ± 0.08	41.32 ± 0.52	50.99 ± 0.70	0.30 ± 0.12	0.40 ± 0.16
KI	69.90	17.23	15	39.90 ± 0.81	49.18 ± 0.48	0.27 ± 0.10	0.32 ± 0.12	40.63 ± 0.84	49.01 ± 0.30	0.21 ± 0.11	0.25 ± 0.13

Table A4 Continued

Saturated Salt Solution	%RH	Moisture, (grams H_2O / 100 grams dry starch)	Storage Temp-erature, (^{o}C)	Nonreversing Signal – 4 week rescan				Total heat flow – 4 week rescan			
				Tm onset, (^{o}C)	Tm peak, (^{o}C)	Enthalpy, (J/g)	Enthalpy, (J/g dry starch)	Tm onset, (^{o}C)	Tm peak, (^{o}C)	Enthalpy, (J/g)	Enthalpy, (J/g dry starch)
KI	67.90	19.14	25	42.79 ± 0.33	52.31 ± 1.09	0.23 ± 0.09	0.28 ± 0.12	39.91 ± 0.61	53.06 ± 0.76	0.47 ± 0.24	0.58 ± 0.30
KI	66.10	13.96	35	54.47 ± 0.56	65.85 ± 0.88	0.37 ±0.13	0.43 ± 0.15	53.16 ± 3.34	66.29 ± 1.10	0.44 ± 0.23	0.51 ± 0.27
50% MC	100.00	100.00	5	42.68 ± 0.22	54.44 ± 0.66	2.48 ± 0.06	4.97 ± 0.13	41.88 ± 0.76	54.03 ± 1.40	2.42 ± 0.15	4.83 ± 0.29
50% MC	100.00	100.00	15	46.93 ± 0.14	56.40 ±0.44	0.62 ± 0.08	1.23 ± 0.16	46.26 ± 1.33	55.31 ± 0.97	0.69 ± 0.19	1.38 ± 0.38
50% MC	100.00	100.00	25	43.04 ± 0.35	52.23 ± 0.65	0.29 ± 0.06	0.58 ± 0.11	43.96 ± 0.52	53.63 ± 0.64	0.26 ± 0.05	0.53 ± 0.10

Table A5. MDSC characterization of the glass transition for intact waxy corn starch granules

Saturated Salt Solution	%RH	Moisture, (grams H_2O / 100 grams dry starch)	Storage Temperature, (^oC)	Tm onset (^oC)	Tm midpoint (^oC)	Tm endpoint (^oC)	ΔCp (J/g ^oC)
$CaSO_4$	0.00	1.48	5	165.91 ± 0.31	170.27 ± 0.02	172.58 ± 0.13	0.13 ± 0.01
$CaSO_4$	0.00	0.75	15	Not detected			
$CaSO_4$	0.00	0.21	25	Not detected			
$CaSO_4$	0.00	1.01	35	Not detected			
LiCl	11.30	7.32	5	Not detected			
LiCl	11.30	6.10	15	Not detected			
LiCl	11.30	5.29	25	Not detected			
LiCl	11.30	5.01	35	Not detected			
$MgCl_2$	33.60	10.54	5	Not detected			
$MgCl_2$	33.30	10.77	15	Not detected			
$MgCl_2$	32.80	8.40	25	Not detected			
$MgCl_2$	32.10	8.47	35	Not detected			
NaBr	62.20	19.21	5	51.96 ± 0.56	54.45 ± 0.04	63.78 ± 0.09	0.11 ± 0.00
NaBr	59.10	14.84	15	Not detected			
NaBr	56.10	12.77	25	Not detected			
NaBr	53.20	12.01	35	Not detected			
KI	72.10	21.04	5	41.81 ± 0.07	44.38 ± 0.02	47.47 ± 0.18	0.09 ± 0.00
KI	69.90	18.09	15	62.89 ± 0.54	66.29 ± 1.03	73.52 ± 1.13	0.07 ± 0.01
KI	67.90	15.19	25	69.81 ± 0.12	74.04 ± 0.01	82.91 ± 0.28	0.17 ± 0.00
KI	66.10	15.77	35	77.06 ± 0.52	81.88 ± 0.00	89.12 ± 0.19	0.14 ± 0.01

Table A6. MDSC characterization of the glass transition for fragmented waxy corn starch granules

Saturated Salt Solution	%RH	Moisture, (grams H_2O / 100 grams dry starch)	Storage Temp-erature, (^{o}C)	Tm onset (^{o}C)	Tm midpoint (^{o}C)	Tm endpoint (^{o}C)	ΔCp (J/g °C)
CaSO$_4$	0.00	1.02	5	165.50 ± 0.21	167.92 ± 0.00	169.48 ± 0.03	0.07 ± 0.00
CaSO$_4$	0.00	1.09	15	Not detected			
CaSO$_4$	0.00	4.08	25	Not detected			
CaSO$_4$	0.00	0.51	35	Not detected			
LiCl	11.30	7.96	5	Not detected			
LiCl	11.30	5.78	15	Not detected			
LiCl	11.30	8.53	25	Not detected			
LiCl	11.30	4.77	35	Not detected			
MgCl$_2$	33.60	10.15	5	Not detected			
MgCl$_2$	33.30	9.44	15	Not detected			
MgCl$_2$	32.80	11.46	25	Not detected			
MgCl$_2$	32.10	8.83	35	Not detected			
NaBr	62.20	17.47	5	54.82 ± 3.46	58.18 ± 3.75	71.00 ± 1.32	0.12 ± 0.03
NaBr	59.10	20.55	15	Not detected			
NaBr	56.10	16.07	25	Not detected			
NaBr	53.20	15.10	35	Not detected			
KI	72.10	24.95	5	48.17 ± 0.11	48.90 ± 0.01	50.70 ± 0.04	0.09 ± 0.00
KI	69.90	17.23	15	64.93 ± 1.52	68.13 ± 0.12	74.50 ± 0.20	0.10 ± 0.02
KI	67.90	19.14	25	76.03 ± 0.32	78.90 ± 0.46	89.76 ± 0.74	0.11 ± 0.01

Table A7. MDSC characterization of endotherm following sub-Tg endotherm for intact waxy corn starch granules

Saturated Salt Solution	%RH	Moisture, (grams H$_2$O / 100 grams dry starch)	Storage Temp-erature, (^{o}C)	Nonreversing Signal – Initial				Total heat flow – Initial			
				Tm onset, (^{o}C)	Tm peak, (^{o}C)	Enthalpy, (J/g)	Enthalpy, (J/g dry starch)	Tm onset, (^{o}C)	Tm peak, (^{o}C)	Enthalpy, (J/g)	Enthalpy, (J/g dry starch)
NaBr	62.20	19.21	5	55.14 ± 0.37	61.87 ± 1.12	0.25 ± 0.15	0.31 ± 0.18	54.66 ± 0.37	62.08 ± 0.99	0.38 ± 0.31	0.47 ± 0.38
NaBr	59.10	14.84	15	77.91 ± 1.03	83.18 ± 0.90	0.25 ± 0.13	0.30 ± 0.16	78.09 ± 0.91	83.89 ± 1.53	0.23 ± 0.11	0.26 ± 0.13
KI	69.90	18.09	15	61.99 ± 0.17	67.62 ± 0.26	0.10 ± 0.02	0.13 ± 0.02	62.97 ± 0.33	68.26 ± 0.21	0.12 ± 0.02	0.14 ± 0.02
KI	67.90	15.19	25	74.49 ± 1.33	79.63 ± 1.60	0.13 ± 0.04	0.15 ± 0.05	76.21 ± 0.34	82.13 ± 0.29	0.15 ± 0.01	0.18 ± 0.01
KI	66.10	15.77	35	80.35 ± 0.74	86.83 ± 0.69	0.15 ± 0.06	0.18 ± 0.07	81.02 ± 0.71	87.45 ± 0.62	0.20 ± 0.03	0.24 ± 0.04

Table A8. MDSC characterization of endotherm following sub-Tg endotherm for fragmented waxy corn starch granules

Saturated Salt Solution	%RH	Moisture, (grams H$_2$O / 100 grams dry starch)	Storage Temp-erature, (ºC)	Nonreversing Signal – Initial				Total heat flow – Initial			
				Tm onset, (ºC)	Tm peak, (ºC)	Enthalpy, (J/g)	Enthalpy, (J/g dry starch)	Tm onset, (ºC)	Tm peak, (ºC)	Enthalpy, (J/g)	Enthalpy, (J/g dry starch)
NaBr	62.20	17.47	5	68.68 ± 0.69	74.28 ± 0.94	0.16 ± 0.04	0.20 ± 0.05	67.00 ± 0.73	75.28 ± 0.67	0.38 ± 0.15	0.47 ± 0.18
KI	69.90	17.23	15	65.41 ± 0.63	71.66 ± 2.57	0.11 ± 0.03	0.13 ± 0.04	64.81 ± 0.55	70.27 ± 0.31	0.13 ± 0.01	0.16 ± 0.01
KI	67.90	19.14	25	81.98 ± 0.36	86.16 ± 0.71	0.11 ± 0.02	0.14 ± 0.03	80.88 ± 0.39	85.81 ± 1.86	0.14 ± 0.02	0.17 ± 0.03
KI	66.10	13.96	35	83.75 ± 0.45	87.11 ± 0.34	0.13 ± 0.02	0.15 ± 0.02	84.36 ± 0.51	87.94 ± 0.78	0.16 ± 0.05	0.19 ± 0.05

Table A9. MDSC characterization of the sub-Tg endotherm in commercial crackers

Application	Saturated Salt Solution	%RH	Moisture, (% wet basis)	Nonreversing Signal			
				Tm onset, (^{o}C)	Tm peak, (^{o}C)	Enthalpy, (J/g)	Enthalpy, (J/g dry starch)
Carr's water crackers	$CaSO_4$	0.00	0.79	30.71 ± 0.87	41.44 ± 0.33	0.11 ± 0.03	0.11 ± 0.03
Carr's water crackers	LiCl	11.30	4.10	33.87 ± 0.69	44.48 ± 2.29	0.21 ± 0.02	0.21 ± 0.02
Carr's water crackers	$KC_2H_3O_2$	22.50	6.36	41.96 ± 1.80	52.00 ± 0.64	0.71 ± 0.10	0.76 ± 0.11
Carr's water crackers	$MgCl_2$	32.80	6.48	38.08 ± 3.93	48.70 ± 3.22	0.72 ± 0.09	0.77 ± 0.10
Carr's water crackers	K_2CO_3	43.20	7.52	41.41 ± 1.31	50.53 ± 0.47	0.91 ± 0.02	0.99 ± 0.02
Carr's water crackers	$Mg(NO_3)_2$	52.90	8.85	39.05 ± 1.14	47.71 ± 0.64	1.21 ± 0.02	1.32 ± 0.03
Carr's water crackers	KI	67.90	12.31	39.54 ± 0.22	47.82 ± 0.13	2.18 ± 0.07	2.49 ± 0.07
Cream crackers	$CaSO_4$	0.00	0.83	32.19 ± 2.30	43.01 ± 1.82	0.19 ± 0.01	0.19 ± 0.01
Cream crackers	LiCl	11.30	3.26	33.97 ± 0.63	46.11 ± 3.92	0.30 ± 0.04	0.31 ± 0.04
Cream crackers	$KC_2H_3O_2$	22.50	5.17	38.10 ± 1.44	52.74 ± 0.49	0.51 ± 0.01	0.54 ± 0.01
Cream crackers	$MgCl_2$	32.80	5.51	38.70 ± 1.81	48.32 ± 1.66	0.56 ± 0.05	0.59 ± 0.05
Cream crackers	K_2CO_3	43.20	6.85	40.41 ± 0.77	49.51 ± 0.01	0.74 ± 0.03	0.80 ± 0.03
Cream crackers	$Mg(NO_3)_2$	52.90	7.99	44.30 ± 1.41	52.55 ± 2.79	0.97 ± 0.03	0.97 ± 0.03
Cream crackers	KI	67.90	11.45	44.06 ± 1.03	49.86 ± 0.63	1.55 ± 0.04	1.75 ± 0.04
Matzo	$CaSO_4$	0.00	0.76	$40.52 \pm 1.`8$	51.71 ± 1.92	0.07 ± 0.04	0.07 ± 0.04
Matzo	LiCl	11.30	4.16	33.46 ± 0.35	43.77 ± 4.35	0.12 ± 0.01	0.13 ± 0.01
Matzo	$KC_2H_3O_2$	22.50	6.30	43.17 ± 2.16	50.30 ± 0.49	0.51 ± 0.07	0.55 ± 0.07
Matzo	$MgCl_2$	32.80	6.47	42.49 ± 1.49	50.90 ± 0.28	0.58 ± 0.05	0.62 ± 0.05
Matzo	K_2CO_3	43.20	7.64	44.59 ± 0.66	50.99 ± 0.24	0.70 ± 0.03	0.76 ± 0.03
Matzo	$Mg(NO_3)_2$	52.90	9.15	38.74 ± 0.42	48.88 ± 0.00	1.12 ± 0.04	1.24 ± 0.04
Matzo	KI	67.90	12.81	43.81 ± 1.51	49.77 ± 1.32	1.69 ± 0.23	1.94 ± 0.26
Melba toast	$CaSO_4$	0.00	0.70	39.45 ± 5.11	47.90 ± 3.52	0.11 ± 0.01	0.11 ± 0.01
Melba toast	LiCl	11.30	3.29	44.75 ± 3.81	53.97 ± 5.08	0.24 ± 0.02	0.25 ± 0.02
Melba toast	$KC_2H_3O_2$	22.50	5.32	42.18 ± 0.63	52.16 ± 0.67	0.73 ± 0.05	0.77 ± 0.05
Melba toast	$MgCl_2$	32.80	5.41	43.20 ± 0.27	52.26 ± 0.16	0.76 ± 0.03	0.80 ± 0.03
Melba toast	K_2CO_3	43.20	6.54	42.78 ± 1.25	51.30 ± 1.91	0.88 ± 0.02	0.94 ± 0.03
Melba toast	$Mg(NO_3)_2$	52.90	8.18	38.90 ± 0.49	46.40 ± 0.27	1.06 ± 0.03	1.16 ± 0.04
Melba toast	KI	67.90	13.44	39.98 ± 1.42	48.67 ± 0.65	2.68 ± 0.06	3.09 ± 0.07
Saltines	$CaSO_4$	0.00	1.52	32.61 ± 1.85	42.73 ± 1.34	0.16 ± 0.02	0.16 ± 0.02
Saltines	LiCl	11.30	4.14	36.25 ± 3.31	45.78 ± 4.36	0.28 ± 0.02	0.29 ± 0.02
Saltines	$KC_2H_3O_2$	22.50	6.00	40.08 ± 1.29	49.44 ± 1.61	0.44 ± 0.01	0.47 ± 0.01
Saltines	$MgCl_2$	32.80	6.21	40.58 ± 0.65	49.87 ± 0.25	0.47 ± 0.02	0.50 ± 0.03

216

Table A9 Continued

Application	Saturated Salt Solution	%RH	Moisture, (% wet basis)	Nonreversing Signal			
				Tm onset, (^{o}C)	Tm peak, (^{o}C)	Enthalpy, (J/g)	Enthalpy, (J/g dry starch)
Saltines	K_2CO_3	43.20	7.19	41.20 ± 0.56	49.96 ± 1.51	0.58 ± 0.04	0.63 ± 0.04
Saltines	$Mg(NO_3)_2$	52.90	8.72	38.68 ± 0.55	46.35 ± 0.93	0.72 ± 0.05	0.79 ± 0.05
Saltines	KI	67.90	13.01	40.53 ± 0.63	47.30 ± 0.08	1.36 ± 0.18	1.56 ± 0.21

APPENDIX B

SUPPORTING DATA FOR CHAPTER 4

Table B1. MDSC characterization of primary sub-Tg endotherm peak and secondary endotherm peak in low moisture pregelatinized waxy maize starch

Saturated Salt Solution	%RH	Moisture, (% wet basis)	Nonreversing Signal - Primary Peak				Nonreversing Signal - Secondary Peak			
			Tm onset, (°C)	Tm peak, (°C)	Enthalpy, (J/g)	Enthalpy, (J/g dry starch)	Tm onset, (°C)	Tm peak, (°C)	Enthalpy, (J/g)	Enthalpy, (J/g dry starch)
$CaSO_4$	0.00	1.10	42.86 ± 1.52	57.53 ± 1.34	0.08 ± 0.01	0.09 ± 0.01	Not observed			
LiCl	11.30	6.09	52.44 ± 0.52	62.20 ± 0.01	0.27 ± 0.03	0.29 ± 0.03	Not observed			
$KC_2H_3O_2$	22.50	7.80	53.40 ± 0.33	61.99 ± 0.01	0.37 ± 0.01	0.40 ± 0.01	Not observed			
$MgCl_2$	32.80	8.46	54.96 ± 0.13	62.36 ± 0.01	0.44 ± 0.02	0.48 ± 0.02	Not observed			
K_2CO_3	43.20	10.21	53.65 ± 0.16	60.58 ± 0.01	0.57 ± 0.02	0.64 ± 0.02	Not observed			
NaBr	56.10	12.16	52.04 ± 0.20	58.74 ± 0.01	0.78 ± 0.03	0.91 ± 0.04	94.77 ± 0.04	100.95 ± 0.01	0.13 ± 0.02	0.15 ± 0.03
KI	67.90	13.91	54.74 ± 0.05	60.82 ± 0.01	1.11 ± 0.02	1.33 ± 0.02	77.70 ± 0.43	87.33 ± 0.61	0.15 ± 0.03	0.18 ± 0.03
50% moisture	n/a	50.00	42.25 ± 0.53	66.27 ± 0.01	5.68 ± 0.10	11.36 ± 0.20	Not observed			

Table B2. MDSC characterization of the glass transition for low moisture pregelatinized waxy maize starch

Saturated Salt Solution	%RH	Moisture, (% wet basis)	Tm onset (^oC)	Tm midpoint (^oC)	Tm endpoint (^oC)	ΔCp (J/g $^\circ$C)	ΔCp (J/g $^\circ$C dry starch)
CaSO$_4$	0.00	1.10	Not observed				
LiCl	11.30	6.09	Not observed				
KC$_2$H$_3$O$_2$	22.50	7.80	Not observed				
MgCl$_2$	32.80	8.46	Not observed				
K$_2$CO$_3$	43.20	10.21	Not observed				
NaBr	56.10	12.16	94.93 ± 1.73	99.22 ± 1.15	103.31 ± 0.64	0.12 ± 0.02	0.12 ± 0.03
KI	67.90	13.91	77.07 ± 1.11	82.15 ± 0.75	86.91 ± 0.55	0.13 ± 0.01	0.13 ± 0.02
50% MC	n/a	50.00	Not observed				

Table B3. FTIR-ATR peak absorbance intensities for low moisture pregelatinized waxy maize starch

Saturated Salt Solution	% RH	Moisture, (% wet basis)	Absorbance Intensity - Before DSC Scan				
			995 cm^{-1}	1022 cm^{-1}	1045 cm^{-1}	1078 cm^{-1}	1151 cm^{-1}
CaSO$_4$	0.00	1.10	0.039 ± 0.000	0.028 ± 0.000	0.011 ± 0.001	0.004 ± 0.000	0.007 ± 0.000
LiCl	11.30	6.09	0.052 ± 0.000	0.035 ± 0.000	0.008 ± 0.002	0.006 ± 0.001	0.008 ± 0.001
KC$_2$H$_3$O$_2$	22.50	7.80	0.072 ± 0.000	0.039 ± 0.000	0.009 ± 0.002	0.004 ± 0.000	0.006 ± 0.000
MgCl$_2$	32.80	8.46	0.098 ± 0.000	0.050 ± 0.001	0.012 ± 0.003	0.055 ± 0.002	0.072 ± 0.004
K$_2$CO$_3$	43.20	10.21	0.115 ± 0.000	0.068 ± 0.000	0.016 ± 0.003	0.007 ± 0.000	0.009 ± 0.001
NaBr	56.10	12.16	0.131 ± 0.000	0.080 ± 0.000	0.018 ± 0.003	0.007 ± 0.000	0.008 ± 0.000
KI	67.90	13.91	0.667 ± 0.002	0.580 ± 0.013	0.213 ± 0.000	0.128 ± 0.002	0.140 ± 0.004
50% moisture	n/a	50.00	0.567 ± 0.003	0.536 ± 0.005	0.192 ± 0.001	0.126 ± 0.002	0.137 ± 0.005
Ungelatinized starch	n/a	11.68	0.289 ± 0.025	0.237 ± 0.017	0.108 ± 0.006	0.061 ± 0.005	0.076 ± 0.010

Table B4. FTIR-ATR peak absorbance intensities for low moisture pregelatinized waxy maize starch immediately after DSC scan

Saturated Salt Solution	% RH	Moisture, (% wet basis)	Absorbance Intensity - After DSC Scan			
			995 cm^{-1}	1022 cm^{-1}	1078 cm^{-1}	1151 cm^{-1}
CaSO$_4$	0.00	1.10	0.164 ± 0.000	0.142 ± 0.000	0.037 ± 0.001	0.046 ± 0.001
LiCl	11.30	6.09	0.255 ± 0.001	0.217 ± 0.002	0.059 ± 0.003	0.074 ± 0.004
KC$_2$H$_3$O$_2$	22.50	7.80	0.254 ± 0.001	0.217 ± 0.001	0.057 ± 0.003	0.070 ± 0.003
MgCl$_2$	32.80	8.46	0.0277 ± 0.001	0.237 ± 0.001	0.062 ± 0.005	0.077 ± 0.005
K$_2$CO$_3$	43.20	10.21	0.294 ± 0.001	0.251 ± 0.001	0.064 ± 0.003	0.080 ± 0.002
NaBr	56.10	12.16	0.300 ± 0.003	0.255 ± 0.003	0.067 ± 0.008	0.083 ± 0.003
KI	67.90	13.91	0.156 ± 0.002	0.136 ± 0.003	0.046 ± 0.004	0.057 ± 0.004

APPENDIX C

SUPPORTING DATA FOR CHAPTER 5

Table C1. Kinetic characterization of the sub-Tg endotherm peak in low moisture pregelatinized waxy maize starch observed by MDSC

Saturated Salt Solution	%RH	Moisture, (% wet basis)	Time, (weeks)	MDSC Nonreversing Signal				Extent of transformation, Y
				Tm onset, (°C)	Tm peak, (°C)	Enthalpy, (J/g)	Enthalpy, (J/g dry starch)	
CaSO$_4$	0.00	1.10	1	39.10 ± 1.41	51.45 ± 3.31	0.10 ± 0.01	0.10 ± 0.01	0.08 ± 0.01
CaSO$_4$	0.00	1.10	2	39.62 ± 0.71	52.98 ± 1.46	0.12 ± 0.01	0.12 ± 0.01	0.09 ± 0.01
CaSO$_4$	0.00	1.10	3	38.97 ± 1.35	50.40 ± 3.11	0.13 ± 0.01	0.13 ± 0.01	0.10 ± 0.01
CaSO$_4$	0.00	1.10	4	37.50 ± 0.60	43.96 ± 2.76	0.14 ± 0.01	0.14 ± 0.01	0.11 ± 0.01
CaSO$_4$	0.00	1.10	8	40.85 ± 1.78	50.32 ± 3.84	0.17 ± 0.03	0.17 ± 0.03	0.13 ± 0.03
CaSO$_4$	0.00	1.10	12	41.52 ± 0.71	48.48 ± 0.90	0.20 ± 0.01	0.20 ± 0.01	0.15 ± 0.01
CaSO$_4$	0.00	1.10	16	41.98 ± 1.25	50.37 ± 2.85	0.22 ± 0.02	0.17 ± 0.02	0.16 ± 0.01
CaSO$_4$	0.00	1.10	20	40.75 ± 1.59	49.24 ± 1.82	0.23 ± 0.01	0.24 ± 0.01	0.18 ± 0.01
CaSO$_4$	0.00	1.10	24	41.83 ± 1.74	49.35 ± 1.29	0.25 ± 0.01	0.25 ± 0.03	0.19 ± 0.01
LiCl	11.30	6.09	1	41.71 ± 1.72	49.02 ± 1.48	0.13 ± 0.01	0.14 ± 0.02	0.10 ± 0.01
LiCl	11.30	6.09	2	39.48 ± 1.89	47.78 ± 2.14	0.15 ± 0.02	0.16 ± 0.02	0.11 ± 0.02
LiCl	11.30	6.09	3	38.39 ± 1.74	46.80 ± 1.62	0.17 ± 0.04	0.18 ± 0.04	0.13 ± 0.03
LiCl	11.30	6.09	4	38.45 ± 0.95	48.10 ± 0.38	0.19 ± 0.02	0.20 ± 0.02	0.14 ± 0.02
LiCl	11.30	6.09	8	39.77 ± 0.96	48.59 ± 1.58	0.23 ± 0.01	0.24 ± 0.01	0.17 ± 0.01
LiCl	11.30	6.09	12	41.30 ± 1.90	50.29 ± 1.55	0.25 ± 0.01	0.26 ± 0.01	0.18 ± 0.01
LiCl	11.30	6.09	16	41.57 ± 1.99	47.96 ± 1.52	0.26 ± 0.01	0.28 ± 0.01	0.20 ± 0.01
LiCl	11.30	6.09	20	39.33 ± 1.09	47.31 ± 2.05	0.27 ± 0.03	0.29 ± 0.03	0.21 ± 0.02
LiCl	11.30	6.09	24	40.73 ± 1.85	49.14 ± 1.37	0.29 ± 0.01	0.31 ± 0.01	0.22 ± 0.01

Table C1 Continued

Saturated Salt Solution	%RH	Moisture, (% wet basis)	Time, (weeks)	MDSC Nonreversing Signal				Extent of transformation, Y
				Tm onset, (^{o}C)	Tm peak, (^{o}C)	Enthalpy, (J/g)	Enthalpy, (J/g dry starch)	
$KC_2H_3O_2$	22.50	7.80	1	37.88 ± 0.78	46.78 ± 1.11	0.14 ± 0.02	0.15 ± 0.02	0.12 ± 0.01
$KC_2H_3O_2$	22.50	7.80	2	37.54 ± 0.94	44.94 ± 1.39	0.17 ± 0.01	0.18 ± 0.01	0.14 ± 0.01
$KC_2H_3O_2$	22.50	7.80	3	41.92 ± 2.00	50.89 ± 2.49	0.19 ± 0.01	0.20 ± 0.01	0.15 ± 0.01
$KC_2H_3O_2$	22.50	7.80	4	38.24 ± 2.19	47.90 ± 1.23	0.20 ± 0.03	0.22 ± 0.04	0.16 ± 0.03
$KC_2H_3O_2$	22.50	7.80	8	38.22 ± 1.54	50.10 ± 4.02	0.24 ± 0.04	0.26 ± 0.04	0.19 ± 0.03
$KC_2H_3O_2$	22.50	7.80	12	40.26 ± 0.37	50.64 ± 1.00	0.25 ± 0.02	0.27 ± 0.02	0.21 ± 0.01
$KC_2H_3O_2$	22.50	7.80	16	39.02 ± 1.57	47.50 ± 2.41	0.27 ± 0.03	0.27 ± 0.03	0.22 ± 0.03
$KC_2H_3O_2$	22.50	7.80	20	40.03 ± 0.89	49.78 ± 1.19	0.29 ± 0.02	0.31 ± 0.02	0.23 ± 0.01
$KC_2H_3O_2$	22.50	7.80	24	40.09 ± 1.30	52.05 ± 0.71	0.30 ± 0.04	0.33 ± 0.05	0.25 ± 0.03
$MgCl_2$	32.80	8.46	1	40.18 ± 3.04	51.17 ± 3.98	0.17 ± 0.02	0.18 ± 0.02	0.14 ± 0.01
$MgCl_2$	32.80	8.46	2	37.44 ± 1.03	48.10 ± 4.21	0.20 ± 0.01	0.22 ± 0.01	0.16 ± 0.01
$MgCl_2$	32.80	8.46	3	38.98 ± 0.88	51.15 ± 4.22	0.23 ± 0.03	0.25 ± 0.03	0.19 ± 0.02
$MgCl_2$	32.80	8.46	4	37.66 ±2.04	49.18 ± 5.30	0.25 ± 0.02	0.27 ± 0.02	0.20 ± 0.02
$MgCl_2$	32.80	8.46	8	39.36 ± 1.01	47.14 ± 3.64	0.29 ± 0.03	0.32 ± 0.03	0.24 ± 0.02
$MgCl_2$	32.80	8.46	12	38.19 ± 1.68	49.28 ± 5.55	0.30 ± 0.04	0.33 ± 0.04	0.25 ± 0.03
$MgCl_2$	32.80	8.46	16	42.89 ± 6.67	52.34 ± 5.16	0.31 ± 0.05	0.34 ± 0.05	0.26 ± 0.04
$MgCl_2$	32.80	8.46	20	40.67 ± 0.77	51.18 ± 0.96	0.32 ± 0.01	0.35 ± 0.02	0.26 ± 0.01
$MgCl_2$	32.80	8.46	24	39.41 ± 0.71	51.14 ± 1.48	0.33 ± 0.02	0.36 ± 0.02	0.27 ± 0.02
K_2CO_3	43.20	10.21	1	47.60 ± 1.06	47.15 ± 1.82	0.19 ± 0.03	0.21 ± 0.03	0.16 ± 0.02
K_2CO_3	43.20	10.21	2	36.45 ± 1.32	46.72 ± 0.74	0.22 ± 0.02	0.25 ± 0.02	0.19 ± 0.01
K_2CO_3	43.20	10.21	3	38.66 ± 0.67	47.08 ± 3.45	0.26 ± 0.01	0.29 ± 0.01	0.21 ± 0.01
K_2CO_3	43.20	10.21	4	37.61 ± 1.62	48.56 ± 5.71	0.28 ± 0.04	0.31 ± 0.04	0.23 ± 0.03

Table C1 Continued

Saturated Salt Solution	%RH	Moisture, (% wet basis)	Time, (weeks)	MDSC Nonreversing Signal				Extent of transformation, Y
				Tm onset, (°C)	Tm peak, (°C)	Enthalpy, (J/g)	Enthalpy, (J/g dry starch)	
K_2CO_3	43.20	10.21	8	36.88 ± 0.42	48.00 ± 0.65	0.31 ± 0.02	0.34 ± 0.02	0.26 ± 0.01
K_2CO_3	43.20	10.21	12	38.24 ± 2.11	50.29 ± 3.96	0.32 ± 0.03	0.36 ± 0.04	0.27 ± 0.03
K_2CO_3	43.20	10.21	16	38.20 ± 0.82	47.72 ± 0.83	0.33 ± 0.01	0.37 ± 0.02	0.28 ± 0.01
K_2CO_3	43.20	10.21	20	47.60 ± 1.13	47.15 ± 1.89	0.19 ± 0.10	0.21 ± 0.10	0.28 ± 0.01
K_2CO_3	43.20	10.21	24	47.60 ± 1.14	47.15 ± 1.90	0.19 ± 0.11	0.21 ± 0.11	0.28 ± 0.02
NaBr	56.10	12.16	1	36.44 ± 2.81	48.38 ± 0.83	0.24 ± 0.02	0.27 ± 0.02	0.20 ± 0.02
NaBr	56.10	12.16	2	37.61 ± 1.69	47.50 ± 3.50	0.29 ± 0.02	0.33 ± 0.03	0.25 ± 0.02
NaBr	56.10	12.16	3	37.08 ± 1.76	47.98 ± 3.98	0.31 ± 0.02	0.35 ± 0.02	0.27 ± 0.01
NaBr	56.10	12.16	4	36.42 ± 0.79	43.04 ± 0.09	0.34 ± 0.02	0.38 ± 0.02	0.29 ± 0.02
NaBr	56.10	12.16	8	38.23 ± 1.63	46.38 ± 0.67	0.37 ± 0.03	0.42 ± 0.03	0.31 ± 0.02
NaBr	56.10	12.16	12	37.67 ± 1.33	49.03 ± 1.78	0.39 ± 0.02	0.44 ± 0.02	0.33 ± 0.02
NaBr	56.10	12.16	16	39.08 ± 1.27	45.73 ± 1.82	0.41 ± 0.03	0.47 ± 0.04	0.35 ± 0.03
NaBr	56.10	12.16	20	39.16 ± 1.27	50.82 ± 1.28	0.42 ± 0.03	0.47 ± 0.03	0.36 ± 0.03
NaBr	56.10	12.16	24	38.93 ± 0.87	50.33 ± 0.69	0.42 ± 0.02	0.47 ± 0.02	0.36 ± 0.01
KI	67.90	13.91	1	36.04 ± 0.04	41.87 ± 1.18	0.33 ± 0.01	0.38 ± 0.02	0.29 ± 0.01
KI	67.90	13.91	2	36.54 ± 0.57	44.27 ± 0.77	0.35 ± 0.02	0.40 ± 0.02	0.30 ± 0.02
KI	67.90	13.91	3	37.75 ± 0.62	44.84 ± 0.73	0.37 ± 0.03	0.43 ± 0.04	0.32 ± 0.03
KI	67.90	13.91	4	35.31 ± 0.75	43.08 ± 1.49	0.38 ± 0.04	0.44 ± 0.04	0.33 ± 0.02
KI	67.90	13.91	8	38.29 ± 1.00	45.46 ± 1.51	0.43 ± 0.02	0.50 ± 0.02	0.37 ± 0.02
KI	67.90	13.91	12	39.99 ± 0.90	48.41 ± 0.46	0.47 ± 0.01	0.54 ± 0.02	0.41 ± 0.01
KI	67.90	13.91	16	40.46 ± 0.99	46.92 ± 0.91	0.50 ± 0.02	0.58 ± 0.02	0.43 ± 0.02
KI	67.90	13.91	20	40.70 ± 0.56	49.48 ± 0.15	0.53 ± 0.03	0.61 ± 0.04	0.46 ± 0.03
KI	67.90	13.91	24	40.66 ± 1.29	49.67 ± 0.15	0.55 ± 0.02	0.64 ± 0.02	0.48 ± 0.02
50% moisture	n/a	50.00	0.14	41.77 ± 3.33	47.89 ± 3.23	0.19 ± 0.04	0.39 ± 0.09	0.29 ± 0.06
50% moisture	n/a	50.00	0.29	38.41 ± 0.44	47.03 ± 0.55	0.27 ± 0.02	0.53 ± 0.04	0.40 ± 0.03

Table C1 Continued

Saturated Salt Solution	%RH	Moisture, (% wet basis)	Time, (weeks)	MDSC Nonreversing Signal				Extent of transformation, Y
				Tm onset, (°C)	Tm peak, (°C)	Enthalpy, (J/g)	Enthalpy, (J/g dry starch)	
50% moisture	n/a	50.00	0.43	40.15 ± 2.08	47.85 ± 1.24	0.30 ± 0.02	0.61 ± 0.05	0.46 ± 0.04
50% moisture	n/a	50.00	0.86	40.57 ± 1.30	50.54 ± 2.37	0.40 ± 0.02	0.81 ± 0.05	0.61 ± 0.03
50% moisture	n/a	50.00	1	38.22 ± 2.32	47.91 ± 2.28	0.43 ± 0.05	0.86 ± 0.11	0.64 ± 0.08
50% moisture	n/a	50.00	2	42.97 ± 1.96	52.52 ± 1.42	0.48 ± 0.03	0.95 ± 0.05	0.71 ± 0.04
50% moisture	n/a	50.00	3	41.79 ± 1.22	52.30 ± 1.82	0.56 ± 0.01	1.12 ± 0.03	0.84 ± 0.02
50% moisture	n/a	50.00	4	40.97 ± 0.42	46.31 ± 1.47	0.60 ± 0.02	1.21 ± 0.04	0.91 ± 0.03

Table C2. Kinetic characterization of FTIR-ATR peak absorbance intensities for low moisture pregelatinized waxy maize starch

Saturated Salt Solution	% RH	Moisture, (% wet basis)	Time, (weeks)	Peak Absorbance Intensity						Extent of transformation, Y
				995 cm^{-1}	1022 cm^{-1}	1045 cm^{-1}	1078 cm^{-1}	1151 cm^{-1}	1078 cm^{-1} / 1151 cm^{-1}	
CaSO$_4$	0.00	1.10	0	0.164 ± 0.004	0.142 ± 0.003	0.055 ± 0.002	0.037 ± 0.002	0.046 ± 0.001	0.797 ± 0.030	n/a
CaSO$_4$	0.00	1.10	1	0.215 ± 0.006	0.187 ± 0.006	0.072 ± 0.002	0.045 ± 0.001	0.056 ± 0.001	0.804 ± 0.019	0.076 ± 0.124
CaSO$_4$	0.00	1.10	2	0.228 ± 0.019	0.198 ± 0.016	0.075 ± 0.005	0.049 ± 0.003	0.060 ± 0.003	0.813 ± 0.009	0.134 ± 0.056
CaSO$_4$	0.00	1.10	3	0.265 ± 0.019	0.229 ± 0.017	0.086 ± 0.006	0.057 ± 0.004	0.070 ± 0.004	0.817 ± 0.008	0.164 ± 0.052
CaSO$_4$	0.00	1.10	4	0.198 ± 0.005	0.171 ± 0.004	0.066 ± 0.002	0.042 ± 0.001	0.051 ± 0.002	0.821 ± 0.019	0.188 ± 0.120
CaSO$_4$	0.00	1.10	8	0.225 ± 0.007	0.197 ± 0.007	0.075 ± 0.003	0.049 ± 0.002	0.059 ± 0.002	0.828 ± 0.010	0.232 ± 0.063
CaSO$_4$	0.00	1.10	12	0.287 ± 0.013	0.248 ± 0.011	0.092 ± 0.004	0.062 ± 0.003	0.075 ± 0.004	0.828 ± 0.016	0.232 ± 0.102
CaSO$_4$	0.00	1.10	16	0.265 ± 0.009	0.230 ± 0.008	0.087 ± 0.003	0.057 ± 0.002	0.060 ± 0.002	0.833 ± 0.007	0.264 ± 0.043
CaSO$_4$	0.00	1.10	20	0.296 ± 0.012	0.256 ± 0.009	0.095 ± 0.003	0.062 ± 0.001	0.074 ± 0.002	0.836 ± 0.012	0.282± 0.079
CaSO$_4$	0.00	1.10	24	0.250 ± 0.016	0.219 ± 0.014	0.084 ± 0.005	0.056 ± 0.004	0.067 ± 0.004	0.842 ± 0.009	0.324 ± 0.060
LiCl	11.30	6.09	0	0.242 ± 0.027	0.207 ± 0.023	0.078 ± 0.007	0.055 ± 0.009	0.070 ± 0.010	0.792 ± 0.006	n/a
LiCl	11.30	6.09	1	0.220 ± 0.009	0.190 ± 0.007	0.072 ± 0.002	0.047 ± 0.002	0.058 ± 0.003	0.807 ± 0.009	0.098 ± 0.058
LiCl	11.30	6.09	2	0.231 ± 0.008	0.200 ± 0.007	0.077 ± 0.003	0.050 ± 0.002	0.061 ± 0.003	0.812 ± 0.013	0.128 ± 0.082
LiCl	11.30	6.09	3	0.150 ± 0.030	0.126 ± 0.029	0.046 ± 0.013	0.030 ± 0.007	0.037 ± 0.008	0.819 ± 0.022	0.174 ± 0.141
LiCl	11.30	6.09	4	0.199 ± 0.002	0.172 ± 0.002	0.066 ± 0.001	0.043 ± 0.001	0.052 ± 0.001	0.820 ± 0.023	0.180 ± 0.147
LiCl	11.30	6.09	8	0.207 ± 0.004	0.179 ± 0.003	0.069 ± 0.001	0.045 ± 0.001	0.055 ± 0.002	0.826 ± 0.025	0.221 ± 0.161
LiCl	11.30	6.09	12	0.247 ± 0.001	0.214 ± 0.008	0.082 ± 0.003	0.054 ± 0.003	0.064 ± 0.003	0.832 ± 0.022	0.257 ± 0.143
LiCl	11.30	6.09	16	0.237 ± 0.001	0.206 ± 0.001	0.079 ± 0.001	0.051 ± 0.001	0.061 ± 0.001	0.836 ± 0.001	0.281 ± 0.007
LiCl	11.30	6.09	20	0.234 ± 0.005	0.204 ± 0.004	0.077 ± 0.001	0.051 ± 0.001	0.061 ± 0.002	0.837 ± 0.015	0.293 ± 0.097
LiCl	11.30	6.09	24	0.284 ± 0.002	0.246 ± 0.001	0.093 ± 0.001	0.060 ± 0.001	0.072 ± 0.001	0.840 ± 0.018	0.308 ± 0.116
KC$_2$H$_3$O$_2$	22.50	7.80	0	0.254 ± 0.002	0.217 ± 0.007	0.082 ± 0.005	0.057 ± 0.005	0.070 ± 0.005	0.809 ± 0.018	n/a
KC$_2$H$_3$O$_2$	22.50	7.80	1	0.307 ± 0.002	0.265 ± 0.003	0.098 ± 0.002	0.065 ± 0.001	0.078 ± 0.001	0.827 ± 0.005	0.227 ± 0.131

Table C2 Continued

| Saturated Salt Solution | % RH | Moisture, (% wet basis) | Time, (weeks) | Peak Absorbance Intensity | | | | | | Extent of transformation, Y |
				995 cm^{-1}	1022 cm^{-1}	1045 cm^{-1}	1078 cm^{-1}	1151 cm^{-1}	1078 cm^{-1} / 1151 cm^{-1}	
KC$_2$H$_3$O$_2$	22.50	7.80	2	0.294 ± 0.027	0.255 ± 0.024	0.095 ± 0.008	0.063 ± 0.005	0.077 ± 0.005	0.827 ± 0.020	0.227 ± 0.131
KC$_2$H$_3$O$_2$	22.50	7.80	3	0.225 ± 0.002	0.197 ± 0.002	0.076 ± 0.001	0.051 ± 0.001	0.062 ± 0.001	0.829 ± 0.014	0.242 ± 0.089
KC$_2$H$_3$O$_2$	22.50	7.80	4	0.212 ± 0.010	0.183 ± 0.009	0.071 ± 0.004	0.045 ± 0.002	0.054 ± 0.002	0.832 ± 0.014	0.255 ± 0.088
KC$_2$H$_3$O$_2$	22.50	7.80	8	0.212 ± 0.030	0.184 ± 0.026	0.072 ± 0.009	0.047 ± 0.005	0.056 ± 0.006	0.841 ± 0.006	0.315 ± 0.039
KC$_2$H$_3$O$_2$	22.50	7.80	12	0.255 ± 0.009	0.221 ± 0.007	0.084 ± 0.002	0.055 ± 0.002	0.066 ± 0.003	0.843 ± 0.013	0.326 ± 0.083
KC$_2$H$_3$O$_2$	22.50	7.80	16	0.303 ± 0.009	0.263 ± 0.006	0.098 ± 0.001	0.065 ± 0.002	0.076 ± 0.001	0.847 ± 0.018	0.354 ± 0.114
KC$_2$H$_3$O$_2$	22.50	7.80	20	0.298 ± 0.043	0.258 ± 0.037	0.096 ± 0.014	0.063 ± 0.008	0.074 ± 0.009	0.847 ± 0.009	0.357 ± 0.058
KC$_2$H$_3$O$_2$	22.50	7.80	24	0.203 ± 0.017	0.246 ± 0.011	0.078 ± 0.006	0.052 ± 0.004	0.062 ± 0.004	0.848 ± 0.031	0.364 ± 0.197
MgCl$_2$	32.80	8.46	0	0.277 ± 0.010	0.237 ± 0.010	0.089 ± 0.002	0.062 ± 0.004	0.077 ± 0.005	0.811 ± 0.032	n/a
MgCl$_2$	32.80	8.46	1	0.184 ± 0.016	0.161 ± 0.015	0.060 ± 0.005	0.038 ± 0.003	0.046 ± 0.004	0.832 ± 0.009	0.257 ± 0.057
MgCl$_2$	32.80	8.46	2	0.309 ± 0.006	0.268 ± 0.004	0.101 ± 0.001	0.066 ± 0.001	0.079 ± 0.000	0.834 ± 0.014	0.269 ± 0.096
MgCl$_2$	32.80	8.46	3	0.291 ± 0.026	0.252 ± 0.022	0.095 ± 0.007	0.064 ± 0.004	0.076 ± 0.005	0.838 ± 0.024	0.294 ± 0.158
MgCl$_2$	32.80	8.46	4	0.262 ± 0.008	0.227 ± 0.007	0.085 ± 0.003	0.055 ± 0.001	0.066 ± 0.002	0.840 ± 0.012	0.312 ± 0.077
MgCl$_2$	32.80	8.46	8	0.266 ± 0.001	0.231 ± 0.001	0.088 ± 0.002	0.060 ± 0.002	0.071 ± 0.003	0.847 ± 0.010	0.352 ± 0.066
MgCl$_2$	32.80	8.46	12	0.277 ± 0.030	0.241 ± 0.026	0.091 ± 0.009	0.061 ± 0.005	0.072 ± 0.007	0.847 ± 0.012	0.358 ± 0.078
MgCl$_2$	32.80	8.46	16	0.284 ± 0.010	0.246 ± 0.009	0.092 ± 0.003	0.061 ± 0.002	0.072 ± 0.002	0.850 ± 0.017	0.374 ± 0.109
MgCl$_2$	32.80	8.46	20	0.226 ± 0.001	0.198 ± 0.001	0.077 ± 0.001	0.052 ± 0.001	0.060 ± 0.001	0.854 ± 0.010	0.398 ± 0.063
MgCl$_2$	32.80	8.46	24	0.229 ± 0.025	0.201 ± 0.021	0.077 ± 0.007	0.052 ± 0.005	0.061 ± 0.005	0.854 ± 0.020	0.398 ± 0.128
K$_2$CO$_3$	43.20	10.21	0	0.294 ± 0.010	0.251 ± 0.008	0.095 ± 0.005	0.064 ± 0.003	0.080 ± 0.002	0.809 ± 0.019	n/a
K$_2$CO$_3$	43.20	10.21	1	0.310 ± 0.037	0.268 ± 0.031	0.100 ± 0.011	0.066 ± 0.005	0.080 ± 0.007	0.835 ± 0.012	0.278 ± 0.075
K$_2$CO$_3$	43.20	10.21	2	0.320 ± 0.026	0.277 ± 0.021	0.103 ± 0.006	0.069 ± 0.005	0.082 ± 0.005	0.841 ± 0.011	0.314 ± 0.074
K$_2$CO$_3$	43.20	10.21	3	0.270 ± 0.012	0.235 ± 0.010	0.089 ± 0.003	0.061 ± 0.002	0.072 ± 0.001	0.842 ± 0.018	0.324 ± 0.118

Table C2 Continued

Saturated Salt Solution	% RH	Moisture, (% wet basis)	Time, (weeks)	Peak Absorbance Intensity						Extent of transformation, Y
				995 cm^{-1}	1022 cm^{-1}	1045 cm^{-1}	1078 cm^{-1}	1151 cm^{-1}	1078 cm^{-1} / 1151 cm^{-1}	
K$_2$CO$_3$	43.20	10.21	4	0.250 ± 0.003	0.219 ± 0.003	0.083 ± 0.001	0.056 ± 0.001	0.066 ± 0.001	0.843 ± 0.006	0.332 ± 0.040
K$_2$CO$_3$	43.20	10.21	8	0.298 ± 0.006	0.258 ± 0.006	0.096 ± 0.002	0.065 ± 0.001	0.077 ± 0.001	0.847 ± 0.006	0.352 ± 0.041
K$_2$CO$_3$	43.20	10.21	12	0.288 ± 0.028	0.249 ± 0.024	0.093 ± 0.008	0.062 ± 0.005	0.073 ± 0.006	0.848 ± 0.026	0.362 ± 0.165
K$_2$CO$_3$	43.20	10.21	16	0.281 ± 0.0`9	0.242 ± 0.016	0.090 ± 0.006	0.061 ± 0.003	0.072 ± 0.003	0.852 ± 0.008	0.385 ± 0.054
K$_2$CO$_3$	43.20	10.21	20	0.254 ± 0.011	0.221 ± 0.010	0.083 ± 0.006	0.058 ± 0.002	0.068 ± 0.002	0.853 ± 0.023	0.391 ± 0.146
K$_2$CO$_3$	43.20	10.21	24	0.272 ± 0.030	0.043 ± 0.026	0.093 ± 0.010	0.062 ± 0.006	0.073 ± 0.006	0.853 ± 0.012	0.394 ± 0.077
NaBr	56.10	12.16	0	0.300 ± 0.057	0.255 ± 0.049	0.100 ± 0.019	0.067 ± 0.009	0.083 ± 0.009	0.811 ± 0.062	n/a
NaBr	56.10	12.16	1	0.323 ± 0.005	0.280 ± 0.004	0.105 ± 0.002	0.072 ± 0.001	0.087 ± 0.001	0.830 ± 0.008	0.248 ± 0.052
NaBr	56.10	12.16	2	0.276 ± 0.012	0.241 ± 0.010	0.093 ± 0.003	0.064 ± 0.002	0.077 ± 0.002	0.839 ± 0.023	0.302 ± 0.148
NaBr	56.10	12.16	3	0.304 ± 0.012	0.264 ± 0.009	0.099 ± 0.003	0.070 ± 0.003	0.083 ± 0.002	0.839 ± 0.010	0.304 ± 0.063
NaBr	56.10	12.16	4	0.260 ± 0.002	0.223 ± 0.001	0.084 ± 0.001	0.059 ± 0.001	0.070 ± 0.001	0.840 ± 0.018	0.311 ± 0.114
NaBr	56.10	12.16	8	0.302 ± 0.005	0.263 ± 0.004	0.100 ± 0.002	0.069 ± 0.001	0.082 ± 0.001	0.843 ± 0.010	0.329 ± 0.067
NaBr	56.10	12.16	12	0.304 ± 0.009	0.273 ± 0.017	0.105 ± 0.007	0.071 ± 0.003	0.084 ± 0.003	0.845 ± 0.006	0.342 ± 0.039
NaBr	56.10	12.16	16	0.294 ± 0.001	0.255 ± 0.001	0.096 ± 0.001	0.063 ± 0.001	0.074 ± 0.001	0.850 ± 0.013	0.377 ± 0.085
NaBr	56.10	12.16	20	0.283 ± 0.014	0.256 ± 0.012	0.092 ± 0.005	0.066 ± 0.003	0.077 ± 0.003	0.853 ± 0.014	0.393 ± 0.089
NaBr	56.10	12.16	24	0.250 ± 0.019	0.217 ± 0.016	0.082 ± 0.005	0.058 ± 0.003	0.068 ± 0.004	0.852 ± 0.017	0.389 ± 0.111
KI	67.90	13.91	0	0.156 ± 0.031	0.136 ± 0.026	0.057 ± 0.009	0.046 ± 0.008	0.057 ± 0.008	0.799 ± 0.025	n/a
KI	67.90	13.91	1	0.297 ± 0.039	0.259 ± 0.034	0.100 ± 0.013	0.069 ± 0.008	0.084 ± 0.008	0.824 ± 0.021	0.205 ± 0.134
KI	67.90	13.91	2	0.310 ± 0.022	0.270 ± 0.020	0.103 ± 0.007	0.073 ± 0.004	0.087 ± 0.003	0.838 ± 0.018	0.298 ± 0.119
KI	67.90	13.91	3	0.300 ± 0.040	0.262 ± 0.034	0.100 ± 0.011	0.069 ± 0.008	0.082 ± 0.008	0.840 ± 0.015	0.312 ± 0.096
KI	67.90	13.91	4	0.268 ± 0.011	0.232 ± 0.010	0.088 ± 0.005	0.062 ± 0.003	0.074 ± 0.004	0.844 ± 0.001	0.332 ± 0.005
KI	67.90	13.91	8	0.501 ± 0.005	0.424 ± 0.044	0.151 ± 0.012	0.102 ± 0.007	0.120 ± 0.004	0.849 ± 0.032	0.365 ± 0.209
KI	67.90	13.91	12	0.260 ± 0.011	0.227 ± 0.009	0.089 ± 0.001	0.062 ± 0.002	0.073 ± 0.001	0.851 ± 0.020	0.381 ± 0.128
KI	67.90	13.91	16	0.326 ± 0.016	0.281 ± 0.012	0.104 ± 0.003	0.072 ± 0.002	0.085 ± 0.002	0.854 ± 0.008	0.400 ± 0.054
KI	67.90	13.91	20	0.274 ± 0.011	0.241 ± 0.011	0.094 ± 0.006	0.066 ± 0.003	0.078 ± 0.003	0.852 ± 0.002	0.389 ± 0.011

Table C2 Continued

Saturated Salt Solution	% RH	Moisture, (% wet basis)	Time, (weeks)	Peak Absorbance Intensity						Extent of transformation, Y
				995 cm⁻¹	1022 cm⁻¹	1045 cm⁻¹	1078 cm⁻¹	1151 cm⁻¹	1078 cm⁻¹ / 1151 cm⁻¹	
KI	67.90	13.91	24	0.243 ± 0.093	0.213 ± 0.080	0.083 ± 0.028	0.058 ± 0.019	0.067 ± 0.018	0.854 ± 0.045	0.399 ± 0.290
50% moisture	n/a	50.00	0	0.473 ± 0.177	0.448 ± 0.184	0.161 ± 0.050	0.105 ± 0.031	0.117 ± 0.029	0.894 ± 0.047	n/a
50% moisture	n/a	50.00	0.14	0.508 ± 0.247	0.424 ± 0.191	0.153 ± 0.096	0.103 ± 0.035	0.113 ± 0.032	0.896 ± 0.055	0.669 ± 0.358
50% moisture	n/a	50.00	0.29	0.558 ± 0.011	0.486 ± 0.010	0.179 ± 0.002	0.118 ± 0.001	0.129 ± 0.01	0.915 ± 0.001	0.792 ± 0.005
50% moisture	n/a	50.00	0.43	0.440 ± 0.177	0.382 ± 0.156	0.140 ± 0.048	0.096 ± 0.032	0.103 ± 0.027	0.914 ± 0.074	0.787 ± 0.479
50% moisture	n/a	50.00	0.86	0.532 ± 0.081	0.436 ± 0.056	0.168 ± 0.016	0.112 ± 0.011	0.122 ± 0.014	0.922 ± 0.023	0.837 ± 0.147
50% moisture	n/a	50.00	1	0.513 ± 0.116	0.458 ± 0.117	0.165 ± 0.035	0.109 ± 0.019	0.117 ± 0.017	0.931 ± 0.026	0.900 ± 0.167
50% moisture	n/a	50.00	2	0.699 ± 0.039	0.595 ± 0.006	0.206 ± 0.004	0.135 ± 0.003	0.143 ± 0.005	0.940 ± 0.024	0.955 ± 0.154
50% moisture	n/a	50.00	3	0.654 ± 0.008	0.580 ± 0.008	0.202 ± 0.002	0.130 ± 0.002	0.138 ± 0.005	0.942 ± 0.039	0.968 ± 0.249
50% moisture	n/a	50.00	4	0.538 ± 0.017	0.502 ± 0.020	0.181 ± 0.005	0.118 ± 0.006	0.125 ± 0.006	0.944 ± 0.007	0.979 ± 0.045

Table D1. MDSC characterization of the sub-Tg endotherm in crackers and baked waxy maize starch at different moisture contents.

Application	Saturated Salt Solution	%RH	Moisture, (% wet basis)	MDSC Nonreversing Signal			
				Tm onset, (^{o}C)	Tm peak, (^{o}C)	Enthalpy, (J/g)	Enthalpy, (J/g dry starch)
Crackers	$CaSO_4$	0.00	1.63	38.74 ± 0.65	46.10 ± 1.19	0.28 ± 0.01	0.28 ± 0.01
Crackers	LiCl	11.30	4.77	43.29 ± 4.80	55.27 ± 0.29	0.32 ± 0.03	0.34 ± 0.03
Crackers	$KC_2H_3O_2$	22.50	6.85	43.20 ± 1.78	54.70 ± 5.35	0.45 ± 0.13	0.49 ± 0.13
Crackers	$MgCl_2$	32.80	7.85	37.94 ± 0.92	45.74 ± 1.60	0.50 ± 0.04	0.54 ± 0.05
Crackers	K_2CO_3	43.20	8.96	42.25 ± 1.19	50.08 ± 1.75	0.62 ± 0.05	0.69 ± 0.06
Crackers	$Mg(NO_3)_2$	52.90	10.35	40.19 ± 0.80	48.03 ± 0.65	0.74 ± 0.03	0.82 ± 0.04
Crackers	KI	67.90	11.97	41.92 ± 2.19	48.12 ± 2.08	0.94 ± 0.08	1.07 ± 0.09
Baked waxy maize starch	$CaSO_4$	0.00	3.39	35.89 ± 3.23	44.67 ± 3.65	0.19 ± 0.07	0.20 ± 0.07
Baked waxy maize starch	LiCl	11.30	5.83	38.72 ± 4.21	53.59 ± 4.32	0.27 ± 0.02	0.29 ± 0.02
Baked waxy maize starch	$KC_2H_3O_2$	22.50	8.61	37.07 ± 1.49	54.65 ± 2.10	0.35 ± 0.05	0.38 ± 0.06
Baked waxy maize starch	$MgCl_2$	32.80	8.95	39.24 ± 2.70	52.77 ± 1.23	0.38 ± 0.02	0.42 ± 0.02
Baked waxy maize starch	K_2CO_3	43.20	10.56	38.37 ± 0.42	52.21 ± 1.51	0.42 ± 0.03	0.47 ± 0.03
Baked waxy maize starch	$Mg(NO_3)_2$	52.90	11.87	37.47 ± 1.56	50.38 ± 6.80	0.45 ± 0.01	0.51 ± 0.01
Baked waxy maize starch	KI	67.90	13.60	43.64 ± 0.65	48.70 ± 0.42	0.55 ± 0.03	0.64 ± 0.03

Table D2. Kinetic characterization of the sub-Tg endotherm peak in crackers and baked waxy maize starch observed by MDSC

| Application | Moisture, (% wet basis) | Time, (weeks) | MDSC Nonreversing Signal | | | | Extent of Transformation, Y |
			Tm onset, (^{o}C)	Tm peak, (^{o}C)	Enthalpy, (J/g)	Enthalpy, (J/g dry starch)	
Crackers	9.59	0	34.32 ± 1.22	41.21 ± 1.08	0.25 ± 0.04	0.27 ± 0.04	n/a
Crackers	9.44	4	41.75 ± 2.78	52.44 ± 4.33	0.35 ± 0.06	0.38 ± 0.06	0.17 ± 0.06
Crackers	8.91	8	41.06 ± 2.04	50.57 ± 5.68	0.39 ± 0.06	0.43 ± 0.07	0.22 ± 0.07
Crackers	6.84	12	33.74 ± 0.87	47.09 ± 7.44	0.45 ± 0.01	0.48 ± 0.01	0.27 ± 0.01
Crackers	6.67	16	38.65 ± 0.65	44.99 ± 1.54	0.50 ± 0.04	0.54 ± 0.04	0.32 ± 0.04
Crackers	6.29	20	38.13 ± 1.47	45.16 ± 2.14	0.52 ± 0.04	0.55 ± 0.04	0.34 ± 0.04
Crackers	7.00	24	37.55 ± 0.91	46.67 ± 1.50	0.54 ± 0.02	0.58 ± 0.02	0.36 ± 0.02
Crackers	6.66	28	36.10 ± 0.62	43.51 ± 1.41	0.55 ± 0.03	0.59 ± 0.04	0.38 ± 0.04
Crackers	7.43	32	37.33 ± 1.09	46.65 ± 1.69	0.55 ± 0.02	0.59 ± 0.02	0.38 ± 0.02
Baked waxy maize starch	10.94	0	34.01 ± 1.36	41.44 ± 3.35	0.19 ± 0.04	0.21 ± 0.05	n/a
Baked waxy maize starch	8.14	4	37.29 ± 2.96	44.90 ± 2.00	0.36 ± 0.05	0.39 ± 0.05	0.18 ± 0.05
Baked waxy maize starch	7.65	8	37.80 ± 1.44	45.78 ± 1.25	0.40 ± 0.08	0.43 ± 0.09	0.22 ± 0.09
Baked waxy maize starch	8.01	12	37.89 ± 0.95	45.60 ± 2.16	0.44 ± 0.03	0.48 ± 0.03	0.27 ± 0.03
Baked waxy maize starch	8.00	16	39.90 ± 2.34	50.87 ± 4.06	0.49 ± 0.03	0.53 ± 0.03	0.32 ± 0.03
Baked waxy maize starch	7.69	20	35.42 ± 1.18	48.68 ± 2.93	0.50 ± 0.03	0.54 ± 0.04	0.33 ± 0.04
Baked waxy maize starch	7.70	24	34.48 ± 0.72	43.94 ± 1.78	0.52 ± 0.02	0.56 ± 0.03	0.35 ± 0.03
Baked waxy maize starch	8.59	28	34.24 ± 0.72	45.84 ± 1.15	0.53 ± 0.02	0.58 ± 0.03	0.37 ± 0.03
Baked waxy maize starch	9.01	32	35.10 ± 0.71	45.75 ± 1.13	0.53 ± 0.04	0.59 ± 0.05	0.38 ± 0.05

Table D3. Kinetic characterization of FTIR-ATR peak absorbance intensities for crackers and baked waxy maize starch

| Application | Moisture, (% wet basis) | Time, (weeks) | FTIR-ATR Absorbance Intensity | | | | | 1080 cm⁻¹ / 1151 cm⁻¹ |
			995 cm⁻¹	1022 cm⁻¹	1045 cm⁻¹	1078 cm⁻¹	1151 cm⁻¹	
Crackers	9.59	0	0.219 ± 0.021	0.164 ± 0.019	0.053 ± 0.009	0.042 ± 0.006	0.004 ± 0.004	0.933 ± 0.052
Crackers	9.44	4	0.267 ± 0.022	0.237 ± 0.020	0.097 ± 0.008	0.060 ± 0.004	0.069 ± 0.005	0.863 ± 0.003
Crackers	8.91	8	0.262 ± 0.030	0.236 ± 0.028	0.095 ± 0.010	0.059 ± 0.006	0.070 ± 0.008	0.844 ± 0.022
Crackers	6.84	12	0.210 ± 0.023	0.188 ± 0.020	0.076 ± 0.008	0.047 ± 0.004	0.057 ± 0.006	0.833 ± 0.018
Crackers	6.67	16	0.194 ± 0.017	0.175 ± 0.015	0.071 ± 0.005	0.044 ± 0.003	0.053 ± 0.003	0.832 ± 0.026
Crackers	6.29	20	0.232 ± 0.020	0.207 ± 0.018	0.081 ± 0.006	0.051 ± 0.004	0.061 ± 0.004	0.830 ± 0.013
Crackers	7.00	24	0.217 ± 0.023	0.195 ± 0.021	0.078 ± 0.007	0.048 ± 0.004	0.058 ± 0.005	0.828 ± 0.021
Crackers	6.66	28	0.188 ± 0.018	0.170 ± 0.017	0.069 ± 0.006	0.043 ± 0.003	0.052 ± 0.003	0.828 ± 0.019
Crackers	7.43	32	0.182 ± 0.012	0.164 ± 0.011	0.067 ± 0.004	0.042 ± 0.003	0.051 ± 0.003	0.827 ± 0.022
Baked waxy maize starch	10.94	0	0.234 ± 0.005	0.152 ± 0.005	0.055 ± 0.003	0.043 ± 0.002	0.038 ± 0.002	1.115 ± 0.025
Baked waxy maize starch	8.14	4	0.192 ± 0.057	0.163 ± 0.047	0.069 ± 0.018	0.045 ± 0.012	0.049 ± 0.014	0.927 ± 0.025
Baked waxy maize starch	7.65	8	0.246 ± 0.016	0.205 ± 0.014	0.086 ± 0.004	0.051 ± 0.003	0.056 ± 0.003	0.914 ± 0.012
Baked waxy maize starch	8.01	12	0.256 ± 0.014	0.213 ± 0.012	0.089 ± 0.005	0.052 ± 0.006	0.057 ± 0.006	0.908 ± 0.010
Baked waxy maize starch	8.00	16	0.188 ± 0.016	0.159 ± 0.013	0.068 ± 0.004	0.041 ± 0.003	0.045 ± 0.002	0.904 ± 0.029
Baked waxy maize starch	7.69	20	0.228 ± 0.016	0.189 ± 0.013	0.079 ± 0.005	0.049 ± 0.003	0.054 ± 0.004	0.902 ± 0.016
Baked waxy maize starch	7.70	24	0.229 ± 0.019	0.190 ± 0.016	0.080 ± 0.006	0.049 ± 0.004	0.055 ± 0.003	0.900 ± 0.019
Baked waxy maize starch	8.59	28	0.209 ± 0.028	0.177 ± 0.025	0.075 ± 0.009	0.047 ± 0.007	0.053 ± 0.007	0.899 ± 0.034
Baked waxy maize starch	9.01	32	0.186 ± 0.029	0.158 ± 0.023	0.068 ± 0.009	0.043 ± 0.006	0.048 ± 0.007	0.898 ± 0.011

D4. 3-point bend texture analysis of crackers stored at 25°C for 32 weeks

Application	Moisture, (% wet basis)	Time, (weeks)	Failure Stress, (kPa)	Failure Strain, (%)	Young's Modulus, (kPa)
Crackers	9.59	0	1517 ± 181	4.60 ± 2.53	197 ± 73
Crackers	9.44	4	1029 ± 230	3.94 ± 1.58	210 ± 64
Crackers	8.91	8	981 ± 173	3.80 ± 1.05	214 ± 92
Crackers	6.84	12	937 ± 274	3.26 ± 1.96	182 ± 93
Crackers	6.67	16	794 ± 78	2.93 ± 1.02	147 ± 46
Crackers	6.29	20	698 ± 124	2.70 ± 1.14	147 ± 58
Crackers	7.00	24	650 ± 184	2.60 ± 0.87	135 ± 59
Crackers	6.66	28	575 ± 193	2.61 ± 0.35	109 ± 34
Crackers	7.43	32	481 ± 181	2.61 ± 0.66	93 ± 33